



universität
wien

Titel der Dissertation

„Development of polar chromatography sorbents and attempts to
describe retention mechanisms of
hydrophilic interaction chromatography systems“

Verfasser

Dipl.-Ing. (FH) Georg Schuster

angestrebter akademischer Grad

Doktor der Naturwissenschaften (Dr. rer. nat)

Wien, März 2013

Studienkennzahl lt. Studienblatt:	A 091 419
Dissertationsgebiet lt. Studienblatt:	Dr.-Studium der Naturwissenschaften Chemie UniStG
Betreuer:	Univ.-Prof. Dr. Wolfgang Lindner

Acknowledgements

Zu Beginn möchte ich mich bei Ihnen Herr Professor Lindner bedanken dass Sie mich in Ihre Arbeitsgruppe aufgenommen haben und mir die Durchführung meiner Dissertation ermöglichten. Danke für die vielen neuen Ideen, die regen Diskussionen und Ihre Unterstützung während der letzten Jahre.

Ich möchte mich auch bei Prof. Lämmerhofer dafür bedanken, dass er immer ein offenes Ohr und einen guten Rat parat hatte.

Ein großer Dank geht an meine Arbeitskollegen: Steffi, Andrea, Denise, Sissy, Reini, Michal, Heli, Roli, Jeannie, Peter und Norbert. Ohne euch wäre diese zeitweilige Berg- und Talfahrt nicht so glimpflich verlaufen. Es war immer gut zu wissen, dass ich jeden von euch um fachlichen Rat bitten konnte, falls etwas mal wieder nicht so glatt lief wie man sich das gedacht hatte. Jedoch möchte ich euch besonders für die Zeit außerhalb des Labors danken. Besonders unsere berühmt-berüchtigten Grillabende werde ich nie vergessen, die so manche Frustration beiseite fegen konnten. In diesem Sinne möchte ich mich besonders bei Steffi und Andrea bedanken, dass ihr stets zu mir gehalten habt und zu so viel mehr als nur Kollegen wurdet.

Ich möchte mich bei Uschi, Monika, Bianca, Teresa, Maria, Björn, Elisa, Kathrin, Aurel, Sarah, Rouwen, Laura, Hannah für ihre Freundschaft und vor allem die schönen gemeinsam verbrachten Stunden und die damit zusammenhängenden Erinnerungen bedanken.

Des Weiteren möchte ich mich von ganzem Herzen bei der Gala-Crew bedanken: Dings, Paul, Paula, Thomas, Kim, Jan, Conny, Micha und Felix, wir haben uns zur richtigen Zeit am richtigen Ort gefunden.

Abschließend danke ich meinen Eltern. Ihr habt mich immer gefördert und mir beigebracht, mein Leben eigenständig zu leben. Danke für den familiären Rückhalt, auf den ich mich zeitlebens verlassen konnte. Dieser Dank gilt auch meinem Bruder Alfred, meiner Schwägerin Barbara und vor allem meinen zwei kleinen Engeln Sophie und Katharina.

„Wohin noch mag mein Weg mich führen?

Närrisch ist er, dieser Weg,

er geht in Schleifen,

er geht vielleicht im Kreise.

Mag er gehen, wie er will,

ich will ihn gehen"

"Siddharta", Hermann Hesse

Table of Contents

List of Figures.....	III
List of Abbreviations.....	VI
Zusammenfassung.....	VII
Abstract.....	IX
1. Introduction.....	1
2. Important factors of HILIC.....	4
2.1 Retention mechanism in HILIC.....	4
2.2 Mobile phases in HILIC.....	7
2.3 The effect of sample diluent on peak shape.....	12
2.4 Stationary phases for HILIC.....	13
2.4.1 Bare silica.....	13
2.4.2 Amine type modified silica.....	16
2.4.3 Silica based diol phases.....	23
2.4.4 Silica based saccharide phases.....	25
2.4.5 Amide type modified silica.....	28
2.4.6 Silica based zwitterionic type phases.....	30
2.5 Characterization strategies of HILIC columns.....	32
2.5.1 Evaluation of HILIC systems by LSER.....	36
3. Study on enantioselectivity outside of the scope of HILIC separations.....	41
4. Concluding remarks.....	43

5. References.....	47
6. List of publications and manuscripts.....	56
Appendix I.....	57
Supplement for Appendix I.....	75
Appendix II.....	81
Supplement for Appendix II.....	105
Appendix III.....	115
Supplement for Appendix III.....	157
Appendix IV.....	171
Curriculum vitae.....	182

List of Figures

I used my best endeavors to seek all claim holders of the pictures and obtain their permission to use their pictures in my thesis. Still, if any copyright infringement should emerge, please inform me.

Fig. 1: Literature research in SciFinder for the keywords HILIC and “Hydrophilic Interaction Chromatography” (march 2013).....	1
Fig. 2: a) Publication type distribution to the study performed in Fig 1. b) area of application for HILIC separations.....	2
Fig. 3: HILIC retention troika (Schuster G., Lindner W., J. Chromatogr. A 2013, © Elsevier; Reprinted with permission)[24].....	4
Fig. 4: Analyte distribution between the water-rich and water-poor bulk phase with additional electrostatic interactions.....	5
Fig. 5: Excess adsorption isotherms for water on four different HILIC sorbents. (Noga et al., J. Chromatogr. A 2013, © Elsevier; Reprinted with permission)[13].....	7
Fig. 6: Effect of different organic solvents on the separation of the water-soluble-vitamins. (A) HILIC diol, (B) bare silica, and (C) amino column. Conditions: (A) diol and silica columns: organic/H ₂ O, 90/10; CH ₃ COONH ₄ , 10 mM; pH 5.0. (C) Amino column: organic/H ₂ O, 85/15; HCOONH ₄ , 5 mM; pH 3.0; flow rate, 0.6 mL/min; column temperature, 25 °C. Detection wavelength, 272 nm. Peak assignment: (1) nicotinamide, (2) pyridoxine, (3) riboflavin, (4) nicotinic acid, (5) L ascorbic acid, and (6) thiamine. (Karatapanis et al., J. Chromatogr. A 2011, © Elsevier; Reprinted with permission)[10].	8
Fig. 7: Influence of analyte solvent on the peak shape of (a,b) small polar compounds (hypoxanthine (1), cytosine (2), nicotinic acid (3), procainamide (4)) and (c,d) peptides (peptide A (1), peptide C (2), peptide D (3), insulin (4)) in HILIC mode. (Ruta et al., J Chromatogr A 2010, © Elsevier; Reprinted with permission)[36].....	12

Fig. 8: <i>Surface silanol groups on bare silica: a) single isolated silanol, b) vicinal hydrogen bonded silanol groups, c) geminal silanol groups and d) surface siloxane groups.</i>	14
.....	
Fig. 9: <i>Schematic representation of ethylene bridged hybrid silica (BEH) adapted from Grumbach et al. [42].</i>	15
.....	
Fig. 10: <i>Amine-type bonded silica phases a) aminopropyl-silica b) sec. and tert. amine-modified sorbent b) triazol bonded SP (exact immobilization strategy not revealed by the supplier).</i>	16
.....	
Fig. 11: <i>Flip mechanism for the APS grafting in dry conditions a) physisorption, b) condensation c) main structure after curing. Adapted from reference [57].</i>	16
.....	
Fig. 12: <i>Comparison of nitrogen content during the ligand immobilization and stress test.</i>	18
.....	
Fig. 13: <i>²⁹Si CP/MAS NMR of a) s'APS and b) APS. T² and T³ correspond to the bidentate or tridentate bonded aminopropylsilyl ligand, respectively. Correspondingly, the surface free silanols and siloxanes are displayed by Q³ and Q⁴.</i>	19
.....	
Fig. 14: <i>Column bleeding study. The blue line represents untreated APS while the red line was achieved for s'APS.</i>	19
.....	
Fig. 15: <i>Selectivity plot for APS and s'APS at pH3.</i>	20
.....	
Fig. 16: <i>separation of mono- and di-saccharides on s'APS and APS. MP: ACN/H₂O (75/25; v/v); flow: 1.0 ml/min; inj.vol: 5 μl; temp: 30°C. Peak annotation: D-fructose (1), D-mannose (2), D glucose (3), D-galactose (4), Sucrose (5), Cellobiose (6), Maltose (7), Lactose (8).</i>	21
.....	
Fig. 17: <i>The chemical structure of a tetrazol modified SP (Dai et al., Chromatographia 2011, © Springer-Verlag; Reprinted with permission)[60].</i>	22
.....	
Fig. 18: <i>a) monomeric brush type diol phase b) undecyl-1,2-diol phase c) cross-linked diol phase.</i>	23
.....	
Fig. 19: <i>The chemical structure of a) non-oxidized thioglycerol phase (TG) b) oxidized thioglycerol phase TGO (respectively SGO in Appendix II + III).</i>	24

Fig. 20: Reaction scheme for glucose-based Chocolate HILIC Phases. (Schuster G., Lindner W., <i>Anal Bioanal Chem</i> 2011, © Springer-Verlag; Reprinted with permission)[78].....	26
.....	
Fig. 21: Evaluation of the separation reproducibility for 50 injections of a vitamin mix with a 17 min HILIC gradient. flow: 1.0 ml/min, inj.vol: 5µl, temp: 20°C; MP-A: ACN + 10 mM NH ₄ AcOH, MP B: H ₂ O + 10mM NH ₄ AcOH., time table: min 0.0 (90%B) → min 2.5 (90%B) → min 10.0 (50 %B) → min 13.0 (50% B) → min 17.0 (90%B).....	27
.....	
Fig. 22: Amide bonded stationary phases. a) TSKgel Amide-80 b) BEH Amide c) propyl urea modified silica.....	28
.....	
Fig. 23: The chemical structure of poly(succinimide) silica derived HILIC-type SPs a) PolyHydroxyethyl ATM b) PolyPolysulfoethyl ATM.....	30
.....	
Fig. 24: Zwitterionic modified HILIC sorbents a) monomeric sulfobetain-type (Nucleodur® HILIC) b) polysulfobetain-type (ZIC® HILIC c) monomeric phosphorylcholin-type (PC HILIC) d) polyphosphorylcholin-type (ZIC® cHILIC).....	30
.....	
Fig. 25: Linear (a) and logarithmic (b) plots of log k vs. volume fraction of water in the MP for adenosine on (■) Atlantis HILIC silica column, (●) multi-hydroxyl column, (▲) single-hydroxyl column, (▼) Venusil HILIC column, (◄) β-cyclodextrin column and (►) BEH HILIC column. (Jin G. et al., <i>Talanta</i> 2008, © Elsevier; Reprinted with permission) [103].....	33
.....	
Fig. 26: The chemical structure of weak anion exchangers QN-AX (left) and QD-AX (right). (Pell et al., <i>J.Sep.Schi.</i> 2012, © Wiley-VCH, Reprinted with permission) [118].....	41
.....	
Fig. 27: Correlation matrix of screened HILIC columns. Red column labels relate to a MP condition of ACN/H ₂ O (90:10, v/v) + 10 mM NH ₄ FA (pH 3) while green SP labels express the analysis with ACN/H ₂ O (90:10, v/v) + 10 mM NH ₄ AcOH (pH 5). The color encryption of the squares is explained in the text.	45

List of Abbreviations

ACN	acetonitrile
APS	aminopropyl silica
APTMS	3-(aminopropyl)trimethoxysilane
BEH	ethylene bridged hybrid silica
CD	cyclodextrin
CP/MAS NMR	cross-polarization magnetic angle nuclear magnetic resonance
CSP	chiral stationary phase
ERLIC	electrostatic repulsion hydrophilic interaction chromatography
ESI-MS	electrospray ionization mass spectrometry
HCA	hierarchical cluster analysis
HILIC	hydrophilic interaction chromatography
LSER	linear solvation energy relationship
MP	mobile phase
NH ₄ AcOH	ammonium acetate
NH ₄ FA	ammonium formate
NMR	nuclear magnetic resonance
NP-LC	normal-phase liquid chromatography
PCA	principle component analysis
RP-LC	reversed-phase liquid chromatography
s'APS	stabilized aminopropyl silica
SP	stationary phase
SWL	stagnant water-rich layer
QN	quinine
QD	quinidine

ZUSAMMENFASSUNG

Seit der Namensgebung der *hydrophilen Interaktionschromatographie* (HILIC) in den 90er Jahren des letzten Jahrhunderts ist ein steiler Anstieg in veröffentlichten Publikationen pro Jahr als starkes Indiz für die hohe Nachfrage und Bedeutung dieser doch noch relativ neuen Chromatographie Methode zu verzeichnen. Neue Methoden zur Analyse polarer Verbindungen sind hierbei ebenso stark vertreten wie die Entwicklung neuer Chromatographiematerialien und Beiträge zur Erläuterung des bis heute noch nicht vollständig aufgeklärten HILIC Mechanismus.

Die Entwicklung und Charakterisierung eines neuen polar modifizierten Säulenmaterials steht im Fokus des ersten Teils der Thesenschrift. Hierbei wurde Aminopropyl-Kieselgel mittels eines innovativen Modifikationsverfahrens, unter Einbezug der sogenannten Maillard Reaktion, zu einem neuen hydrophilen Adsorbens umgesetzt. Die somit erhaltenen „Chocolate HILIC“ Säulen zeichnen sich durch ihre bräunliche Färbung aus. Dabei werden primäre Aminofunktionen, welche sich an der Oberfläche des Startmaterials befinden, mit reduzierenden Zuckern (Glucose, Lactose, Maltose und Cellobiose) und mit Hilfe der nicht-enzymatischen Bräunungsreaktion umgesetzt. Im Zuge des Evaluierungsprozess zeichnete sich Cellobiose als vielversprechendste und effizienteste Liganden-Vorstufe aus. Als Ergebnis der vorgelegten Reaktionskaskade wurde das Amin-Grundgerüst mit Hydroxylgruppen und wahrscheinlich auch mit stickstoffhaltigen Heterozyklen überzogen. Die Überprüfung mehrerer Test-Sets in Kombination mit unterschiedlichen mobilen Phasen zeigte, dass sowohl adsorptive als auch schwache ionische Wechselwirkungen neben den prädominierenden Verteilungsvorgängen gegenwärtig sind. Im Vergleich zu reinen Diol modifizierten HILIC Säulen ermöglichen die zusätzlichen Interaktionspunkte zwischen den Test-Analyten und dem Amin-Hintergrund des Basismaterials eine deutliche Manipulation der Retentionsselektivitäten. Des Weiteren wurde die Stabilität der „Chocolate HILIC“ Säulen bezüglich ihrer chromatographischen Reproduzierbarkeit mittels Gradientenelution evaluiert. 50 aufeinanderfolgende Injektionen eines Test Gemisches, bestehend aus sechs Vitaminen, wurden mit einem 17 minütigen HILIC Gradienten untersucht. Die Säule zeichnete sich hierbei durch eine schnelle Re-Äquilibrierung hinsichtlich der Startbedingungen aus, was ein Indiz für die schnelle Wiederanpassung der stillstehenden adsorbierten Wasserschicht sein kann. Desweiteren ermöglicht der „Mixed Mode“ Charakter des

Retentionsmechanismus auch die Untersuchung lipophiler Verbindungen unter Einbezug mobiler Phasen mit einem sehr hohen Wasseranteil. In Rahmen dieser Studie wurde der höchste Lipophilie Grad auf „Chocolate HILIC“ Phasen verzeichnet, welche mit Glucose anstelle von Cellobiose als Liganden-Vorstufe synthetisiert wurden.

Den zweiten Teil und zugleich den Schwerpunkt dieser Dissertation stellt die nähere Betrachtung all jener Kräfte dar, welche die Interaktionen zwischen den Analyten und dem Adsorbens und somit die Retention in HILIC Systemen gewährleisten. Das Konzept der „linear solvation energy relationships“ (LSER) wurde hierbei angewandt um mit Hilfe von kalkulierten Systemkonstanten Retentions-Korrelationen zu erläutern. Obgleich dies eine bekannte und verbreitete Vorgehensweise im Zuge der Aufklärung von Retentionsmechanismen innerhalb von Umkehrphasensystemen ist, gibt es kaum Veröffentlichungen dieser Methode in Kombination mit HILIC Systemen. Das untersuchte Säulenset bestand dabei aus 23 polaren Adsorbentien und wies unterschiedliche Oberflächenmodifikationen (neutral, basisch, sauer und zwitterionisch) auf. Diese wurden entweder käuflich erworben oder innerhalb der Arbeitsgruppe synthetisiert. Nach dem Erfassen von Retentionsdaten von sich hinsichtlich der Struktur unterscheidender Verbindungen, wurden diese Werte mitsamt den dazugehörigen strukturspezifischen Abraham Parametern (A, B, S und V), sowie den kürzlich eingeführten D Deskriptoren (D^+ und D^-), zum Aufstellen des LSER basierten Retentionsmodells verwendet. Die HILIC Systeme wurden mittels mobilen Phasen, welche einen hohen Gehalt an Acetonitril aufwiesen, und unter Verwendung zweier unterschiedlicher Pufferzusammensetzungen (pH 3 und pH 5) evaluiert. Hierbei konnte gezeigt werden, dass der Ansatz der Solvatisierungs Parameter nicht nur zu einer näheren Erklärung des HILIC Mechanismus beiträgt, sondern ebenfalls als hilfreiches Werkzeug im Verlauf der Entwicklung von Säulenmaterialien eingesetzt werden kann. Durch den Ersatz von Ammoniumformiat als Puffergegenion mit Ammoniumacetat, und den zusätzlichen Anstieg des pH Wertes, wurde eine signifikante Erhöhung der Wasserstoffbrücken Basizität der HILIC Systeme verzeichnet. Des Weiteren wurden auf Säulen, welche sich hinsichtlich des Selektivitätsprofils im Laufe der Datenakquirierung glichen (z.B. Shiseido PC HILIC und Nucleodur HILIC), unterschiedliche Kräfte bestimmt, die zum generellen Rückhalt von Analyten auf den jeweiligen Säulen beitragen. Schlussfolgernd lässt sich sagen, dass die Selektivität in HILIC Systemen durch das Zusammenspiel und somit aus der Summe des additiven und multiplikativen Charakters der Wasserstoffbrückenbindungen, ionischen Wechselwirkungen und Verteilungsvorgängen erreicht wird.

ABSTRACT

Since the advent of hydrophilic interaction liquid chromatography (HILIC) in the 1990's an increase in the number of published papers on this subject can be found per year, which shows the importance and demand of this still rather new chromatography method. Not only new methods for the analysis of polar analytes but also the developments of polar packing materials are found alongside contributions to the revelation of the still not fully elucidated mechanism of HILIC retention characteristics.

The first part of the thesis deals with the development and characterization of a polar packing material for HILIC type separations. A novel and innovative modification of aminopropylsilica by the Maillard Reaction was used to prepare the hydrophilic sorbent. As a result, the new "Chocolate HILIC" packing materials feature a brown color due to the non-enzymatic browning reaction of reducing sugars (glucose, lactose, maltose and cellobiose) with primary amino residues on the base material. In course of the column evaluation cellobiose was found to be the most efficient "ligand-primer". The reaction cascade resulted in hydroxyl groups and most likely aza-heterocycles over an amino-backbone. The screening of test sets in combination with different mobile phases revealed that adsorptive including weak ionic interactions in addition to partition phenomena are present. The additionally introduced interaction sites between the test probes and the amine backbone enabled a convenient selectivity manipulation compared to pure diol type HILIC phases. Furthermore, the chromatographic stability of "Chocolate HILIC" phases was investigated under gradient elution conditions. A test mix of 6 vitamins was analyzed with 50 consecutive runs using a 17 minute HILIC gradient. Thereby, the column showed a fast re-equilibration towards the starting conditions which may be the result of a fast and reproducible readjustment of the stagnant water layer. The mixed modal retention mechanism enabled retention of lipophilic analytes with a high amount of water in the mobile phase. Compared to cellobiose, glucose as ligand primer exhibited the highest overall lipophilicity of the Chocolate HILIC type columns.

In the second and main part of the thesis, a more in depth study on the forces which facilitate solute-sorbent interactions and thus retention within HILIC systems was carried out. The concept of linear solvation energy relationship (LSER) was applied in order to explain the correlations via computed system constants. Despite the fact that this methodology is common for the elucidation of retention mechanisms within reversed phase

packing materials it is still a rather scarcely used routine for HILIC mechanistic studies. 23 home-made and commercially available polar modified sorbents with different surface modifications (neutral, basic, acidic, zwitterionic) served as screening set. Acquired retention data of differently structured test compounds, Abraham solute parameters (A, B, S and V) and recently introduced charge descriptors (D^+ and D^-) were implemented to generate LSER based retention models. The HILIC systems were evaluated under acetonitrile-rich conditions and two different buffer compositions (pH 3 and pH 5). The solvation parameter approach was found to be useful not only during the elucidation of HILIC retention mechanisms but also as a tool during column development. The hydrogen bond basicity of HILIC systems was found to be significantly enhanced under elevated pH conditions and using ammonium acetate instead of ammonium formate as buffer counter ion. Different retentive forces which contribute to the overall retention were found on columns which showed similar selectivity profiles during the acquisition of raw retention data (e.g. Shiseido PC HILIC and Nucleodur HILIC). Thus selectivity in HILIC systems is achieved by the sum of additive or multiplicative phenomena of hydrogen bonding, ionic interactions and partition phenomena.

1. Introduction

In 1990, A. J. Alpert “revolutionized” the world of chromatography by introducing Hydrophilic Interaction Chromatography (HILIC) as an alternative to reversed-phase chromatography (RP-LC) [1]. Up until that point, normal-phase liquid chromatography (NP-LC) was the method of choice for the analysis of semi polar compounds which can be rather difficult or even impossible when RP-LC is applied. Similar to NP-LC using merely plain silica he used a polar stationary phase (PolySulfoethyl ATM and PolyHydroxy ATM) however exchanged the non-polar non-aqueous mobile phase (MP) with an aqueous organic mixtures. These mobile phases contained mainly high proportions of acetonitrile (ACN) (> 60 %) and were able to separate proteins, peptides, amino acids, oligonucleotides and carbohydrates. The obtained selectivities showed complementary pattern compared to NP-LC or RP-LC. Indeed, Alpert was the first one to give a name to this alternative form of chromatography. However, literature can be found which dates back more than 40 years. Martin and Synge separated amino acids on water saturated unmodified silica and used a MP composed of chloroform and alcohol [2]. A famous separation example which resembles even more the HILIC methodology was published by Rabel et al. in 1976. A number of mono-, di- and trisaccharides was analyzed on a permanently polar amino-cyano bonded 10µm silica gel with secondary amine groups by applying a mixture of ACN and water as MP [3]. Although the term aqueous-normal phase started to arise, it took ten more years until the name HILIC was coined and almost another 20 years until it became a buzz. Until 2006 not more than 50 publications were released per year which drastically changed in 2007 and a steep rise can be found until today with around 350 publications in 2012 and already over 60 publications until the end of February 2013 (see Fig. 1).

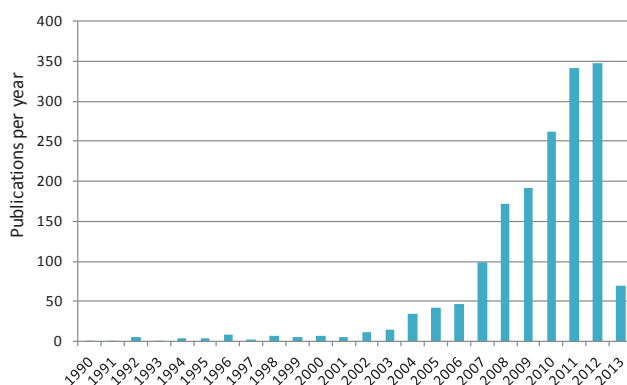


Fig. 1: Literature research in SciFinder for the keywords HILIC and “Hydrophilic Interaction Chromatography” (March 2013).

Out of these publications, 89 % are journal articles, 7 % reviews and 4 % HILIC-related patents (see Fig. 2a). Fig. 2b displays the main areas of application. With the rising interest of polar compounds in the field of biochemistry, genetics and molecular biology but also chemical engineering and studies on pharmaceutical related fields, HILIC is starting to become the method of choice in solving separation problems that cannot be addressed easily by RP-LC.

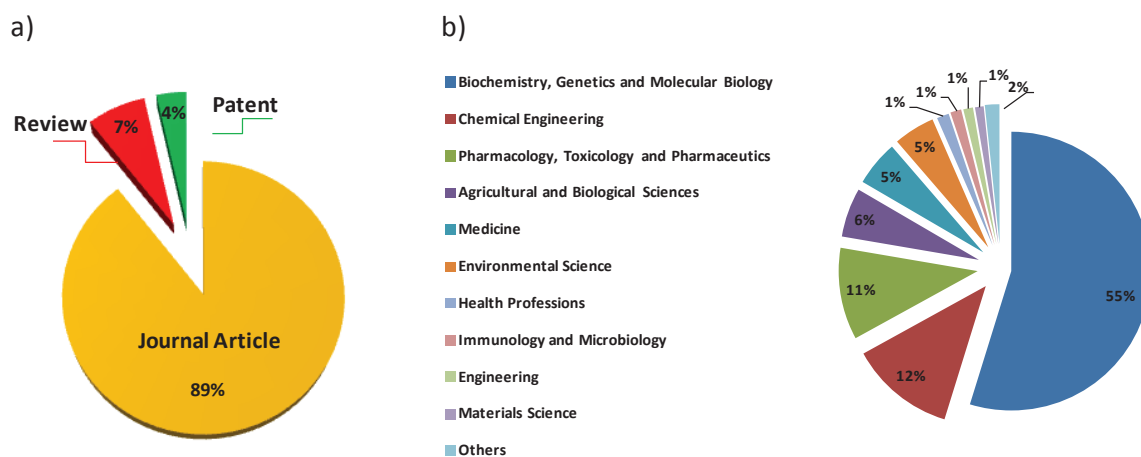


Fig. 2: a) Publication type distribution to the study performed in Fig 1. b) area of application for HILIC separations.

Thus, the literature is filled with new separation methods and publications on the development and evaluation of new polar packing materials alongside contributions to the elucidation and better understanding of the still vaguely deciphered HILIC retention mechanism. Now that more research groups work on probing various influential parameters on HILIC separations (e.g. [4-14]), one aspect starts to clearly crystallize. The stationary phase (SP) has the highest impact on tuning selectivity and optimizing separation due to the rather restricted diversity in usable MPs (see section 2.2.). The vast availability of different HILIC columns from different suppliers does not make it easy for someone to initially choose the most appropriate one. Furthermore, during method development it is important to know which columns are to some extent interchangeable and which columns clearly experience different selectivity. Thus it is important that HILIC columns are very well characterized and understood.

The first aim of these doctoral studies was the development of a new polar sorbent on the basis of (3-aminopropyl)trimethoxysilane modified silica starting materials to extend the available HILIC selectivity. Furthermore, the mechanism within HILIC columns and the retention forces inside these systems were studied by multivariate methods and a set of

different SPs with a neutral, acidic, basic or zwitterionic character generated via surface modifications. Reviews on HILIC are now released at least once a year which enlighten, inform and give an insight on new developments. Consequently, addressing all important HILIC related issues would go beyond the scope of this thesis. Therefore, the following chapters will mainly try to address important factors which are directly related to my research projects summarized in this thesis. In order to provide more information and accessibility on the vast growing field of HILIC I hereby refer the readers to some recent reviews [15-23]. The main results generated during my time as a PhD student are published in scientific articles (**Appendix I, II, IV**) or were recently submitted to a peer-reviewed journal (see manuscript **Appendix III**).

A discussion of the results appearing in the papers and the manuscript will follow in the appropriate sections of the thesis.

2. Important factors of HILIC

2.1 Retention mechanism in HILIC

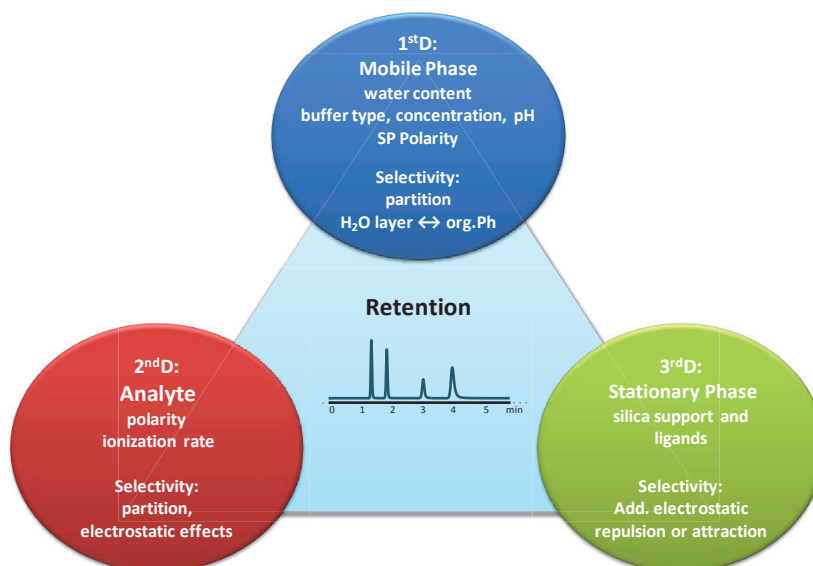


Fig. 3: HILIC retention troika (Schuster G., Lindner W., J. Chromatogr. A 2013, © Elsevier; Reprinted with permission)[24].

Originally Alpert proposed a partition driven mechanism in which the polar surface of the SP attracts water molecules which are subsequently adsorbed to form a stagnant water-rich layer (SWL). ACN molecules are allocated opposed to this SWL to form a water-poor organic layer. Thus, analytes are separated according to their repartition between the organic-rich bulk phase and the SWL. While this explanation was long thought to be true or better said, there were simply no other studies which would oppose this suggestion, it is nowadays generally accepted that not only partition driven phenomena but also electrostatic interactions (attractive or repulsive), hydrophilic adsorptive interactions (hydrogen bonding, dipole-dipole) and also to some extent hydrophobic interactions take place to facilitate the retention of analytes within a HILIC system [4-14]. Fig. 3 describes the interplay between the three factors that explain a HILIC system. During my experimental work I started to think of HILIC as a three dimensional process. It starts all with a separation problem. In general, it is the analysis or determination of a specific analyte type or mixture (2nd dimension of the troika). The analytes stay more or less independent and do not change, unless derivatization strategies or tuning of the 1st dimension, namely the MP, are applied. The scientist in charge of method development can

affect the 2nd and 3rd dimension of a HILIC system (Fig. 3). For example, changing the pH value of the MP will either enhance or decrease the analytes' polarity due to a change in the charge state of ionizable compounds which contributes to the partition-driven increments of the retention mechanism. Furthermore, due to the pH change, chargeable HILIC supports (see section 2.4) may be ionized and additional electrostatic repulsion or attraction between the analytes and the support can occur (Fig. 4).

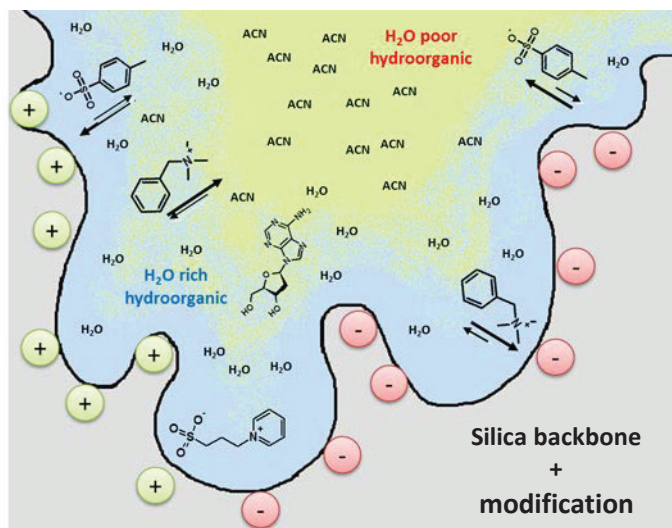


Fig. 4: Analyte distribution between the water-rich and water-poor bulk phase with additional electrostatic interactions.

While these are factors that the operator can influence, he has no immediate engagement during the production process of SPs. I found myself placed in the section which is restricted for a column developer. As an inventor of new HILIC phases, we have the responsibility to enlarge the line-up of available selectivity since the rather restriction of applicable MPs leave the SP as one of the most important factors for the adjustment of HILIC separations. Furthermore, due to the complexity of the HILIC mechanism (see later) and the interplay between all three retention dimensions, it is important to offer characterization tools that on the one hand help us in the course of developing new HILIC-type SPs but more importantly, on the other hand offer the user more valuable information to better understand the HILIC process.

Nevertheless, it is undeniable that the water layer plays an important role in the whole retention mechanism of HILIC systems. Thus, it is no wonder that research groups are trying to find methods to qualitatively and quantitatively evaluate and characterize the adsorption of water on the surface of HILIC-type SPs. In 2011 the group of Ulrich Tallarek published an article on the investigation of the equilibration of H₂O-ACN mixtures

between a cylindrical silica pore and two bulk reservoirs [25]. They were able to show that the solvent composition inside the silica nanopore was significantly different from the bulk reservoirs. Within a radial position of < 0.45 nm ACN is excluded and only water molecules were found to be strongly adsorbed to the hydrophilic silanol surface via hydrogen bonding, thus forming the postulated SWL. Inside this region the solvent density, molecule coordination and orientation are independent of the bulk H₂O-ACN ratio. After this water-occupied immediate surface region, ($> 0 - 45$ nm) ACN-water hydrogen bonding starts to occur next to the prevailing water-water hydrogen bonds which is accompanied by a decrease in solvent coordination until the molecules reach their bulk behavior at the pore center. Although the experimental design does not completely mimic typical HILIC conditions, due to the lack of buffer ions, it is a first attempt to confirm the ability of silica surfaces to govern solvent partitioning and an equilibrium composition inside the pore. Note that not only plain silica works as a HILIC-type SP but also polar modified silica surfaces. In the same year, another publication from the group of Knut Irgum featured a ²H nuclear magnetic resonance (NMR) study as a tool to probe the influence and the state of water in HILIC type chromatography materials [26]. The amount of non-freezable water in silica as well as zwitterionic modified sorbents was detected by the phase transitions in the thawing curves. A considerably higher amount of non-freezable water was found on polymeric zwitterionic SPs in contrast to neat silica. Thus, they correlated the stronger retention of test compounds on the zwitterionic phase opposed to the silica support to a higher amount of liquid water in the adsorbed SWL on these phases. Consequently, this result should support the partition driven mechanism. The most recent investigation related to the existence and the thickness of the SWL was performed by the group of Bogusław Buszeski [13]. They measured the amount of adsorbed water by the minor disturbance method. The received excess adsorption isotherms showed that polar SPs are able to extract water from the organic-rich MP (Fig. 5). This effect gets stronger when less water is used and is in agreement with the general observation, that the retention of analyte increases with a lower amount of water and vice versa. Furthermore, this methodology showed that it can be applied during column development to screen if the new SPs are able to facilitate retention under HILIC conditions. As immediate outcome of this study, one can expect a change of the SWL in case of MP gradient elution conditions (see later).

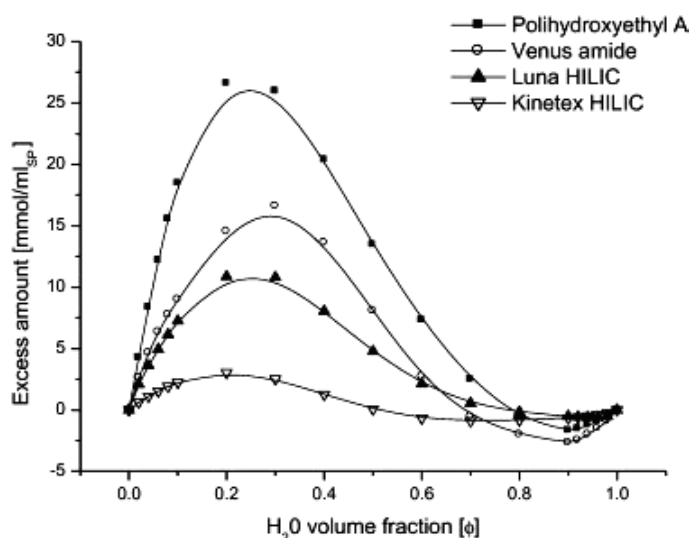


Fig. 5: Excess adsorption isotherms for water on four different HILIC sorbents. (Noga *et al.*, *J. Chromatogr. A* 2013, © Elsevier; Reprinted with permission)[13].

2.2 Mobile phases in HILIC

Similar to RP-LC eluents, HILIC MPs are of hydro-organic character with the exception that water is now the stronger eluent in contrast to the polar organic solvent (mainly ACN). Thus, a high percentage of organic solvent, typically between 95 - 60 %, is mixed with 5 - 40 % water or aqueous buffer. Volatile buffer salts with a high solubility in organic-rich mixtures are usually used. Ammonium formate (NH₄FA) and ammonium acetate (NH₄AcOH) perfectly fit these requirements and are usually the buffer of choice not least because of the good electrospray ionization mass spectrometry (ESI-MS) compatibility. Since HILIC is based to some extent on liquid-liquid partition and extraction, the strong and the weak eluent should be of an adequately different polarity. Mixtures of ACN with water have been found to be the most efficient MP for this task. Yet, ACN can be quite costly and can face delivery shortage as it occurred around the end of 2008 and 2009. To overcome this disadvantage scientists tried to find alternatives within the range of protic and aprotic solvents. Both, Li *et al.* and Karatapanis *et al.* showed the effect of organic modifiers different from ACN [10,27]. As can be seen in Fig. 6, the retention decreases drastically and almost all analytes co-elute while using methanol or 2-propanol instead of ACN. Thus, aprotic solvents seem to be superior due the lower polarity and the lack of a hydrogen donating functional group. Yet, also with tetrahydrofuran a significant loss in

retention was observed, which was attributed to its higher hydrogen-bonding acceptor capability.

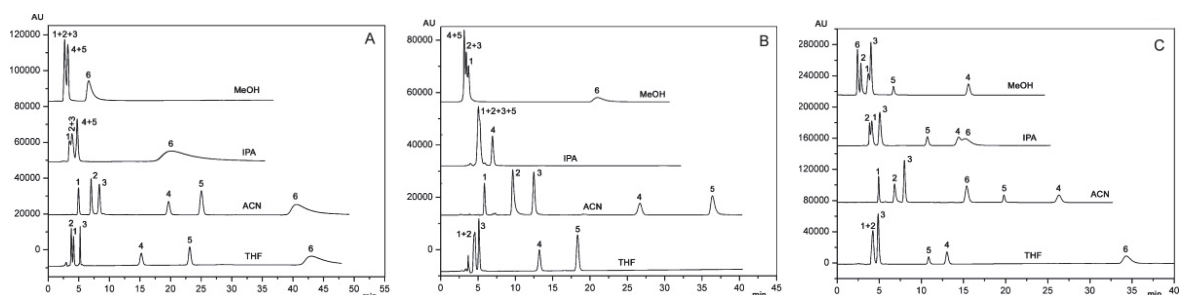


Fig. 6: Effect of different organic solvents on the separation of the water-soluble-vitamins. (A) HILIC diol, (B) bare silica, and (C) amino column. Conditions: (A) diol and silica columns: organic/H₂O, 90/10; CH₃COONH₄, 10 mM; pH 5.0. (C) Amino column: organic/H₂O, 85/15; HCOONH₄, 5 mM; pH 3.0; flow rate 0.6 mL/min; column temperature 25 ° C. Detection wavelength 272 nm. Peak assignment: (1) nicotinamide, (2) pyridoxine, (3) riboflavin, (4) nicotinic acid, (5) L-ascorbic acid, and (6) thiamine. (Karatapanis *et al.*, *J. Chromatogr. A* 2011, © Elsevier; Reprinted with permission)[10].

As an addition to these observations, Karatapanis used toluene as marker analyte to show a possible decrease in the hydrophilicity of the adsorbed layer. If the water layer is disrupted by the organic solvent molecules the layer should increase in its hydrophobicity and an increase in the retention of toluene should be visible. Methanol displayed the highest disruption of the water layer followed by 2-propanol, tetrahydrofuran and ACN. Li attributes this effect to the replacement of water with methanol molecules. Another study which supports this theory was carried out by Anna J. Barnett and Seong H. Kim [28]. They studied the co-adsorption of n-propanol and water on SiO₂. Although they decreased the concentration inside the vapor phase to zero, a residual amount of n-propanol molecules was still found to stay in the adsorbed water layer on the silica surface. In 2010 Fountain et al. investigated the exchange of ACN with acetone [9]. The aprotic character, the similar relative polarity and the solubility in water could make it an appropriate solvent. Shorter retention times and higher selectivity differences between pH 3 and pH 9 were observed for acetone compared to ACN. In principle, this outcome is not generally negatively afflicted and acetone may be used as ACN alternative during method development. However, the incompatibility with UV detectors due to the high cut-off at 330 nm and the inferior performance in terms of background noise and ionization rate under HILIC-ESI-MS, opens only a limited application range for acetone as an alternative to ACN.

Apart from trying to exchange the weakly eluting organic MP component, Bicker et al. showed that it is possible to replace the strong eluent water by protic organic solvents. Methanol, ethanol and 1,2-ethandiol were probed as water alternatives on diol modified columns [29]. Retention for nucleobases and nucleosides increased on Luna HILIC and ProntoSil Diol column (for structure see section 2.4.3) in the order 1,2-ethandiol < methanol < ethanol. Furthermore, different elution orders were observed for nucleobases when changing the strong eluent, while the retention order was unaffected for the nucleosides. Thus, it is also possible to perform HILIC in totally nonaqueous elution mode to have a tool for tuning selectivity during the method development. Despite all these achievements, the mixture of ACN and water is still the most favorable and efficient eluent.

The amount of organic modifier has a crucial influence on the retention observed in HILIC. Generally, the retention of polar analytes decreases with decreasing amount of organic modifier. Thus, while more water is applied in the MP the distinction between the more strongly bound water-enriched layer and the more diffuse layer, which is more loosely associated to the SP, decreases and the elution of polar analytes is amplified. In other words, if the amount of organic modifier is increased, a stronger interaction between the water molecules and the polar SP takes place. In this case, ACN molecules are not able to penetrate the closely bound water molecules to interact with the SP. By using excess adsorption isotherms, Buzewski et al. found a maximum of adsorbed water at around 80 % of organic modifier and vice versa. The investigations of McCalley and Neue showed that with a MP composition of 75 - 90 % ACN, around 4 - 13 % of the silica phase pore volume is occupied by a water-enriched layer [30]. In addition to these results, studies on the effect of a variation in the percentage of organic modifier on HILIC SPs showed that due to the modification of the silica base material, U-shaped retention motifs are found for several modified SPs. In that case, the retention of analytes decreases and exhibits a minimum at around 70 - 40 % ACN. Thus, these columns are not limited only to HILIC separations but can also be used to a certain extent in RP-LC or 2D HPLC separation concepts (e.g. reference [31] and **Appendix I**).

A change of the eluents' pH can have various effects on either the analyte or the SP. A pH above an acids' *pKa* leads to the dissociation of the proton associated to the acidic group. Thus, the compound gets negatively charged and is rendered more hydrophilic. The opposite effect occurs for bases and the charged amine group loses its proton which in turn

results in a hydrophilicity loss of the basic solute (now uncharged). Consequently, the analytes retain either longer or shorter. Furthermore, the pH of the MP can affect the SP in terms of ionizing chargeable ligand groups (e.g. aminopropyl groups or residual silanols) which in turn enables electrostatic attraction e.g. between a positively charged SP and a negatively charged analyte. Moreover, the charged SP exhibits a higher polarity which in turn attracts more water molecules and a thicker water layer is formed. The effect of attraction and repulsion between an analyte and the SP was introduced by Alpert under the name electrostatic repulsion hydrophilic interaction chromatography (ERLIC) [32]. Basic and acidic peptides as well as phosphopeptides were analyzed on a weak anion exchanger (WAX) column. Acidic peptides exhibited electrostatic attraction and showed longer retention than basic peptides. The latter eluted in the time frame of neutral peptides due to electrostatic repulsion. However, since the mixed mode character of HILIC is now accepted, the term ERLIC is interchangeable with HILIC and only scarcely found in literature anymore.

Increasing the buffer concentration usually increases the retention of analytes on neutrals non-ionic SPs. An increase in hydrogen-bond interactions between the sorbent and the solutes may be attributed to this effect as the amount of solvated salt ions increases in the MP. Kumar et al. found a decrease for basic compounds with an increase of buffer counter ions and related this result to a displacement of the analytes which are associated with residual silanol groups by the buffer counter ion [12]. In analogy, the retention of acidic solutes increased due to a reduction of ionic repulsion. The opposite effect can take place on basic modified SPs (see section 2.4.2). However, this study showed that the effect of the used buffers was rather low compared to other parameters screened.

The type of buffer can have also an effect on the retention and selectivity on HILIC phases. While triethylammonium phosphate buffers increase the retention of basic peptides, sodium methylphosphonate can be of advantage for phosphopeptides [32]. The use of trifluoroacetic acid can induce changes in selectivity due to the formation of ion pairs, this was shown e.g. by McCalley et al. for small polar compounds [33], or by Ding et al. during the separation of glycopeptides [34]. Another example may be found in **Appendix I**. Trifluoroacetic acid reduced the retention of acidic compounds on my newly developed SPs due to the inhibition of the amine moieties of the HILIC sorbent. Sanchez and Kansal investigated the effects of formic acid without salt additives for the HILIC type analysis of basic compounds [35]. The result was less promising since bad peak shapes and lower

retention were obtained compared to NH_4FA buffered systems. However, the addition of Li^+ , K^+ and Na^+ improved the performance when formic acid was used without salt additives. This emphasizes the importance of a buffered system in HILIC to obtain a better peak performance. Although the buffer concentration can alter the ionic interactions between the SP and the solute, the elution does not show a linear relationship with the amount of used counter ions [4,7,8]. Thus, retention is not explained by the stoichiometric displacement model, hence, it is not purely based on a cation or anion exchange mechanism. While we did not study this effect for the HILIC mode, the general approach and theory of the displacement model can be found in **Appendix IV**, where we investigated the influence of counterion type and strength for chiral sulfonates on weak anion-exchange chiral SPs (see section 3).

During my experimental work I investigated the MP-related change of HILIC systems via multivariate statistics (**Appendix III**). The substitution of NH_4FA (pH 3) with NH_4AcOH (pH 5) ensued an elevated hydrogen bond acceptor property of the HILIC system. Moreover, apart from some exceptions which are specified in **Appendix III**, the hydrogen bond donor property generally increased, too. Analytes tended to retain longer except if electrostatic repulsion occurred. The effect was independent of the character of the SP. One reason for this outcome may be a higher solvation of the chromatographic support due to the elevated pH value which can render the SP more hydrophilic (e.g. ionization of residual silanol groups). In addition, acetate ions not only exhibit a higher molecular volume than formate ions which can lead to a swelling of the water layer, but may also contribute to the HILIC system in terms of salt bridge formations between the SP and the analyte. Consequently, the results indicate that the SP is surrounded by more water molecules. In addition, the higher retention and clear rise of the hydrogen basicity can be attributed to the buffer salt change which promotes the dissociation of silanol functions on modified SPs based on silica support materials.

2.3 The effect of sample diluent on peak shape

Another crucial factor in HILIC is the use of appropriate sample diluents to obtain good peak efficiency, shape and symmetry. Although the effect is known, not many studies can be found on this subject. In 2010, a systematic study on band broadening due to the effect of the sample diluents was published by Ruta et al. [36]. The test set included peptides with a molecular weight range of 1000-6000 Da and small solutes. Protic solvents (water, methanol, ethanol, 2-propanol), aprotic solvents (dimethyl sulfoxide and ACN) and mixtures thereof were screened on an Acquity BEH HILIC and Acquity BEH amide-type column. Best peak shapes for the small analytes were obtained with ACN (Fig. 7a). The amount of water should not exceed 10 % within the dilution solvent (Fig. 7b). As an alternative for solutes which face solubility problems in pure ACN, they suggested a mixture of 2-propanol/ACN (50:50, v/v). For peptides, ACN and 2-propanol and to a smaller extend ethanol seemed appropriate (Fig. 7c). Water should again be avoided as much as possible (Fig. 7d). These conclusions show that the appropriate dilution solvent is an important factor which should be investigated during method development.

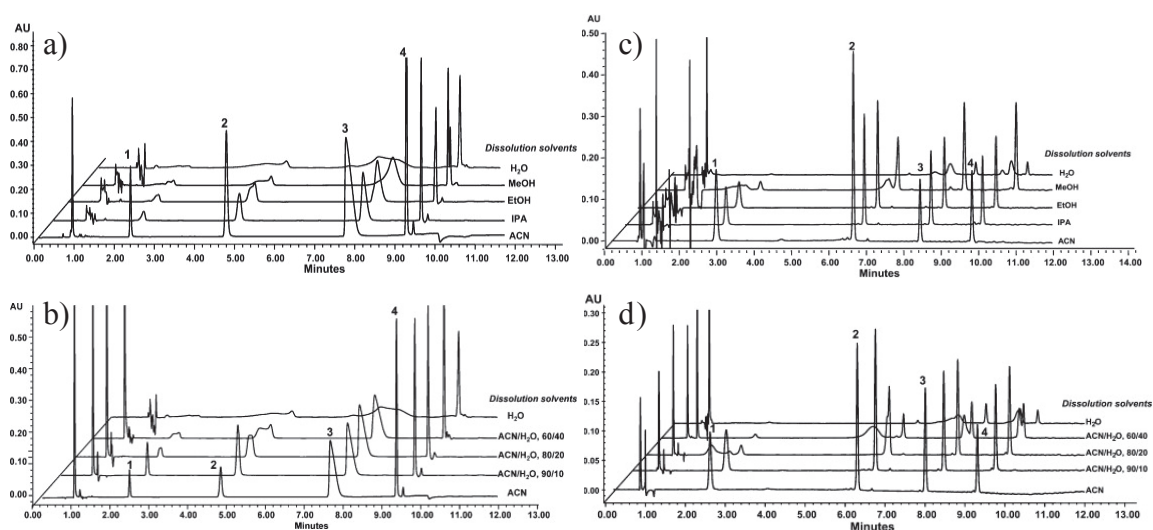


Fig. 7: Influence of analyte solvent on the peak shape of (a,b) small polar compounds (hypoxanthine (1), cytosine (2), nicotinic acid (3), procainamide (4)) and (c,d) peptides (peptide A (1), peptide C (2), peptide D (3), insulin (4)) in HILIC mode. (Ruta *et al.*, J Chromatogr A 2010, © Elsevier; Reprinted with permission)[36].

2.4 Stationary phases for HILIC

As already stated earlier in this thesis, the amount of available HILIC phases is continuously growing and most suppliers of chromatography sorbents develop and offer their own sparticular column. However, all these columns can be arranged into roughly four to five groups. One of the oldest and still often used classes is plain or naked silica, which is available in different purity, surface activated grades and different particle size. A newer development of this kind is BEH silica which is an ethylene bridged hybrid material and offers less acidic silanol groups on the surface than regular silica. Both can be either used as standalone HILIC columns or as base material which is then further modified with different ligand types and functional groups. One of this modifications which is historically as old as silica in combination with HILIC separations are amino-modified packing materials which belong to the group of basic columns.

Due to the rising interest in HILIC, new polar sorbents were developed which offered non-ionizable hydrophilic modifications that possessed e.g. diol or amide groups attached via a linker to the silica surface. The latest achievement, however, was the introduction of zwitterionic motifs either attached via a brush-type linker or via a hydrophilic polymer on top of the silica particle or to a polymeric support, respectively. Yet, this is just a very basic and simplified arrangement of available column types. Each of these groups further offer many different modification chemistries, ligand structures, particle sizes and particle types which results in a continuous increase in available HILIC sorbents. Due to this complexity, excellent reviews have been published in the last years which I highly recommend to the reader for a more in-depth information on this topic [16,18-20,37,38]. Consequently, I will mainly discuss column types that were used during my studies which are primarily silica-based materials.

2.4.1 Bare silica

Underivatized silica has been used many years before HILIC was even known as a chromatographic methodology and as a term. It is a typical SP for NP-LC. Retention is based on the adsorption of polar analytes due to the existence of silanol groups and of a water layer on the sorbent's surface, while elution is enabled by the addition of a polar

organic modifier (e.g. ethanol, 2-propanol) in the nonpolar MP (usually hexan/heptane). In HILIC, the polar silanol groups attract water molecules which are adsorbed and form an aqueous layer. Moreover, the surface of unmodified silica can be ionized due to the acidity of the silanols which results not only in an enhanced surface polarity and higher water adsorption, but also in stronger ionic interaction sites which can either attract positively charged analytes or repulse acidic compounds. These hydrophilic moieties are results of the preparation process (condensation-polymerization of $\text{Si}(\text{OH})_4$) of spherical silica [39]. Fig. 8 illustrates the different types of silanol groups on the sorbent surface. Isolated or free silanol groups (Fig. 8a) are hardly involved in hydrogen-bonding to neighboring Si-OH groups due a sufficient spatial distance. Vicinal silanols (Fig. 8b) are two single or associated silanol groups which are in close proximity. The distance between the O and the OH is close enough to form a hydrogen bond. The last type of silanols are silanediol groups called geminal silanols (Fig. 8c). Thermal dehydration creates surface siloxanes (Fig. 8d) which can be rehydroxylated to silanol groups. According to Fyfe et al., the silanol type ratio in commercially available silica, determined by ^{29}Si cross polarization magic-angle nuclear magnetic resonance (CP/MAS NMR) spectroscopy, is 8.8 (siloxanes)/5.7 (single and vicinal)/1 (geminal) [40].

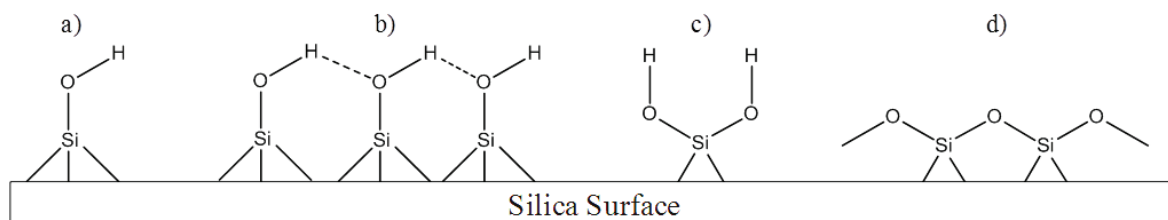


Fig. 8: Surface silanol groups on bare silica: a) single isolated silanol, b) vicinal hydrogen bonded silanol groups, c) geminal silanol groups and d) surface siloxane groups.

Rehydrolysis of siloxanes increases again the silanol group density. Silica gels for liquid chromatography are available in different grades of purity. Type A can be prepared by precipitation of silicate solutions [37,41]. These materials are rendered acidic due to a reasonable amount of metal impurities (mostly aluminum and iron) which activate silanol groups in close proximity. Hence, basic analytes are strongly retained, exhibit bad peak shape or are irreversibly adsorbed. However, Type A silica is not used anymore for modern HPLC columns. Type B silica is of high purity and prepared by the aggregation of silica sols in air [37]. Consequently, the amount of present metal ions and thus the acidity of the material are reduced. Hydride silica materials are now available as Type C silica. Around 95 % of the Si-OH groups are exchanged by Si-H. These materials are more hydrophobic

and used in aqueous normal-phase chromatography, which by consensus, is based on a different retention mechanism than HILIC.

A modification of Type B silica, ethylene bridge hybrid (BEH) silica for HILIC, has been developed and introduced by Waters and described by Grumbach *et al.* [42]. Two neighboring silanol groups are exchanged by an ethylene bridge (Fig. 9). As a result, nearly one third of all silanol groups are claimed to be removed. Furthermore, the ethylene bridged groups are embedded within the particle which enhances their chemical durability at elevated pH and temperature. The surface is more alkaline rendered and the retention and adsorption of basic analytes is reduced compared to Type A or Type B silica.

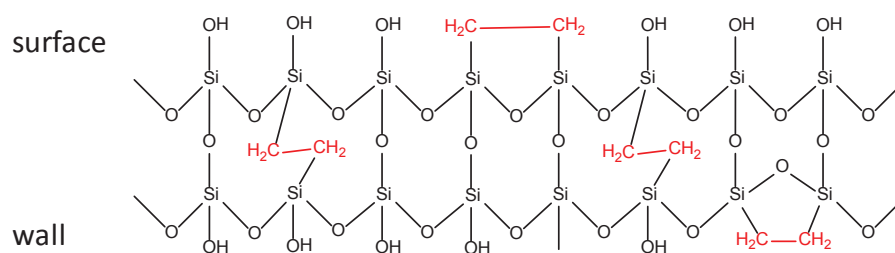


Fig. 9: Schematic representation of ethylene bridged hybrid silica (BEH) adapted from Grumbach *et al.* [42].

Unmodified silica columns are available from various suppliers and are either developed for NP-LC or directly for HILIC separations. They can show significant differences in purity and, thus, observed selectivity due to the use of either Type A or Type B silica [43,44]. Kromasil (EKA Chemicals), Betasil (Thermo Scientific), NUCLEODUR® SiOH (Macherey & Nagel), Atlantis HILIC (Waters) and Zorbax HILIC plus (Agilent) are just some examples of commercially available bare silica materials. The latter two columns were specifically developed for HILIC separations. Compared to bonded phases, naked silica columns may be advantageous in liquid chromatography-tandem mass spectrometry (LC-MS/MS) due to the lack of ligand bleeding which eventually results in a lower background noise.

Despite the disadvantage of the prominent strong adsorption of basic solutes, silica columns are still applied e.g. in the bio-analytical field [45,46] or the analysis of small polar compounds [47-49].

2.4.2 Amine type modified silica

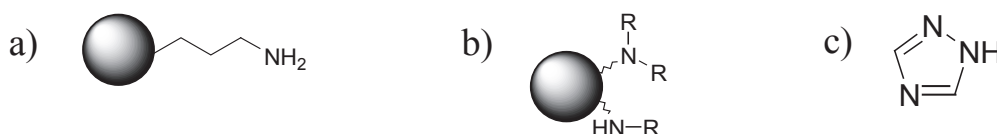


Fig. 10: Amine-type bonded silica phases a) aminopropyl-silica b) sec. and tert. amine-modified sorbent b) triazol bonded SP (exact immobilization strategy not revealed by the supplier).

Next to plain silica, aminopropyl silica (APS, see Fig. 10a) is one of the first used column types for HILIC separations and can be bought from many different suppliers. It goes way back to the origin of NP-LC and is still widely used, for instance for the separation of tetracyclines, carbohydrates, amino acids, carboxylic acids or biomarkers [50-55].

During our study we used home-made APS and Luna Amino (Phenomenex), but also YMC-PACK NH₂ (YMC, Kyoto Japan) or Zorbax NH₂ (Agilent) are examples for commercially available materials. A big drawback of interchanging amine type columns during method development is the significant difference in retention on varied columns [56]. Guo et al. suggest that this is due to different silica starting materials or the phase preparation process which may end up with an dissimilar amount of bound amino groups [18]. Finally, column bleeding during usage need also be considered as a variable of surface coverage with aminoalkyl groups (see also later).

APS can be produced for example via silylation of bare silica with (3-aminopropyl)trimethoxysilane (APTMS) in water-free toluene (Fig. 11).

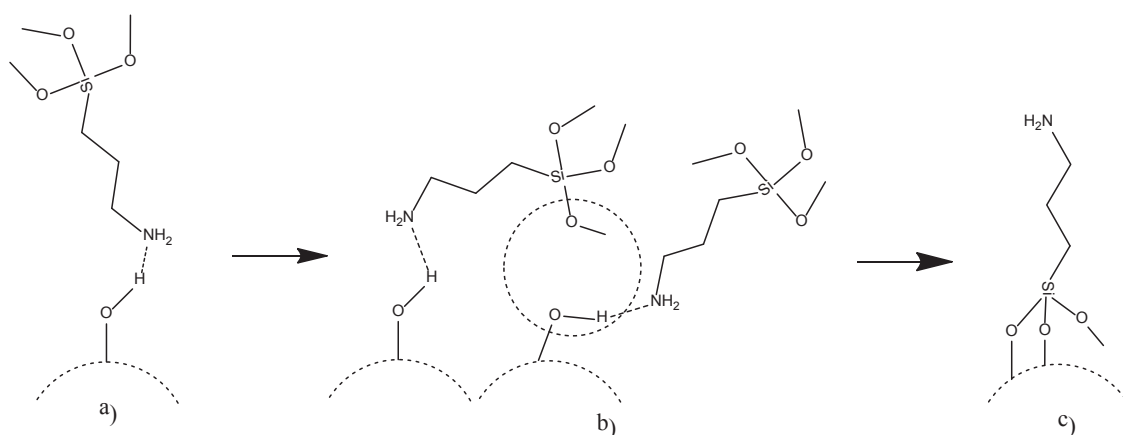


Fig. 11: Flip mechanism for the APS grafting in dry conditions a) physisorption, b) condensation c) main structure after curing. Adapted from reference [57].

During the physisorption process, aminosilane molecules are rapidly adsorbed by hydrogen bonding to the silanol groups on the silica surface (Fig. 11a). Subsequently, proton transfer may occur for some hydrogen bonded molecules. This process is reversible and is promoted by the presence of residual surface water. Moreover, during the loading or curing step, the formation of siloxane bonds is catalyzed by the hydrogen-bonded aminosilane (Fig. 11b). In other words, the aminosilane molecule “turns over” (the so called “flip mechanism”) from its initial amine-down position and points towards the pore center, while the alkyl chain is located between the free primary amino group and the siloxane bonded silicon atom on the support surface (Fig. 11c). However, this mechanism is only valid under fully dry conditions and may vary if other factors interfere [57].

A selectivity difference compared to silica can be exhibit due to the chargeable primary amino group and the quality may vary greatly among the different suppliers. Although they can be very powerful separation materials, drawbacks sometimes overshadow their usability. For example, the strong affinity towards acidic molecules can result in very long retention times with bad peak shapes. While the retention issue can be adjusted by an appropriate MP composition, the analyte adsorption may still be too strong and a signal loss will be observed. This effect is crucial as the surface of the material change while analytes start to adsorb and block the amino functionalities. Thus, a shift in retention time or a very long column equilibration is the result. However, the adsorption is not only limited to acids, since the highly reactive primary amino group could also form a Schiff base with an aldehyde or keto group of certain sugar molecules.

Another drawback of APS is the tendency to undergo autohydrolysis. The local basicity of the silica is enhanced by the close vicinity of the basic amino group. Even at low pH, deprotonated amine groups stimulate the hydrolysis of silica which usually occurs around pH 9. Residual silanols are deprotonated and form a zwitterionic species. The silicon atom is attacked by the free amine group via a S_N2 reaction, which causes the hydrolysis of the silica and bleeding of the ligand if water is present [58]. Since water is essential for HILIC, the stability of aminopropyl bonded silica is often low. Especially the hyphenation of HILIC with ESI-MS suffers from this high ligand bleeding due to an increase in background noise. A way to stabilize aminopropyl phases was introduced by Khaled et al. who blocked silanol groups with TiO_2 or ZrO_2 [58].

During my experimental work on APS, a way was found to stabilize the ligand by applying an additional base treatment, with an aqueous polar-organic sodium borohydride solution after the ligand formation step (**unpublished results**). The new, stabilized material, named s'APS, showed higher durability under aqueous conditions compared to common APS. Elemental analysis was used to estimate the remaining amount of nitrogen which correlates with the bound aminopropyl ligand (Fig. 12). Regular APS lost 62 % of its nitrogen content after an acidic wash of six hours. In comparison, the total loss of nitrogen on s'APS was only 18 % after a 20 hour basic stress (apparent pH ~ 10) with a subsequent six hour acidic stress (apparent pH ~ 2.8).

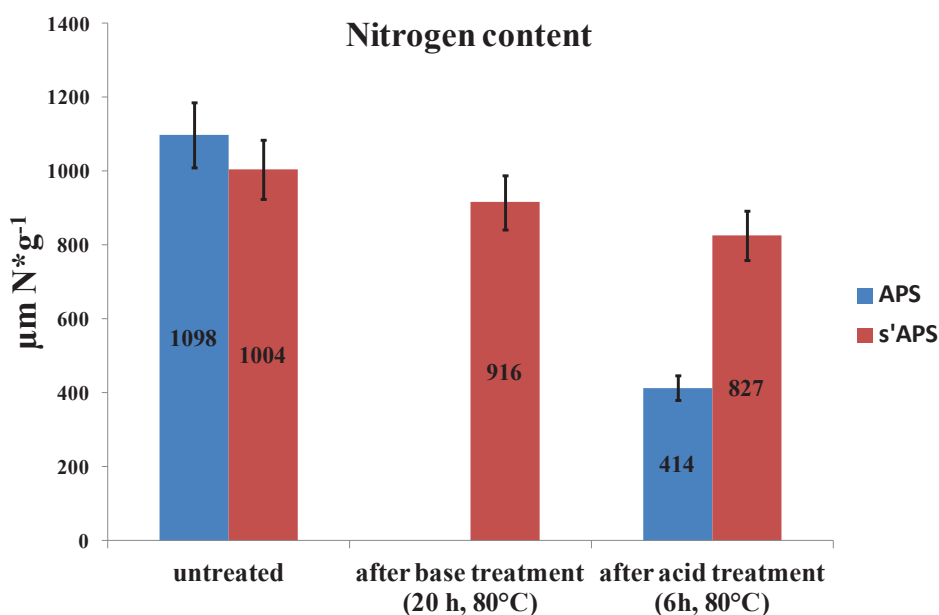


Fig. 12: Comparison of nitrogen content during the ligand immobilization and stress test.

NMR experiments were carried out to evaluate the obtained materials. The ¹³C spectra of s'APS and APS was in accordance with published ¹³C spectra for aminopropyl modified silica [59] and clearly confirmed the modification of the surface with trifunctional aminopropylsilane on both materials (data not shown). In addition, while considering ²⁹Si CP/MAS NMR spectra (Fig. 13), we found a clear decrease of the resonance at the chemical shift of $\delta = -58$ ppm (T^2) for s'APS as opposed to untreated APS, which corresponds to a reduction of bidentate bonded APTMS molecules to the silica surface. Consequently, almost solely tridentate or in other words completely cross-linked silyl species were found (T^3 , $\delta = -66$ ppm). This result could indicate that a condensation of the residual free methoxy group of the partially cross-linked silane species converts into a siloxane group; either with a neighboring partially cross linked silane molecule or with the silica surface (see schematical description of T^3 in Fig. 13). Thus, this interconversion indicates the stabilization process, and more cross-linked ligands are present.

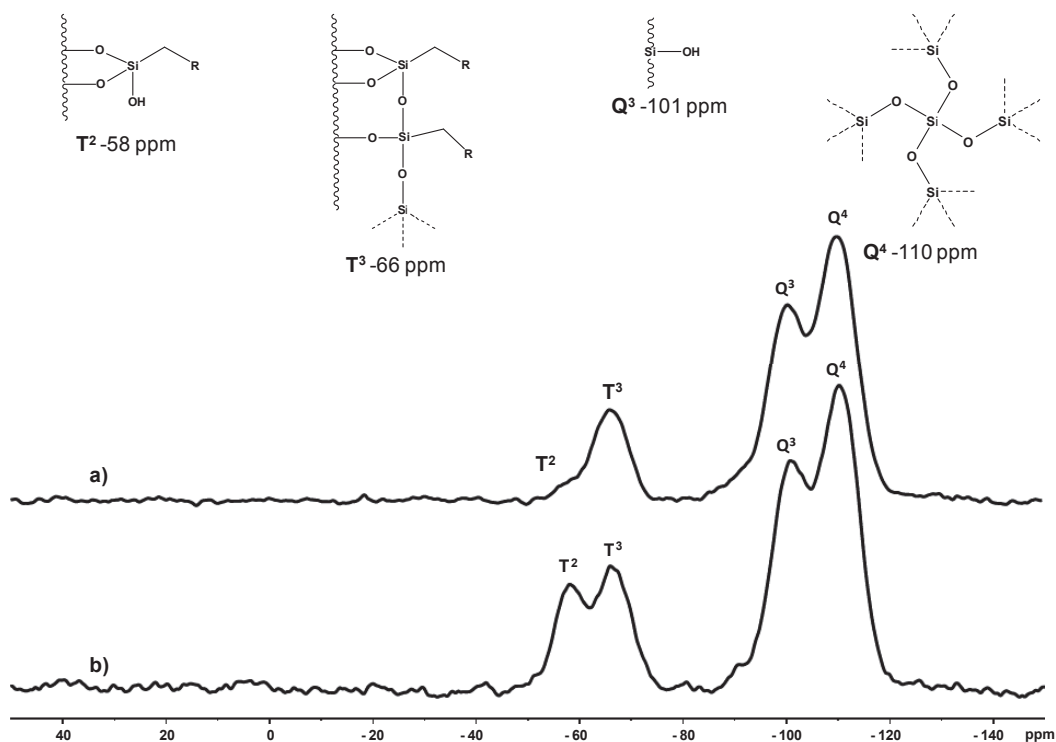


Fig. 13: ^{29}Si CP/MAS NMR of a) s'APS and b) APS. T^2 and T^3 correspond to the bidentate or tridentate bonded aminopropylsilyl ligand, respectively. Correspondingly, the surface free silanols and siloxanes are displayed by Q^3 and Q^4 .

In addition, the column bleeding was evaluated with ESI-MS. Columns were equilibrated for 30 minutes with a MP composed of ACN/ H_2O + 10 mM NH_4FA (pH 3). Subsequently, the effluent was analyzed by mass spectrometry in positive ion (scan) mode. Although both columns exhibit a certain degree of ligand bleeding, it was significantly decreased for s'APS compared to APS (Fig. 14).

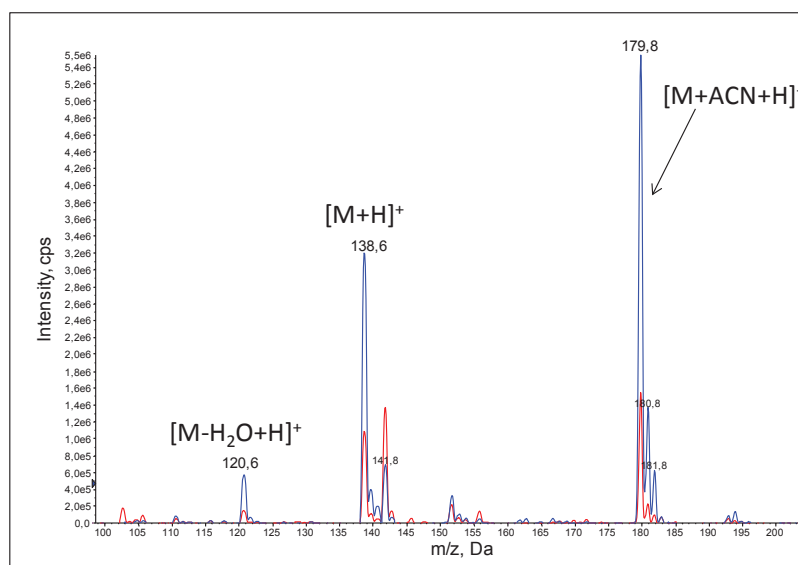


Fig. 14: Column bleeding study. The blue line represents untreated APS while the red line was achieved for s'APS.

Chemical as well as chromatographic evaluations showed a decreased reactivity of free (addressable) primary amino groups. For instance, the derivatization of APS and s'APS with epoxydodecane resulted in $575 \mu\text{mol}\cdot\text{g}^{-1}$ and $220 \mu\text{mol}\cdot\text{g}^{-1}$ dodecane motifs, respectively. This corresponds to 64 % derivatized primary amine groups on APS and only 26 % on s'APS.

Although the retention on the stabilized material was found to be lower compared to the untreated APS, the material still exhibits retention for various analytes (e.g. acids, bases, zwitterionic compounds) under HILIC conditions with similar selectivity to the unstabilized form (Fig. 15). The test set was analogous to test set 1-3 found in **Appendix I**.

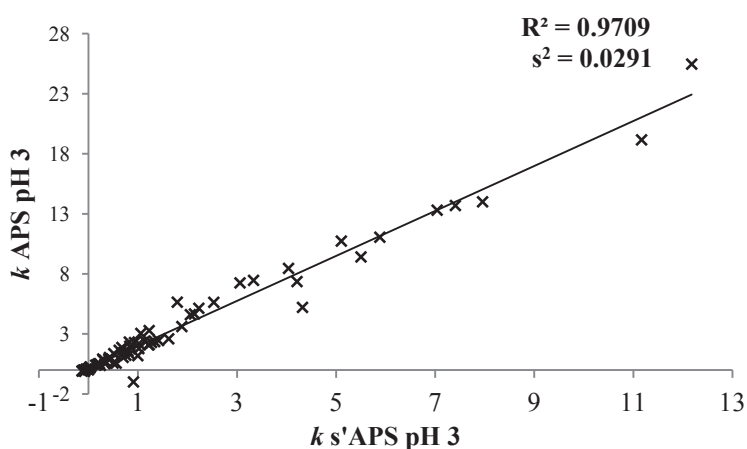


Fig. 15: Selectivity plot for APS and s'APS at pH3.

We further examined the new material in combination with carbohydrates, which is a typical application for amino-modified silica. Detection was achieved on a Corona charged aerosol detector (CAD). Elution order was equal on both packing materials. However, the selectivity suffered because of lower peak efficiency. Nevertheless, overall analyte retention and background noise was reduced for s'APS compared to APS. Both axes (time and picoampere) in Fig. 16 are in the same scale. The gained signal intensity and the better peak shape are two clear advantages of s'APS compared to APS and correspond to the reduced chemical activity of the primary amino groups.

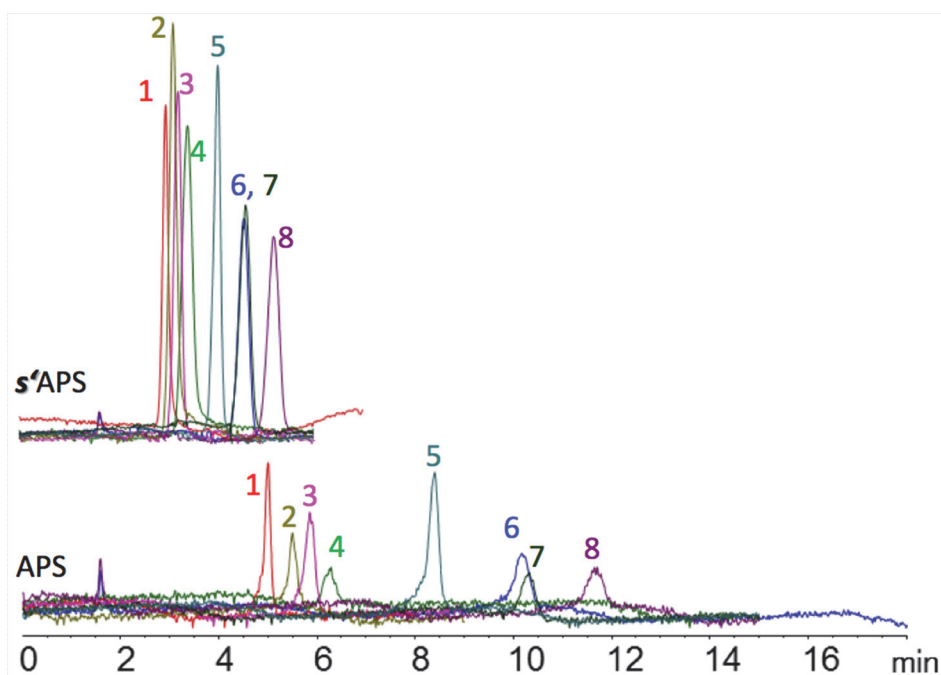


Fig. 16: Separation of mono- and di-saccharides on s'APS and APS. MP: ACN/H₂O (75/25; v/v); flow: 1.0 ml/min, inj.vol: 5 μ l; temp: 30°C. Peak annotation: D-fructose (1), D-mannose (2), D-glucose (3), D-galactose (4), sucrose (5), cellobiose (6), maltose (7), lactose (8).

Consequently, a way was found to overcome the two main disadvantages of standard APS, despite the fact that it is not yet fully clear if the additional basic treatment solely results in a formation of completely cross-linked aminopropylsilyl species which are responsible for the stabilization or if other structural variations occur. The reduced retention time and the efficiency loss display an inferior drawback. Longer packing cartridges, an optimized packing procedure or a smaller particle size can be used to overcome this limitation.

Although these results are quite promising, the clear structure for s'APS is still unknown. Thus, it will take further investigations until the proposed material treatment may be applied to industrial processes.

Another strategy to overcome the drawbacks of primary amino modified columns, was either to crosslink the primary amino ligands to obtain also secondary amino groups (former mentioned Luna NH₂) or the introduction of only secondary and tertiary amine groups (e.g. Cosmosil Sugar D) (Fig. 10b). The latter cannot form Schiff bases with carbonyl groups, which reduces the compound adsorption and results in higher signal intensities. Furthermore, they are less prone to autohydrolysis which results in a longer life time of the column.

Another more recent amine-related SP type are imidazol, triazol and tetrazol modified supports. These phases are silica-based and in terms of the tetrazole ligand, prepared by nitrile-modification applying a (3+2) azide-nitrile cycloaddition [60] (Fig. 17).

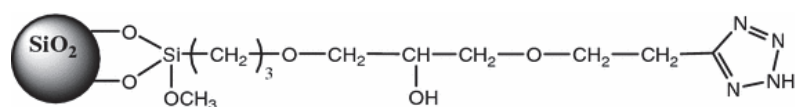


Fig. 17: The chemical structure of a tetrazol modified SP (Dai *et al.*, *Chromatographia* 2011, © Springer-Verlag; Reprinted with permission)[60].

Unfortunately, the exact immobilization strategy of the 1,2,4-triazol modified silica, which is commercially available as Cosmosil HILIC, has not been made public (Fig. 10c). The typical pH range of HILIC applications allows to positively charge the imidazol ring which enables electrostatic interactions and groups the triazol modified material as a basic to neutral column (**Appendix II+III**).

2.4.3 Silica based diol phases

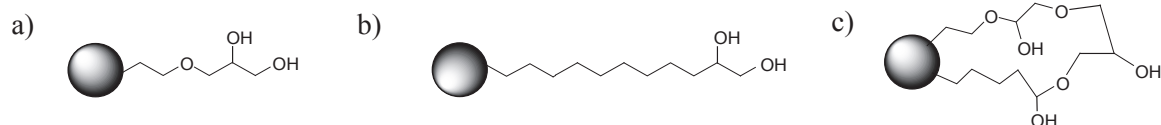


Fig. 18: a) Monomeric brush type diol phase b) undecyl-1,2-diol phase c) cross-linked diol phase.

The neutral bonded diol phases were originally developed to overcome the drawback of strong adsorption of basic analytes on bare silica. Two types of immobilization strategies are usually applied. The monomeric brush-type phases (Fig. 18a) are produced by bonding glycidoxypropyltrimethoxy silane to the silica surface and subsequently hydrolyzing the epoxy groups under acidic conditions [61]. These SPs are of neutral character and lack ionizable interaction sites except for potential residual silanol groups. Some commercialized diol phases can be purchased under the trade names NUCLEOSIL[®] OH (Macherey-Nagel), ProntoSil[®] Diol (Bischoff Chromatography), LiChrospher[®] 100 Diol (Merck) or Intersil[®] Diol (GL Sciences). The diol groups offer hydrogen bond acceptor and donor characteristics and are well solvated by water molecules. A similar polarity close to silica gel was proposed for these materials by the groups of Claessens and Abraham [62,63]. However, the aliphatic linker group adds a hydrophobic character which enables additional selectivity.

A mixed mode column was developed by Dionex and is available under the brand name Acclaim[®] Mixed-Mode HILIC-1. This SP is able to facilitate retention under RP-LC and HILIC conditions due to the exchange of the propyl linker with a C₁₁ chain to get an undecyl-1,2-diol ligand (Fig. 18b). Mechanistic studies show that this column exhibits strong ionic repulsion for acidic compounds under elevated pH (**Appendix II + III**). This pinpoints to a very limited ligand density with high amount of addressable silanol groups on the support surface.

Another type of a diol modified SP is known under the brand name Luna[®] HILIC (Fig. 18c). A polymer layer is formed which shields residual silanol groups by covalently cross-linking diol groups with an ether bridge. As a result, the phases are less affected by harsh conditions, thus, more stable under a broader pH range compared to monomeric diol phases. The “end-capping” of residual silanol groups with the diol-ether network disables to a significant extent the adsorption of basic analytes due to anionic interactions [64].

Separation targets can be the analysis of phenolic compounds, polar pharmaceutical ingredients, small molecular metabolites and even proteins [61,65-69]. Although the propyl anchor can introduce additional selectivity, these columns suffer often from low retention and the selectivity is also limited compared to newer developed phases. In terms of the previous mechanistic discussion, one may also speculate that the adsorbed water layer of the surface gets thinner. Thus, nowadays, amide-type SPs have displaced diol-type phases since they offer higher selectivity and longer retention (indication of a thicker water layer).



Fig. 19: The chemical structure of a) non-oxidized thioglycerol phase (TG) b) oxidized thioglycerol phase TGO (respectively SGO in Appendix II + III).

An additional type of nonionic polar SPs of the diol-type was introduced in 2008 by Lindner and co-workers [64]. These phases were obtained by anchoring either 2-mercaptoethanol or 1-thioglycerol using a radical immobilization strategy onto vinylised and end-capped silica particles. Furthermore, they introduced additional hydrophilicity by transforming the embedded sulphide group into a sulphoxide moiety via on-phase oxidation by means of excess of hydrogen peroxide in aqueous medium. The sorbents derived from 1-thioglycerol are displayed in Fig. 19. Evaluation with nucleosides and vitamins showed that these phases can be used either in RP-LC or HILIC mode. The polarity increases from the non-oxidized form to the oxidized and from 2-mercaptoethanol derived sorbents to 1-thioglycerol packing materials. A very interesting outcome is the reduction of hydrophilicity by exchanging the ether linking groups of the propyl-diol (Fig. 18a) with the sulphide group (Fig. 19a). A loss in retention and selectivity is observed. Wu et al. showed that the oxidized thioglycerol phase (Fig. 19b) obtains similar selectivity compared to the commercially available propyl diol phase and proposed this outcome to be due to the higher polarity of the oxidized sulphide group. However, they were not able to directly quantify this proposal. Undoubtedly, this assumption is true and was confirmed by the later described linear solvation energy relationship studies (LSER) (see section 2.5.1.) The enhanced hydrogen acceptor characteristic of these phases was quantified by a higher estimated *a* coefficient. (see Appendix II).

2.4.4 Silica based saccharide phases

Saccharide based SPs exhibit, similar to diol-bonded phases, OH groups which offer hydrogen bond acceptor and donor characteristics. Oligosaccharide derived phases of the Cyclodextrin (CD) type feature α 1-4 linked D-glucose units which are circular arranged. Depending on the number of linked monosaccharides they are grouped either as α (six), β (seven) or γ (seven) CD. The predominant domain of such SPs is chiral liquid chromatography due to the optically active sugar moieties which define a chiral cavity within the cone of the inner spatially shaped CD molecule. The interior of the CD ring is rather hydrophobic and allows less polar compounds to penetrate the inside of the toroid structure to form inclusion complexes. Moreover, polar analytes can interact with the hydroxyl groups which are located on the outside of the CD. This high degree of hydrophilicity allows water molecules to accumulate and form a water layer by hydrogen bonding which facilitates a HILIC-type retention mechanism. Separations of nucleosides, phosphorylated carbohydrates or sugar alcohols are some examples of possible applications. Risley et al. used a CD-derivatized SP for chiral separations of polar compounds under HILIC-type separation conditions [70]. As the supported water layer (SWL) of this SP is not chiral, it is again a clear indication that in case of enantiomer separations analyte adsorption phenomena must be dominantly in place besides partitioning processes in HILIC-type columns. A native β -CD SP was prepared by Guo et al. who used Huisgen [3+2] dipolar cycloaddition to immobilize the β -CD on azide-activated silica. The column exhibited hydrophilic partitioning as well as ion exchange and electrostatic repulsive interactions. Good selectivity and retention were achieved for polar analytes such as nucleosides and oligosaccharides. Furthermore, chiral separation of ibuprofen was obtained under typical HILIC-type elution conditions [71].

The group of Daniel Armstrong developed a fructan derived oligosaccharide-type phase, by covalently bonding isopropyl-carbamate functionalized cyclofructan6 to a silica support. These can be used for the separation of polar analytes e.g. nucleic acid compounds, xanthenes, salicylic acid derivatives, β -blockers or maltooligosaccharides [72]. Compared to CD-derivatized SPs, native cyclofructan6 based SPs have only limited capabilities as chiral selectors [73]. In addition, Armstrong and coworkers introduced a sulfonated cyclofructan6 based SP which offers additional electrostatic repulsive and attractive interactions, and thus, provides superior selectivity and retention for the

β -blockers compared to native cyclodextrin columns. However, acidic analytes may not retain well on sulfonated cyclodextrin SPs under certain MP conditions [74].

In another attempt, APS was modified with mono- or disaccharides by creating a carbamoyl group between the primary amine and the carboxy group of the saccharides and was published by the group of L. M. Yuan [75,76]. The sugar moieties kept their optical activity and were able to separate D and L amino acids under NP-LC conditions.

Moni et. al. created a sugar-based SP by immobilizing C-galactoside and propargyl O-lactoside via copper-catalyzed azide-alkyne cycloaddition on azido-activated silica. The materials showed good retention and selectivity for carbohydrates, amino acids and flavones. Furthermore, the materials were able to achieve a full separation of sugar anomers. Similarly, Huang et al. applied copper-catalyzed azide-type click chemistry to bind N₃-glycosyl-D-phenylglycine to alkyne modified silica [77]. Polar organic acids, bases and nucleosides were used as test samples and could be separated by a MP composition of ACN and water without the addition of buffer salt.

During my experimental work I was able to develop a different methodology to immobilize reducing sugars on APS by applying non-enzymatic browning. The results have been released in the following publication: G. Schuster, W. Lindner, Journal of Analytical and Bioanalytical Chemistry, 2011, 400, 2539-2554 (for the full article see **Appendix I**). The schematic reaction cascade is displayed in Fig. 20.

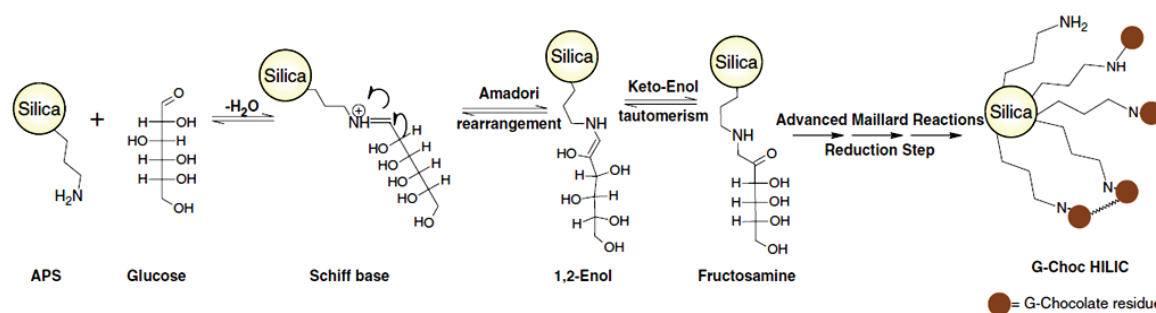


Fig. 20: Reaction scheme for glucose-based Chocolate HILIC Phases. (Schuster G., Lindner W., Anal Bioanal Chem 2011, © Springer-Verlag; Reprinted with permission)[78].

The use of water-free medium at elevated temperature facilitated a reaction cascade based on the Maillard reaction. This methodology was new since it does not only rely on a simple formation of a carbamoyl bond or on azide click chemistry. As a result, I obtained a deeply brown ligand that released a sweet sugary to pastry-like odor during the manufacturing process. The immobilization method was different from the former mentioned saccharide

immobilization as the sugars were decomposed to a certain degree and lost their potential enantioselectivity. However, the reaction scheme was found to be easily applied, cheap in the production process and highly reproducible. Chromatographic evaluation with bases, acids, nucleosides and vitamins showed that this material exhibits WAX moieties due to residual aminopropyl groups. An enhanced selectivity for purine-based compounds was found compared to diol bonded phases. The long term evaluation under isocratic conditions showed that these phases are very stable and obtain reproducible retention times. Moreover, it is possible to separate lipophilic compounds with a highly aqueous MP. Therefore, a mixed-modal character is introduced due to the decomposed sugar molecules and the formed Maillard product. The most lipophilic “chocolate” ligand was obtained with glucose as monosaccharide primer. Generally, it was found that the lipophilicity and RP applicability of Chocolate HILIC columns is between the cross linked Luna HILIC phase and the XBridge Amide. The later realized LSER study (**Appendix II + III**) arranged the cellobiose (disaccharide) derived Chocolate HILIC column between the Cosmosil HILIC and Diol phases. This indirectly affirmed our speculations of forming aza heterocycles in the course of the Maillard reaction next to diol groups within the ligand. However, due to the complexity of the on-phase Maillard chemistry, we were not able to directly confirm this speculation.

The chromatographic stability of Chocolate HILIC phases was further investigated under gradient elution conditions (unpublished results).

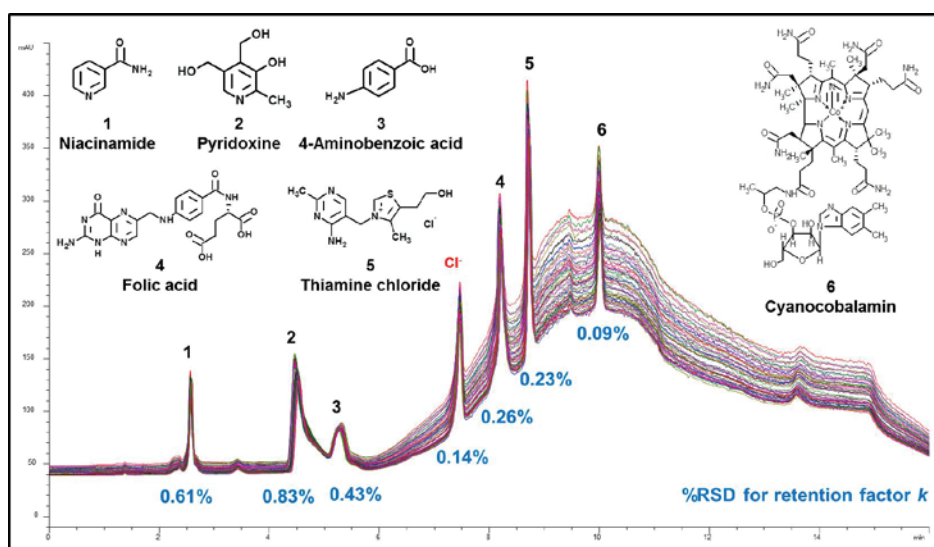


Fig. 21: Evaluation of the separation reproducibility for 50 injections of a vitamin mix with a 17 min HILIC gradient. flow: 1.0 ml/min, inj.vol: 5 μ l, temp: 20°C; MP-A: ACN + 10 mM NH₄AcOH, MP-B: H₂O + 10mM NH₄AcOH, time table: min 0.0 (90%B) → min 2.5 (90%B) → min 10.0 (50 %B) → min 13.0 (50% B) → min 17.0 (90%B).

A test mix consisting of 6 vitamins was analyzed using a 17 min HILIC gradient. The stability was evaluated by calculating the %RSD for the retention factor k of all analytes of 50 consecutive injections. Thereby, the column showed a fast re-equilibration towards the starting conditions and a low %RSD of < 1 (Fig. 21), which may be the result of a fast and reproducible readjustment of the stagnant water layer and a retention mechanism highly based on adsorptive interactions.

2.4.5 Amide type modified silica

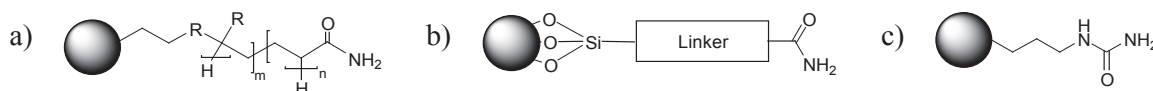


Fig. 22: Amide bonded SPs. a) TSKgel Amide-80 b) BEH Amide c) propyl urea modified silica.

Amide-modified SPs are one of the most commonly used, so-called “neutral” HILIC sorbents. They have started to displace diol-bonded SPs due to generally longer analyte retention times and superior selectivity. The lower chemical reactivity compared to amine-modified sorbents and lower susceptibility to MP pH changes make them ideal for carbohydrate analysis. In particular, the absence of Schiff base formation and reduced irreversible analyte adsorption results in improved long-term stability [79,80]. Moreover, they show less ligand bleeding which makes them superior to amino silica in combination with ESI-MS. Nevertheless, depending on the preparation strategy, ionic interactions may still take place due to accessible residual silanol groups, which is often observed for TSKgel Amide-80 (Tosoh) (Fig. 22a). This SP features carbamoyl groups which are covalently bound to the silica surface by a short aliphatic linker. Many publications can be found using this very popular HILIC phase. Applications range for example from the analysis of saccharides and glycosides to peptides, amino acids and even of a paralytic shellfish poison (PSP)-toxin [81-85].

Another type of amide bonded phase is supplied by Waters with the brand name XBridge Amide. In contrast to TSKgel Amide-80, the base material is not Type B silica but ethylene bridged hybrid (BEH) silica (see section 2.4.1). Although the exact bond

chemistry is not revealed by the supplier they specify the column modification as trifunctional amide. BEH silica is stated to contain a controlled number of less residual (acidic) silanol groups. Consequently, the SP offers higher stability over a broad pH range combined with a high peak efficiency. When comparing XBridge Amide and Luna HILIC under highly aqueous RP-LC like conditions (**Appendix I**), the column was able to retain and separate toluene, ethylbenzene, butylbenzene, pentylbenzene and trans-stilbene oxide to a higher magnitude than the cross-linked diol type. This indicates on the one hand the lower hydrophilicity of Type C to Type B silica but more importantly the considerably higher hydrophobicity and addressability of the anchor group. The area of application is similar to the aforementioned TSKgel Amide-80 column [86-88].

In addition to carbamoyl and amide-bonded silica phases, Bicker et al. carried out a study on the retention and selectivity effects of different ligand densities of polar urea-modified packing materials. They modified silica particles with 1-[3-(trimethoxysilyl)propyl] urea as chromatographic ligand (Fig. 22c). Evaluation was carried out with small basic, acidic, amphoteric and non-charged compounds. Retention was achieved for all analytes screened and the mechanism resembled the mixed-modal character of typical HILIC separations.

Unisol Amide (Agela Technology) is another commercially available HILIC column that is claimed to feature amide moieties. However, no clear statement on the structure or on the immobilization chemistry is given by the supplier. Results from Bicker et al. but also from my studies revealed that most likely urea functional groups are present on the surface of the Unisol Amide material since the retention interaction forces (**Appendix II + III**) and the selectivity are quite similar to the highly loaded ($3.67 \mu\text{mol}\cdot\text{m}^{-2}$) urea phase.

Alpert himself developed another type of amide-containing SPs which are based on poly(succinimide)-silica. At first he created a poly(succinimide) network covalently attached to APS. This was further modified by means of either alkaline hydrolysis, reaction with ethanolamine or with 2-aminoethylsulfonic acid. In the end, he obtained four poly(succinimide)-silica based materials which are available under the brand name PolyGlycoplexTM, PolyCAT ATM, PolyHydroxyethyl ATM, and PolySulfoethyl ATM and are supplied by PolyLC Inc. The latter two phases (Fig. 23) were used in Alper's first paper on HILIC and were found to be suitable for the separation of carbohydrates, glycosides, oligosaccharides, polar peptides and proteins [1,32,44,89-91].

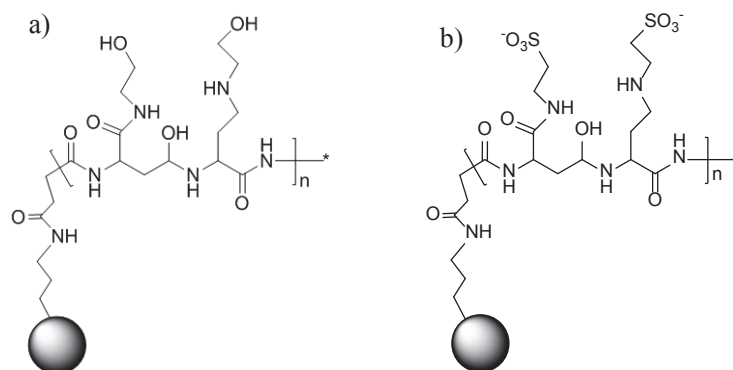


Fig. 23: The chemical structure of poly(succinimide) silica derived HILIC-type SPs a) PolyHydroxyethyl ATM b) PolyPolysulfoethyl ATM.

The HILIC system of PolySulfoethyl ATM (Fig. 23b) exhibits high hydrogen bond donor characteristics (**Appendix III**) and a strong anion exchange property. The retention mechanism consists of partition phenomena and the sorbent enables a high amount of water to penetrate the polymeric network. However, acids may be repelled due to the negatively charged sulfonic acid group (low d' coefficient, see **Appendix III**).

2.4.6 Silica based zwitterionic type phases

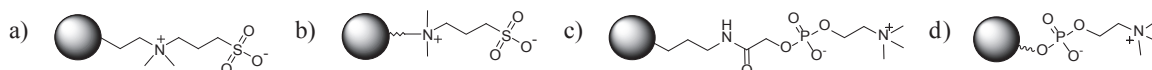


Fig. 24: Zwitterionic modified HILIC sorbents a) monomeric sulfobetain-type (Nucleodur[®] HILIC) b) polysulfobetain-type (ZIC[®] HILIC c) monomeric phosphorylcholin-type (PC HILIC) d) polyphosphorylcholin-type (ZIC[®] cHILIC).

A very popular group of HILIC columns consists of zwitterionic modified SPs, either monomeric immobilized on silica, immobilized via a polymeric structure on silica or on fully polymeric support. The group of Knut Irgum used wide-pore silica and introduced 3-sulfopropyltrimethylammonium inner salt moieties in the form of a grafted polymeric layer [92]. The SPs exhibit an intrinsic charge of zero due to the equal distribution of sulfonic acid to quaternary ammonium groups. High hydrophilicity and the ability to uptake a high amount of water is one of the advantages of these phases which are available under the brand name ZIC[®]-HILIC and ZIC[®]-pHILIC (for the full polymeric

support) (Merck SeQuant[®]). Although originally invented for the separation of small ionic compounds, inorganic salts and proteins, they were found to offer good retention and selectivity under HILIC elution conditions. Separation targets involve for example peptides, proteins, small organic compounds, pharmaceuticals and various other compounds [19,46,93-101]. The reaction mechanism involves partition, but also ionic interactions due to the charged functional groups. Basic and acidic analytes are drawn towards the interaction surface due to partition phenomena. However, the phase exhibits stronger acidic character under electrostatically driven conditions (low amount of water, low amount of buffer counter ions) due to the sulfonic acid groups which are directed towards the bulk MP. In analogy to the ZIC[®]-HILIC phase, Macherey-Nagel developed a monomeric brush-type sulfobetain phase which is distributed under the trademark Nucleodur[®] HILIC. Although selectivity is quite similar, both phases may not be directly interchangeable [11]. More precisely, we found that Nucleodur[®] HILIC is slightly more acidic (**Appendix II + III**), which could be either due to the monomeric ligand on which analytes may be able to better form ionic interactions. On the other hand, residual silanol groups, which are present on almost all brush-type modified silica materials, may add up to the overall acidity of this phase. Furthermore, mass transfer seems to be enhanced on the monomeric zwitterionic phase, which is reflected in higher plate numbers of the columns.

In addition to the sulfobetain-type zwitterionic columns, phosphorylcholin-type residues immobilized onto silica materials are available nowadays. Again, a monomeric and a polymeric form can be obtained from either Shiseido under the brand name PC-HILIC (Fig. 24c, structure adapted from reference [102]) or from Merck SeQuant[®] under the trademark ZIC[®]-cHILIC (Fig. 24d). Although the selectivity of PC-HILIC is quite similar to Nucleodur[®] HILIC, a somewhat different distribution of the retention interactions motifs was obtained while consulting LSER models. Namely, the ionic interaction was much more pronounced on the phosphorylcholin (PC-HILIC) than on the monomeric sulfobetain phase (Nucleodur[®] HILIC). As mentioned before, the group of Knut Irgum published a ²H NMR study in which they investigated the amount of non-freezable water on SPs [26]. The polyphosphorylcholin-based phases showed significant differences to the polysulfobetain-type. Most probably the phosphoric acid moiety is too bulky to self-assemble easily and thus the formation of a neutral inner salt is reduced. Despite the fact that the phosphoric acid group is adjusted between the silica and the quaternary amine group, its influence on the mechanism is still overpowering the positively charged amine function which is oriented away from the surface towards the center of the pores.

2.5 Characterization strategies of HILIC columns

Hemström et al. used model equations which are originally based on RP-LC and NP-LC to investigate the retention mechanism in HILIC [19]. In RP-LC, retention is considered to be mainly controlled by partition and the distribution coefficient between the more lipophilic SP and the more polar MP depends on whether the analyte is better “dissolved” in the hydrophobic ligand or the MP. The retention, by a partition-like mechanism is explained by the empirical equation Eq. (1).

$$\text{Eq. (1)} \quad \log k = \log k_w - S \varphi$$

The concentration (volume fraction or mole fraction) of the stronger eluent of a binary MP system is displayed by φ , k_w is the theoretical retention factor when the MP consists only of the strong eluent and S is the slope of $\log k$ versus φ in a linear regression model.

In analogy, adsorption chromatography, or in other words NP-LC, can be described by the Snyder-Soczewinski equation (Eq. (2)) which illustrates the relationship between the concentration (mole fraction N_B) of the stronger eluent B and the analytes retention:

$$\text{Eq. (2)} \quad \log k = \log k_B - \frac{A_S}{n_B} \log N_B$$

where A_S and n_B are the cross-sectional areas occupied by the solute molecule on the adsorption surface and the B molecules, respectively. The retention factor of the analytes, if the eluent consists only of the strong eluent B, is expressed by k_B . The mole fraction of the stronger component B in the MP is described by N_B .

As a result, the linear fit of either a plot of $\log k$ versus the mole fraction of water or versus the logarithm of the mole fraction should indicate if partition or adsorption is the predominant mechanism in HILIC.

Hemström used $\log k$ values from several publications and constructed these plots [19]. However, the obtained results could not be used to draw a clear conclusion on the actual mechanism and pinpointed more towards a mixed modal character of the HILIC retention mechanism. In 2010, McCalley used this methodology to investigate the retention mechanism on several HILIC columns [7]. His experimental design had the advantage that all retention data were produced on one instrument and the more correct mole fraction of

water was used instead of the volume fraction. Yet again the obtained plots were inconclusive. He suggested that these plots should not be used for the determination of the retention mechanism, but they can be very useful to visualize selectivity changes as a function of the MP composition. An example of these rather inconclusive plots to determine the retention mechanism is exemplified in Fig. 25.

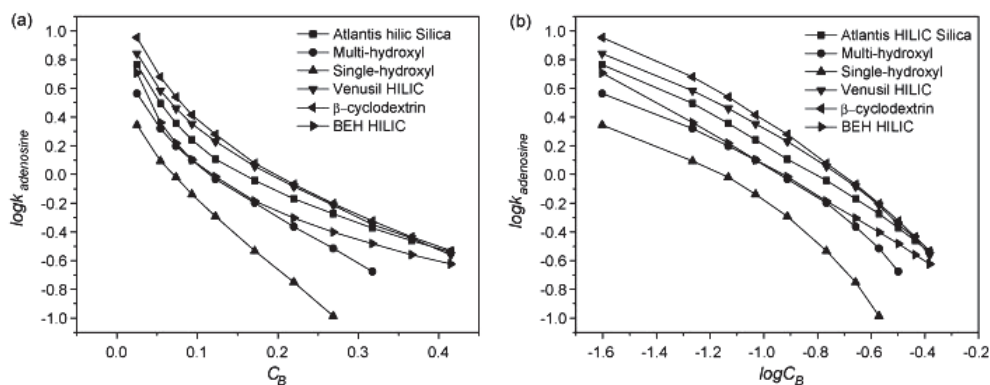


Fig. 25: Linear (a) and logarithmic (b) plots of $\log k$ vs. volume fraction of water in the MP for adenosine on (■) Atlantis HILIC silica column, (●) multi-hydroxyl column, (▲) single-hydroxyl column, (▼) Venusil HILIC column, (◄) β -cyclodextrin column and (►) BEH HILIC column. (Jin G. *et al.*, *Talanta* 2008, © Elsevier; Reprinted with permission) [103].

One drawback of this characterization method is that the obtained plots more or less only reflect the behavior of single compounds. Furthermore, it is very difficult to arrange available HILIC columns into groups of similar behavior with this method. Albeit the recommendation that these plots are rather inconclusive a lot of publications still use these adsorption and partition equations to evaluate newly developed materials (e.g.[55,69,104-106])

Due to the overall acceptance of the multimodal mechanism of HILIC, the main focus lays now more on the characterization and assimilation of available HILIC columns, to enlighten which types are rather orthogonal and lead to a different chromatographic selectivity if exchanged during method development.

One way is to analyze a sufficient set of test solutes on different columns and create selectivity plots. In other words, the retention factors k for each compound at two different conditions (different SP) are plotted against each other (e.g. Fig. 15). The obtained linear regression coefficient (r^2), which is obtained by fitting a linear trend line, displays the degree of similarity between these two columns. By this, not only the effect of different columns but also of different elution condition on the HILIC system can be evaluated.

Another way to compare the obtained results is by using the selectivity difference values which can be calculated according to Eq. (3).

$$\text{Eq. (3)} \quad s^2 = 1 - r^2$$

An s^2 value of 1 indicates complete orthogonality of the two compared conditions, while a value of 0 indicates that the probed conditions have no influence on selectivity. This method has been used by Neue et al. to investigate the separation performance of different packing materials and MPs under RP conditions [107-109]. A study which is based on selectivity plots was recently released by the group of David McCalley. They investigated factors that affect the selectivity in HILIC (e.g. pH, buffer type and concentration, temperature) [12]. Additional examples of selectivity plots used during column characterization can be found in references [8,9,29,110].

Kawachi et al. characterized fourteen commercially available HILIC SPs with derivatives of nucleosides, phenyl glucosides, xanthenes, sodium *p*-toluenesulfonate and trimethylphenylammonium chloride [5]. They evaluated the grade of hydrophilicity, the selectivity for hydrophilic-hydrophobic substituents, the molecular shape selectivity as well as electrostatic interactions and the acidic-basic nature of the HILIC material. Selectivity values α were calculated for solute pairs of interest. Radar-shaped diagrams were created to summarize partial structural differences. Concordances between diagrams indicate similar retention behavior of the corresponding columns.

Principal component analysis (PCA) and hierarchical cluster analysis (HCA) are two structure finding statistical approaches which are often used for the characterization and evaluation of HILIC columns. HCA of raw retention data or selectivity values can cluster SPs into similar groups. The big advantage is that no information on possible mechanistic relationships is needed in advance. Consequently, the structure-finding algorithm of HCA can find latent relationships that may be hard to estimate due to the vast number of data. The result is represented by a vertical or horizontal tree diagrams (e.g. **Appendix II** Fig 5). References [8,13,14] are examples of HCA related publications.

A more powerful multivariate statistical method is PCA. Observations which may have a certain degree of correlation are orthogonally transformed to obtain linearly uncorrelated variables named principle components (PC). The number of mathematically acquired PCs can be less or equal to the number of originally inserted variables. They can be e.g.

retention data, selectivity values, resolution factors or any descriptors that are thought to explain a given system which in our case is a chromatographic system.

The orthogonal transformation is defined that the largest possible variance of the data matrix is associated to the first PC obtained. In that manner, every following component has in turn the largest variance possible with the prerequisite that it is orthogonal to the previous components. In other words, the information of the analytes' screening data can be analyzed by PCA to obtain two or more PCs. By plotting two components, columns may be grouped in an x/y diagram in which e.g. the first PC may represent the polarity of the SP followed by the second PC which displays e.g. ionic interactions. Lämmerhofer et al. used PCA to evaluate various RP/WAX and polar columns under HILIC conditions and subsequently found groups of comparable SPs [110]. Irgum and co-workers surveyed the interaction mode in HILIC by means of shape selectivity, hydrophilic, hydrophobic, hydrogen-bonding, dipole-dipole, electrostatic and $\pi - \pi$ interactions. At first, specific analytes were associated with the aforementioned interactions. In addition, separation factors were calculated from pairs of similar substances and used as data matrix for a subsequent PCA evaluation [6]. Chirita et al. used PCA to investigate appropriate columns for the analysis of neurotransmitters [111]. Relevant parameters for method development in ultra-high performance HILIC were screened under gradient elution conditions by Periat et al. [14]. The column set contained unmodified silica, hybrid silica, diol-, amide- and zwitterionic-modified columns. 82 pharmaceutical compounds of diverse polarity were analyzed by variations in MP pH, buffer ionic strength and amount of organic modifier. PCA and HCA were used to group and represent changes in similarity between the column systems.

2.5.1 Evaluation of HILIC systems by linear solvation energy relationships

Linear solvation energy relationship (LSER) is opposed to PCA or HCA a exploratory structure detection approach. The statistical setup requires predefined descriptors (independent variables) which are considered to explain a certain condition (dependent variable). To put it more simply, in terms of chromatography, specific characteristics of analytes are displayed by descriptors. These values are the independent variables since the analytes do not change. The dependent variable is the achieved retention factor of the analyte. The multivariate regression calculates system constants which can be attributed to the magnitude of difference for the particular property between the MP and the SP. Thus the LSER approach can give detailed descriptions of the influence and extent of different molecular interactions which take place between the analytes and the chromatographic system. These specific interactions which facilitate retention can be explained by Eq. (4).

$$\text{Eq. (4)} \quad \log k = c + eE + sS + aA + bB + vV$$

Solute descriptors are represented by capital letters while the complementary effect on these interactions by the SP is explained by the lower case letters, namely the system constants. E is the excess molar refraction which models the polarizability contributions of n and π electrons. Solute dipolarity/polarizability is described by S while the hydrogen bond acidity and basicity are A and B, respectively. The molar volume of a molecule is associated to the McGowan characteristic volume in units of $\text{cm}^3 \cdot \text{mol}^{-1} / 100$, and represented by the V term. The system constants (e, s, a, b, v) reflect whether the analyte prefer the interaction with the SP (positive constants) or the MP (negative constants). For more in-depth information on the history and methodology of solvation parameter models I would like to refer the readers to **Appendix II** or references [11,112].

For a long time, LSER has been used to describe retention in RP-LC. However, the methodology is scarcely applied for the characterization of HILIC systems. Jandera et al. used LSER to investigated effects of MP composition on the retention of flavonic antioxidants and phenolic acids on five polar SPs [31]. The investigated columns showed a dual HILIC-RP retention mechanism while the composition of the MP affected more the selectivity in HILIC than in RP. Chirita et al. investigated the retention mechanism of zwitterionic modified SP. The evaluation set consisted of 75 small molecules which are relevant to pharmaceutical and biomedical studies. They expanded Eq. (4) by two

additional descriptors (D^- and D^+) to characterize the contribution of coulomb interactions to the retention of ionizable compounds. The obtained equation (Eq. (5)) was found to yield a better goodness of fit in terms of R^2_{adj} and enabled prediction of solute retention. The equations for calculating the D descriptors can be obtained from **Appendix II + III** or reference [11].

$$\text{Eq. (5)} \quad \log k = c + eE + sS + aA + bB + vV + d^-D^- + d^+D^+$$

The working group of Claire Elfakir used an eluent of ACN/H₂O (80/20; v/v) with 20 mM NH₄AcOH to down-regulate potential secondary strong electrostatic or adsorptive interactions and mainly screen the HILIC system under a predominant partition driven mechanism. This study made me think and the question arose: Is it also possible to use LSER during column development and to screen the background of the newly synthesized SPs by deliberately increasing the amount of organic modifier and further reduce the amount of buffer counter-ions to enhance possible electrostatic interactions or in other words make them more visible. Under these circumstances, the obtained system constants should more closely reflect the influence of the SPs background in terms of its charge state and of adsorptive interactions. This information can be of demanding interest since e.g. on phase chemistry is not always straightforward and the characterization of ligands obtained by this synthesis route can be very difficult. Thus, it is important to use every available evaluation method to fully understand the obtained material. With that in mind, the modified equation of Elfakirs group was used to investigate the retention interactions of 23 different HILIC columns and systems, respectively.

In the following section, I want to shortly recapitulate the studies which have been released in the following publications: G. Schuster, W. Lindner, *Journal of Chromatography A*, 2013, 1273, 73-94; (for the full article see **Appendix II**) and G. Schuster, W. Lindner, (submitted manuscript, under review; for the full article see **Appendix III**).

HILIC-type SPs of neutral, acidic, basic and zwitterionic character were compared under HILIC conditions. Retention models based on a LSER approach were generated with prior acquired retention data of 68 differently structured test solutes. Indeed, the new constructed solute D descriptors were found to represent adequately the coulomb interactions within the screened HILIC systems. Moreover, the method proved to be a valuable and very helpful tool during column development. The solvation parameter model was able to dismiss or affirm the preceding heuristic on which predominant mechanistic interactions

will take place under HILIC conditions or how certain immobilized ligands will behave. This was for example displayed for our in-house produced sulfobetain modified column which was found to belong to the group of basic SPs instead of zwitterionic neutral columns (see **Appendix II**). However, the introduction of the sulfonic acid group was able to counterbalance the repulsion of basic solutes on this column which was expressed by a more equal d^- to d^+ distribution compared to unmodified APS. The amido-aminophosphonate modified SPs (developed by the group member Andrea Gargano, manuscript is in process) which were originally developed as neutral rendered zwitterionic SPs. However, both columns were found to operate under a predominant cation-exchange mechanism and some hydrogen-bond interactions for neutral sorbents. Chocolate HILIC (section 2.4.4) could be arranged between the triazol-modified and diol-modified columns. It confirmed our expectations that next to diol groups also aza-heterocycles are formed due to the reaction cascade of the non-enzymatic browning (Maillard reaction). In the same way, we were able to show that the addition of a hydrogen bond donor group is able to compensate repulsive effects on acidic columns (see **Appendix II**). This was expressed by a higher b coefficient on the strong acidic sulfonic acid modified column compared to bare silica or Acclaim Mixed Mode HILIC 1.

Although our achieved solvation models experienced a lower goodness of fit compared to the two previous publications on LSER in HILIC, I think that this is due to the mixed modal character of the mechanism under the chosen conditions. Despite the lower R^2_{adj} , prediction was still possible to a certain degree which is one of the big advantages, compared to HCA or PCA as column classification methods. A drawback however is the lack of information on column performance in terms of selectivity, efficiency or stability.

The first LSER study (**Appendix II**) confirmed to be a valuable tool for the characterization of different HILIC columns even under enhanced electrostatic interaction conditions. In a follow-up study I tried to examine a mechanistic change in the HILIC system when the ^wpH of the MP is elevated from 3 to 5 and the NH_4FA buffer is exchanged with NH_4AcOH buffer (see **Appendix III**). The first result was quite unexpected since the obtained adjusted multiple correlation coefficient (R^2_{adj}) was quite low when acidic, basic and neutral compounds were inserted altogether into the multivariate algorithm. It is attributed that this is due the change of the ionization degree of acidic analytes and the SP. Consequently, I performed a fragmented LSER modeling which

consisted on the one side of acids and neutral analytes and on the other side of bases and neutrals.

The goodness of fit of the individual equations was found to be comparable to the previous study under pH 3. Additionally, a combined mean equation was formed to display the general change in interaction forces. This mean model was further evaluated by using a validation set to predict retention factors (**Appendix III**, Supplement, Fig. S2 - S6). The comparison of the experimental versus the computed retention data showed that not all interactions are adequately displayed since the estimated values were generally higher than the experimental ones. Especially interactions those are more favorable between the analyte and the MP. This is most likely due to the high correlation of the S and B descriptors in the test set of mainly aromatic UV-active compounds which define the ability of solutes to form dipole-dipole interactions and the hydrogen bond acceptor probability. Still, the results were in good agreement with publications from other working groups who used PCA, HCA or selectivity plots to evaluate different packing materials [6,12,111]. In particular the predictive character of LSER is a big advantage and is considered superior to other characterization methods.

To conclude at this point, it is to hope that the work of Jandera, Elfakir and my own as described here, is able to motivate research groups to carry out further investigations on solvation parameter models in HILIC, thus, enriching the pool of information related to mechanistic aspects of HILIC systems.

Clearly, more experimental work needs to be done on the accurate estimation or the new development of solute descriptors for ionizable compounds. Undoubtedly, the unadjusted solute parameters for charged anions and cations enter a significant uncertainty to the statistic model. For example, a molecule's capability to act as a hydrogen bond donor or acceptor is changing with its ionization state: thus it plays an important role if adsorption becomes one of the dominant "hydrophilic retention interactions".

Generally, the work on LSER model in HILIC can be summarized as following:

- A better goodness of fit is obtained when a MP composition is chosen which enhances partition phenomena if a multitude of molecules with different functionalities and characteristics are entered into the multivariate algorithm. In other words, a MP with a higher amount of water (> 15 %) and a higher buffer ion concentration of ≥ 20 mM [11] is to be used as first choice.
- The evaluation test set should offer a high diversity of functional groups to get a global view on the retention interactions in HILIC systems. It is important to enter aliphatic compounds to break the correlation between the descriptors for the contribution from n and π electrons (E), the dipolarity and polarizability (S) and the hydrogen bond basicity (B).
- The behavior of single compound groups (e.g. specific types of acids) can be screened by LSER with a high goodness of fit. However, the experimental design of this study does not allow a global view of the HILIC system [31]
- LSER can be used during column development to see the influence of the charge state of the SP when the MP composition is designed to allow stronger ionic interactions. Fragmented LSER models may be advantageous compared to a global LSER (**Appendix III**) when a higher number of ionized analytes is present and descriptors which are by conception developed for neutral species should be adjusted to the ionized forms.

3. Study on enantioselectivity outside of the scope of HILIC separations

Direct separations of enantiomers in analytical but also preparative scale are nowadays generally accomplished by liquid chromatography using chiral stationary phases (CSPs) [113]. Chiralpak[®] QN-AX and QD-AX (see Fig. 26) are *tert*-butylcarbamoyl-quinine (QN)- and -quinidine (QD) modified CSPs which offer remarkable enantiodiscrimination properties towards chiral acids, such as *N*-protected amino acids, aryl carboxylic acids, *N*-protected aminophosphonic, and phosphinic acids [114-117].

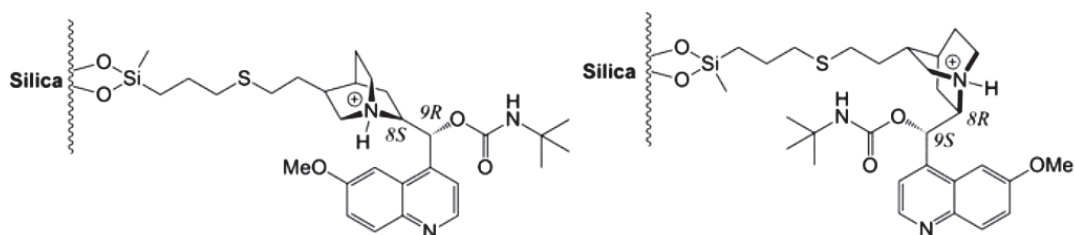


Fig. 26: The chemical structure of weak anion exchangers QN-AX (left) and QD-AX (right). (Pell *et al.*, *J.Sep.Sci.* 2012, © Wiley-VCH, Reprinted with permission) [118].

So far, only the separation of camphorsulfonic acid, three *N*-protected aminosulfonic acids and alpha-perfluoromethyl branched perfluorooctane sulfonate (*1m*-PFOS) on a quinine carbamate-type weak anion-exchange CSP [115,116,119] and the indirect enantioseparation of camphorsulfonic acid with an achiral diol SP and the chiral MP additive quinine have been reported. However, there are no literature reports on the enantioresolution of a broad set of free sulfonic acids via chiral chromatography. Chiral sulfonic acids (or their sulfonate salts, respectively) can be used for example as chiral resolving agents (e.g. camphor sulfonic acid, 3-bromocamphorsulfonic acid, and 1-phenylethanesulfonic acid [120]) but also have the potential to be applied as pharmaceuticals (e.g. 6-gingsulfonic acid or (R)-Saclofen [121-123]).

An application was developed for HPLC and subcritical fluid chromatography (SubFC) to enantioseparate sodium ketosulfonates such as sodium chalconesulfonates and derivatives thereof on *tert*-butylcarbamoyl-QN and -QD CSPs. Moreover, the influence of co- and counterion type and amount on retention and enantioresolution was investigated with polar organic MPs.

Both *Cinchona* alkaloid-based columns afforded remarkable enantiodiscrimination properties for the investigated sodium ketosulfonates. The QD-based column showed slightly stronger retention and better enantioselectivity for solutes tested, compared to the QN-derived CPS.

The protonation of the quinuclidine tertiary amine of the chiral selector under slightly acidic conditions allows deprotonated acidic analytes to experience ionic attraction. This long range electrostatic interaction predominates separation and retention via a weak anion-exchange mechanism. Additionally, further interactions (hydrogen bonding, π - π stacking, solvophobic/van der Waals, or steric interactions between the chiral selector and the analyte) support the spatially determined ion pairing process and thus facilitate enantiodiscrimination [124,125].

The anion-exchange retention mechanism is strongly dependent on the type and amount of counterions in the MP and follows a stoichiometric displacement model. Consequently, we investigated the influence of five different mono-, bi-, and trivalent acids as acidic additives (counterions) in a polar organic MP with methanol as bulk solvent. Triethylamine was used to adjust the apparent pH to 6.1. Retention times for all sulfonates decreased with an increase of the competitor acid (counterion) concentration. The anion-exchange mechanism was affirmed by plotting the logarithm of the retention factor ($\log k$) versus the logarithm of the counterion concentration ($\log [C]$). The obtained linear relationship clearly indicates that the stoichiometric displacement model can explain the anion-exchange mechanism. The elution strength of the investigated counterions was found to be: citric acid > malonic acid > formic acid = succinic acid > acetic acid. However, acetic acid may be preferential since peak shape and reproducibility are enhanced when a higher counterion concentration is applied.

Moreover, the type and concentration of the counterion (acidic additive) were found to have only a minor influence on the enantioselectivity. Thus, retention can easily be adjusted by the type and amount of acidic additive without significantly changing enantioselectivity. However, the ion exchange process is superimposed by the acid–base equilibria which means that the ratio or type of the acidic and basic additives, respectively, causes a distinct influence on retention, enantioselectivity and peak shape.

HPLC turned out to be superior to SubFC in terms of fast solute elution with the same co- and counterion strength in the MP. Indeed, SubFC allowed the highest magnitude of resolution values for some analytes and thus can be used as an alternative to HPLC.

The results have been released in the following publication: R. Pell., G. Schuster, M. Lämmerhofer, W. Lindner, *Journal of Separation Science* 2012, 35, 2521–2528; (for the full article see **Appendix IV**)

4. Concluding remarks

In its main part, the present dissertation and the experimental work described therein combine the synthesis and development of a new saccharide-derived SP, the evaluation of chromatography sorbents and the systematic investigation of increments to HILIC retention phenomena by applying multivariate statistical methods.

At first, a polar SP was synthesized by applying a non-enzymatic browning (Maillard) reaction on APS. Water free toluene was found to be the most efficient medium to form the initial “Maillard type” ligand. A subsequent stabilization step with NaBH₄ and a final acidic washing procedure guaranteed a reproducible formation of the dark-orange to dark-brown “chocolate” ligand. Consequently, the transformed reducing sugar moieties, which are of hydrophilic character, facilitate retention for polar compounds (e.g. nucleosides, nucleobases, acids, bases, vitamins) under HILIC elution conditions. Selectivity was observed to be of a hybrid type between diol and amine modified columns. Indeed, the columns offered good peak efficiencies and retention similar to commercially available columns. Out of all saccharides observed, cellobiose created the most efficient “chocolate” ligand. Moreover, convenient selectivity manipulation can be applied when operated under acidic conditions, due to residual primary amino groups. A mixed modal retention mechanism is present which enables retention of lipophilic analytes under RP-LC like conditions. In particular, the mono-saccharide ligand-primer glucose exhibits the highest overall lipophilicity of the “Chocolate HILIC” columns. Chromatographic stability tests under isocratic and gradient elution conditions showed a high reproducibility in terms of retention time with a max %RSD of 1. The SP guaranteed a fast re-equilibration towards the starting conditions which may be the result of a fast and reproducible readjustment of the stagnant water layer.

Additional experiments which did not directly correlate with HILIC separations but with the methodology of the evaluation of chromatographic separation materials was carried out on *tert*-butylcarbamoyl- quinine and quinidine-modified CSPs (Chiralpak[®] QN-AX and QD-AX). HPLC and SubFC have been applied and compared to assist enantioseparation of sodium ketosulfonates. Chiralpak[®] QD-AX was slightly superior in terms of retention time and enantioseparation as opposed to Chiralpak[®] QN-AX. The elution mechanism follows the stoichiometric displacement model and implies anion-exchange driven retention. Monovalent acids may be preferably used as competitor ions due to a better peak shape

and a lower observed drift in retention times. However, the counter-ion type does not affect the enantioselectivity. Nevertheless, the acid–base equilibria or in other words the ratio or type of the acidic and basic additives, respectively, can alter retention, enantioselectivity and peak shape. Although, SubFC permitted the highest magnitude of resolution values for some analytes and may be used as an alternative chromatography method. The fast enabled solute elution with the same co- and competitor ion strength in the MP clearly makes HPLC superior to SubFC.

The last part of the thesis focused on the evaluation of different HILIC phases by screening a multitude of test compounds and subsequent elucidation of retention forces by multivariate linear regression. Solute-sorbent interactions were analyzed on 23 polar modified HILIC-type SPs which featured acidic, neutral, basic and zwitterionic modifications. The generally accepted LSER model with Abraham (A, B, S and V) and charge descriptors (D^+ and D^-) proved to be a valuable tool to find similarities within HILIC columns and furthermore to characterize new sorbents during the development process.

The solvation parameter models showed that electrostatic interactions may dominate the HILIC mechanism. Bare silica and acidic modified columns exhibit high cation-exchange characteristics and the mechanism seems predominated by adsorptive interactions. Consequently, acids may observe strong electrostatic repulsion and elute with the void volume. Although basic modified columns undergo anion-exchange interactions, the electrostatic repulsive effect on bases is less strongly affected and basic analytes may be still analyzable on this column type. Since LSER does not imply a direct correlation between retention interactions and observed analyte selectivity, HCA was applied to compare column alignments obtained either by standardized retention factors k or by the obtained system constants. Although the SPs are combined into similar groups for both HCAs, distinct differences in retentive force and obtained selectivity were observed. Consequently, it seems that selectivity in HILIC systems is achieved by the sum of additive or multiplicative phenomena and may not only rely on partition.

A change in the MP pH and type of buffer salt (10 mM NH_4FA \rightarrow 10 mM NH_4AcOH) caused an increase in the hydrogen bond basicity. Consequently, a general trend towards longer retention times was observed except when ionic repulsion took place.

As a summary of the experimental data, Fig. 27 combines all the retention and selectivity data in one correlation matrix. This multivariate method uses the correlation coefficient of selectivity plots to create a graphic representation which indicates columns and conditions that achieve similar or orthogonal results in terms of retention pattern. The color gradient is encoded in the way that red represents a high correlation while white illustrates high orthogonality.



Fig. 27: Correlation matrix of screened HILIC columns. Red column labels relate to a MP condition of ACN/H₂O (90:10, v/v) + 10 mM NH₄FA (pH 3) while green SP labels express the analysis with ACN/H₂O (90:10, v/v) + 10 mM NH₄AcOH (pH 5). The color encryption of the squares is explained in the text.

One interesting result is that most of the columns show a quite high correlation which indicates that the retention mechanism, albeit of mixed-modal character and the fact that columns have different modifications seems to be driven by one dominating process. Furthermore, unmodified silica, strong acidic modified columns, and strong basic columns show the least correlation with the rest of the columns. Consequently, this plot can provide an answer to the question of how many columns a chromatographer, who is working in the field of HILIC, should at least have in his toolbox to cover a wide spread range of selectivity. Based on our studies, as a rule of thumb we advise one acidic, one strong basic and one “neutral” HILIC column as starting set. Although neutral and basic columns are more preferable for HILIC applications due to weaker repulsive interactions, acidic columns can give alternative selectivity which may be of advantage during method development. However, for the installation of a robust HILIC system, one might choose a “neutral” modified column of the zwitterionic or BEH amide type.

5. References

- [1] A.J. Alpert, *Journal of Chromatography*, (1990), 499, 177. *Hydrophilic-interaction chromatography for the separation of peptides, nucleic acids and other polar compounds*
- [2] A.J. Martin, R.L. Synge, *Biochemical Journal*, (1941), 35, 1358. *A new form of chromatogram employing two liquid phases: A theory of chromatography. 2. Application to the micro-determination of the higher monoamino-acids in proteins*
- [3] F.M. Rabel, A.G. Caputo, E.T. Butts, *Journal of Chromatography A*, (1976), 126, 731. *Separation of carbohydrates on a new polar bonded phase material*
- [4] Y. Guo, S. Gaiki, *Journal of Chromatography A*, (2005), 1074, 71. *Retention behavior of small polar compounds on polar stationary phases in hydrophilic interaction chromatography*
- [5] Y. Kawachi, T. Ikegami, H. Takubo, Y. Ikegami, M. Miyamoto, N. Tanaka, *Journal of Chromatography A*, (2011), 1218, 5903. *Chromatographic characterization of hydrophilic interaction liquid chromatography stationary phases: Hydrophilicity, charge effects, structural selectivity, and separation efficiency*
- [6] N.P. Dinh, T. Jonsson, K. Irgum, *Journal of Chromatography A*, (2011), 1218, 5880. *Probing the interaction mode in hydrophilic interaction chromatography*
- [7] D.V. McCalley, *Journal of Chromatography A*, (2010), 1217, 3408. *Study of the selectivity, retention mechanisms and performance of alternative silica-based stationary phases for separation of ionised solutes in hydrophilic interaction chromatography*
- [8] W. Bicker, J.Y. Wu, H. Yeman, K. Albert, W. Lindner, *Journal of Chromatography A*, (2011), 1218, 882. *Retention and selectivity effects caused by bonding of a polar urea-type ligand to silica: A study on mixed-mode retention mechanisms and the pivotal role of solute-silanol interactions in the hydrophilic interaction chromatography elution mode*
- [9] K.J. Fountain, J. Xu, D.M. Dieh, D. Morrison, *Journal of Separation Science*, (2010), 33, 740. *Influence of stationary phase chemistry and mobile-phase composition on retention, selectivity, and MS response in hydrophilic interaction chromatography*
- [10] A.E. Karatapanis, Y.C. Fiamegos, C.D. Stalikas, *Journal of Chromatography A*, (2011), 1218, 2871. *A revisit to the retention mechanism of hydrophilic interaction liquid chromatography using model organic compounds*
- [11] R.I. Chirita, C. West, S. Zubrzycki, A.L. Finaru, C. Elfakir, *Journal of Chromatography A*, (2011), 1218, 5939. *Investigations on the chromatographic behaviour of zwitterionic stationary phases used in hydrophilic interaction chromatography*
- [12] A. Kumar, J.C. Heaton, D.V. McCalley, *Journal of Chromatography A*, (2013), 1276, 33. *Practical investigation of the factors that affect the selectivity in hydrophilic interaction chromatography*
- [13] S. Noga, S. Bocian, B. Buszewski, *Journal of Chromatography A*, (2013), 1278, 89. *Hydrophilic interaction liquid chromatography columns classification by effect of solvation and chemometric methods*

- [14] A. Periat, B. Debrus, S. Rudaz, D. Guillarme, *Journal of Chromatography A*, **(2013)**, 1282, 72. *Screening of the most relevant parameters for method development in ultra-high performance hydrophilic interaction chromatography*
- [15] J. Bernal, A.M. Ares, J. Pól, S.K. Wiedmer, *Journal of Chromatography A*, **(2011)**, 1218, 7438. *Hydrophilic interaction liquid chromatography in food analysis*
- [16] B. Buszewski, S. Noga, *Analytical & Bioanalytical Chemistry*, **(2012)**, 402, 231. *Hydrophilic interaction liquid chromatography (HILIC)-a powerful separation technique*
- [17] M.R. Gama, R.G. da Costa Silva, C.H. Collins, C.B.G. Bottoli, *TrAC Trends in Analytical Chemistry*, **(2012)**, 37, 48. *Hydrophilic interaction chromatography*
- [18] Y. Guo, S. Gaiki, *Journal of Chromatography A*, **(2011)**, 1218, 5920. *Retention and selectivity of stationary phases for hydrophilic interaction chromatography*
- [19] P. Hemström, K. Irgum, *Journal of Separation Science*, **(2006)**, 29, 1784. *Hydrophilic interaction chromatography*
- [20] T. Ikegami, K. Tomomatsu, H. Takubo, K. Horie, N. Tanaka, *Journal of Chromatography A*, **(2008)**, 1184, 474. *Separation efficiencies in hydrophilic interaction chromatography*
- [21] R. Li, Y.i. Guo, Q. Yuan, *Journal of Liquid Chromatography & Related Technologies*, **(2011)**, 34, 1112. *Recent applications of hydrophilic interaction chromatography in environmental analysis*
- [22] E. Ponten, *LC-GC Europe*, **(2012)** 21. *Advances in the understanding of stationary phases for HILIC*
- [23] G. Zauner, A.M. Deelder, M. Wuhler, *ELECTROPHORESIS*, **(2011)**, 32, 3456. *Recent advances in hydrophilic interaction liquid chromatography (HILIC) for structural glycomics*
- [24] G. Schuster, W. Lindner, *Journal of Chromatography A*, **(2013)**, 1273, 73. *Comparative characterization of hydrophilic interaction liquid chromatography columns by linear solvation energy relationships*
- [25] S.M. Melnikov, A. Holtzel, A. Seidel-Morgenstern, U. Tallarek, *Analytical Chemistry*, **(2011)**, 83, 2569. *Composition, structure, and mobility of water-acetonitrile mixtures in a silica nanopore studied by molecular dynamics simulations*
- [26] E. Wikberg, T. Sparrman, C. Viklund, T. Jonsson, K. Irgum, *Journal of Chromatography A*, **(2011)**, 1218, 6630. *A H-2 nuclear magnetic resonance study of the state of water in neat silica and zwitterionic stationary phases and its influence on the chromatographic retention characteristics in hydrophilic interaction high-performance liquid chromatography*
- [27] R. Li, J.X. Huang, *Journal of Chromatography A*, **(2004)**, 1041, 163. *Chromatographic behavior of epirubicin and its analogues on high-purity silica in hydrophilic interaction chromatography*
- [28] A.L. Barnette, S.H. Kim, *Journal Physical Chemistry C*, **(2012)**, 116, 9909. *Coadsorption of n-propanol and water on SiO₂: study of thickness, composition, and structure of binary adsorbate layer using attenuated total reflection infrared (ATR-IR) and sum frequency generation (SFG) vibration spectroscopy*

- [29] W. Bicker, J. Wu, M. Lämmerhofer, W. Lindner, *Journal of Separation Science*, (2008), 31, 2971. *Hydrophilic interaction chromatography in nonaqueous elution mode for separation of hydrophilic analytes on silica-based packings with noncharged polar bondings**
- [30] D.V. McCalley, U.D. Neue, *Journal of Chromatography A*, (2008), 1192, 225. *Estimation of the extent of the water-rich layer associated with the silica surface in hydrophilic interaction chromatography*
- [31] P. Jandera, T. Hajek, V. Skerikova, J. Soukup, *Journal of Separation Science*, (2010), 33, 841. *Dual hydrophilic interaction-RP retention mechanism on polar columns: Structural correlations and implementation for 2-D separations on a single column*
- [32] A.J. Alpert, *Analytical Chemistry*, (2008), 80, 62. *Electrostatic repulsion hydrophilic interaction chromatography for isocratic separation of charged solutes and selective isolation of phosphopeptides*
- [33] D.V. McCalley, *Journal of Chromatography A*, (2007), 1171, 46. *Is hydrophilic interaction chromatography with silica columns a viable alternative to reversed-phase liquid chromatography for the analysis of ionisable compounds?*
- [34] W. Ding, H. Nothaft, C.M. Szymanski, J. Kelly, *Molecular & cellular proteomics : MCP*, (2009), 8, 2170. *Identification and quantification of glycoproteins using ion-pairing normal-phase liquid chromatography and mass spectrometry*
- [35] C. Sanchez, M. Kansal, *LC-GC The Peak*, (2007), November 2007, 16 *Deleterious effects of formic acid without salt additives on the HILIC analysis of basic compounds*
- [36] J. Ruta, S. Rudaz, D.V. McCalley, J.-L. Veuthey, D. Guillarme, *Journal of Chromatography A*, (2010), 1217, 8230. *A systematic investigation of the effect of sample diluent on peak shape in hydrophilic interaction liquid chromatography*
- [37] P. Jandera, *Analytica Chimica Acta*, (2011), 692, 1. *Stationary and mobile phases in hydrophilic interaction chromatography: a review*
- [38] T.L. Chester, *Analytical Chemistry*, (2012), 85, 579. *Recent developments in high-performance liquid chromatography stationary phases*
- [39] H.E. Bergna, American Chemical Society, (1994), *The colloid chemistry of silica Colloid chemistry of silica*
- [40] C.A. Fyfe, G.C. Gobbi, G.J. Kennedy, *Journal of Physical Chemistry*, (1985), 89, 277. *Quantitatively reliable Si-29 magic-angle spinning nuclear magnetic-resonance spectra of surfaces and surface-immobilized species at high-field using a conventional high-resolution spectrometer*
- [41] H. Qiu, X. Liang, M. Sun, S. Jiang, *Analytical & Bioanalytical Chemistry*, (2011), 399, 3307. *Development of silica-based stationary phases for high-performance liquid chromatography*
- [42] E.S. Grumbach, D.M. Diehl, U.D. Neue, *Journal of Separation Science*, (2008), 31, 1511. *The application of novel 1.7 µm ethylene bridged hybrid particles for hydrophilic interaction chromatography*
- [43] A.P. McKeown, M.R. Euerby, H. Lomax, C.M. Johnson, H.J. Ritchie, M. Woodruff, *Journal of Separation Science*, (2001), 24, 835. *The use of silica for liquid chromatographic/mass spectrometric analysis of basic analytes*

- [44] B.A. Olsen, *Journal of Chromatography A*, (2001), 913, 113. *Hydrophilic interaction chromatography using amino and silica columns for the determination of polar pharmaceuticals and impurities*
- [45] N.D. Weng, *Journal of Chromatography B-Analytical Technologies in the Biomedical and Life Sciences*, (2003), 796, 209. *Bioanalytical liquid chromatography tandem mass spectrometry methods on underivatized silica columns with aqueous/organic mobile phases*
- [46] B. Dejaegher, D. Mangelings, Y. Vander Heyden, *Journal of Separation Science*, (2008), 31, 1438. *Method development for HILIC assays*
- [47] K. Heinig, T. Wirz, A. Gajate-Perez, S. Belli, *Journal of Chromatography B-Analytical Technologies in the Biomedical and Life Sciences*, (2011), 879, 436. *Determination of ganciclovir and its prodrug valganciclovir by hydrophilic interaction liquid chromatography-tandem mass spectrometry*
- [48] Q. Song, W. Naidong, *Journal of Chromatography B-Analytical Technologies in the Biomedical and Life Sciences*, (2006), 830, 135. *Analysis of omeprazole and 5-OH omeprazole in human plasma using hydrophilic interaction chromatography with tandem mass spectrometry (HILIC-MS/MS)--eliminating evaporation and reconstitution steps in 96-well liquid/liquid extraction*
- [49] R.P. Li, J.X. Huang, *Journal of Chromatography A*, (2004), 1041, 163. *Chromatographic behavior of epirubicin and its analogues on high-purity silica in hydrophilic interaction chromatography*
- [50] Z.G. Shi, Y.B. Wu, Y.B. Luo, Y.Q. Feng, *Chromatographia*, (2010), 71, 761. *Analysis of pterins in urine by HILIC*
- [51] M.J. Christopherson, K.J. Yoder, J.T. Hill, *Journal of Liquid Chromatography & Related Technologies*, (2006), 29, 2545. *Hydrophilic interaction liquid chromatographic (HILIC)/Ion exchange separation of picolinic and nicotinic acids*
- [52] T. Kind, V. Tolstikov, O. Fiehn, R.H. Weiss, *Analytical Biochemistry*, (2007), 363, 185. *A comprehensive urinary metabolomic approach for identifying kidney cancer*
- [53] M. De Person, A. Hazotte, C. Elfakir, M. Lafosse, *Journal of Chromatography A*, (2005), 1081, 174. *Development and validation of a hydrophilic interaction chromatography-mass spectrometry assay for taurine and methionine in matrices rich in carbohydrates*
- [54] B. Beilmann, P. Langguth, H. Häusler, P. Grass, *Journal of Chromatography A*, (2006), 1107, 204. *High-performance liquid chromatography of lactose with evaporative light scattering detection, applied to determine fine particle dose of carrier in dry powder inhalation products*
- [55] R.P. Li, Y. Zhang, C.C. Lee, L.M. Liu, Y.P. Huang, *Journal of Separation Science*, (2011), 34, 1508. *Hydrophilic interaction chromatography separation mechanisms of tetracyclines on amino-bonded silica column*
- [56] Y. Guo, A. Huang, *Journal of Pharmaceutical and Biomedical Analysis*, (2003), 31, 1191. *A HILIC method for the analysis of tromethamine as the counter ion in an investigational pharmaceutical salt*
- [57] E.F. Vansant, P. Van Der Voort, K.C. Vrancken (Editors), Elsevier, (1995), p. 193. *Studies in Surface Science and Catalysis Chapter 9 - Modification with silicon compounds: mechanistic studies*

- [58] K.S. Abou-El-Sherbini, C. Pape, O. Rienetz, D. Schiel, R. Stosch, P.G. Weidler, W.H. Höll, *Journal of Sol-Gel Science and Technology*, **(2010)**, 53, 587. *Stabilization of n-aminopropyl silica gel against hydrolysis by blocking silanol groups with TiO₂ or ZrO₂*
- [59] K. Albert, R. Brindle, J. Schmid, B. Buszewski, E. Bayer, *Chromatographia*, **(1994)**, 38, 283. *CP/MAS NMR investigations of silica-gel surfaces modified with aminopropylsilane*
- [60] X. Dai, X. Qian, B. Gong, Y. Wei, *Chromatographia*, **(2011)**, 73, 865. *Tetrazole-functionalized silica for hydrophilic interaction chromatography of polar solutes*
- [61] F.E. Regnier, R. Noel, *Journal of Chromatographic Science*, **(1976)**, 14, 316. *Glycerolpropylsilane bonded phases in the steric exclusion chromatography of biological macromolecules*
- [62] R. Kaliszan, M.A. van Straten, M. Markuszewski, C.A. Cramers, H.A. Claessens, *Journal of Chromatography A*, **(1999)**, 855, 455. *Molecular mechanism of retention in reversed-phase high-performance liquid chromatography and classification of modern stationary phases by using quantitative structure–retention relationships*
- [63] M.H. Abraham, *Chemical Society Reviews*, **(1993)**, 22, 73. *Scales of solute hydrogen-bonding: their construction and application to physicochemical and biochemical processes*
- [64] J.Y. Wu, W. Bicker, W. Lindner, *Journal of Separation Science*, **(2008)**, 31, 1492. *Separation properties of novel and commercial polar stationary phases in hydrophilic interaction and reversed-phase liquid chromatography mode*
- [65] W. Li, D. Nadig, H.T. Rasmussen, K. Patel, T. Shah, *Journal of Pharmaceutical and Biomedical Analysis*, **(2005)**, 37, 493. *Sample preparation optimization for assay of active pharmaceutical ingredients in a transdermal drug delivery system using experimental designs*
- [66] X. Wang, W. Li, H.T. Rasmussen, *Journal of Chromatography A*, **(2005)**, 1083, 58. *Orthogonal method development using hydrophilic interaction chromatography and reversed-phase high-performance liquid chromatography for the determination of pharmaceuticals and impurities*
- [67] P. Jandera, T. Hájek, *Journal of Separation Science*, **(2009)**, 32, 3603. *Utilization of dual retention mechanism on columns with bonded PEG and diol stationary phases for adjusting the separation selectivity of phenolic and flavone natural antioxidants*
- [68] F. Marclay, M. Saugy, *Journal of Chromatography A*, **(2010)**, 1217, 7528. *Determination of nicotine and nicotine metabolites in urine by hydrophilic interaction chromatography-tandem mass spectrometry: Potential use of smokeless tobacco products by ice hockey players*
- [69] A.E. Karatapanis, Y.C. Fiamegos, C.D. Stalikas, *Chromatographia*, **(2010)**, 71, 751. *Study of the behavior of water-soluble vitamins in HILIC on a diol column*
- [70] D.S. Risley, M.A. Strege, *Analytical Chemistry*, **(2000)**, 72, 1736. *Chiral separations of polar compounds by hydrophilic interaction chromatography with evaporative light scattering detection*
- [71] Z.M. Guo, Y. Jin, T. Liang, Y.F. Liu, Q. Xu, X.M. Liang, A.W. Lei, *Journal of Chromatography A*, **(2009)**, 1216, 257. *Synthesis, chromatographic evaluation and hydrophilic interaction/reversed-phase mixed-mode behavior of a "Click beta-cyclodextrin" stationary phase*

- [72] H. Qiu, L. Loukotková, P. Sun, E. Tesařová, Z. Bosáková, D.W. Armstrong, *Journal of Chromatography A*, (2011), 1218, 270. *Cyclofructan 6 based stationary phases for hydrophilic interaction liquid chromatography*
- [73] P. Sun, C. Wang, Z.S. Breitbach, Y. Zhang, D.W. Armstrong, *Analytical Chemistry*, (2009), 81, 10215. *Development of dew HPLC chiral stationary phases based on native and derivatized cyclofructans*
- [74] N.L.T. Padivitage, D.W. Armstrong, *Journal of Separation Science*, (2011), 34, 1636. *Sulfonated cyclofructan 6 based stationary phase for hydrophilic interaction chromatography*
- [75] W.Z. Sun, L.M. Yuan, *Journal of Liquid Chromatography & Related Technologies*, (2009), 32, 553. *Arabinose, fucose, ribodeseose, lyxose, and ribose used as chiral stationary phases in HPLC*
- [76] J.Y. Wang, F. Zhao, M. Zhang, Y. Peng, L.M. Yuan, *Chinese Chemical Letters*, (2008), 19, 1248. *Glucose, cellobiose, lactose and raffinose used as chiral stationary phases in HPLC*
- [77] H. Huang, H. Guo, M. Xue, Y. Liu, J. Yang, X. Liang, C. Chu, *Talanta*, (2011), 85, 1642. *Click novel glycosyl amino acid hydrophilic interaction chromatography stationary phase and its application in enrichment of glycopeptides*
- [78] G. Schuster, W. Lindner, *Analytical & Bioanalytical Chemistry*, (2011), 400, 2539. *Chocolate HILIC phases: development and characterization of novel saccharide-based stationary phases by applying non-enzymatic browning (Maillard reaction) on amino-modified silica surfaces*
- [79] D.S. Risley, W.Q. Yang, J.A. Peterson, *Journal of Separation Science*, (2006), 29, 256. *Analysis of mannitol in pharmaceutical formulations using hydrophilic interaction liquid chromatography with evaporative light-scattering detection*
- [80] T. Yoshida, *Analytical Chemistry*, (1997), 69, 3038. *Peptide separation in normal phase liquid chromatography*
- [81] P. Ciminiello, C. Dell'Aversano, E. Fattorusso, M. Forino, S. Magno, F. Santelia, M. Tsoukatou, *Toxicon*, (2006), 47, 174. *Investigation of the toxin profile of greek mussels *mytilus galloprovincialis* by liquid chromatography—mass spectrometry*
- [82] G. Kratz, T. Yoshida, *LC-GC Europe*, (2003) 40. *Separation of peptides by hydrophilic interaction chromatography using TSKgel Amide-80*
- [83] H. Schlichtherle-Cerny, M. Affolter, C. Cerny, *Analytical Chemistry*, (2003), 75, 2349. *Hydrophilic interaction liquid chromatography coupled to electrospray mass spectrometry of small polar compounds in food analysis*
- [84] G. Karlsson, S. Winge, H. Sandberg, *Journal of Chromatography A*, (2005), 1092, 246. *Separation of monosaccharides by hydrophilic interaction chromatography with evaporative light scattering detection*
- [85] M.J. van der Werf, K.M. Overkamp, B. Muilwijk, L. Coulier, T. Hankemeier, *Analytical Biochemistry*, (2007), 370, 17. *Microbial metabolomics: toward a platform with full metabolome coverage*
- [86] R. Zhang, Y. Wang, Y. Ji, B.-J. Shi, Z.-P. Zhang, H.-Y. Zhang, M. Yang, Y.-M. Wang, *Journal of Chromatography A*, (2013), 1272, 73. *Quantitative analysis of oleic acid and*

three types of polyethers according to the number of hydroxy end groups in Polysorbate 80 by hydrophilic interaction chromatography at critical conditions

- [87] P. Rodriguez, A. Alfonso, P. Otero, P. Katikou, D. Georgantelis, L.M. Botana, *Food Chemistry*, **(2012)**, 132, 1103. *Liquid chromatography-mass spectrometry method to detect tetrodotoxin and Its analogues in the puffer fish Lagocephalus sceleratus (Gmelin, 1789) from european waters*
- [88] L. Novakova, I. Kaufmannova, R. Janska, *Journal of Separation Science*, **(2010)**, 33, 765. *Evaluation of hybrid hydrophilic interaction chromatography stationary phases for ultra-HPLC in analysis of polar pteridines*
- [89] B.Y. Zhu, C.T. Mant, R.S. Hodges, *Journal of Chromatography*, **(1991)**, 548, 13. *Hydrophilic-interaction chromatography of peptides on hydrophilic and strong cation-exchange columns*
- [90] Y. Wang, X. Lu, G. Xu, *Journal of Chromatography A*, **(2008)**, 1181, 51. *Development of a comprehensive two-dimensional hydrophilic interaction chromatography/quadrupole time-of-flight mass spectrometry system and its application in separation and identification of saponins from Quillaja saponaria*
- [91] T. Tetaz, S. Detzner, A. Friedlein, B. Molitor, J.L. Mary, *Journal of Chromatography A*, **(2011)**, 1218, 5892. *Hydrophilic interaction chromatography of intact, soluble proteins*
- [92] W. Jiang, K. Irgum, *Analytical Chemistry*, **(1999)**, 71, 333. *Covalently bonded polymeric zwitterionic stationary phase for simultaneous separation of inorganic cations and anions*
- [93] S. Di Palma, P.J. Boersema, A.J.R. Heck, S. Mohammed, *Analytical Chemistry*, **(2011)**, 83, 3440. *Zwitterionic hydrophilic interaction liquid chromatography (ZIC-HILIC and ZIC-cHILIC) provide high resolution separation and increase sensitivity in proteome analysis*
- [94] B. Dejaegher, Y.V. Heyden, *Journal of Separation Science*, **(2010)**, 33, 698. *HILIC methods in pharmaceutical analysis*
- [95] S. Cubbon, T. Bradbury, J. Wilson, J. Thomas-Oates, *Analytical Chemistry*, **(2007)**, 79, 8911. *Hydrophilic interaction chromatography for mass spectrometric metabonomic studies of urine*
- [96] C. Antonio, T. Larson, A. Gilday, I. Graham, E. Bergstrom, J. Thomas-Oates, *Rapid communications in mass spectrometry : RCM*, **(2008)**, 22, 1399. *Hydrophilic interaction chromatography/electrospray mass spectrometry analysis of carbohydrate-related metabolites from Arabidopsis thaliana leaf tissue*
- [97] G. Marrubini, B.E.C. Mendoza, G. Massolini, *Journal of Separation Science*, **(2010)**, 33, 803. *Separation of purine and pyrimidine bases and nucleosides by hydrophilic interaction chromatography*
- [98] R. Oertel, U. Renner, W. Kirch, *Journal of Pharmaceutical and Biomedical Analysis*, **(2004)**, 35, 633. *Determination of neomycin by LC-tandem mass spectrometry using hydrophilic interaction chromatography*
- [99] H.E. Cho, S.Y. Ahn, I.S. Son, S. In, R.S. Hong, D.W. Kim, S.H. Woo, D.C. Moon, S. Kim, *Forensic Science International*, **(2012)**, 217, 76. *Determination and validation of tetrodotoxin in human whole blood using hydrophilic interaction liquid chromatography-tandem mass spectroscopy and its application*
- [100] S. Di Palma, S. Mohammed, A.J.R. Heck, *Nature Protocols*, **(2012)**, 7, 2041. *ZIC-cHILIC as a fractionation method for sensitive and powerful shotgun proteomics*

- [101] Q.X. Liu, L.Y. Xu, Y.X. Ke, Y. Jin, F.F. Zhang, X.M. Liang, *Journal of Pharmaceutical and Biomedical Analysis*, (2011), 54, 623. *Analysis of cephalosporins by hydrophilic interaction chromatography*
- [102] http://www.esainc.com/docs/spool/Poster_Pittcon2009_PC_HILIC.pdf, acc. date 18.03.2013
- [103] G. Jin, Z. Guo, F. Zhang, X. Xue, Y. Jin, X. Liang, *Talanta*, (2008), 76, 522. *Study on the retention equation in hydrophilic interaction liquid chromatography*
- [104] G. Greco, S. Grosse, T. Letzel, *Journal of Chromatography A*, (2012), 1235, 60. *Study of the retention behavior in zwitterionic hydrophilic interaction chromatography of isomeric hydroxy- and aminobenzoic acids*
- [105] M.G. Kokotou, N.S. Thomaidis, *Chromatographia*, (2012), 75, 457. *Behavior and retention models of melamine and its hydrolysis products*
- [106] C. Lamouroux, G. Foglia, G. Le Rouzo, *Journal of Chromatography A*, (2011), 1218, 3022. *How to separate ionic liquids: Use of hydrophilic interaction liquid chromatography and mixed mode phases*
- [107] U.D. Neue, B.A. Alden, T.H. Walter, *Journal of Chromatography A*, (1999), 849, 101. *Universal procedure for the assessment of the reproducibility and the classification of silica-based reversed-phase packings II. Classification of reversed-phase packings*
- [108] U.D. Neue, A. Mendez, *Journal of Separation Science*, (2007), 30, 949. *Selectivity in reversed-phase separations: general influence of solvent type and mobile phase pH*
- [109] U.D. Neue, J.E. O'Gara, A. Méndez, *Journal of Chromatography A*, (2006), 1127, 161. *Selectivity in reversed-phase separations: Influence of the stationary phase*
- [110] M. Lämmerhofer, M. Richter, J. Wu, R. Nogueira, W. Bicker, W. Lindner, *Journal of Separation Science*, (2008), 31, 2572. *Mixed-mode ion-exchangers and their comparative chromatographic characterization in reversed-phase and hydrophilic interaction chromatography elution modes*
- [111] R.I. Chirita, C. West, A.L. Finaru, C. Elfakir, *Journal of Chromatography A*, (2010), 1217, 3091. *Approach to hydrophilic interaction chromatography column selection: Application to neurotransmitters analysis*
- [112] M. Vitha, P.W. Carr, *Journal of Chromatography A*, (2006), 1126, 143. *The chemical interpretation and practice of linear solvation energy relationships in chromatography*
- [113] E. Francotte, W. Lindner, Wiley-VCH, Weinheim, (2006). *Chirality in drug research*
- [114] M. Laemmerhofer, *Journal of Chromatography A*, (2005), 1068, 3. *Chiral separations by capillary electromigration techniques in nonaqueous media. I. Enantioselective nonaqueous capillary electrophoresis*
- [115] M. Lämmerhofer, W. Lindner, *Journal of Chromatography A*, (1996), 741, 33. *Quinine and quinidine derivatives as chiral selectors I. Brush type chiral stationary phases for high-performance liquid chromatography based on cinchonan carbamates and their application as chiral anion exchangers*
- [116] M. Lämmerhofer, W. Lindner, E. Grushka, N. Grinberg, Editors, CRC Press LLC, (2008). *Advances in Chromatography, Volume 46*

- [117] E. Zarbl, M. Lämmerhofer, F. Hammerschmidt, F. Wuggenig, M. Hanbauer, N.M. Maier, L. Sajovic, W. Lindner, *Analytica Chimica Acta*, (2000), 404, 169. *Direct liquid chromatographic enantioseparation of chiral α - and β -aminophosphonic acids employing quinine-derived chiral anion exchangers: determination of enantiomeric excess and verification of absolute configuration*
- [118] R. Pell, G. Schuster, M. Lämmerhofer, W. Lindner, *Journal of Separation Science*, (2012), 35, 2521. *Enantioseparation of chiral sulfonates by liquid chromatography and subcritical fluid chromatography*
- [119] Y. Wang, S. Beeson, J.P. Benskin, A.O. De Silva, S.J. Genuis, J.W. Martin, *Environmental Science & Technology*, (2011), 45, 8907. *Enantiomer fractions of chiral perfluorooctanesulfonate (PFOS) in human sera*
- [120] P. Newman, Optical Resolution Information Center, Manhattan College, Riverdale, N.Y., (1978). *Optical resolution procedures for chemical compounds*
- [121] A. Macchiarulo, R. Pellicciari, *Journal of Molecular Graphics and Modelling*, (2007), 26, 728. *Exploring the other side of biologically relevant chemical space: Insights into carboxylic, sulfonic and phosphonic acid bioisosteric relationships*
- [122] D.I.B. Kerr, J. Ong, C. Vaccher, P. Berthelot, N. Flouquet, M.-P. Vaccher, M. Debaert, *European Journal of Pharmacology*, (1996), 308, R1. *GABAB receptor antagonism by resolved (R)-saclofen in the guinea-pig ileum*
- [123] M. Yoshikawa, S. Yamaguchi, K. Kunimi, H. Matsuda, Y. Okuno, J. Yamahara, N. Murakami, *Chemical & pharmaceutical bulletin*, (1994), 42, 1226. *Stomachic principles in ginger. III. An anti-ulcer principle, 6-gingesulfonic acid, and three monoacyldigalactosylglycerols, gingerglycolipids A, B, and C, from Zingiberis Rhizoma originating in Taiwan*
- [124] N.M. Maier, S. Schefzick, G.M. Lombardo, M. Feliz, K. Rissanen, W. Lindner, K.B. Lipkowitz, *Journal of the American Chemical Society*, (2002), 124, 8611. *Elucidation of the chiral recognition mechanism of cinchona alkaloid carbamate-type receptors for 3,5-dinitrobenzoyl amino acids*
- [125] A. Mandl, L. Nicoletti, M. Lämmerhofer, W. Lindner, *Journal of Chromatography A*, (1999), 858, 1. *Quinine- versus carbamoylated quinine-based chiral anion exchangers: A comparison regarding enantioselectivity for N-protected amino acids and other chiral acids*

6. List of publications and manuscripts

Appendix I

G. Schuster, W. Lindner.; *Chocolate HILIC phases: development and characterization of novel saccharide-based stationary phases by applying non-enzymatic browning (Maillard reaction) on amino-modified silica surfaces.*

Journal of Analytical and Bioanalytical Chemistry 2011, 400, 2539-2554.

Appendix II

G. Schuster, W. Lindner.; *Comparative characterization of hydrophilic interaction liquid chromatography columns by linear solvation energy relationships.*

Journal of Chromatography A 2012, 1273, 73-94

Appendix III

G. Schuster, W. Lindner.; *Additional investigations into the retention mechanism of Hydrophilic Interaction Liquid Chromatography by Linear Solvation Energy Relationships.*

Submitted Manuscript under review

Appendix VI

R.Pell, G. Schuster, M. Lämmerhofer, W. Lindner; *Enantioseparation of chiral sulfonates by liquid chromatography and subcritical fluid chromatography.*

Journal of Separation Science 2012, 35, 2521-2528

APPENDIX I

Chocolate HILIC phases: development and characterization of novel saccharide-based stationary phases by applying non-enzymatic browning (Maillard reaction) on amino-modified silica surfaces

G. Schuster, W. Lindner.

Journal of Analytical and Bioanalytical Chemistry 2011, 400, 2539-2554.

Chocolate HILIC phases: development and characterization of novel saccharide-based stationary phases by applying non-enzymatic browning (Maillard reaction) on amino-modified silica surfaces

Georg Schuster · Wolfgang Lindner

Received: 28 October 2010 / Revised: 4 January 2011 / Accepted: 28 January 2011 / Published online: 17 March 2011
© Springer-Verlag 2011

Abstract Novel saccharide-based stationary phases were developed by applying non-enzymatic browning (Maillard Reaction) on aminopropyl silica material. During this process, the reducing sugars glucose, lactose, maltose, and cellobiose served as “ligand primers”. The reaction cascade using cellobiose resulted in an efficient chromatographic material which further served as our model Chocolate HILIC column. (Chocolate refers to the fact that these phases are brownish.) In this way, an amine backbone was introduced to facilitate convenient manipulation of selectivity by additional attractive or repulsive ionic solute–ligand interactions in addition to the typical HILIC retention mechanism. In total, six different test sets and five different mobile phase compositions were investigated, allowing a comprehensive evaluation of the new polar column. It became evident that, besides the so-called HILIC retention mechanism based on partition phenomena, additional adsorption mechanisms, including ionic interactions, take place. Thus, the new column is another example of a HILIC-type column characterized by mixed-modal retention increments. The glucose-modified materials exhibited the relative highest overall hydrophobicity of all grafted Chocolate HILIC columns which enabled retention of lipophilic analytes with high water content mobile phases.

Keywords HILIC · Hydrophilic interaction chromatography · Weak anion exchanger · Stationary phase · Maillard reaction

Introduction

Interest in hydrophilic interaction liquid chromatography (HILIC) has steadily increased since its introduction by Alpert in the early 1990s [1]. Because the elution characteristics of HILIC are orthogonal to those of the more commonly applied reversed-phase chromatography (RP-LC), HILIC was found to be a powerful tool for the analysis of polar compounds which would elute more or less unretained and unresolved on the lipophilic RP materials. The wide application field of HILIC includes food and drug analysis, bioanalysis, proteomics, metabolic profiling, toxicology, drug metabolism, and other fields like environmental analysis which requires the verification of (very) polar pollutants. Further applications can be found elsewhere [2]. Typical HILIC conditions, i.e., polar sorbents and eluents with a high fraction of acetonitrile (ACN), usually 75–95%, facilitate the formation of a dynamically enriched stagnant water-rich layer on the surface of the polar stationary phase. The mobile phases in particular contribute some additional advantages of HILIC separations: a low back pressure due to the low viscosity of organic-rich solvents and the improved ESI-LC-MS/MS compatibility [3, 4]. Thereby, lower detection limits in MS detection are provided by the high volatility of these eluents which increases the electrospray ionization efficiency. Retention in HILIC, being merely a form of aqueous normal phase chromatography, was originally thought to be due to partition between the water-rich layer and the organic bulk eluent rather than the result of adsorption

Published in the special issue *Analytical Sciences in Austria* with Guest Editors G. Allmaier, W. Buchberger, and K. Francesconi.

Electronic supplementary material The online version of this article (doi:10.1007/s00216-011-4745-5) contains supplementary material, which is available to authorized users.

G. Schuster · W. Lindner (✉)
Department of Analytical Chemistry, University of Vienna,
Wahringer Strasse 38,
1090 Vienna, Austria
e-mail: wolfgang.lindner@univie.ac.at

events. However, numerous studies of the retention mechanism in HILIC mode have clarified that a more complicated mixed-modal retention mechanism needs to be taken into account [5–9]. Binding increments derived from hydrogen bonding, dipole–dipole interactions as well as ionic and even hydrophobic interactions can affect selectivity and retention on so-called HILIC columns. Today, a range of polar modified column materials are available in parallel with HILIC's steadily increasing fields of application. Silica functionalized with amino, amide, poly(succinimide), sulfoalkylbetaine, and diol groups are only some of the many HILIC phases discussed in recent reviews and publications [5–7, 10–14]. It is generally agreed that ligands suitable for HILIC columns should be hydrophilic (polar) in nature derived from diverse polar functional groups. Saccharides, which feature various hydroxyl groups and have unique structures, seem to be ideal for this task. Carbohydrates in the form of cyclodextrins (oligosaccharides) and cellulose with its derivatives (polysaccharides) are already well-established chromatography materials [15–18]. In contrast, monosaccharide- or disaccharide-modified silica is less often discussed in the literature. Huisden et al. [19] used glucose-modified silica for the separation of proteins. Enantioseparations under normal phase conditions using mono- and disaccharides as chiral ligands were presented by Yuan and co-workers [20, 21]. Furthermore, “click chemistry” was applied by Guo et al. [22, 23] and Moni et al. [24] to prepare saccharide-modified separation materials for hydrophilic chromatography. However, to the best of our knowledge, there are no publications introducing the non-enzymatic browning reaction cascade, better known as the Maillard reaction, as a procedure for the immobilization of saccharides.

Because of the complexity of this reaction, only a short introduction to its mechanism can be provided. For a deeper insight into the reaction cascade itself the large amount of available literature may be consulted [25–35]. Louis Camille Maillard (1878–1936), after whom the reaction is named, was the first scientist who explored non-enzymatic browning [25]. While investigating milder conditions for Emil Fischer's peptide synthesis, Maillard found that reducing sugars showed particular reactivity. Even though he was the first one to publish the discovered reaction, the work of J.E. Hodge is nowadays regarded as the foundation for research in this field [30]. Considering its incredible complexity, the reaction is more appropriately ascribed as a chemical pathway with several junctions than a mere single reaction. Hodge classified the Maillard reaction into three stages: initial, intermediate, and final. These stages are also often named in the literature as early, advanced, and final stage, respectively. Figure S1 (see “Electronic supplementary material”) gives an outline of the Maillard reaction proposed by Hodge

[30]. However, taking into account the information obtained during the past decade, this classification may be too general and oversimplifying [35]. The number of reactive functional groups during the initial stage of the reaction is very limited (OH, NH₂, COOH, and C=O). The amino–carbonyl reaction is in this respect the most important one, because it proceeds fast and without the aid of catalysts. After the initial reversible formation of a Schiff base, irreversible Amadori (for aldoses) and Heyns (for ketoses) products are formed which perpetuate a cascade of complex reactions (e.g., dehydration, oxidation, cyclization). Final Maillard products are called melanoidins which are brown nitrogenous compounds.

The Maillard reaction was chosen in order to create a unique HILIC-type ligand with multiple interaction sites: including hydroxyl groups, a weak cationically behaving backbone, and aza-heterocycles. Despite the aforementioned complexity of the reaction itself, we believe that our course of reaction results in a much more restricted Maillard pathway by using brush-type aminopropyl-modified silica as primary amine component instead of, e.g., amino acids. The reaction is performed on the surface and in water-free media, decreasing substantially the degree of freedom and flexibility of the surface-bound aminopropyl moiety. This is in agreement, for example, with comparing the reactions of xylose with glycine and glucose with ammonia, which result in around 100 compounds and only around 15 or even less, respectively [31].

In this work, we developed new and innovative silica-based polar stationary phases—Chocolate HILIC phases—and demonstrate their applicability in HILIC elution mode. As only reducing sugars are able to form the initial Schiff base, D-glucose, lactose (4-*O*-β-D-galactopyranosyl-D-glucose), maltose (4-*O*-α-D-glucopyranosyl-D-glucose), and cellobiose (4-*O*-β-D-glucopyranosyl-D-glucose) were employed as “ligand primers”. The name “Chocolate” introduced in this publication, refers to the brown color of the Maillard-modified silica material; the prefixes (G-, M-, L-, C-) refer to the employed saccharide-primer (i.e., glucose, lactose, maltose, and cellobiose, respectively). Various test probes (acids, bases, purines, methylxanthines, polyphenols, and hydroxyacids) and HILIC-type mobile phase compositions with different pH values were studied to gain an understanding of the columns' retention characteristics. Results are discussed in terms of chromatographic parameters (retention, efficiency, selectivity, stability etc.) and are compared to data obtained by in-house prepared aminopropyl-modified silica and more common and commercially available HILIC phases: Phenomenex Luna HILIC as diol-bonded phase and Waters XBridge Amide column as a neutral bonded phase.

Experimental

Materials

Chemicals

HPLC gradient grade acetonitrile (ACN), methanol (MeOH), ethanol, isopropyl alcohol, acetone, and toluene were supplied by VWR International (Vienna, Austria). 3-Aminopropyltrimethoxysilane was from ABCR (Karlsruhe, Germany). Water was double distilled in-house. Acetic acid (AcOH), ammonium acetate (NH₄Ac), formic acid (FA), ammonium formate (NH₄FA), trifluoroacetic acid (TFA), triethyl amine, *O,O*-diethyl chlorothiophosphate, 1,2-epoxydodecane (95%), allyl isothiocyanate (95%), sodium borohydride (NaBH₄; 98%), sodium cyanoborohydride (>95%), D-(+)-glucose (G), D-(+)-lactose monohydrate (L), D-(+)-maltose monohydrate (M), and D-(+)-cellobiose (C) were all of analytical grade and purchased from Sigma–Aldrich (Vienna, Austria). *N-tert*-Butoxycarbonyl-prolyl-phenylalanine (Boc-Pro-Phe) was obtained from Bachem (Buchs, Switzerland). Test compounds as listed in Fig. 1 were obtained in the highest purity grade available from Sigma–Aldrich. *O,O*-Diethyl thiophosphate (DETP) was prepared by hydrolysis of *O,O*-diethyl chlorothiophosphate in a mixture of ACN/H₂O (3:1, v/v) in the presence of an equimolar amount of triethylamine.

Other stationary phases and columns

To compare the retention characteristics of the newly developed Chocolate HILIC phases with more common and commercially available HILIC phases the following columns were used: (i) Luna HILIC column (5 μm, 200 Å, 200 m² g⁻¹, 150×4.6-mm id, typical carbon content reported to be 5.7% [36]) (Luna HILIC) supplied by Phenomenex (Vienna, Austria); (ii) XBridge Amide (3.5 μm, 135 Å, 185 m² g⁻¹, ligand density 7.5 μmol m⁻²; 150 mm×3-mm id) obtained from Waters Corporation (Milford, MA, USA); (iii) Daisogel (5 μm, 120 Å, 300 m² g⁻¹) as a bare silica analogue, obtained from Daiso Chemical (Osaka, Japan).

Preparation of chromatographic materials and column packing

Preparation of aminopropylsilica (APS) column packing material

Batches of 10 g bare silica (either 5 μm or 3 μm in particle size) were suspended in 150 mL dry toluene and 1.7 mmol 3-aminopropyltrimethoxysilane per gram silica was added. The mixture was refluxed for 7 h under a continuous stream of nitrogen and with stirring. The modified silica was washed

with toluene and MeOH and dried at 60 °C for 12 h in vacuo. Three batches, namely, APS-5 μ-1, APS-5 μ-2, and APS-3 μ, were generated with an aminopropyl ligand coverage of 1.1 mmol N g⁻¹ silica for APS-5 μ-1, 1.0 mmol N g⁻¹ silica for APS-5 μ-2, and 1.2 mmol N g⁻¹ silica for APS-3 μ, determined by elemental analysis. The reproducibility of the elemental analysis protocol carried out by a service unit of the Faculty of Chemistry, University of Vienna, was measured with ±8% relative at a level of 0.8–3% N absolute of the modified silica.

Preparation of Chocolate HILIC column packings

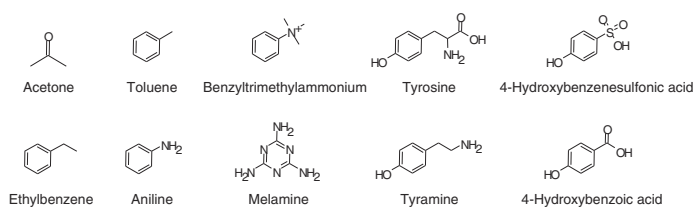
As outlined in Fig. 2 the Chocolate HILIC silica gels were prepared in four steps: At first, APS was coated with the reducing sugar in a molar ratio of 1.0 mmol per gram silica which is roughly stoichiometric. However, as not all amino groups can react due to a restricted accessibility, the sugars are in excess. APS was then suspended in a solution of the reducing sugar (dissolved in either pure MeOH for maltose, or in a mixture of H₂O/MeOH (58:42, v/v) for lactose, cellobiose, and glucose) and subsequently evaporated under reduced pressure.

The second and crucial step of the reaction was the formation and binding of the “Chocolate” ligand. The sugar-coated APS silica material (e.g., 5 g) was suspended in 100 mL dry toluene and stirred at 120 °C for 20 h under nitrogen. After filtration, the now brownish material was washed twice with toluene, three times with MeOH, transferred into a round-bottomed flask, and again refluxed in MeOH for 15 min. Subsequently, the material was dried at 60 °C for 12 h in vacuum. For the reduction of possibly remaining imine and carbonyl groups, the modified silica was stirred in MeOH containing 2 mmol NaBH₄ per gram silica at 80 °C for 14 h under constant nitrogen flow. Finally, to remove any possible unbound ligand, the Maillard-modified silica material was filtered and subsequently stirred in a mixture of MeOH/H₂O (50:50, v/v) with 5% acetic acid (pH=3.6) at 80 °C for 6 h. After collection by filtration, the modified stationary phase was washed three times with MeOH containing 1% triethylamine and subsequently washed with MeOH until the amine odor was gone. As a final point, the obtained modified silica materials, namely M-, L-, C-, and G-Chocolate HILIC (according to the used sugar primer), were dried at 60 °C for 24 h using the vacuum dry box. From now on, the materials are named M-, L-, C-, and G-Choc HILIC when referring to the specific material or Chocolate HILIC when the Chocolate material as such is discussed.

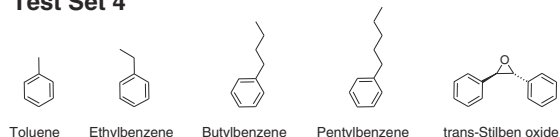
Preparation of Chocolate HILIC and APS derivatives

To evaluate the amount of remaining chemically reactive and accessible amino groups on our Chocolate HILIC material we

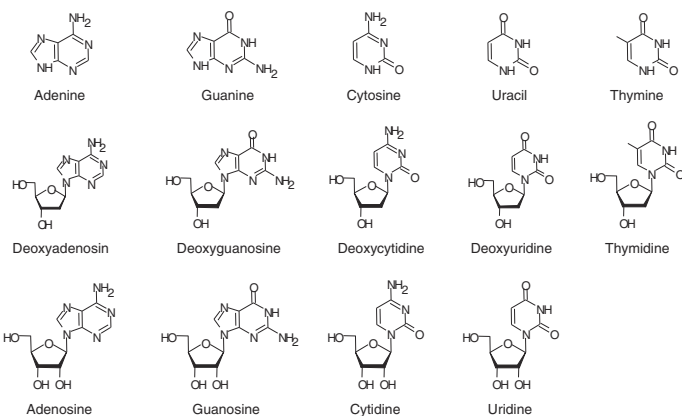
Test Set 1



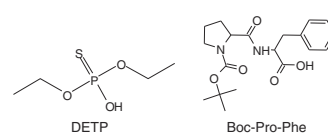
Test Set 4



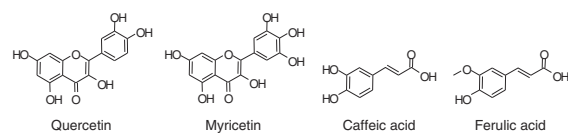
Test Set 2



Test Set 5



Test Set 6



Test Set 3

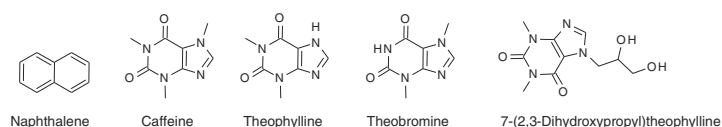


Fig. 1 Structural formulas of test compounds used in the evaluation of Chocolate HILIC phases

performed two on-phase derivatizations, resulting in dodecane and allylthiourea modifications. Both reactions can involve primary and secondary but not tertiary amines. As a control experiment we also modified APS with epoxydodecane, whereby the oxirane can react via a nucleophilic addition with primary and secondary amino functions.

Dodecane-modified L-Choc HILIC and APS

L-Choc HILIC column packing material (3.5 g, coverage 0.8 ± 0.06 mmol N g⁻¹ silica) and 2.6 g of APS-5 μ -2 (coverage 1.0 ± 0.08 mmol N g⁻¹ silica) were separately suspended in ca. 50 mL isopropyl alcohol. Then, 1.0 mmol

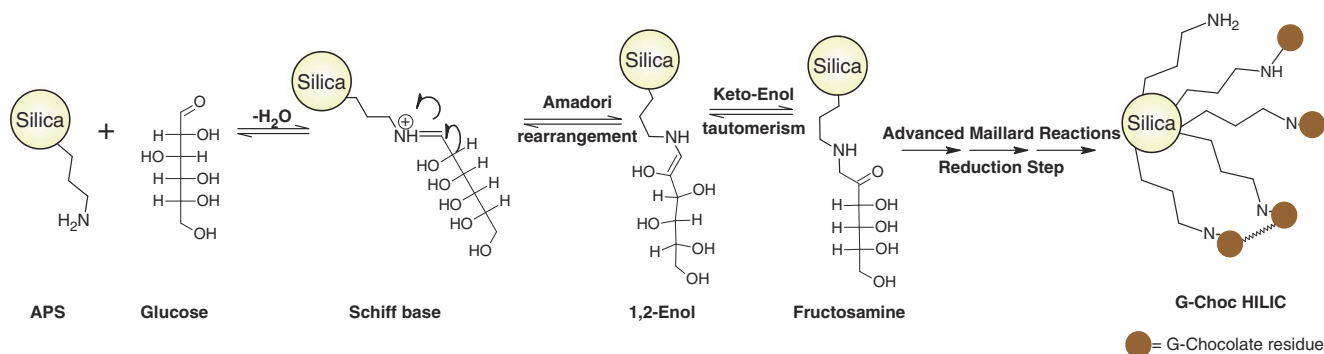


Fig. 2 Proposed reaction scheme for Chocolate HILIC packings, exemplified for glucose-modified G-Choc HILIC. The brown circles represent the as yet structurally less defined Chocolate ligands

1,2-epoxydodecane per gram silica was added and the mixtures were both refluxed for 24 h. The dodecane-modified silicas—RP-WAX-L-Choc and RP-WAX-APS (in reference to the weak anion exchanging character of the backbone and the introduced lipophilic alkyl chain, respectively)—were collected by filtration and washed in isopropyl alcohol and thoroughly in MeOH and dried at 60 °C for 24 h in vacuo.

Allylthiourea-modified C-Choc HILIC

C-Choc HILIC column packing material (1.04 g, coverage 0.8 ± 0.06 mmol N g⁻¹ silica) was suspended in 52 mL MeOH and 1.8 mmol allylthiocyanate per gram silica was added. The pH was adjusted to 9.0 with triethylamine. The mixture was reacted at 90 °C for 5 h. After filtration the modified silica was thoroughly washed in MeOH and dried at 60 °C for 24 h in vacuo.

Column packing

The obtained Chocolate HILIC packings, the dodecane-modified RP-WAX-L-Choc and RP-WAX-APS materials, APS-5 μ -1, and bare silica were slurry-packed in-house in 150 \times 4-mm-id stainless steel columns at 600 bar using MeOH as a carrier solvent.

Methods

Ninhydrin test

A 100- μ L aliquot of Ninhydrin solution (0.3% ninhydrin in ethanol containing 3% AcOH) was added to 100 mg stationary phase and heated up to 100 °C. A color change towards blue indicates a primary amino function. APS-5 μ -1, RP-WAX-L-Choc, RP-WAX-APS, and C-Choc HILIC were used for a preliminary evaluation with Daisogel as control standard.

Preparation of eluents

NH₄Ac and NH₄FA stock solutions were prepared at a concentration of 100 mM in double distilled water. pH values of the aqueous buffers were adjusted to pH 5 with AcOH or to pH 3 with FA. Mobile phases were obtained by mixing ACN, double distilled water, and the required buffer stock solutions or additives (TFA, FA).

RP-LC conditions To estimate the overall hydrophobicity of our Chocolate HILIC material with test set 4, a mobile phase composition containing H₂O/ACN (90:10, v/v) without further additives was used. Furthermore, an ACN/H₂O (40:60, v/v) combination containing in total 0.29% v/v AcOH (later on referred to as RP-WAX conditions) was

used to estimate the weak anion exchange character of the developed materials (test set 5) [37]. The pH was adjusted to pH 6 with analytical grade ammonia (Merck).

HILIC conditions The HILIC mobile phases in combination with test set 1 and test set 2 (Fig. 1) were composed of ACN/buffer (90:10, v/v) with either NH₄Ac buffer (100 mM, pH 5) or NH₄FA buffer (100 mM, pH 3), respectively. The methylxanthine test (test set 3) was eluted with a mixture of ACN/H₂O in a ratio of 98:2 (v/v) containing 2 mM NH₄Ac. Furthermore, to estimate the WAX character under HILIC conditions (with test set 6) eluents consisting of ACN/H₂O (90:10, v/v) with a specific amount of additives (10 mM NH₄Ac, 10 mM NH₄FA, 0.1% FA, and 0.05% TFA) were prepared.

Instrumentation

Chromatographic runs were carried out with a 1200 series or 1290 Infinity HPLC system from Agilent (Waldbronn, Germany) each equipped with a diode array detector. If not otherwise stated, elution in HILIC mode was achieved under isocratic conditions with a flow rate of 1.0 mL min⁻¹, except for the XBridge Amide column, where a flow rate of 0.6 mL min⁻¹ was applied to keep a constant linear flow velocity. Furthermore, the RP-WAX elution was performed at 1.7 mL min⁻¹. The column compartment temperature was set throughout the study to 25 °C. The detection wavelength was 254 nm, unless stated otherwise. Depending on their solubility, analytes were dissolved at concentrations of 0.02–1.0 mg mL⁻¹ in ACN/H₂O v/v ratios of either 50:50 or 90:10 and injected in volumes of 5–10 μ L. Acetone was used as a void time marker. Columns were equilibrated with about 15–20 column volumes of each new mobile phase to guarantee a stable baseline.

Results and discussion

Material development

Influence of reaction media, temperature, and reaction time on the Chocolate ligand formation

Throughout the process development, lactose was used as a model reducing sugar. Cellobiose, maltose, and glucose were further used to generate analogue Chocolate HILIC phases according to the protocol (see “**Experimental**” section). The name Chocolate originates from the color of the final Maillard-functionalized silica, which is dark orange to brown with a very slight sweet odor.

In general, the protocol was optimized according to the following parameters: reaction media, reaction temperature, and reaction time. Furthermore, different reducing agents and variations in the acid wash duration were applied. The yield of immobilized ligands was evaluated by means of color and additional carbon loading (refer to following section for ligand coverage calculations). Table 1 summarizes the whole process development.

As expected, in terms of the Chocolate ligand formation, the temperature as well as the reaction medium was found to play a crucial role. The higher the temperature and the less water was present during the reaction, the darker the final Maillard ligand obtained and the higher the additional carbon loading (see Table 1). Thus, toluene at 120 °C for 24 h was finally chosen as reaction media.

According to the concept of Maillard reactions [30, 31], first, a Schiff base is formed by condensation and elimination of water, followed by Amadori rearrangement and keto–enol tautomerization. The reversibility of these steps means that the 1,2-*O*-enol can rearrange back to the Schiff base which then could be hydrolyzed again, resulting in loss of the bound sugar. Thus, water-free media, which reduce the chance of hydrolysis, are expedient in terms of

reaction kinetics and reproducibility. The browning occurs to a higher degree and much faster when toluene in combination with high temperature is applied. Furthermore, the volatile compounds which are unavoidably formed are stronger in fragrance. Nevertheless, this indicates a foreseeable carbon loss according to the reaction cascade (see Fig. S1 in the “Electronic supplementary material”).

We treated the phase originally with sodium cyanoborohydride and later with sodium borohydride to reduce possibly existing imine and carbonyl groups in order to enhance bond and thus phase stability. Actually the imine groups may already be transformed during advanced Maillard reactions due to the initial excess of the reducing sugar in the reaction medium, thus behaving as an auto-reduction medium. To evaluate this effect, one Chocolate HILIC phase was made without the extra reduction step and loss in %N was only 3% relative which is insignificant due to the standard deviation of the element analysis method. Also the chromatographic performance of this HILIC phase was relatively similar (data not shown). Hence, reducing agents are not necessary to transform the imine groups into amino groups. However, to ensure complete reduction we kept the protocol with borohydride constant.

Table 1 Protocol optimization steps during the Chocolate HILIC development

Binding process				
Binding temperature (°C)	Reaction time	Color	mmol C g ⁻¹ silica	C/N ratio
30	7 days	White	1.0	3.6
60	24 h	Bright yellow	2.9	5.5
120 ^a	24 h ^a	Dark orange-brown ^a	7.7 ^a	10.6 ^a
Reaction media				
Reaction media	Reaction conditions	Color	mmol C g ⁻¹ silica	C/N ratio
H ₂ O	24 h; reflux	Slight yellow	2.1	4.6
H ₂ O+10% ethyl acetate	24 h; reflux	Yellow	2.0	6.0
Toluene ^a	24 h; reflux ^a	Dark orange-brown ^a	7.7 ^a	10.6 ^a
Reduction step ^b				
Reducing agent	Color	Loss C g ⁻¹ (%)	Loss N g ⁻¹ (%)	C/N ratio
NaCNBH ₃ , MeOH/H ₂ O; 80 °C; 24 h	Dark orange-brown	12.6	3.0	7.1
NaBH ₄ , MeOH/H ₂ O; 80 °C; 24 h ^a	Dark orange-brown ^a	4.5 ^a	0.0 ^a	9.8 ^a
None	Dark orange-brown	16.3	3.8	6.3
Acid wash step (H ₂ O/MeOH 50:50 (v/v) + 5% AcOH; 80 °C)				
Duration (h)	Color	%C	%N	C/N ratio
0.0	Dark orange-brown	7.9	1.3	6.2
0.5	Dark orange-brown	7.8	1.3	6.2
8.0 ^c	Dark orange-brown	7.6	1.2	6.1

The accuracy of the elemental measurements is by specification ±8% relative

^a Indicates final chosen parameter

^b Loss of C g⁻¹ and N g⁻¹ in % are in reference to the former binding step

^c Final acid wash, shortened to 6 h, was chosen

An additional optimization protocol was required for the acid wash (pH~3.6) in which loose bound ligands, sugar residues, or acid-labile molecules are stripped off the material. Thirty minutes or 8 h was chosen to evaluate the influence of wash duration. Within 7.5 h, further loss of N was only 3.8% correlated by a C/N ratio of 6.2 and 6.1. Finally we selected a 6-h acid treatment at 80 °C as an adequate protocol.

To remove residual acetate from the acid-wash step the stationary phases were then washed three times with 1% triethylamine in MeOH followed by thorough washing with MeOH. Elemental analyses before and after the wash indicated a slight change of %C (9.5% before, 9.2% after) which could be due to the acetate removal; no increase in % N was observed (1.0%N before wash, 1.0% after wash; data not shown in Table 1). Hence, the wash protocol was successful, without any unwanted triethylamine adsorption or degradation of the Chocolate HILIC phase.

To confirm that the browning is due to the Maillard reaction and not a result of thermochemical decomposition which occurs during the sugar caramelization process [38], a control reaction cascade according to the Chocolate protocol was performed with mercaptopropyl-modified or bare silica, separately (data not shown). Furthermore, sucrose was applied to APS. As a non-reducing disaccharide, no Maillard product should be formed. As expected, none of these control reactions showed carbon loading or browning, confirming the Maillard reaction as the dominant reaction pathway during the Chocolate ligand formation.

In separate attempts we wanted to characterize the residual amino groups. For this reason, a preliminary ninhydrin test was performed which indicates only primary amine groups. Whereas APS-5 μ -1 (1.1 ± 0.08 mmol N g⁻¹) turned dark blue, the originally white RP-WAX-APS (0.9 ± 0.07 mmol N g⁻¹) showed a lighter blue coloring,

signifying a reduction in primary amines. Furthermore, C-Choc HILIC (0.8 ± 0.06 mmol N g⁻¹) and RP-WAX-L-Choc (0.8 ± 0.06 mmol N g⁻¹) exhibit only a very light, for the latter almost unnoticeable, green coloring of the original brown silica. Hence, it indicates a strong reduction of primary amine groups. Daisogel, hereby used as control silica, showed no coloring at all. As already mentioned in the “Experimental” section, two on-phase derivatizations were carried out to support these observations with more precise and measurable experiments (see Fig. S2 in the “Electronic supplementary material”). In order to involve primary and secondary but not tertiary amines, a dodecane and allylthiourea modification was chosen. The amount of remaining total N is given in Table 2. By applying the epoxydodecane reaction we were only able to derivatize 3% of the amine groups on the RP-WAX-L-Choc judged by the C analysis and representing ca. 25 μ mol additional dodecane g⁻¹ modified silica. But 64% of the amine groups on the RP-WAX-APS could be modified with 580 μ mol dodecane g⁻¹ modified silica. However, on the C-Choc HILIC column, around 8% of the calculated amine groups (based on the N analysis data) were converted into allylthiourea groups. The discrepancy between the dodecane and thiourea modification could relate to the different reactivity and accessibility of the reaction partners. Epoxydodecane is highly hydrophobic and may not be able to draw as near as allylthiocyanourea towards the polar surface of the packing material and/or steric hindrance plays a role in the lower yield. However, both results underline our previously gained insight and confirm the strong diminishment of “active” primary amino groups, which were also consolidated during the chromatographic characterization (see following section). Whether the nitrogen on the packing material is transformed into tertiary amines, or is present in the form of nitrogen-containing

Table 2 Results for the elemental analysis of our in-house-made APS and Chocolate HILIC packings

	Modification	%C	%N	%S	Surface area (m ² g ⁻¹)	mmol C g ⁻¹	μ mol C m ⁻²	mmol N g ⁻¹	μ mol N m ⁻²	C/N
APS-5 μ -1	Aminopropyl	4.4	1.5		300	3.6	12.1	1.1 ± 0.09	3.7	2.9
APS-5 μ -2	Aminopropyl	4.6	1.4		300	3.8	12.7	1.0 ± 0.08	3.3	3.3
APS-3 μ	Aminopropyl	5.1	1.7		300	4.3	14.2	1.2 ± 0.10	4.0	3.0
G-Choc HILIC	Glucose	8.3	1.1		300	4.5	15.0	0.8 ± 0.06	2.7	7.5
L-Choc HILIC	Lactose	10.2	1.1		300	6.1	20.2	0.8 ± 0.06	2.7	9.3
M-Choc HILIC	Maltose	9.2	1.0		300	5.6	18.6	0.7 ± 0.06	2.4	9.2
C-Choc HILIC	Cellobiose	10.0	1.2		300	5.8	19.2	0.8 ± 0.06	2.8	8.3
C-Choc HILIC-3	Cellobiose	10.5	1.1		300	6.3	20.9	0.8 ± 0.06	2.7	9.5
RP-WAX-L-Choc	Lactose+C ₁₂	10.5	1.1		300	6.4	21.2	0.8 ± 0.06	2.7	9.5
RP-WAX-APS	C ₁₂	10.8	1.3		300	6.3	21.1	0.9 ± 0.07	3.0	8.3
Allylthiourea C-Choc	Allylthiourea	10.3	1.4	0.2	300	5.6	18.8	1.0 ± 0.08	3.3	7.4

Ligand loading in mmol C g⁻¹ was calculated as described in the “Results and discussion” section. The accuracy of the elemental measurements is by specification $\pm 8\%$ relative

heterocycles, which can be formed during the Maillard reaction [29], could not be elucidated so far.

Calculation of the Chocolate HILIC ligand coverage

Because of the complexity and diversity of the “Maillard-type ligand” the estimation of the exact ligand loading was difficult. However, as a reference value, the Chocolate HILIC column coverage was calculated according to the amount of *additional carbon* to that already present in the APS base material. Because the bound sugar molecule is no longer fully intact, the ligand coverage is stated in units of mmol C g^{-1} silica and not the expected mmol sugar g^{-1} . An additional characterization of the loading process is given by the changed C/N ratio (derived from %C and %N values) during the preparation of the chromatographic material. Because of the known instability of APS [39], the initial carbon content was not used to calculate the ligand loadings. Instead, the coverage was estimated by multiplying the obtained mmol N g^{-1} silica value times three (derived from aminopropyl group) and subtracting this result from the achieved overall mmol C g^{-1} silica value. The accuracy of the elemental measurements is by specification $\pm 8\%$ relative.

Chromatographic characterization

The new Chocolate HILIC phases were chromatographically evaluated according to their overall hydrophobicity and their ionic interaction character. Moreover, polar non-charged test compounds which are commonly used in HILIC (nucleobases, nucleosides, deoxynucleosides) as well as RP elution mode (e.g., methylxanthines) were monitored to obtain an overview of the columns retention behavior. By this means the data were compared to those obtained with commercial diol-type and amide-bonded HILIC columns as well as in-house made amino-functionalized and bare silica columns (Daisogel) (the latter only for methylxanthines). The mentioned methylxanthines were also used to test the column stability of a freshly prepared 3- μm particle C-Choc HILIC column.

Characterization of Chocolate phase used in RP elution mode

As stated in the literature, saccharides undergo various reactions including rearrangements and degradation during the non-enzymatic browning, resulting in less polar products. Hence, it was important to characterize the introduction of considerable hydrophobic compartments. Thus, basic experiments were performed following the RP-LC test conditions according to Lämmerhofer et al. [37] listed in the “Experimental” section.

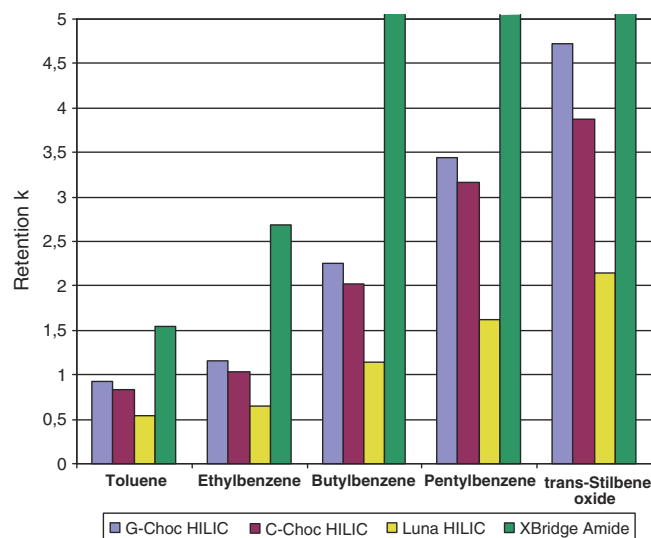


Fig. 3 Retention factor k alterations for toluene, ethylbenzene, butylbenzene, and pentylbenzene on G-Choc HILIC, C-Choc HILIC, Luna HILIC, and XBridge Amide in correlation with overall material hydrophobicity. Mobile phase, $\text{H}_2\text{O}/\text{ACN}$ (90:10, v/v). Additional chromatographic details are given in the “Experimental” section

Butylbenzene and pentylbenzene eluted around t_0 on any disaccharide-functionalized Chocolate HILIC column without separation, using a 60% aqueous hydroorganic mobile phase. Glucose as ligand primer achieves k values of 0.12 and 0.11 for pentylbenzene and butylbenzene, respectively. Even though this does not explicitly imply hydrophobic interactions, it points toward the expected depletion of the carbohydrate structural element into more hydrophobic moieties during the Maillard reaction. Consequently a lipophilicity test with only 10% ACN in combination with test set 4 was conducted. As a result, the overall retention on all Chocolate HILIC columns was prolonged and the introduced hydrophobic backbone imparted the ability to separate single CH_2 increments (see Fig. 3). Thereby, enhanced retention correlated with

Table 3 Retention values k obtained on packings with different ligand structures

	Retention factor k	
	DETP	Boc-Pro-Phe
G-Choc HILIC	0.60	0.77
M-Choc HILIC	0.55	0.50
L-Choc HILIC	0.58	0.52
C-Choc HILIC	0.40	0.39
RP-WAX-APS	2.68	9.79
RP-WAX-L-Choc	0.54	0.80
Luna HILIC	-0.03	-0.04

Mobile phase comprised $\text{ACN}/\text{H}_2\text{O}$ (40:60, v/v)+0.29% v/v AcOH , pH 6.0

the alkyl chain length and the test probes retained longer on the monosaccharide material than on the disaccharide-functionalized phase. Thus, the outcome is in agreement with our preliminary expectations. As can be deduced from Fig. 3 the overall hydrophobicity of our Chocolate HILIC columns is more pronounced than for the commercially available Luna HILIC column but less than for the XBridge Amide column. On the latter, only toluene and

ethylbenzene could be analyzed under the given conditions. Even after 70 min, neither butyl- nor pentylbenzene could be eluted, corroborating a pronounced hydrophobic backbone of this phase.

In addition to the examined absolute hydrophobicity and hydrophobic selectivity, the weak anion exchange character was evaluated by taking the retention of DETP and Boc-Pro-Phe (at 60% H₂O and pH 6.0) into account (see Table 3

Table 4 Log *D* values calculated for pH 5.0 and calculated p*K*_a values for test solutes of test set 1–6 in alphabetical order

	Log <i>D</i> ^{pH 5.0}	p <i>K</i> _{a1}	p <i>K</i> _{a2}	p <i>K</i> _{a3}	p <i>K</i> _{a4}	p <i>K</i> _{a5}	p <i>K</i> _{a6}
4-Hydroxybenzenesulfonic acid	0.85	8.66±0.13	-0.23±0.50				
4-Hydroxybenzoic acid	-5.16	9.22±0.13	4.57±0.10				
7-(2,3-Dihydroxypropyl)theophylline	-1.10	15.05±0.10	13.66±0.20	0.70±0.70	-4.05±0.20		
Acetone	-0.16						
Adenine	-0.11	10.01±0.27	3.91±0.45				
Adenosine	-1.04	14.46±0.70	14.09±0.70	13.11±0.70	3.40±0.50		
Aniline	0.79	4.91±0.10					
Benzyltrimethylammonium	-2.31						
Boc-Pro-Phe	0.34	15.84±0.20	3.56±0.10	-1.07±0.20	-4.16±0.40		
Butylbenzene	4.27						
Caffeic acid	0.42	12.79±0.31	9.97±0.10	4.04±0.40			
Caffeine	-0.13	0.73±0.70	-3.93±0.20				
Cytidine	-1.94	14.70±0.70	14.33±0.70	13.48±0.70	3.27±0.70		
Cytosine	-1.77	12.20±0.50	4.18±0.37				
Deoxyadenosine	-0.57	14.44±0.10	13.79±0.60	3.40±0.50			
Deoxycytidine	-1.89	14.44±0.10	14.03±0.60	3.59±0.70			
Deoxyguanosine	-1.36	14.44±0.10	13.96±0.60	9.31±0.20	1.90±0.50	-3.41±0.20	
Deoxyuridine	-1.70	14.44±0.10	14.05±0.60	8.39±0.20	-2.35±0.20		
DETP	-2.56	1.42±0.50					
Ethylbenzene	3.21						
Ferulic acid	0.42	10.22±0.31	4.04±0.40				
Guanine	-0.99	12.60±0.40	9.63±0.20	3.15±0.30	-3.26±0.20		
Guanosine	-1.72	14.63±0.70	14.26±0.70	13.37±0.70	9.23±0.20	1.69±0.50	-3.46±0.20
Melamine	-2.11	5.66±0.16	-3.26±0.14				
Myricetin	2.11	15.14±0.40	10.46±0.15	8.95±0.15	8.62±0.20	8.13±0.60	6.89±0.60
Naphthalene	3.45						
Propylbenzene							
Quercetin	2.07	12.55±0.35	9.46±0.10	8.74±0.20	8.14±0.60	6.90±0.60	
Theobromine	-0.72	9.90±0.50	0.59±0.70				
Theophylline	-0.18	8.60±0.50	1.70±0.70	-4.19±0.20			
Thymidine	-1.11	14.44±0.10	14.05±0.60	9.23±0.41	-2.31±0.40		
Thymine	-0.12	16.21±0.40	9.84±0.40	-1.61±0.40			
Toluene	2.68						
<i>trans</i> -Stilbene oxide	3.39						
Tyramine	-2.37	10.49±0.10	9.51±0.26				
Tyrosine	-2.12	10.01±0.15	9.35±0.15	2.25±0.10			
Uracil	-0.71	16.18±0.20	9.20±0.21	-1.65±0.20			
Uridine	-1.61	14.72±0.70	14.35±0.70	13.50±0.70	8.28±0.70	-2.41±0.70	

Data were estimated with ACD Labs 7.0 Log *D* and p*K*_a calculator

for results). Both co-elute and are only slightly retained on Chocolate columns, indicating only minor anion exchange capacities. The hydrophobic selectivity of our material should be able to further separate DETP and Boc-Pro-Phe. However, as previously mentioned, the given elution conditions were too strong for the weak anion exchange character. With the APS-5 μ -1 material, DETP and Boc-Pro-Phe still co-elute, yet, retention is quite enhanced (e.g., for DETP, $k_{C\text{-Choc}}=0.40$ and $k_{\text{APS-5}\mu\text{-1}}=2.59$) showing significantly higher anion interactions for the APS material. This result underlines the discussion in the “Experimental” section, confirming the reduction of chromatographically addressable amine groups for the Chocolate phases. After the dodecane modification of the L-Choc HILIC material (RP-WAX-L-Choc), the weak anionic character stays constant ($k_{\text{DETP L-Choc}}=0.58$, $k_{\text{DETP RP-WAX-L-Choc}}=0.54$) but Boc-Pro-Phe retention is enhanced due to the additional hydrophobic interactions (for Boc-Pro-Phe, $k_{\text{L-Choc}}=0.52$ and $k_{\text{RP-WAX-L-Choc}}=0.80$). In comparison, more active-amine groups were found on the APS-5 μ -1 material and could be modified with C₁₂ alkyl chains. Thus, as expected, we found comparable ionic interactions but a dramatic increase in hydrophobic selectivity on the RP-WAX-APS material ($k_{\text{DETP RP-WAX-APS}}=2.68$, $k_{\text{Boc-Pro-Phe RP-WAX-APS}}=9.79$).

Characterization of Chocolate phase in HILIC elution mode

Because the packing procedure for commercially available columns is specifically optimized, they exhibit slightly better peak performance than our homemade materials. Thus, comparison between our new and the commercial materials focuses mainly on retention and selectivity profiles. Whereas, in comparing the Chocolate phases with each other, higher peak performance was our main factor. From all the Chocolate materials, cellobiose as ligand primer achieved the highest plate numbers and was therefore the most favorable starting material for us. The cellobiose-functionalized Chocolate HILIC column even outperformed the efficiency of the commercial Luna HILIC.

In the first attempt, HILIC properties of the separation materials were evaluated using test set 1 (acids/bases/ neutrals/zwitterions) and 2 (nucleobases/nucleosides/deoxynucleosides) as standard HILIC test analytes (for name, structure, and corresponding log*D* values consult Fig. 1 and Table 4). Furthermore, two different pH values of the aqueous buffer fractions were applied (NH₄Ac pH 5 and NH₄FA pH 3) to screen possible pH effects on the chromatography. The ACN/H₂O (90:10, v/v) mobile phase mixtures each contained 10 mM salt. Acetone was used as void volume marker. Results are presented in Table 5 (for test set 1) and Table 6 (for test set 2).

Table 5 Column efficiency (N m⁻¹) and *k* values obtained for G-, L-, M-, C-Choc HILIC and APS-5 μ -1, Luna HILIC, and XBridge Amide during the HILIC mode evaluation of acids, bases, neutrals, and zwitterions at pH 3 and pH 5

	G-Choc		L-Choc		M-Choc		C-Choc		APS-5 μ -1		Luna HILIC		XBridge Amide	
	pH 5		pH 3		pH 5		pH 3		pH 5		pH 3		pH 5	
	<i>k</i>	N m ⁻¹	<i>k</i>	N m ⁻¹	<i>k</i>	N m ⁻¹	<i>k</i>	N m ⁻¹	<i>k</i>	N m ⁻¹	<i>k</i>	N m ⁻¹	<i>k</i>	N m ⁻¹
Acetone	0.00	31,000	0.00	28,000	0.00	29,000	0.00	26,000	0.00	32,000	0.00	27,000	0.00	41,000
4-HBA	0.36	8,000	4.69	50,000	0.36	8,100	6.27	57,000	0.30	10,000	4.78	54,000	0.31	50,000
4-HBSA	2.74	59,000	1.96	45,000	3.53	26,000	2.71	46,000	3.06	21,000	2.05	49,000	2.87	53,000
BTM	0.50	33,000	1.07	38,000	0.54	27,000	1.02	32,000	0.66	29,000	1.02	42,000	0.47	4,000
Melamine	2.32	50,000	2.05	50,000	3.16	58,000	2.96	51,000	3.27	61,000	2.94	52,000	2.89	64,000
Tyramine	1.73	25,000	3.94	15,000	2.20	24,000	4.30	32,000	2.30	48,000	3.89	27,000	1.64	60,000
L-Tyrosine	8.53	27,000	12.22	11,000	13.88	25,000	19.01	22,000	14.37	59,000	16.58	17,000	13.19	18,000
Aniline	-0.01	27,000	-0.02	23,000	-0.03	24,000	-0.03	20,000	-0.03	22,000	-0.04	19,000	-0.08	23,000
Toluene	-0.09	32,000	-0.10	25,000	-0.11	28,000	-0.11	23,000	-0.12	23,000	-0.11	22,000	-0.11	42,000
Ethylbenzene	-0.10	49,000	-0.11	24,000	-0.12	56,000	-0.12	21,000	-0.12	24,000	-0.12	23,000	-0.16	39,800

4-HBA 4-hydroxybenzoic acid, 4-HBSA 4-hydroxybenzene sulfonic acid

^aCompound detected as split peak

Table 6 Column efficiency ($N\ m^{-1}$) and k values obtained for G-, L-, M-, C-Choc HILIC and APS-5 μ -1, Luna HILIC, and XBridge Amide during the HILIC mode evaluation of nucleobases, deoxynucleosides, and nucleosides at pH 3 and pH 5

	G-Choc		L-Choc		M-Choc		C-Choc		APS-5 μ -1		Luna HILIC		XBridge Amide															
	pH 3	pH 5	pH 3	pH 5	pH 3	pH 5	pH 3	pH 5	pH 3	pH 5	pH 3	pH 5	pH 3	pH 5														
	k	$N\ m^{-1}$	k	$N\ m^{-1}$	k	$N\ m^{-1}$	k	$N\ m^{-1}$	k	$N\ m^{-1}$	k	$N\ m^{-1}$	k	$N\ m^{-1}$	k	$N\ m^{-1}$												
Adenine	1.99	29,000	2.39	26,000	2.42	31,000	2.81	29,000	2.48	35,000	2.52	28,000	2.10	16,000	2.61	38,000	1.16	6,000	2.27	35,000	1.02	29,000	1.14	33,000	2.03	40,000	2.21	39,000
Adenosine	1.95	41,000	2.36	46,000	2.66	45,000	3.08	44,000	2.78	48,000	2.81	49,000	2.35	31,000	2.95	54,000	1.96	39,000	3.39	55,000	1.04	47,000	1.14	51,000	2.78	57,000	2.97	54,000
Deoxyadenosine	1.46	34,000	1.67	36,000	1.88	31,000	2.07	30,000	1.98	34,000	1.90	32,000	1.72	35,000	1.99	35,000	1.19	8,000	2.06	20,000	0.77	27,000	0.83	27,000	1.82	23,000	1.93	22,000
Guanine	4.66	11,000	5.67	36,000	6.19	14,000	7.37	44,000	5.97	16,000	6.71	13,000	5.48	48,000	6.77	63,000	4.03	13,000	8.54	60,000	1.83	8,000	2.06	68,000	5.85	65,000	6.09	64,000
Guanosine	5.78	37,000	7.32	35,000	8.31	19,000	10.73	45,000	8.22	65,000	9.06	53,000	7.65	64,000	10.11	61,000	7.75	46,000	17.27	58,000	2.12	48,000	2.52	45,000	10.69	70,000	11.70	75,000
Deoxyguanosine	4.23	59,000	5.36	51,000	5.86	53,000	7.07	54,000	5.75	58,000	6.03	29,000	5.14	63,000	6.70	64,000	4.80	52,000	9.74	53,000	1.58	57,000	1.84	56,000	6.18	52,000	6.74	54,000
Cytosine	2.62	42,000	2.84	45,000	3.70	48,000	4.02	51,000	3.85	53,000	3.75	55,000	3.35	38,000	3.88	63,000	3.35	48,000	5.88	61,000	1.28	48,000	1.45	50,000	3.97	60,000	4.12	68,000
Cytidine	3.74	52,000	4.54	50,000	5.91	52,000	7.01	47,000	6.15	61,000	6.34	62,000	5.43	49,000	6.74	68,000	7.11	59,000	13.32	59,000	1.83	68,000	2.10	68,000	7.89	74,000	8.39	76,000
Deoxyuridine	2.81	41,000	3.28	44,000	4.10	44,000	4.69	47,000	4.31	50,000	4.28	52,000	3.73	56,000	4.54	56,000	4.15	46,000	7.61	63,000	1.37	48,000	1.56	46,000	4.80	72,000	5.12	68,000
Thymine	0.46	6,000	0.49	15,000	0.55	12,000	0.61	30,000	0.54	22,000	0.59	27,000	0.46	18,000	0.59	29,000	0.59	23,000	1.01	62,000	0.80	22,000	0.29	25,000	- ^a	- ^a	0.64	32,000
Thymidine	0.73	37,000	0.85	35,000	0.96	32,000	1.07	29,000	0.97	33,000	0.98	29,000	0.73	4,000	1.03	34,000	0.97	16,000	1.56	22,000	0.38	23,000	0.41	21,000	- ^b	- ^b	1.13	9,000
Deoxyuridine	0.86	22,000	1.01	25,000	1.19	21,000	1.36	22,000	1.22	22,000	1.25	22,000	1.10	24,000	1.30	23,000	1.31	13,000	2.10	27,000	0.36	27,000	0.50	13,000	1.43	21,000	1.55	21,000
Uracil	0.62	31,000	0.73	35,000	0.85	31,000	0.97	37,000	0.85	35,000	0.91	35,000	0.69	5,000	0.92	39,000	0.84	27,000	1.28	20,000	0.71	43,000	0.38	30,000	0.93	11,000	1.02	18,000
Uridine	1.29	35,000	1.61	43,000	1.94	35,000	2.33	43,000	1.97	45,000	2.12	47,000	1.75	25,000	2.22	51,000	2.49	43,000	4.163	53,000	0.46	12,000	0.79	43,000	2.79	49,000	3.00	46,000

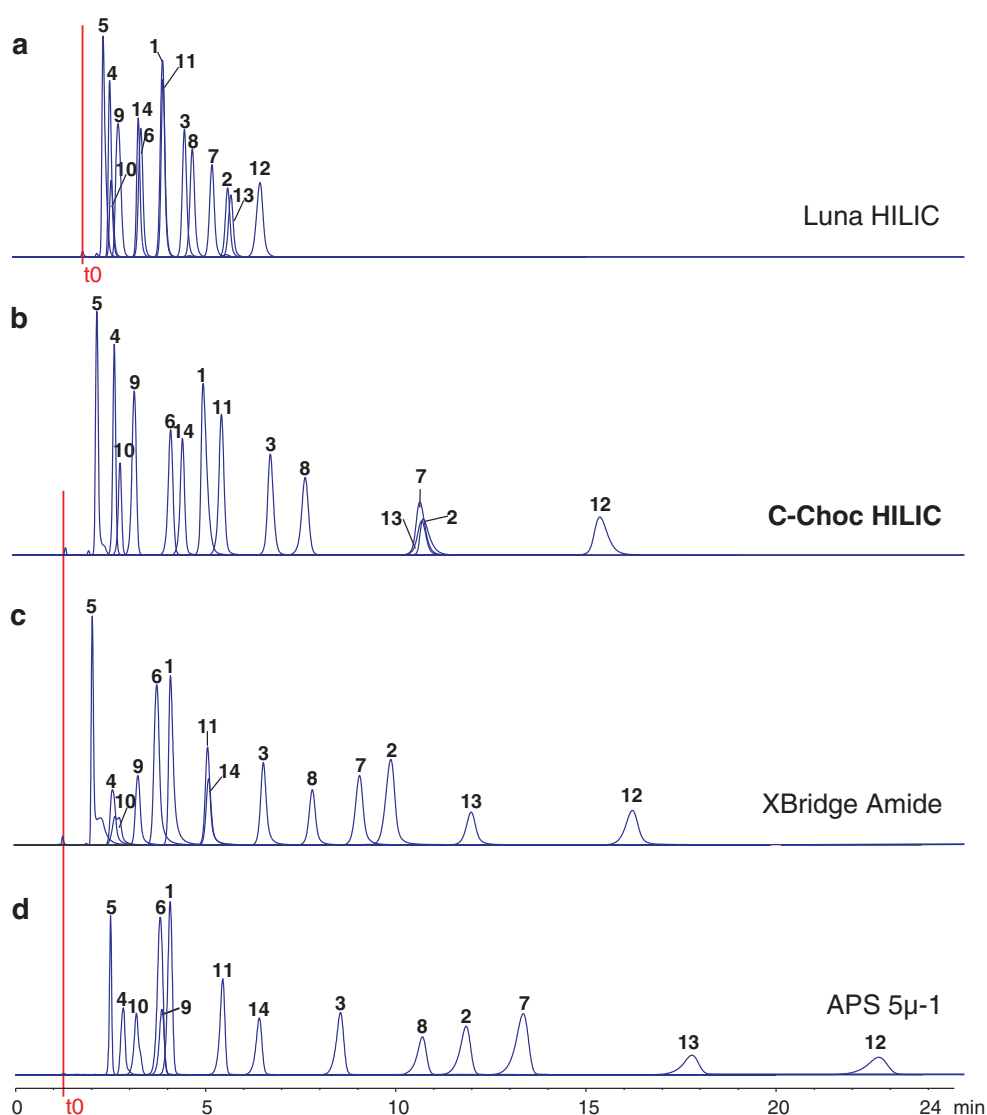
^a Compound detected as split peak

^b Compound detected as plateau peak

As already elucidated, at various amounts ACN in the mobile phase (40–100%), each column elutes aniline, toluene, and ethylbenzene with the void volume, and pH values show no impact on the chromatography. However, acidic and basic compounds are more prone to the effects of pH changes. For the APS-5 μ -1, Luna HILIC, and XBridge Amide column, k values for 4-hydroxybenzene sulfonic acid (4-HBSA) under both pH conditions are comparable within a range of 3–13%, whereas the loss in retention is more pronounced on our Chocolate HILIC material (20–50%). The latter packing seems to achieve retention with a mixed-modal mechanism (amine backbone plus Chocolate ligand) and solutes may get retained by ionic interactions in addition to their partition in the stagnant water-rich layer within the pores. At acidic pH the amine backbone is protonated, thus the retention of the strong acid 4-HBSA seems to be prolonged due to auxiliary ionic solute–ligand interactions with the charged backbone. Comparing 4-

HBSA with the weaker acid 4-hydroxybenzoic acid (4-HBA), the carboxylic group of the latter is protonated and therefore cannot undergo additional ionic interactions. Retention is comparably low on all tested columns. However, at pH 5 the polarity of 4-HBA increases due to the initial dissociation of the carboxylic group, resulting in a longer retention. Whether this is due to an increased partition or an activated ion attraction mechanism or a combination of both effects remains open. Benzyltrimethylammonium cation (BTM), tyramine, and tyrosine experience an increase in retention on the Chocolate HILIC, Luna HILIC, and XBridge Amide material when changed from pH 3 to 5. The Chocolate HILIC amine backbone may repel positively charged basic compounds at low pH and thereby shift their retention characteristics towards an increased partition to the organic layer. For the Luna HILIC this mixed-mode mechanism may not exist (see Table 5). Moreover, this observation is paralleled with a possible

Fig. 4 Comparison of obtained chromatograms for nucleobases (1–5), deoxynucleosides (6–9), and nucleosides (10–14) on **a** Luna HILIC, **b** C-Choc HILIC, **c** XBridge Amide, **d** APS-5 μ -1. 1 Adenine, 2 guanine, 3 cytosine, 4 uracil, 5 thymine, 6 deoxyadenosine, 7 deoxyguanosine, 8 deoxycytidine, 9 deoxyuridine, 10 thymidine, 11 adenosine, 12 guanosine, 13 cytidine, 14 uridine. Mobile phase comprised ACN/H₂O (90:10, v/v) + 10 mM NH₄Ac pH 5, temperature 25 °C. Additional chromatographic details are given in the “Experimental” section

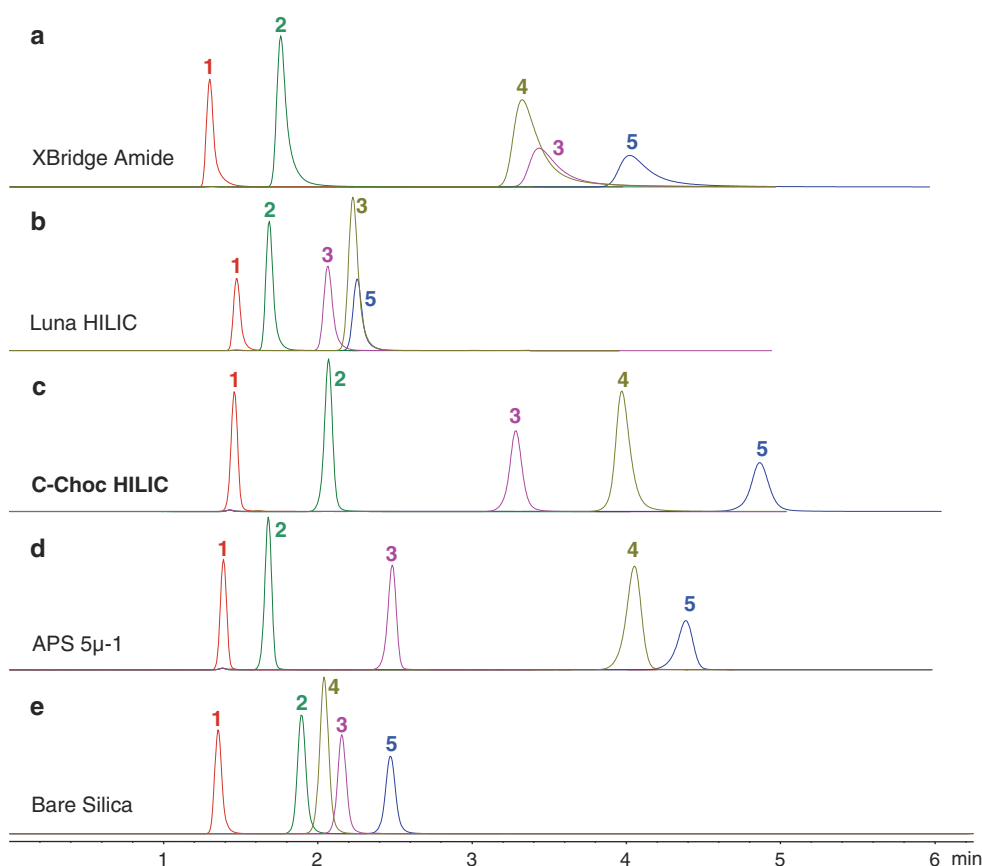


accessibility of residual surface silanol activity. The higher the pH the more silanol groups will be dissociated; hence, basic compounds experience an increase in retention via ionic solute–silanol interactions. The effect is stronger for tyramine, because the phenolic hydroxyl group, which BTM lacks, allows further HILIC-type interactions with the stationary water-rich layer, thus prolonging retention. In their recent study on solute–silanol interactions in HILIC, Bicker et al. [5] observed a true “mixed-mode” retention process composed of solute–silanol cation exchange and HILIC-type interactions for tyramine. On the basis of their study, we also consider mixed-modal interactions for tyramine on Chocolate HILIC columns but with additional anionic exchange interactions as a result of the amine backbone. On the APS-5 μ -1 column only BTM and tyrosine exhibit enhanced retention, whereas tyramine elutes earlier when the pH is changed from 3 to 5. Melamine retention is decreased on all columns by changing from pH 3 to 5, except for the Luna HILIC (see Table 5).

The neutral nucleobases (test set 2) with their conjugated nucleosides and deoxynucleosides retain according to the number of hydroxyl groups present and hence their polarity (e.g., guanine < deoxyguanosine < guanosine). Guanosine is thereby retained the longest on all columns, whereas

thymine is eluted first. Retention profiles and trends are shown in Fig. 4 and Table 6. However, the elution order of all 14 compounds is altered to some extent on all columns. Guanine, deoxyguanosine, and cytidine co-elute on the C-Choc HILIC column, whereas APS-5 μ -1 and XBridge Amide columns are able to resolve these compounds. Nevertheless, APS-5 μ -1 is not able to separate adenine, deoxyadenosine, and deoxyuridine. Uracil and thymidine are only partly resolved on the C-Choc HILIC column and unresolved on the XBridge Amide with thymidine even detected as a split peak. Additionally, adenine and uridine co-elute on the amide column. Luna HILIC was identified to possess overall limited HILIC separation capabilities for test set 2 under the chosen conditions, compared to the XBridge Amide, APS-5 μ -1, or Chocolate HILIC. Regarding the selectivity pattern, it seems that the Chocolate ligand has various “recognition sites” which enables superior selectivity for purine bases and pyrimidine bases in addition to the HILIC partition process, when compared to the commercially available columns. Thereby, selectivity seems to be more pronounced between the glycosylamines and their bases but less between the latter. As already mentioned, the formation of nitrogen-containing (aza-aromatic) heterocycles is likely during the Maillard reaction (in correlation with the brown color) which may add

Fig. 5 Comparison of obtained chromatograms for test set 3 (1 naphthalene, 2 caffeine, 3 theobromine, 4 theophylline, and 5 7-(2,3-dihydroxypropyl)-theophylline) on **a** XBridge Amide, **b** Luna HILIC, **c** C-Choc HILIC, **d** APS-5 μ -1, **e** Daisigel. Mobile phase comprised ACN/H₂O (98:2, v/v) + 2 mM NH₄Ac. Additional chromatographic details are given in the “Experimental” section



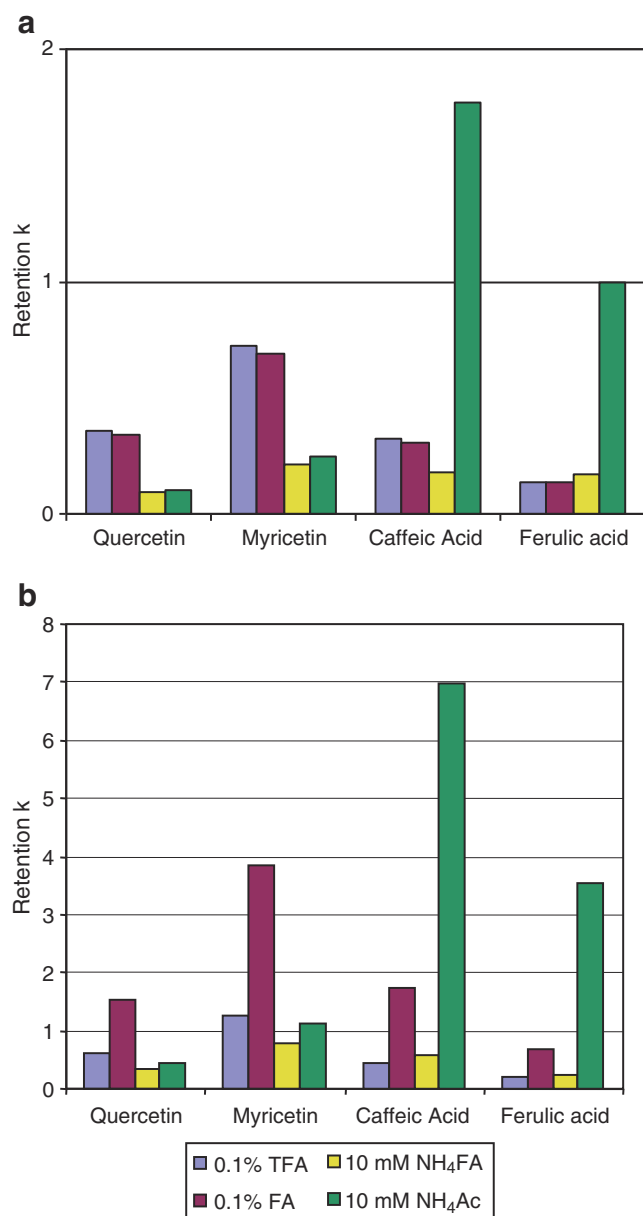


Fig. 6 Change of retention factor k for quercetin, myricetin, caffeic acid, and ferulic acid on **a** Luna HILIC and **b** C-Choc HILIC as a function of pH change. Mobile phase comprised ACN/H₂O (90:10, v/v) with a specific amount of additives (10 mM NH₄Ac, 10 mM NH₄FA, 0.1%FA, and 0.05%TFA)

additional π - π and shape selectivity increments. However, this would again relate to a contributing adsorption mechanism overlaying the partition model.

Lämmerhofer et al. [37] showed that the separation of methylxanthines, which are commonly separated on RP material, can also be performed in HILIC mode when applied on mixed-mode columns. In this context we screened our C-Choc HILIC column towards purine bases, and compared its separation with other dedicated HILIC columns including weak anion exchange columns. Thereby,

it could be demonstrated that the constitutional isomers theophylline and theobromine are challenging analytes to be separated, which resulted only at 98% ACN content of the mobile phase. It was not possible to fully resolve them on the commercially available columns or bare silica. However, theophylline and theobromine are not only resolved on our C-Choc HILIC phase but also on the APS-5 μ -1 column, with slightly different selectivity (see Fig. 5).

Although this result indicates a “purine selectivity” of our C-Choc HILIC, it cannot be clearly affirmed whether or not the separation is triggered to some extent by the protonated amino function of the backbone, due to the formed Maillard ligand motif, or by a mixed-mode mechanism.

HILIC WAX test: influence of buffer additive and pH on the ionic interactions

Test set 6 incorporates polyphenols and hydroxyl acids. With this set it should be possible to observe auxiliary ionic as well as hydrogen donor/acceptor interactions in addition to the partition effects under HILIC conditions. With ammonium buffers (NH₄Ac pH 5 or NH₄FA pH 3), retention was found to be mainly due to the pK_a of the test compounds, thus due to their polarity and the partition between the stationary water-rich phase and the organic-rich bulk eluent. Hence,

Table 7 Interday chromatographic stability for 150 injections of methylxanthines on C-Choc HILIC-3 material over 3 days (50 injections/day), evaluated using standard chromatographic parameters

	Naphthalene	Caffeine	Theobromine	Theophylline
	Plate number ($N\ m^{-1}$)			
Mean	33,114	48,543	54,893	44,358
RSD	496	531	980	974
%RSD	1.50	1.09	1.79	2.20
	Tailing			
Mean	0.90	0.91	0.82	0.57
RSD	0.01	0.01	0.01	0.02
%RSD	0.66	0.68	1.47	3.18
	Retention factor (k)			
Mean	0.00	0.36	1.18	1.94
RSD	0.00	0.00	0.01	0.02
%RSD	0.00	0.55	0.94	1.07
	$\alpha_{\text{theophylline/theobromine}}$			
Mean				1.64
RSD				0.02
%RSD				1.37

Mobile phase comprised ACN/H₂O (98:2, v/v) + 2 mM NH₄Ac pH 5; flow rate 1 mL/min; temperature 25 °C

similar effects were observed for the Luna HILIC and Chocolate HILIC phases. Using TFA instead of FA an additional effect was introduced and caused by the WAX backbone. With TFA the amino group more easily formed a hydrophilic ion pair, which “deactivates” the ionic interactions of acidic analytes thus giving the preference for HILIC-type interactions. As a result, one observes a shorter retention for all four test compounds compared to FA as additive (see Fig. 6b). The diol phase (Luna HILIC) does not exhibit this effect (see Fig. 6a). Another observation is the exchanged elution order on both columns. With FA and TFA, all compounds are fully protonated and the retention correlates with the amount of available hydroxyl groups (myricetin > quercetin > caffeic acid > ferulic acid) (for chemical structures see Fig. 1) thus referring to a HILIC mechanism. Those basic experiments demonstrated that by using different mobile phase additives and pH values, Chocolate HILIC phases can be superior in terms of selectivity adjustments, compared to pure diol phases.

To test the stability of our material, a new column with cellobiose as ligand primer but with a particle size of 3 μm (C-Choc HILIC-3), was generated. The methylxanthine test set (test set 3) was used to examine the long-term stability. As mentioned before, theobromine and theophylline are a crucial pair to be separated on HILIC columns, yet very well resolved on our materials. A loss or degradation of our ligand should result in a loss of selectivity. Multiple injections of the test set 3 were carried out to test the column stability in terms of retention factor k , selectivity α (theobromine/theophylline), and efficiency ($N\text{ m}^{-1}$) (see Table 7, Fig. S3 in the “Electronic supplementary material”). The total mobile phase volume that was pumped through the column during the xanthine reproducibility study amounts to 1,500 column volumes. The stability was evaluated by calculating the mean and percent relative standard deviation (%RSD) of three sets with 50 injections and a total number of 150 injections. Each set was achieved on a different day to evaluate the intraday reproducibility (mean and %RSD within each set) and interday reproducibility (mean and %RSD of all 150 injections). Results are listed in Table 7.

The column stability test revealed that the C-Choc HILIC-3 column is stable over a long period of time. Both intraday and interday %RSD regarding the retention factor are under 1%, except for the interday deviation of theophylline which is 1.1%. The interday column performance with reference to the plate number is below 2% for caffeine and theobromine and under 2.5% for theophylline.

In addition to the methylxanthine reproducibility, we analyzed test set 1 and 2 at pH 5 and 3 after 1 or 1,500 column volumes to see the stability of the column towards charged acidic and basic compounds. Comparing the column performance with test set 2 at pH 5 versus pH 3,

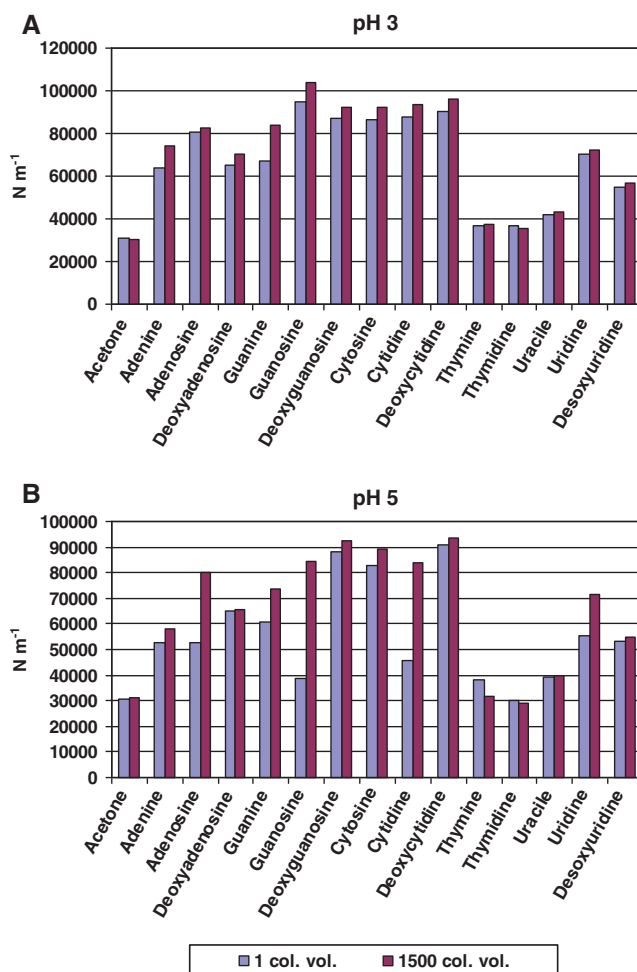


Fig. 7 Plate numbers ($N\text{ m}^{-1}$) achieved for C-Choc HILIC-3 column at **a** pH 3 and **b** pH 5 after 1 and 1,500 column volumes (col. vol.) respectively. Mobile Phase: ACN/ H_2O (90:10, v/v)+10 mM NH_4FA (pH 3) or 10 mM NH_4Ac (pH 5). Additional chromatographic details are given in the “Experimental” section

we could observe slightly better peak shape and enhanced retention for most of the analytes for the aged column. Figure 7 shows the achieved plate numbers at pH 5 and 3 for 1 or 1,500 column volumes. Especially at pH 5, prolonged retention was observed. During the nucleoside/nucleobase test at pH 5 the plate number increased significantly for the nucleosides. However, it is noticeable that the column runs more stably regarding the analyte retention and plate number when operated at pH 3 than at pH 5. Overall, a total flow-through of around 2,200 column volumes was applied to the C-Choc-3 μ .

Conclusions

The straightforward concept of immobilizing reducing sugars as ligand primers on aminopropyl-modified silica particles by applying a Maillard reaction scheme was

demonstrated. As a result, polar stationary phases suitable for use in HILIC mode were created. Out of all the sugars investigated, cellobiose was found to be the most promising primer resulting in the most efficient packing material. Cellobiose is composed of two glucose subunits which are clearly superior to other reducing sugars in the course of Maillard product formation on a surface.

High temperature (120 °C) and water-free media (toluene) during the immobilization step showed most promising results in terms of reproducibility and C/N ratio. Higher values indicate less depletion of primer and/or more stable phases. However, the presented “controlled” and reproducible Maillard reaction on surfaces is not yet fully understood in terms of the reaction cascade and future work will be carried out along that line. In the course of the comprehensive evaluation of Chocolate phases and columns it became evident that they are used preferentially in the HILIC mode. They are largely deficient for hydrophobic interactions and show no retention and separation for pure lipophilic compounds. The additional amine backbone, which is absent in a diol-bonded phase (i.e., Luna HILIC), exhibits quite an impact on the separation of methylxanthines, purines, and pyrimidine bases possibly due to underlying ionic interactions. Selectivity and elution order can be altered to some extent by variations in mobile phase pH, which can be of advantage compared to pure diol phases for certain applications. In terms of retention mechanisms, the new Chocolate phases behave as mixed-modal stationary phases when used in the HILIC mode, meaning that adsorption (including ionic interactions) and partition phenomena are responsible for the observed retention and selectivity characteristics.

Acknowledgements The financial support of our industry partner AstraZeneca (Mölnådal, Sweden) is gratefully acknowledged. Our special thanks go to Shalini Andersson and Tomas Leek for constructive discussions and valuable scientific input. The authors also thank Tobias Hüser for his strong help in synthesizing the different Chocolate HILIC columns.

References

- Alpert AJ (1990) *J Chromatogr* 499:177–196
- Lämmerhofer M (ed) (2008) Special issue: hydrophilic interaction chromatography. *J Sep Sci* 31(9):1419–1653
- Nguyen HP, Schug KA (2008) *J Sep Sci* 31(9):1465–1480
- Hsieh Y (2008) *J Sep Sci* 31(9):1481–1491
- Bicker W, Wu J, Yeman H, Albert K, Lindner W (2010) *J Chromatogr A*. doi:10.1016/j.chroma.2010.10.073
- Hemström P, Irgum K (2006) *J Sep Sci* 29(12):1784–1821
- McCalley DV (2010) *J Chromatogr A* 1217(20):3408–3417
- Fountain KJ, Xu J, Dieh DM, Morrison D (2010) *J Sep Sci* 33(6–7):740–751
- Guo Y, Gaiki S (2005) *J Chromatogr A* 1074(1–2):71–80
- Chauve B, Guillaume D, Cléon P, Veuthey JL (2010) *J Sep Sci* 33(6–7):752–764
- Ikegami T, Tomomatsu K, Takubo H, Horie K, Tanaka N (2008) *J Chromatogr A* 1184(1–2):474–503
- Wu JY, Bicker W, Lindner W (2008) *J Sep Sci* 31(9):1492–1503
- Bicker W, Wu JY, Lämmerhofer M, Lindner W (2008) *J Sep Sci* 31(16–17):2971–2987
- Chirita R-I, West C, Finaru A-L, Elfakir C (2010) *J Chromatogr A* 1217(18):3091–3104
- Ali IA-E, Hassan Y (2007) *Curr Pharm Anal* 3(1):71–82
- Yashima E (2001) *J Chromatogr A* 906(1–2):105–125
- Mitchell C, Desai M, McCulla R, Jenks W, Armstrong D (2002) *Chromatographia* 56(3):127–135
- Soukup K, Tsoukali H, Raikos N, Gika H, Wilson ID, Theodoridis G (2009) *J Sep Sci* 33(6–7):716–727
- Huisden RE, Kraak JC, Poppe H (1990) *J Chromatogr* 508(2):289–299
- Sun WZ, Yuan LM (2009) *J Liq Chromatogr Relat Technol* 32(4):553–559
- Wang JY, Zhao F, Zhang M, Peng Y, Yuan LM (2008) *Chin Chem Lett* 19(10):1248–1251
- Guo Z, Lei A, Liang X, Xu Q (2006) *Chem Commun* (43):4512–4514
- Guo Z, Lei A, Zhang Y, Xu Q, Xue X, Zhang F, Liang X (2007) *Chem Commun* (24):2491–2493
- Moni L, Ciogli A, D'Acquarica I, Dondoni A, Gasparini F, Marra A (2010) *Chem Eur J* 16(19):5712–5722
- Maillard LC (1912) *Compt Rend* 154:66–68
- Schleicher E, Schieberle P, Hoffmann T, Somoza V (eds) (2008) *The Maillard reaction: recent advances in food and biomedical sciences*. Wiley–Blackwell, New York
- Cerny C (2008) *Ann N Y Acad Sci* 1126(1):66–71
- Friedman M (1996) *J Agric Food Chem* 44(3)
- Fujimaki M, Namiki M, Kato H (eds) (1986) *Developments in food science, 13: amino-carbonyl reaction in food and biological systems*. Kodansha, Tokyo; Elsevier, Amsterdam
- Hodge JE (1953) *J Agric Food Chem* 1(15):928–943
- Ikan R (1996) *The Maillard reaction*. Wiley, Chichester
- Nursten HE (2005) *Maillard reaction: chemistry, biochemistry and implications*. Royal Society of Chemistry, Cambridge
- Westphal G, Kroh L (1985) *Food/Nahrung* 29(8):765–775
- Westphal G, Kroh L (1985) *Food/Nahrung* 29(8):757–764
- Yaylayan VA (1997) *Trends Food Sci Technol* 8(1):13–18
- Phenomenex (2007) *Explore Luna HILIC—discover HPLC polar retention*. Phenomenex, Torrance
- Lämmerhofer M, Richter M, Wu J, Nogueira R, Bicker W, Lindner W (2008) *J Sep Sci* 31(14):2572–2588
- Purlis E (2010) *J Food Eng* 99(3):239–249
- Etienne M, Walcarus A (2003) *Talanta* 59(6):1173–1188

Supporting Information for Appendix I

Chocolate HILIC phases: development and characterization of novel saccharide-based stationary phases by applying non-enzymatic browning (Maillard reaction) on amino-modified silica surfaces

G. Schuster, W. Lindner.

Journal of Analytical and Bioanalytical Chemistry 2011, 400, 2539-2554.

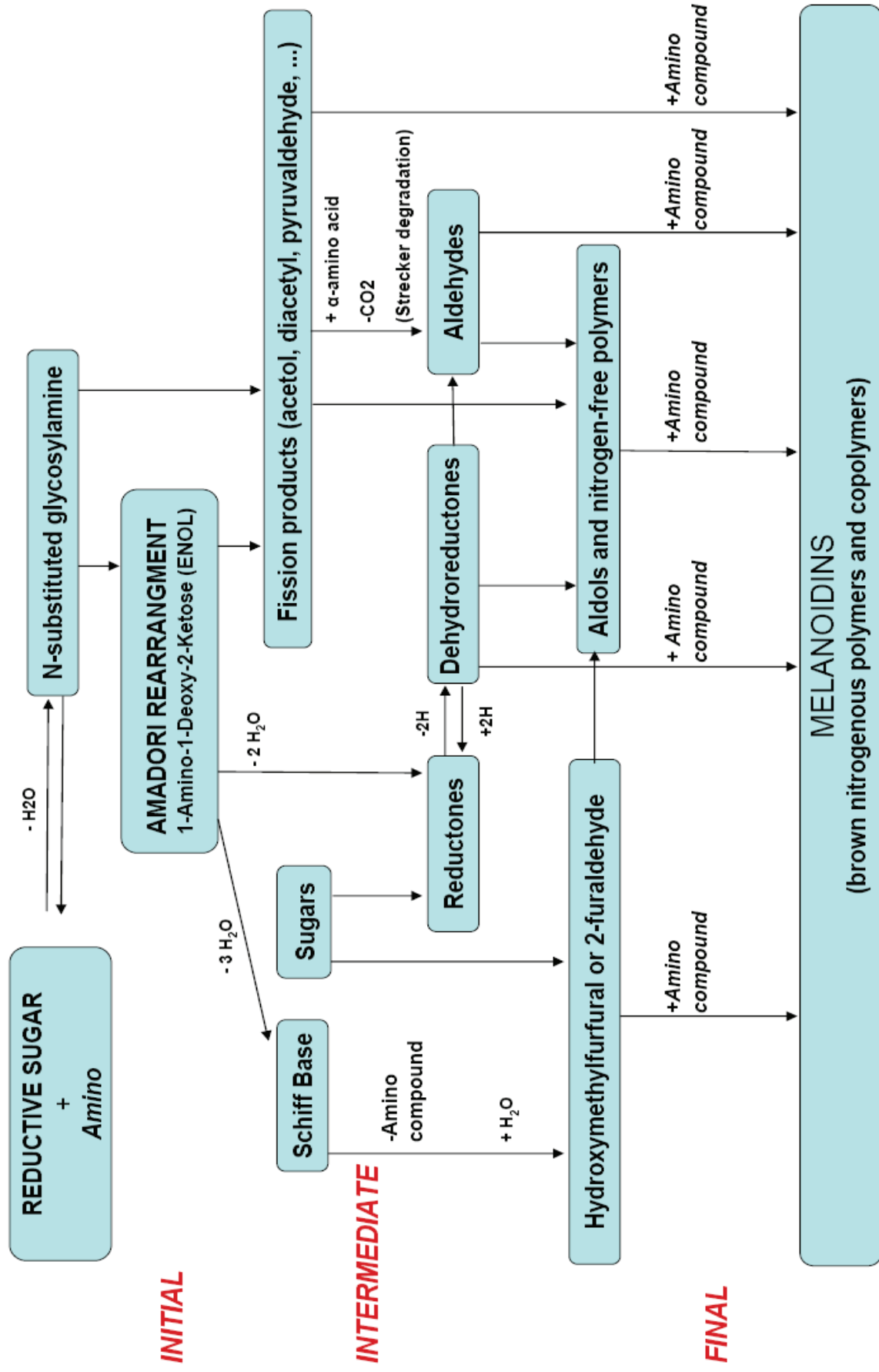


Fig. S1 Maillard reaction pathway scheme, modified from Hodge JE (1953). *J. Agric. Food Chem.* 1 (15):928-943

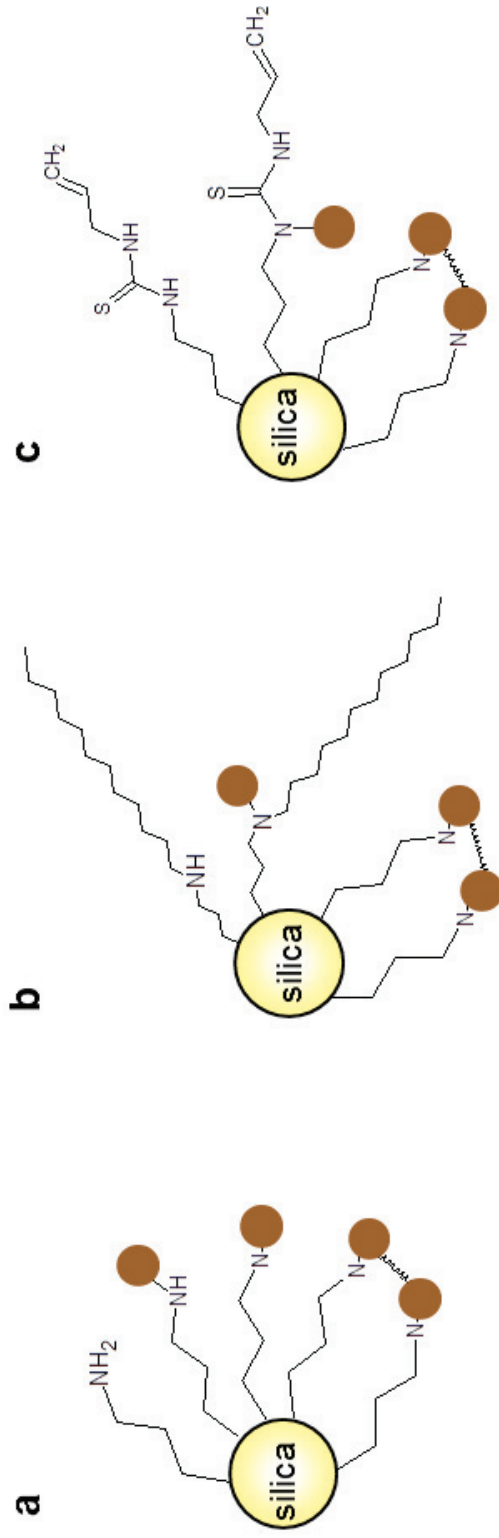


Fig. S2 Chocolate HILIC derivatives: **(a)** Chocolate HILIC, **(b)** RP-WAX-Choc, **(c)** Allylthiourea modified Choc HILIC

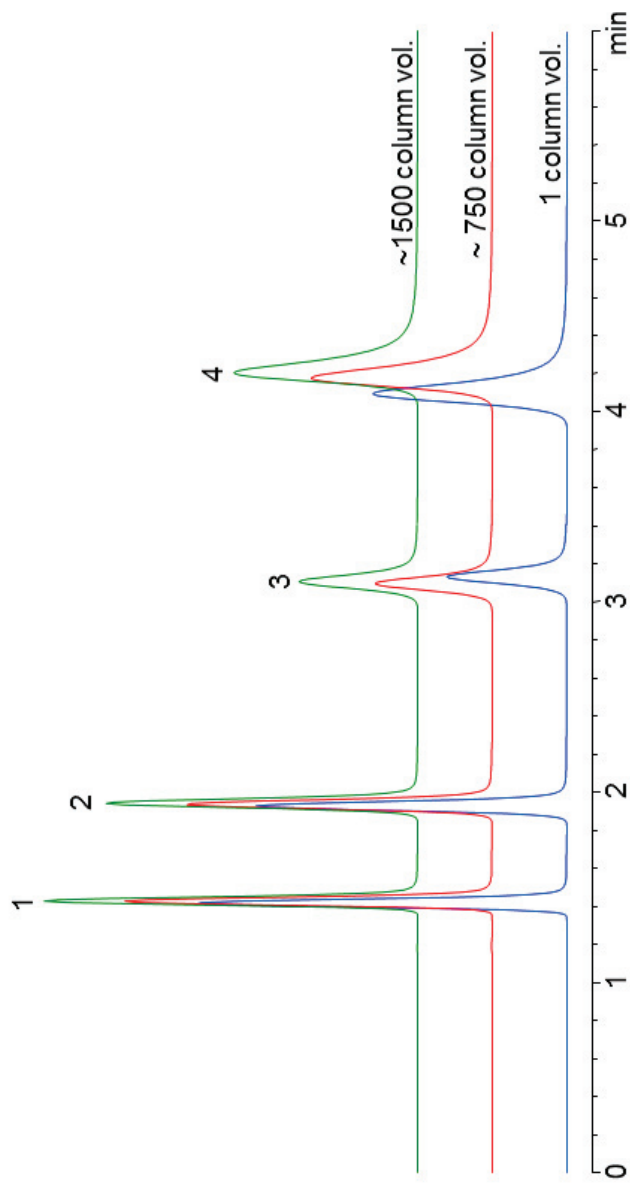


Fig. S3 Long-term stability of C-Choc HILIC-3, stability of chromatographic runs from 1 to 1500 col. vol.
 Mobile Phase: ACN/H₂O (98:2; v/v) + 2 mM NH₄Ac pH 5; flow:1 ml/min, temp:25°
 (1) naphthalene, (2) caffeine, (3) theobromine, (4) theophylline.
 Additional chromatographic details are given in the experimental section.

APPENDIX II

Comparative characterization of hydrophilic interaction liquid chromatography columns by linear solvation energy relationships.

G. Schuster, W. Lindner.

Journal of Chromatography A 2012, 1273, 73-94



Comparative characterization of hydrophilic interaction liquid chromatography columns by linear solvation energy relationships[☆]

Georg Schuster, Wolfgang Lindner*

Department of Analytical Chemistry, University of Vienna, Waehringer Strasse 38, A-1090 Vienna, Austria

ARTICLE INFO

Article history:

Received 3 October 2012
Received in revised form
23 November 2012
Accepted 26 November 2012
Available online 5 December 2012

Keywords:

HILIC
Hydrophilic interaction liquid chromatography
LSER
Linear solvation energy relationship
Column characterization

ABSTRACT

22 commercially available and home-made stationary phases with different surface modifications were compared under hydrophilic interaction liquid chromatographic (HILIC) conditions. The column set comprised neutral, basic, acidic, zwitterionic and mixed surface modifications. Retention data of 68 differently structured test solutes were acquired to generate retention models based on a linear solvation energy relationship (LSER) approach. A recently modified solvation parameter model with two additional molecular descriptors was evaluated in terms of its universal applicability when electrostatic forces are enabled in addition to predominant partition phenomena. The suggested method could not be confirmed to be a standardized way to characterize HILIC systems when different operating conditions are applied. However, the significant contribution of the recently introduced charge descriptors (D^- and D^+) on explaining the interactions within HILIC systems was confirmed. The solvation parameter model was found to be a useful tool in the course of column development, to affirm or dismiss the preceding educated guess on how certain immobilized ligands will behave. Acidic modified surfaces (stationary phases) exhibit a very small hydrogen bond acceptor property and are less versatile when it comes to an even distribution of solutes along the retention window. Furthermore, the results indicate that basic and neutral columns are more preferable for HILIC applications and might explain why only a limited variety of strong acidic modified HILIC columns, although found in literature, are available commercially.

© 2012 Elsevier B.V. All rights reserved.

1. Introduction

The name hydrophilic interaction liquid chromatography (HILIC) roams the realm of scientific writing since the 1990s with its first appearance by Alpert [1]. Even though this publication gave birth to the name HILIC, the concept of a polar sorbent in combination with a hydro-organic mobile phase (MP) already dates back to the early days of liquid chromatography (analysis of carbohydrates [2,3]). Initially, Alpert suggested a partition driven retention mechanism in which the analytes distribute between the stationary phase (SP) which consists of a stagnant water rich layer adsorbed onto the polar sorbent (Si-OH) and the water poor organic bulk phase without contributions from the sorbent backbone. This “pseudo” SP is formed using a MP composition of 2–40% water in acetonitrile (ACN). Although working groups tried to elucidate the existence/thickness and to ascribe the actual contribution of the water layer to the HILIC retention mechanism, fully conclusive results could not be described so far [4–8]. Furthermore, in addition

to the hydrophilic partition, various publications on applications but also mechanistic studies showed the existence of electrostatically driven (repulsive and attractive) interaction effects under HILIC conditions which originate from interactions between the analytes and the solid sorbent (e.g. [9–16]). Thus, at the current state a true mixed mode retention mechanism is widely accepted to facilitate retention in HILIC. For a better illustration, we introduce the “LC Retention Troika” (Fig. 1) which emphasizes the intermolecular interplay between the solutes, the SP and the MP.

HILIC applications can be found in the fields of e.g. glycomics [17–20], metabolomics [21–24], peptidomics [9,25–29] and the analysis of polar compounds from natural products [30–33]. More and more different polar SPs are now commercially available and even more are published in scientific literature. While originally bare silica was used as polar sorbent, these newly developed phases feature various silica surface modifications such as aminopropyl, sulfobetaine, amide, and urea [4,34–37]. Due to the mixed modal character of HILIC, these functionalities introduce additional interaction sites which may not always be predicted in their effect on the overall observed chromatographic selectivity by educated guess. Thus, it is important to develop chromatographic tests which can characterize, compare and segment SPs into groups of similar selectivity. To handle this task, several tests are accepted in RP-LC (e.g. Tanaka and Engelhardt test). For a deeper insight we

[☆] Presented at the 29th International Symposium on Chromatography, Torun, Poland, 9–12 September 2012.

* Corresponding author. Tel.: +43 1 4277 52300; fax: +43 1 4277 52301.
E-mail address: wolfgang.lindner@univie.ac.at (W. Lindner).

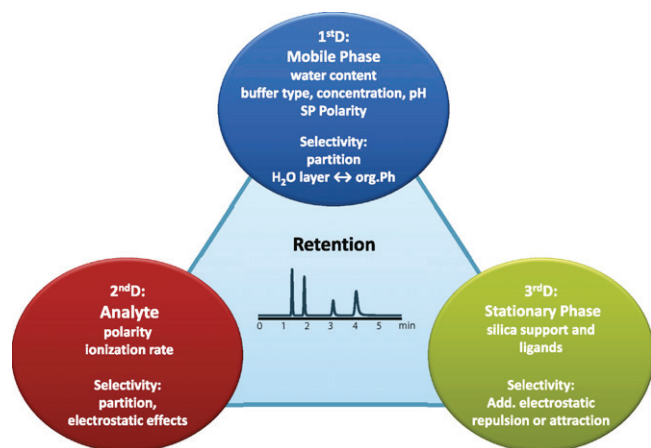


Fig. 1. LC retention "Troika".

suggest the review on such column classifications by Lesellier and West [38]. Although Kawachi et al. [39], Dinh et al. [40] and the group of Lucy [41] published tests on how to probe the interaction mode in HILIC, they are not yet as established and universally recognized as the former mentioned RP tests. There are two main characterization approaches. One method is to analyze different test solutes and only verbally describe the columns with regard to the observed retention behaviors. Another way is the application of statistical methods like hierarchical cluster analysis (HCA), principal component analysis (PCA) or multiple linear regression (MLR). The chromatographic results are added to the algorithm to describe and get an insight into the mechanistic contributions, retention behavior, but also to group the tested SPs. The prediction of retention and selectivity becomes more challenging as more different types of HILIC columns become available. Thus, we aimed by this contribution to help to further understand the importance of a well-known column chemistry in order to choose alternative HILIC columns to gain a wide spread range in selectivity. For this purpose, we applied the previously published methodology by Chirita et al. [42] which is based on a MLR approach and more precisely on linear solvation energy relationships (LSER). The goal was to evaluate this method during column development as it was stated to may be a general approach for characterizing HILIC columns according to the predominant retention mechanism. Since one focus of our working group is column development, it is a crucial factor to also incorporate and examine the underlying electrostatic effects of the packing material. Therefore, we modified the MP composition according to the amount of buffer salt and water. On the one hand, this was done to get a grasp on the already mentioned additional electrostatic effects and on the other hand to facilitate sufficient retention on weakly retaining columns. Another change was the choice of test solutes since we wanted to use a different set of analytes that might be more diverse in their chemical nature. Opposed to Ref. [42] all LSERs were performed with *D* descriptors calculated for pH 3 and not 5.4. The argumentation for this decision is more closely discussed in Section 4.1. Furthermore, we used hierarchical cluster analysis (HCA) to group the tested columns by their obtained coefficients. As a conclusion we want to see if this methodology can direct column development strategies and give an insight into which factors are important to gain a well performing HILIC column.

2. Theory

In the following section, only a short introduction on LSER will be given, mainly focusing on the equations applied throughout this study. We do not think that it is important to enroll the history

of LSER since it has already been published by several authors. We highly recommend Refs. [42,43] to get a deeper insight into the field of solvation parameter models, their historical development and their advantages and limitations. Since the origin of liquid chromatography, scientists have been trying to investigate the interactions and forces that underlie the retention and the selectivity mechanism which take place in chromatographic systems while analyzing solutes. One approach is the application of LSER models. Thereby a linear relationship is estimated between the logarithm of achieved retention factor ($\log k$) values and solute descriptors using MLR. Thus, the chromatographic system is described by parameters determined by combining a multitude of measured retention factors of test solutes with their individual chemical property descriptors. Abraham solute parameters have found particularly acceptance in the field of column characterization. The big advantage of LSER models is the quantitative character of the obtained phase descriptors (regression coefficients). They can allow a direct comparison of the influential parameters which contribute to the observed retention mechanism. The drawback, however, is that in contrast to structure finding methodologies, like PCA or HCA, a valid linear model must be developed prior to the statistical evaluation which will provide the best regressions. Not only the goodness of fit by means of *t*-scores, *F* statistics and standard deviation but also the chemical reasonability of the obtained coefficients is consulted to evaluate the obtained results. Although several publications can be found throughout literature dealing with column evaluation under reversed phase (RP), normal phase and supercritical fluid chromatography (SFC) conditions [44–49] only few publications are available on the characterization of columns used in HILIC mode [42,50]. The reason for this might be the diverse retention mechanisms within HILIC columns. The model must be able to evaluate the adsorptive and electrostatic interactions between the analytes and the support but also the partition of the solutes between the formed water rich stagnant layer and the water poor hydro-organic bulk MP. Recently, Chirita et al. published an article about the application of LSER models on zwitterionic SPs [42]. We applied this methodology for our column study and evaluated the universal application thereof.

Eq. (1) shows the LSER equation which correlates the retention of solutes in a specific system to their characteristics as described by the Abraham parameters.

$$\log k = c + eE + sS + aA + bB + vV \quad (1)$$

The capital letters refer to solute descriptors, hence the particular interaction properties of the analytes, while italic lower case letters are computed regression coefficients which describe the system constants related to the complementary property of the SP.

The system constant *c* is independent of the probe solutes and is dominated by the phase ratio, specific column parameters as e.g. porosity as well as other properties that do not depend on solute characteristics and the selected solute descriptors [46]. However the interpretation of the intercept is not straightforward due to the complex contributions of the void volume and other interactions.

E displays polarizability contributions from *n* and π electrons and is the excess molar refraction calculated with the McGowan's volume (MR_x) minus the molar refraction of an alkane with the same McGowan volume (Eq. (2)) [51].

$$E = (MR_x) - 2.83196V + 0.52553 \quad (2)$$

Solute dipolarity and polarizability is characterized by the *S* parameter which is determined experimentally. *A* and *B* express the overall hydrogen bond acidity (H-donor) and basicity (H-acceptor), respectively. *V* is a measurement of the cavity effect, i.e. the endoergic effect of disrupting solvent–solvent bonds. It is displayed by the McGowan characteristic volume in $\text{cm}^3 \text{mol}^{-1}/100$ [51]. The

regression coefficients c , e , s , a , b , and ν reflect the magnitude of difference for that particular property between the MP and SP. Thus, it is important to keep in mind that a displays the system's (SP and stagnant water rich layer) hydrogen bond basicity (H-acceptor) and b the system's hydrogen bond acidity (H-donor).

Due to the restriction of Abraham parameters to neutral compounds any difference in the ionization state of analytes under different MP compositions cannot be represented by Eq. (1). Thus ionized species are treated equal to their neutral form. However, the ionization state has a high impact on the polarity of the solute which, in turn, has a strong effect on the retention in HILIC systems. The group of Claire Elfakir modified Eq. (1) with two additional parameters to include the analytes charge states into the solvation equation (Eq. (3)). The solute D parameters are calculated according to Eqs. (4) and (5).

$$\log k = c + eE + sS + aA + bB + \nu V + d^- D^- + d^+ D^+ \quad (3)$$

$$D^- = \frac{10^{(\text{pH}^* - \text{pK}^*)}}{1 + 10^{(\text{pH}^* - \text{pK}^*)}} \quad (4)$$

$$D^+ = \frac{10^{(\text{pK}^* - \text{pH}^*)}}{1 + 10^{(\text{pK}^* - \text{pH}^*)}} \quad (5)$$

Originally pH^* is the effective pH obtained for the mixed hydro-organic MP and is different from the pH of the aqueous buffer. However, the estimation of pH^* is more difficult as the pH electrode needs to be calibrated with calibration buffers representative for the organic medium. Therefore the apparent pH is often used, which is the pH measured for a water poor hydro-organic solvent but the system is calibrated with aqueous calibration buffers. The additional D parameters facilitate the description of the retention for acidic, basic and zwitterionic species. For neutral species, D^+ and D^- are zero and Eq. (3) is reduced to Eq. (1) [42]. Although several approaches for the incorporation of the analyte's ionization state can be found in literature, D descriptors were applied since they are rather easy to compute and result in a convenient goodness of fit.

3. Experimental

3.1. Materials

HPLC gradient grade ACN and acetone were supplied by VWR International (Vienna, Austria). Formic acid (FA) and ammonium formate (NH_4FA), both of analytical grade, were obtained from Sigma-Aldrich (Vienna, Austria). All 68 test compounds were of analytical grade and commercially available by different manufacturers. Table 1 lists the solutes with their structures and associated molecular descriptors. Water was bi-distilled in-house. The SPs used throughout the study alongside their dimensions, structures and manufacturers can be found in Table 2.

3.1.1. Sample and eluent preparation

Depending on their solubility, analytes were dissolved in concentrations of 0.02–1.0 mg mL^{-1} in ACN/ H_2O (v/v) ratios of either 80:20 or 90:10. NH_4FA stock solutions were prepared by dissolving 100 mM NH_4FA in bi-distilled water. The pH values of the aqueous buffers were adjusted to pH 3 with FA. Eluents were obtained by mixing ACN and the buffer stock solutions, resulting in a MP composed of ACN/buffer (90:10; v/v) (10 mM NH_4FA). The apparent MP pH was measured with a glass electrode calibrated with aqueous calibration buffers and was pH 5.4. Throughout the paper, as suggested by IUPAC, we will refer to the aqueous pH and the apparent hydro-organic pH as pH and pH^* , respectively.

3.1.2. Instrumentation

Chromatographic runs were carried out on a 1200 series HPLC system from Agilent (Waldbronn, Germany) equipped with a diode array detector. Elution was achieved under isocratic conditions with a linear flow velocity of 1.6 mm/s. The column compartment temperature was set to 25 °C throughout the study. Columns were equilibrated with about 15–20 column volumes to guarantee stable equilibrium situations. The detection wavelengths were 254 nm and 230 nm. Analytes were injected in volumes of 2 μL . Acetone was used as a void time marker.

3.2. Methods

Only the modifications compared to Ref. [42] shall be discussed in this part. As it is important to characterize newly developed sorbents, the additional interactions resulting from the background modifications (interaction sites) should be considered as well. Hence, we chose a lower salt content and changed it from 20 mM to 10 mM formate buffer. Another alteration was the increase of organic solvent from 80 to 90% ACN. Since different type of columns were evaluated during the study, from home-made to commercially available materials and with diverse SP chemistry, we had to increase the ACN amount to be able to facilitate sufficient retention on “weakly HILIC retaining” sorbents. We selected these conditions as most suitable compromise.

As stated in the introduction, a different set of analytes as described in [42] was used in order to further evaluate the usability and universality of the given method in terms of solute choice. We introduced permanently charged zwitterionic compounds to expand our analyte set according to a more diverse chemical nature. However, this approach might lead to outliers or leverage values. Thus, we found it more convenient to perform a robust regression (robR) compared to ordinary least squares regression (OLSR). Like in OLSR, robR seeks to find relationships between independent variables and a dependent variable. Least square regression estimates may be influenced by outliers or influential observations resulting in misleading results. One way would be to remove these influential data from the least-square fit. Another approach is the use of robust methods. They can be applied if outlying observations are found which should stay in the analysis since they are not data entry errors and still belong to the same population as the rest of the observations. In robR a fitting criterion is employed which is less vulnerable as least square to unusual data. Thus, the observations are weighted differently due to the chosen fitting criteria which leads to a form of weighed and reweighted least squares regression. For more information on the theoretical background see e.g. Refs. [52,53]. M-Estimates were used to down-weight outliers. Influential data were checked by plotting the studentized deleted residuals against centered leverage values.

3.2.1. Data analysis

All Abraham solute descriptors (A , B , S , E , and V) were obtained by ACD/Labs i.Lab [54]. If an exact match was found, database descriptors were used; otherwise, the calculated values were employed. pK and $\log D$ at pH 3.0 were calculated using ACD Labs 7.0 calculator. Charge related descriptors D^+ and D^- at pH 3.0 were calculated with Eqs. (4) and (5). robR with M Estimators as robust scale weights was performed with SPSS 20.0 (PAWS Statistics) equipped with the R essential package and Robust Regression dialog box [55]. As dependent variable, the logarithm of the retention factor ($\log k$) was used with the Abraham solute descriptors and charge descriptors as independent variables.

3.2.2. Choice of solutes

The number of solutes to perform the MLR should be large enough to obtain at least four times the amount of the computed

Table 1
Test analytes considered during the LSER study with their corresponding descriptors and structures.

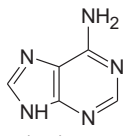
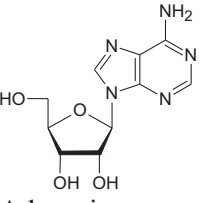
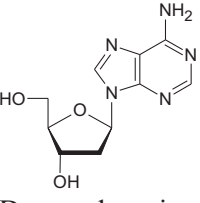
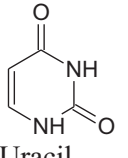
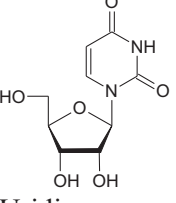
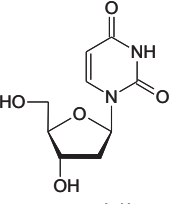
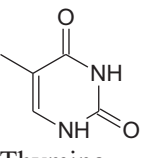
Nr.	Analytes	A	B	S	E	V	$D_{3.0}^-$	$D_{3.0}^+$	Log $D_{o/w}$ (pH 3.0)	Acid pK	Basic pK
1	 Adenine	0.70	1.13	1.80	1.68	0.923	0.00	0.94	-1.36	9.85	4.20
2	 Adenosine	0.97	2.22	2.64	2.69	1.754	0.00	0.72	-1.77	13.11, 9.23	3.40
3	 Deoxyadenosine	0.72	1.94	2.38	2.49	1.695	0.00	0.72	-1.29	13.79	3.40
4	 Uracil	0.44	1.00	1.00	0.81	0.752	0.00	0.00	-0.71	9.20	
5	 Uridine	0.90	2.29	2.35	1.88	1.582	0.00	0.00	-1.61	13.58, 8.28	
6	 Deoxyuridine	0.74	1.92	2.14	1.65	1.524	0.00	0.00	-1.70	13.37, 9.23	1.69
7	 Thymine	0.44	1.03	1.00	0.80	0.893	0.00	0.00	-0.12	9.84	

Table 1 (Continued)

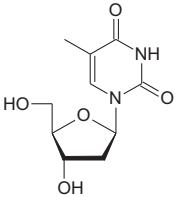
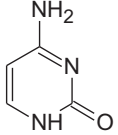
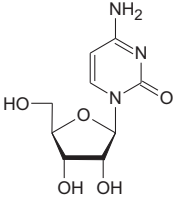
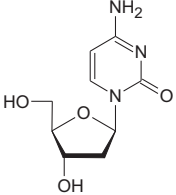
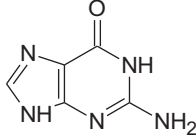
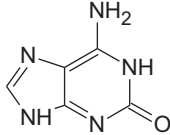
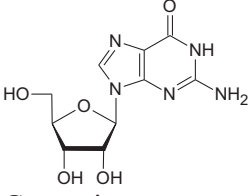
Nr.	Analytes	A	B	S	E	V	$D_{3.0}^-$	$D_{3.0}^+$	Log $D_{o/w}$ (pH 3.0)	Acid pK	Basic pK
8	 Thymidine	0.74	1.93	2.09	1.62	1.665	0.00	0.00	-1.11	14.04, 9.23	
9	 Cytosine	0.60	1.02	1.90	1.43	0.793	0.00	0.94	-2.38	12.20	4.18
10	 Cytidine	0.87	2.62	2.21	2.09	1.623	0.00	0.65	-2.86	13.43	3.27
11	 Deoxycytidine	0.71	2.25	2.00	1.86	1.565	0.20	0.00	-2.55	14.03, 3.59	
12	 Guanine	0.97	1.20	1.60	1.80	0.982	0.00	0.59	-1.57	12.6, 9.63	3.15
13	 Isoguanine	0.96	1.52	1.82	1.64	0.982	0.00	1.00	-4.32	8.62	5.86
14	 Guanosine	1.34	2.86	2.82	2.56	1.812	0.00	0.05	-1.76	13.37, 9.28	1.69

Table 1 (Continued)

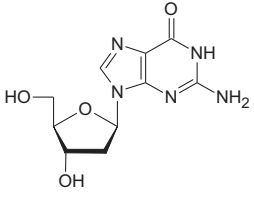
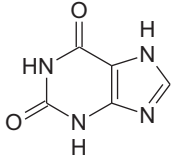
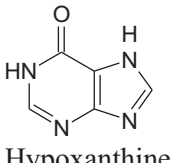
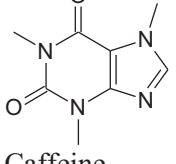
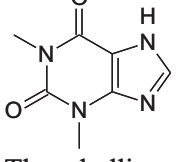
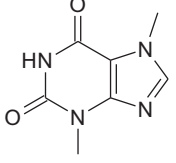
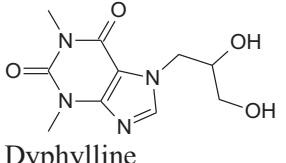
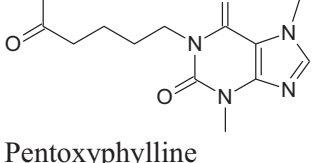
Nr.	Analytes	A	B	S	E	V	$D_{3.0}^-$	$D_{3.0}^+$	Log $D_{o/w}$ (pH 3.0)	Acid pK	Basic pK
15	 Deoxyguanosine	1.09	2.58	2.56	2.36	1.754	0.00	0.07	-1.41	13.96, 9.31	1.90
16	 Xanthine	0.97	1.07	1.60	1.50	0.941	0.00	0.01	-0.82	13.93, 7.60	1.00
17	 Hypoxanthine	0.60	1.18	1.82	1.38	0.882	0.00	0.14	-1.31	8.90	2.20
18	 Caffeine	0.05	1.28	1.72	0.50	1.363	0.00	0.01	-0.13		0.73
19	 Theophylline	0.54	1.34	1.60	1.50	1.222	0.00	0.05	-0.21	8.60	1.70
20	 Theobromine	0.50	1.38	1.60	1.50	1.222	0.00	0.00	-0.72	9.90	0.59
21	 Dyphylline	0.54	1.86	2.44	1.88	1.762	0.00	0.00	-1.11	15.05, 13.66	0.70
22	 Pentoxyphylline	0.00	1.84	2.28	1.64	2.083	0.00	0.00	0.32		0.16

Table 1 (Continued)

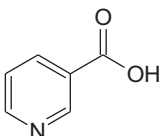
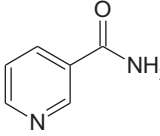
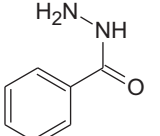
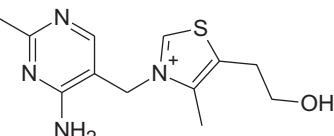
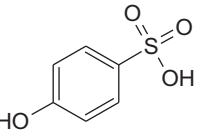
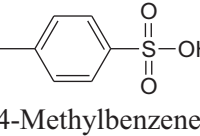
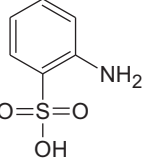
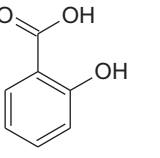
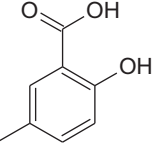
Nr.	Analytes	A	B	S	E	V	$D_{3.0}^-$	$D_{3.0}^+$	$\text{Log } D_{o/w}$ (pH 3.0)	Acid pK	Basic pK
23	 Nicotinic acid	0.57	0.73	1.21	0.79	0.891	0.86	0.98	-1.23	2.20	4.80
24	 Nicotinamide	0.63	1.00	1.09	1.01	0.932	0.00	0.78	-0.75		3.54
25	 Isoniazid	0.47	1.39	1.85	1.19	1.032	0.00	0.53	-0.09	12.55	3.06
26	 Thiamine	0.54	1.04	1.58	1.58	2.010	0.00	1.99	-3.51	14.17	4.77
27	 4-Hydroxybenzenesulfonic acid	0.81	1.15	2.02	1.10	1.115	1.00	0.00	-4.71	8.66, -0.23	
28	 4-Methylbenzenesulfonic acid	0.31	0.88	1.72	0.89	1.197	1.00	0.00	-2.23	-0.43	2.45
29	 2-Aminobenzenesulfonic acid	0.54	1.19	2.17	1.15	1.156	1.00	0.22	-2.81	-1.41	2.45
30	 Salicylic acid	0.71	0.38	0.84	0.89	0.990	0.49	0.00	1.76	3.01	
31	 5-Methylsalicylic acid	0.70	0.40	1.04	0.93	1.131	0.33	0.00	2.24	13.99, 3.30	

Table 1 (Continued)

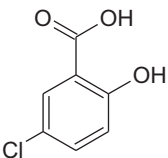
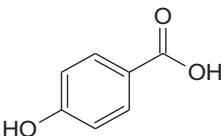
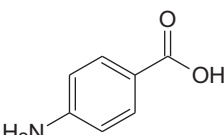
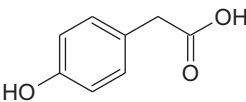
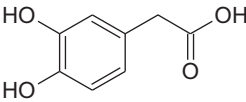
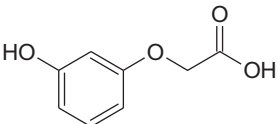
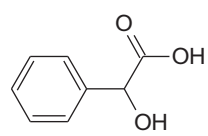
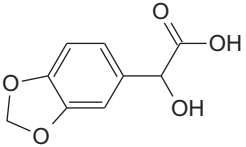
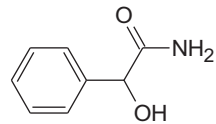
Nr.	Analytes	A	B	S	E	V	$D_{3.0}^-$	$D_{3.0}^+$	Log $D_{o/w}$ (pH 3.0)	Acid pK	Basic pK
32	 5-Chlorosalicylic acid	0.95	0.38	1.21	1.06	1.113	0.70	0.00	2.90	13.25, 2.64	
33	 4-Hydroxybenzoic acid	0.81	0.56	0.90	0.93	0.990	0.03	0.00	1.41	9.22, 4.57	
34	 4-Aminobenzoic acid	0.94	0.60	1.65	1.08	1.032	0.01	0.24	0.68	4.86	2.51
35	 4-Hydroxyphenylacetic acid	0.97	0.78	1.32	0.94	1.131	0.03	0.00	0.75	10.19, 4.50	
36	 3,4-Dihydroxyphenylacetic acid	1.35	0.86	1.47	1.12	1.190	0.04	0.00	0.15	9.84, 4.42	
37	 3-Phenoxyacetic acid	0.72	0.76	0.93	0.91	1.131	0.06	0.00	0.49	9.59, 4.19	
38	 Mandelic acid	0.74	0.89	1.05	0.9	1.131	0.28	0.00	0.78	15.65, 3.41	
39	 3,4-(Methylenedioxy) mandelic acid	0.74	1.28	1.33	1.22	1.281	0.29	0.00	0.63	15.65, 3.39	
40	 Mandelamide	0.66	1.10	1.52	1.15	1.172	0.00	0.00	-0.17	12.46	-0.80

Table 1 (Continued)

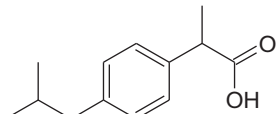
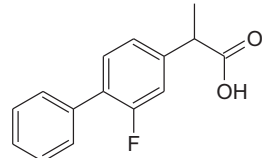
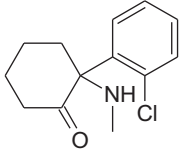
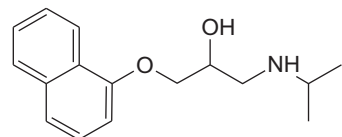
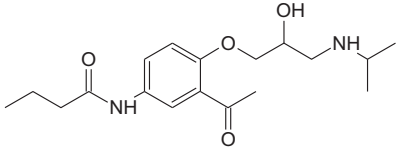
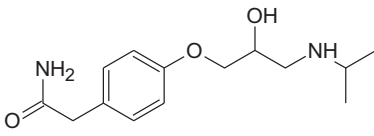
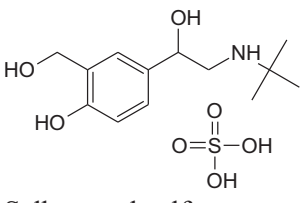
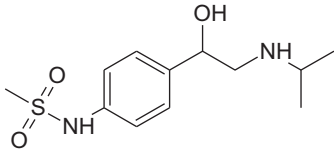
Nr.	Analytes	A	B	S	E	V	$D_{3.0}^-$	$D_{3.0}^+$	Log $D_{o/w}$ (pH 3.0)	Acid pK	Basic pK
41	 Ibuprofen	0.59	0.81	0.59	0.73	1.777	0.04	0.00	3.71	4.41	
42	 Flurbiprofen	0.57	0.58	1.51	1.50	1.839	0.07	0.00	4.08	4.14	
43	 Ketamine	0.13	0.89	1.42	1.28	1.832	0.00	1.00	-0.76		6.46
44	 Propranolol	0.17	1.42	1.43	1.88	2.148	0.00	1.00	0.00	13.84	9.14
45	 Acebutolol	0.90	2.10	2.42	1.60	2.756	0.00	1.00	-1.15	13.78	9.10, 0.20
46	 Atenolol	0.69	2.00	1.88	1.45	2.176	0.00	1.00	-3.00	13.88	9.16
47	 Salbutamol sulfate	1.19	1.82	1.26	1.43	1.978	0.00	1.00	-3.08	9.99	9.22
48	 Sotalol	0.74	1.75	1.86	1.52	2.101	0.00	1.00	-2.78	9.55	9.18

Table 1 (Continued)

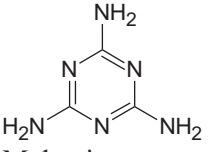
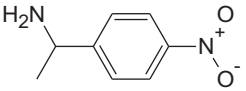
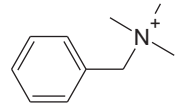
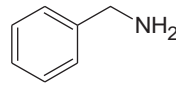
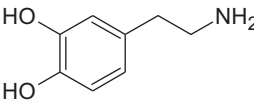
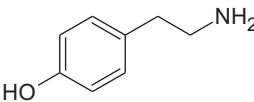
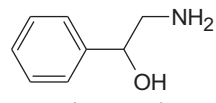
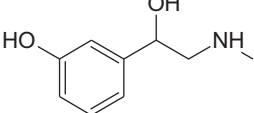
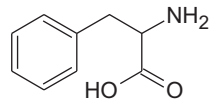
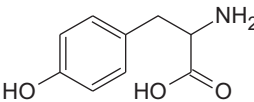
Nr.	Analytes	A	B	S	E	V	$D_{3.0}^-$	$D_{3.0}^+$	Log $D_{o/w}$ (pH 3.0)	Acid pK	Basic pK
49	 Melamine	0.68	1.21	1.88	1.61	0.893	0.00	1.00	-3.64		5.66
50	 1-(4-nitrophenyl)ethanamine	0.21	0.79	1.51	1.06	1.272	0.00	1.00	-1.93		8.65
51	 Benzyltrimethylammonium	0.00	0.15	0.56	0.36	1.401	0.00	1.00	-2.31		
52	 Benzylamine	0.15	0.72	0.77	0.83	0.957	0.00	1.00	-2.01		9.22
53	 Dopamine	1.20	1.04	1.46	1.35	1.215	0.00	1.00	-2.98	12.68, 9.39	10.11
54	 Tyramine	0.71	0.94	1.17	1.01	1.157	0.00	1.00	-2.38	9.51	10.49
55	 2-Amino-1-phenylethanol	0.46	1.19	1.10	1.03	1.157	0.00	1.00	-2.64	12.04	8.43
56	 Phenylephrine	0.88	1.37	1.17	1.20	1.356	0.00	1.00	-3.13	9.76	9.22
57	 Phenylalanine	0.78	1.02	1.39	0.95	1.313	0.86	1.00	-1.43	2.21	9.20
58	 Tyrosine	1.28	1.29	1.60	1.18	1.372	0.85	1.00	-2.17	10.01, 2.25	9.35

Table 1 (Continued)

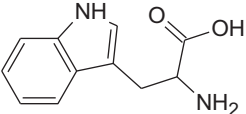
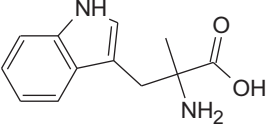
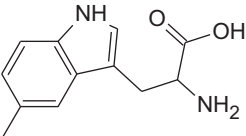
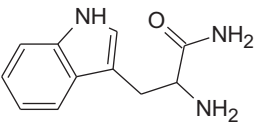
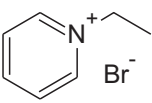
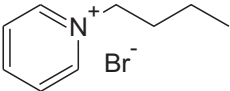
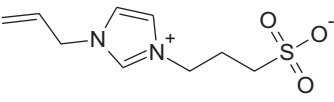
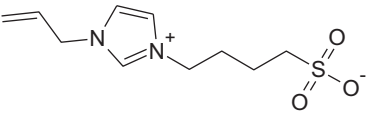
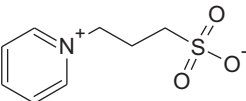
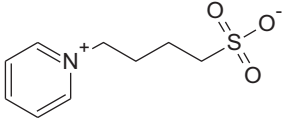
Nr.	Analytes	A	B	S	E	V	D _{3.0} ⁻	D _{3.0} ⁺	Log D _{0/w} (pH 3.0)	Acid pK	Basic pK
59	 Tryptophan	1.09	1.23	1.80	1.62	1.543	0.83	1.00	-1.52	2.30	9.51
60	 α-Methyltryptophan	1.09	1.24	1.75	1.59	1.684	0.82	1.00	-1.17	2.34	9.51
61	 5-Methyltryptophan	1.09	1.23	1.74	1.64	1.684	0.85	1.00	-1.06	2.26	9.52
62	 Tryptophaneamide	1.01	1.45	2.27	1.87	1.584	0.00	1.00	-2.99		8.18
63	 1-Ethylpyridin-1-ium bromide	0.00	0.11	0.58	0.39	0.979	0.00	1.00	-3.66		
64	 1-Butylpyridin-1-ium bromide	0.00	0.12	0.59	0.39	1.260	0.00	1.00	-3.30		
65	 1-(Prop-2-en-1-yl)-3-(3-sulfopropyl)- 1H-imidazol-3-ium	0.31	1.08	1.81	0.75	1.700	0.97	1.00	-1.97	1.41	
66	 1-(Prop-2-en-1-yl)-3-(4-sulfopropyl)- 1H-imidazol-3-ium	0.31	1.08	1.81	0.75	1.841	0.95	1.00	-1.97	1.67	
67	 1-(3-Sulfopropyl)pyridin-1-ium	0.31	0.89	1.74	0.67	1.459	0.97	1.00	-5.58	1.47	

Table 1 (Continued)

Nr.	Analytes	A	B	S	E	V	$D_{3.0}^-$	$D_{3.0}^+$	Log $D_{o/w}$ (pH 3.0)	Acid pK	Basic pK
68	 1-(4-Sulfobutyl)pyridin-1-ium	0.31	0.89	1.74	0.67	1.600	0.95	1.00	-5.59		1.70

system constants. We chose an initial amount of 68 test compounds which comprised small neutral, basic, acidic, zwitterionic and amphoteric molecules (Table 1) with a wide variety of functional groups. Thus, our set was around 11 times the amount of the computed constants. The set was different to Ref. [42]. Fig. 2 and Table 3 display the solute descriptor distributions and their descriptive statistics, respectively.

Due to the nature of the D descriptors, as they define the magnitude of charge, neutral analytes exhibit a value of zero while acids and bases obtain a value close to 1 depending on their ionization state. The number of negatively charged molecules as a factor of the D^- descriptor is low under the given conditions. However, the calculated charge state was in agreement with observations made during the experimental setup. Thus, it is important to keep in mind that the observations and discussions made during this publication reflect the chromatographic system under the given conditions. The effect on retention of negatively charged analytes compared to positively charged molecules might be underestimated to a certain degree and can be distributed differently under conditions with a higher MP pH. Nevertheless, d^- coefficients were found significant for almost all columns examined (see Section 4.2). We think that despite an uneven D^- to D^+ distribution, the results at the given conditions are of good quality. Strong correlation between the independent variables should be avoided as highly correlating parameters would describe the same forces within the HILIC mechanism, and thus be redundant. Table 4 shows the correlation matrix for A , B , S , E and V . Although all parameters correlate to a certain extent with each other, E was found to show the highest correlation with all descriptors. Due to this observation, we decided to exclude E from the linear regression model. The correlation between E , S and B may be the result of a relatively high number of aromatic compounds within the analyzed test set. According to Vitha and Carr, the introduction of additional aliphatic solutes might help to break this correlation [43]. Yet, due to the limitation of UV-detection this alteration of the test set was not possible in our set-up. To reinforce our decision we initially computed the LSERs with E (data not shown) and found the obtained regression coefficient e to be insignificant for all systems, which was also the case for Chirita et al. Moreover, consolidation was found in literature. Dinh et al. used principal component analysis (PCA) to probe the interaction mode in HILIC and could also not see any noticeable effects from π - π interactions [40].

4. Results and discussion

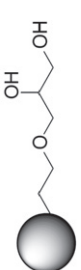
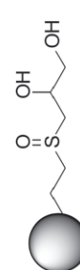
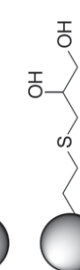
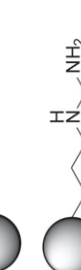
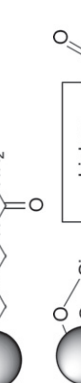

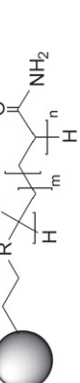
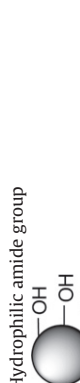
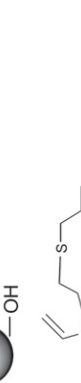
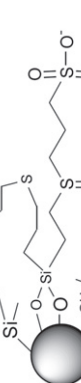

4.1. Apparent hydro-organic s_w^s pH versus aqueous w^w pH

A crucial factor for the determination of the system parameters is the choice of the pH used in Eqs. (4) and (5) to compute D^+ and D^- . Due to a difference in the exhibited pH between the buffer with w^w pH 3.0 compared to the MP apparent hydro-organic s_w^s pH of 5.4, a severe difference in the obtained D factors was found. Thus, a pH value must be chosen that will most likely reflect the pH present near the interaction sites. To evaluate this factor, we performed all LSER regression calculations under both theoretical

pH values (data not shown). Comparing both results, we found a significant difference in the obtained s coefficient. Applying D^+D^- computed at w^w pH 3.0 the s coefficient is negative and accounts for the dispersion into the MP, while at s_w^s pH 5.4 s coefficients are positive and reflect a contribution of the polarizability to the overall retention. Consulting already published literature along that line, a negative s coefficient was usually found indicating that for our experiments w^w pH 3.0 seems more suitable. Another result obtained by applying s_w^s pH 5.4 contradicting preliminary considerations is the stronger attraction of positively charged analytes on amine phases compared to negatively charged solutes (higher d^+ compared to d^- coefficient). Regardless of whether w^w pH 3.0 or s_w^s pH 5.4 is most likely present near the SP, the primary amine groups on brush type aminopropyl modified silica (e.g. APS-5) (pKa \sim 9) should be positively charged; consequently repulsive forces reduce retention of also positively charged and protonated basic compounds. The final step to verify our choice of incorporating w^w pH 3.0 into Eqs. (4) and (5) was done by PCA. In consideration that PCA is a structure finding method while LSER is a conformational statistical approach, we decided to compute three PCA's. The first two calculations used the obtained LSER system coefficients for either w^w pH 3.0 (PCA1) or s_w^s pH 5.4 (PCA2) as independent variables to compute and extract later on principal component 1 (PC1) and principal component 2 (PC2). Hence, the reduction and explanation of the variances of the underlying interaction mechanism were predefined by our statistic setup and could only be explained by the information found in the system constants s , v , a , b , d^+ and d^- . As a control, a third PCA was performed using the raw retention data (log k -values) as loadings (PCA3). Thus, PCA3 is not predefined and is capable of finding structures and similarities that influence the interaction within the HILIC system, without being confined by the system coefficients. All values were normalized (centered and reduced) prior to the calculation of the PCA. The comparison and evaluation was carried out with a linearity plot, applying both extracted PC1 + PC2 of PCA3 on the x -axis and the extracted PC1 + PC2 of PCA1 and PCA2 on the y -axis, respectively (Fig. 3).

To recapitulate the thoughts behind this experiment: We should gain the same mechanistic information out of the system coefficients obtained by MLR that we get from the latently incorporated mechanistic information from the solutes log k values. Hence, the extracted PC1 + PC2's should be linear to each other. In accordance to our prior evaluations, the factors obtained with w^w pH 3.0 showed a linearity of $R^2 = 0.7181$ compared to $R^2 = 0.0012$ for s_w^s pH 5.4. The negative correlation of PCA1 and PCA3 might be due to an opposite distribution of the mechanistic information behind PC1 and PC2 of PCA1 and PCA3, respectively. Thus, in contrast to previous publications, we decided to use not the apparent but the aqueous buffer pH value for determining the charge state. This observation would support the HILIC theory of a formed water layer. At the SP surface and within the stagnant water layer the aqueous pH should be present as the water is largely separated from the hydro-organic modifier, thus suppressing the pH shifting effect of the organic modifier. Nevertheless, we are aware that w^w pH 3.0 might also not reflect the correct pH at the interaction site but helped us to obtain better quality results. This is the main drawback

Table 2 (Continued)

Abbreviation	Stationary phase	Manufacturer	Modification	Ligand density	Dimensions	Particle size (μm)	Pore size (\AA)	Surface ($\text{m}^2 \text{g}^{-1}$)
Diol	ProntosilDiol	Bischoff Chromatography		4% C	150 mm \times 4.0 mm	5.0	100	300
SGO	Sulfinylglycerol	In-house		2.3 $\mu\text{mol}/\text{m}^2$	150 mm \times 4.0 mm	5.0	100	300
TG	Thioglycerol	In-house		2.7 $\mu\text{mol}/\text{m}^2$	150 mm \times 4.0 mm	5.0	100	300
propU	nPropUrea	In-house		1.81 $\mu\text{mol}/\text{m}^2$	150 mm \times 4.0 mm	5.0	100	300
Xamide	XBridge Amide	Waters Corporation		7.5 $\mu\text{mol}/\text{m}^2$	150 mm \times 3.0 mm	3.5	135	185
Amide80 UniAmide	TSK Gel Amide80 UniAmide (HILIC)	Tosoh Agela Techn. Inc.		n/a 8% C	150 mm \times 2.0 mm 150 mm \times 4.6 mm	3.0 5.0	100 100	450 410
Daiso	Daisogel (bare silica)	Daiso Chemical		–	150 mm \times 4.0 mm	5.0	100	300
SSO	Sulfosulfoxide	In-house		0.85 $\mu\text{mol}/\text{m}^2$	150 mm \times 4.0 mm	5.0	100	300
CosH	CosmosilHILIC	Nacalai Tesque		n/a	150 mm \times 4.6 mm	5.0	120	300
CChoc	C-Choc HILIC	In-house		19.2 $\mu\text{mol}/\text{m}^2$	150 mm \times 4.0 mm	3.0	100	300
MMH1	Acclaim Mixed Mode HILIC 1	Dionex		8.5% C	150 mm \times 4.6 mm	5.0	120	300

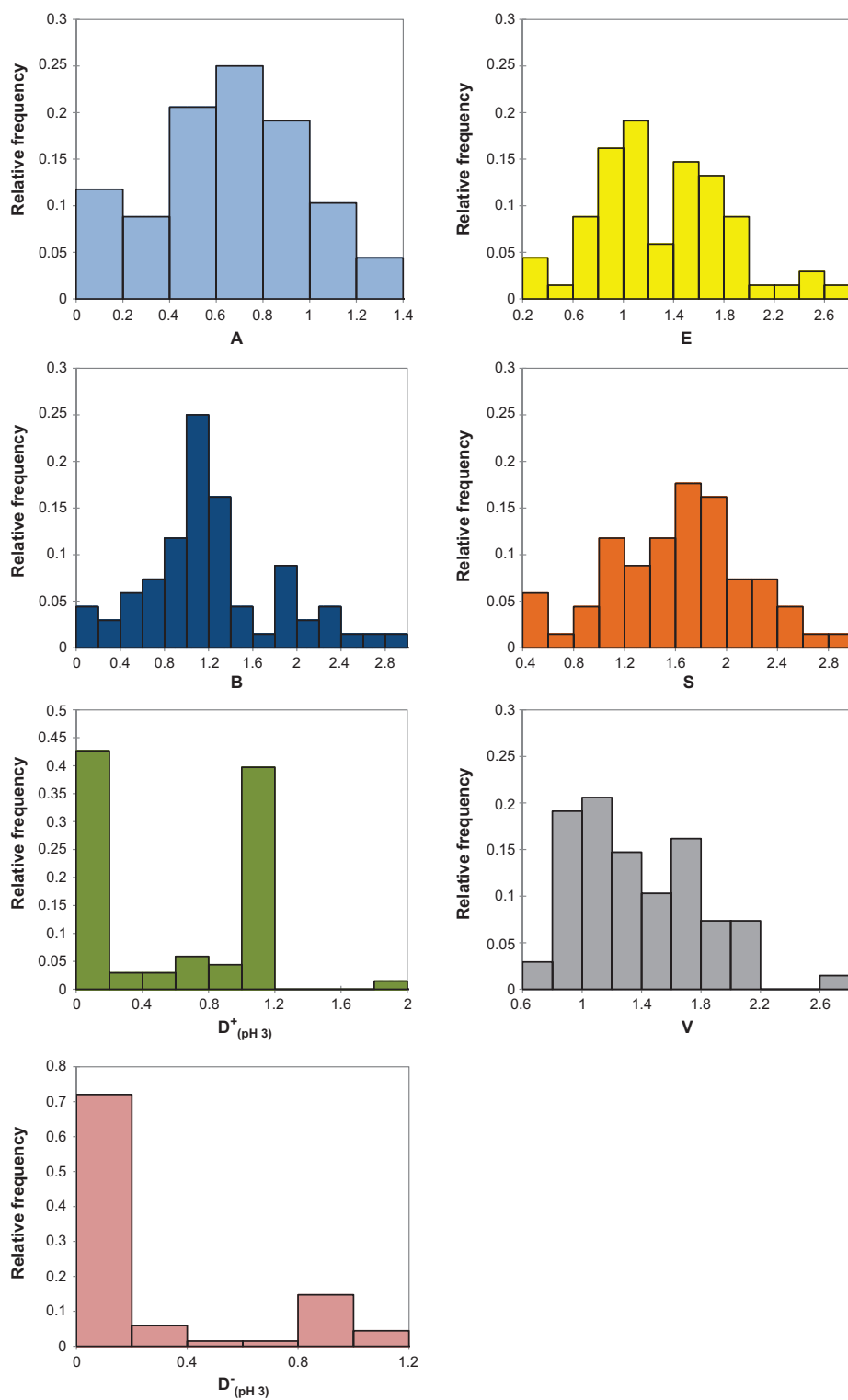


Fig. 2. Frequency plots of the Abraham and D descriptors of the test solute set.

Table 3

Descriptive statistic for the solute set in Table 1.

	E	S	A	B	V	D^-	D^+
Minimum	0.360	0.560	0.000	0.100	0.750	0.000	0.000
Maximum	2.690	2.820	1.350	0.280	2.760	1.000	1.990
Mean	1.300	1.604	0.668	1.224	1.388	0.000 ^a	0.685 ^a
Standard deviation	0.513	0.527	0.339	0.593	0.411	0.365	0.500

^a For D^- and D^+ the measure for the central tendency refers to the median not the mean value.

Table 4
Correlation matrix for the solute descriptors of the probes listed in Table 1.

	A	B	S	E	V	D ⁻	D ⁺
A	1.000	0.387	0.334	0.513	0.038	0.023	-0.110
B		1.000	0.811	0.809	0.529	-0.219	-0.080
S			1.000	0.774	0.451	0.040	-0.059
E				1.000	0.409	-0.291	-0.025
V					1.000	-0.012	0.244
D ⁻						1.000	0.108
D ⁺							1.000

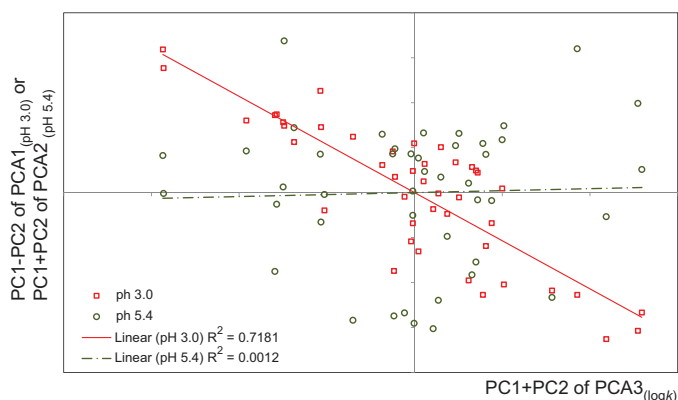


Fig. 3. PCA linearity plots. The red line resembles the correlation between the extracted PC1 + PC2 of PCA1_(pH 3.0) versus the extracted PC1 + PC2 of PCA3_(log k). The green disconnected line displays the extracted PC1 + PC2 for PCA1_(pH 5.4) versus the extracted PC1 + PC2 for PCA3_(log k). (For interpretation of the references to color in this figure legend, the reader is referred to the web version of the article.)

of the *D* descriptors as the whole HILIC system is rather complicated and not straight forward and an adequate pH for calculating the LSERs needs to be evaluated and may always enter an error to the final result. We recommend to calculate both *D* descriptors either for w pH as well as s pH and evaluate the effect according to the individual test setup, if LSER experiments are performed with Eq. (3).

4.2. Evaluation of system coefficients for robR w pH 3.0

Initially, OLSR was performed to obtain the system constants. However, after plotting the studentized deleted residuals versus the centered leverage values, outliers as well as influential data points were found. Since we wanted to keep the solute set as big and diverse as possible, we decided to perform a robR using M-Weights to compensate for outliers. These results were again re-validated by OLSR in which all outliers and influential points were removed previous to the calculations (data not shown). Fig. S1 (Supporting information) shows the comparison of the obtained R_{adj}^2 for robR and OLSR. Almost equal and comparable goodness of fit and system coefficients were recorded for both approaches, thus, robR was maintained since more solutes can be incorporated into the model. Throughout the LSER calculations some descriptors were found to be insignificant for describing $\log k$ on several columns. The model equations were finally recomputed by neglecting these solute descriptors. All calculated model coefficients and regression statistics are summarized in Table 5. Empty fields display former mentioned insignificant descriptors. Unfortunately, the number of solute retention data used for the solvation parameter model varies within the column set as some analytes eluted with the void time.

As a result, two main observations could be made. First, the coefficient directions are in accordance to previous publications and second the R_{adj}^2 values are lower compared to the literature [42]. In the following, the results will be discussed generally for all columns

followed by a deeper look in reference to the SP groups. As already mentioned, throughout our experimental setup electrostatic repulsive and attractive forces became active overlaying the HILIC type partition mechanism. Positive directed coefficients are considered to contribute to the retention of analytes and the partition towards the SP, while negative coefficients display the contribution and solute dispersion into the MP. The higher the value, the bigger is the difference between the SP and the MP for this characteristic. Small values or insignificant descriptors emphasizing the comparability and similarity of these properties between the two phases will not considerably contribute to the retention or elution process. For all columns, the system constants for the hydrogen bond acceptor and donor (*a*, *b*) character as well as *d*⁺ and *d*⁻ are positive, while *c*, *v* and *s* are negative. This is in agreement with published data for HILIC systems as well as orthogonal to results found for RP material. The strongest contribution to the retention process is found by the hydrogen bond donor characteristics (*b*) of the HILIC systems and can be correlated to the stagnant water layer. While water and acetonitrile have similar hydrogen acceptor properties ($B_{H_2O} = 0.35$, $B_{ACN} = 0.32$ [56]), H₂O is a better hydrogen bond donor than ACN ($A_{H_2O} = 0.82$, $A_{ACN} = 0.07$ [56]) which also explains the lower contribution of the *a* coefficient. Thus, the hydrogen bond acceptor property *a* is generally lower than the hydrogen bond donor property *b*. Furthermore, *a* was not significant to describe the retention on TG, Amide80, UniAmide, ShPCHILIC, PC-FA, Daiso and SSO (see Table 5). It seems that the acidity of the SP support or the acidity of the immobilized ligand of the packing materials may have an impact on this phenomenon.

The intercept *c* is negative for all columns and represents the phase ratio as well as interactions which are not described by the chosen solute descriptors. A clear discussion is not possible due to the diversity of the phenomena that contribute to the intercept.

For all columns, *v* has the highest impact on the partition towards the hydrophobic MP. The coefficient *v* reflects the difference in the ease of cavity formation between two solvents [43]. The energy which is needed for a solute to form a cavity within a highly organized and very cohesive solvent is higher than to transfer into a less organized liquid, therefore, the higher the value of the *V* parameter (non-polar molecular volume) of a solute, the more likely it is to remain in the organic layer as it is much easier to break interactions between ACN than H₂O molecules. Furthermore, the magnitude of the obtained *v* coefficient reflects the polarity of the SP surface. Low *v* coefficient reflects a lower surface polarity and vice versa. In addition it partially correlates with the overall retention span range for the examined columns under the pre-set conditions. Another description of non-polar interactions was found in the *s* coefficient which is an indication of the interaction between dipolar and/or polarizable solutes with the MP. The polarizability of ACN is higher compared to H₂O ($S_{H_2O} = 0.45$, $S_{ACN} = 0.9$ [56]), thus the dipole–dipole interactions between the analytes and the MP are slightly stronger than with the SP. Furthermore, for almost all columns *s* was not found to be significant. This was especially of interest within the frame of ongoing column development projects for which the implementation of LSER was significant.

Table 5

System constants for 22 stationary phases computed according to Eq. (3) with the corresponding statistics. R_{adj}^2 is the adjusted correlation coefficient, SE is the standard error of the fit, F the Fisher's statistics, n the number of solutes considered in the regression. Italic numbers represent the standard errors of the coefficient while number in brackets represent the standardized coefficients \hat{b}_j .

	<i>c</i>	<i>s</i>	<i>a</i>	<i>b</i>	<i>v</i>	<i>d</i> ⁻	<i>d</i> ⁺	<i>n</i>	R_{adj}^2	SE	<i>F</i>
SugD	-0.144 <i>0.154</i>		0.838 <i>0.132</i> (0.446)	0.469 <i>0.097</i> (0.447)	-0.843 <i>0.134</i> (-0.541)	1.136 <i>0.109</i> (0.672)	0.344 <i>0.090</i> (0.265)	64	0.763	0.302	42
LunaNH	-0.103 <i>0.150</i>		0.827 <i>0.121</i> (0.435)	0.472 <i>0.088</i> (0.433)	-0.791 <i>0.117</i> (-0.503)	1.105 <i>0.106</i> (0.624)	0.397 <i>0.081</i> (0.302)	67	0.782	0.296	49
APS-5	-0.356 <i>-0.138</i>		0.454 <i>0.112</i> (0.279)	0.471 <i>0.082</i> (0.503)	-0.555 <i>0.110</i> (-0.408)	0.948 <i>0.097</i> (0.626)	0.583 <i>0.075</i> (0.519)	66	0.753	0.276	41
APS-3	-0.242 <i>0.156</i>	-0.257 <i>0.124</i> (-0.234)	0.488 <i>0.111</i> (0.298)	0.641 <i>0.119</i> (0.681)	-0.532 <i>0.109</i> (-0.389)	1.023 <i>0.103</i> (0.672)	0.558 <i>0.074</i> (0.495)	66	0.762	0.273	36
Sulfbet	-0.229 <i>0.149</i>	-0.255 <i>0.119</i> (-0.246)	0.502 <i>0.106</i> (0.324)	0.616 <i>0.117</i> (0.692)	-0.500 <i>0.108</i> (-0.385)	0.894 <i>0.099</i> (0.623)	0.613 <i>0.072</i> (0.575)	66	0.757	0.259	35
NucH	-0.497 <i>0.141</i>		0.327 <i>0.117</i> (0.208)	0.426 <i>0.090</i> (0.468)	-0.382 <i>0.122</i> (-0.289)	0.598 <i>0.101</i> (0.408)	0.842 <i>0.080</i> (0.778)	65	0.723	0.280	35
ShPCHILIC	-0.334 <i>0.131</i>		0.491 <i>0.083</i> (0.539)	-0.384 <i>0.121</i> (-0.293)	0.537 <i>0.104</i> (0.365)	0.886 <i>0.082</i> (0.823)		65	0.703	0.287	39
PC-MME	-0.454 <i>0.118</i>	-0.264 <i>0.087</i> (-0.257)	0.371 <i>0.083</i> (0.242)	0.427 <i>0.083</i> (0.466)	-0.305 <i>0.082</i> (-0.238)	0.970 <i>0.056</i> (0.918)		67	0.837	0.201	70
PC-FA	-0.772 <i>0.147</i>	-0.227 <i>0.110</i> (-0.206)	0.461 <i>0.102</i> (0.477)	-0.253 <i>0.097</i> (-0.18)	1.097 <i>0.069</i> (0.938)		64	0.803	0.257	66	
LunaH	-0.559 <i>0.110</i>		0.373 <i>0.091</i> (0.284)	0.401 <i>0.071</i> (0.522)	-0.517 <i>0.094</i> (-0.469)	0.554 <i>0.080</i> (0.453)	0.690 <i>0.062</i> (0.764)	65	0.759	0.213	42
Diol	-0.403 <i>0.099</i>		0.394 <i>0.080</i> (0.308)	0.419 <i>0.060</i> (0.564)	-0.577 <i>0.080</i> (-0.537)	0.489 <i>0.070</i> (0.410)	0.657 <i>0.054</i> (0.745)	66	0.798	0.195	53
TG	-0.382 <i>0.099</i>		0.478 <i>0.061</i> (0.633)	-0.457 <i>0.089</i> (-0.417)	0.458 <i>0.077</i> (0.375)	0.765 <i>0.060</i> (0.853)		66	0.758	0.215	53
SGO	-0.354 <i>0.125</i>	-0.229 <i>0.100</i> (-0.247)	0.342 <i>0.089</i> (0.247)	0.633 <i>0.091</i> (0.791)	-0.495 <i>0.091</i> (-0.422)	0.572 <i>0.084</i> (0.439)	0.736 <i>0.060</i> (0.767)	66	0.789	0.217	42
propU	-0.298 <i>0.142</i>	-0.259 <i>0.113</i> (-0.273)	0.213 <i>0.101</i> (0.150)	0.678 <i>0.114</i> (0.825)	-0.431 <i>0.104</i> (-0.360)	0.669 <i>0.096</i> (0.502)	0.728 <i>0.068</i> (0.741)	66	0.740	0.244	32
Xamide	-0.460 <i>0.144</i>		0.249 <i>0.119</i> (0.155)	0.637 <i>0.091</i> (0.691)	-0.605 <i>0.124</i> (-0.448)	0.644 <i>0.104</i> (0.427)	0.831 <i>0.081</i> (0.751)	65	0.724	0.285	35
Amide80	-0.276 <i>0.151</i>		0.660 <i>0.096</i> (0.672)	-0.603 <i>0.140</i> (-0.426)	0.608 <i>0.119</i> (0.386)	0.904 <i>0.094</i> (0.779)		65	0.663	0.331	33
UniAmide	-0.179 <i>0.128</i>		0.516 <i>0.081</i> (0.577)	-0.527 <i>0.115</i> (-0.429)	0.756 <i>0.096</i> (0.501)	0.756 <i>0.077</i> (0.752)		59	0.716	0.262	38
Daiso	-0.894 <i>0.138</i>		0.256 <i>0.081</i> (0.222)	0.784 <i>0.147</i> (0.686)	-0.335 <i>0.139</i> (-0.200)	0.290 <i>0.125</i> (0.158)	1.229 <i>0.092</i> (0.904)	63	0.710	0.357	53
SSO	-0.313 <i>0.176</i>	-0.362 <i>0.149</i> (-0.273)	0.784 <i>0.147</i> (0.686)	-0.335 <i>0.139</i> (-0.200)	0.290 <i>0.125</i> (0.158)	1.229 <i>0.092</i> (0.904)		63	0.775	0.317	44
CosH	-0.391 <i>0.113</i>		0.448 <i>0.092</i> (0.312)	0.489 <i>0.069</i> (0.588)	-0.602 <i>0.092</i> (-0.497)	0.769 <i>0.080</i> (0.574)	0.569 <i>0.061</i> (0.571)	66	0.791	0.224	51
CChoc	-0.115 <i>0.137</i>	-0.245 <i>0.110</i> (-0.235)	0.456 <i>0.098</i> (0.293)	0.716 <i>0.106</i> (0.801)	-0.634 <i>0.098</i> (-0.485)	0.715 <i>0.091</i> (0.493)	0.725 <i>0.065</i> (0.678)	65	0.801	0.238	44
MMH1	-0.846 <i>0.157</i>		-0.406 <i>0.130</i> (-0.202)	0.526 <i>0.099</i> (0.444)	-0.290 <i>0.125</i> (-0.176)	0.543 <i>0.129</i> (0.263)	1.195 <i>0.087</i> (0.863)	62	0.801	0.298	51

Next, the results will be discussed according to the chemical nature of the SPs. Basically, columns are classified according to their ligands grafted on silica. However, the solvation parameter approach showed that they do not always fit into the

predefined column group. For the evaluation, the obtained system coefficients, the standardized coefficients as well as the experimental versus the predicted $\log k$ values have been consulted. While the regression coefficients are important to set up the

linear solvation equation which explains the mechanism within the system, they do not directly depict which independent variable has more influence on the retention. Therefore, the standardized coefficients also known as beta (\hat{b}_j) values are formed according to Eq. (6) which eliminates the different scale dimensions of the variables.

$$\hat{b}_j = b_j \frac{\sigma_{x_j}}{\sigma_y} \quad (6)$$

Thereby, b_j is the value of the regression coefficient j while σ_y and σ_{x_j} display the standard deviation of the dependent variable ($\log k$) and of the obtained regression coefficient j , respectively.

4.2.1. Basic columns

The group of basic columns includes APS-5, APS-3, SugD and LunaNH. APS-5 and APS-3 are both home-made aminopropyl modified packings but of a different batch and different particle size while LunaNH is a commercially available amino phase. The repulsive effect for positively charged analytes is stronger on LunaNH and SugD compared to APS-5 and APS-3. However, d^- is comparable on all basic columns. Fig. S2 shows a plot of the experimental $\log k$ against the predicted $\log k$ values. A wider distribution along the trendline indicates a broader retention span width and a higher selectivity under the given conditions. On APS-5 (Fig. S2a) and APS-3 (Fig. S2b), neutral and basic analytes are equally distributed along the retention window while acidic compounds can be found in the upper half with zwitterionic solutes being the most strongly retained compounds. As the predictive character of the model is not applicable due to the low R_{adj}^2 it can be said that the estimation error is equally distributed along the molecule groups and no specific solute type is predominately over- or under-estimated. Changing from in-house columns to commercially available columns LunaNH and SugD, a wider retention range was observed (Fig. S2c and d). The solute distribution is not as uniform as the previously discussed columns with acidic and zwitterionic analytes being more focused on the upper retention limit followed up by neutral and basic compounds. Furthermore, retention factors of basic and zwitterionic solutes tend to be underestimated with the established LSER retention model. An equal prediction error for $\log k$ of neutral, and a tendency to overestimate the retention of acidic molecules can be witnessed. LunaNH shows the same coefficient magnitude compared to the secondary and tertiary amino modified SugD (Fig. 4c and d). In comparison to the primary amino modified columns APS-5 (Fig. 4a) and APS-3 (Fig. 4b), the introduction of tert. and sec. amino groups seem to counterbalance the influence of A and B on the mechanism, as shown by the equal magnitude of the standardized a and b regression coefficient for LunaNH and SugD.

4.2.2. Zwitterionic modified columns

The commercially available Nuch (Fig. S3a and Fig. 4e) and ShPCHILIC (Fig. S3b and Fig. 4f) show similar retention patterns. Neutral and acidic compounds are concentrated from the lower left up to the center and the basic and zwitterionic analytes from the center to the upper right of the trendline. Although the modified ligands are orthogonal with reference to the orientation of the acidic and basic group towards the silica surface they exhibit similar retention and selectivity behavior. The coefficients b , ν , d^- and d^+ are comparable for both systems; hence the different zwitterionic modification has no considerable influence on the forces connected to the retention mechanism. On both columns, d^- and d^+ are not equal with a higher attraction towards the SP for positively charged analytes. However, zwitterions are able to form intrinsic salts which should compensate attractive or repulsive electrostatic forces. The results show that under the given conditions, the acidic residue contributes stronger to the retention of basic compounds.

However, since few analytes are negatively charged at w pH 3.0 and more basic compounds exhibit a positive charge, the charge effect may not be adequately distributed and thus described by the used solute set.

Although PC-MME (Fig. S3d and Fig. 4h) and PC-FA (Fig. S3e and Fig. 4i) are similar, in reference to the chemical modification of the phosphocholin type column ShPCHILIC, the acidic group is oriented towards the water layer and introduces strong electrostatic repulsive effects on acidic compounds. Acidic and neutral compounds as well as basic and zwitterionic compounds build a cluster, respectively. No equal distribution along the retention window is observed, which makes this type of columns limited to specific separation issues mainly focused on basic compounds. Due to these results, the columns are removed from the zwitterionic cluster and classified as acidic columns. The high coefficient value for positively charged analytes affirms this consideration. Also the stronger acidity of PC-FA with two acidic groups compared to PC-MME, with one free acid and one methylester, is reasonably well covered by the regression coefficients. Again, this shows that LSER can be used as characterization tool during column development, as solid phase chemistry is not always straight-forward and the structure elucidation of the immobilized ligands on the silica surface can be very difficult.

The third group within the betaine modified sorbents is represented by the in-house made Sulfbet column (Fig. S3c and Fig. 4g). It shows an equal distribution for all compound groups, except for the zwitterionic molecules which are usually focused on the upper limit of the retention window. The prediction error is equally well distributed along the compound groups. As Sulfbet was created in analogy to Nuch we expected to obtain similar retention behavior. However, the LSER results and the $\log k$ plots showed a higher basic character of the Sulfbet column, which can be explained by the aminopropyl-silica starting material. Thus, not all amino groups were converted into sulfobetaine groups and primary amine groups are still present on the surface. However, they facilitate a more even distribution of the tested analytes along the retention window. The standardized coefficients show that the repulsive electrostatic effects for positively charged solutes are slightly reduced while all other systems constants are comparable to APS-5 and APS-3. Hence, Sulfbet is transferred from zwitterionic to basic modified columns.

4.2.3. Diol modified columns

Compared to e.g. amide or basic modified columns, the overall retention of analytes on diol type columns was generally found to be lower. The test solutes were similarly distributed along the retention window on all diol columns (Fig. S4). An interesting outcome was the significance of the a and s coefficient on the SGO column (Fig. 4m). This may be due to the sulphoxide group which is not present on the other diol columns and also explains the longer solute retention on the SGO column compared to the TG column [57]. A lower d^- and a higher d^+ value were found for TG compared to SGO. This is in agreement with Wu et al. who observed a lower silanophilic interaction on the SGO column than on the TG column and ascribed this to a shielding effect of the sulphoxide moiety compared to the sulphide group [57]. Furthermore, the ν coefficient shows a higher magnitude on LunaH (Fig. 4j) and Diol (Fig. 4k) compared to TG (Fig. 4l) and SGO. A thiol group is used for linking the diol-type ligands on the two latter columns. The higher lipophilicity of sulfur (thioether group) compared to oxygen (ether group) may reduce the ν coefficient hence makes the packing material less hydrophilic. The diol column exhibits generally higher coefficients than LunaH except for the d values, which may be due to the brush-type immobilized ligand compared to a cross linked diol group backbone.

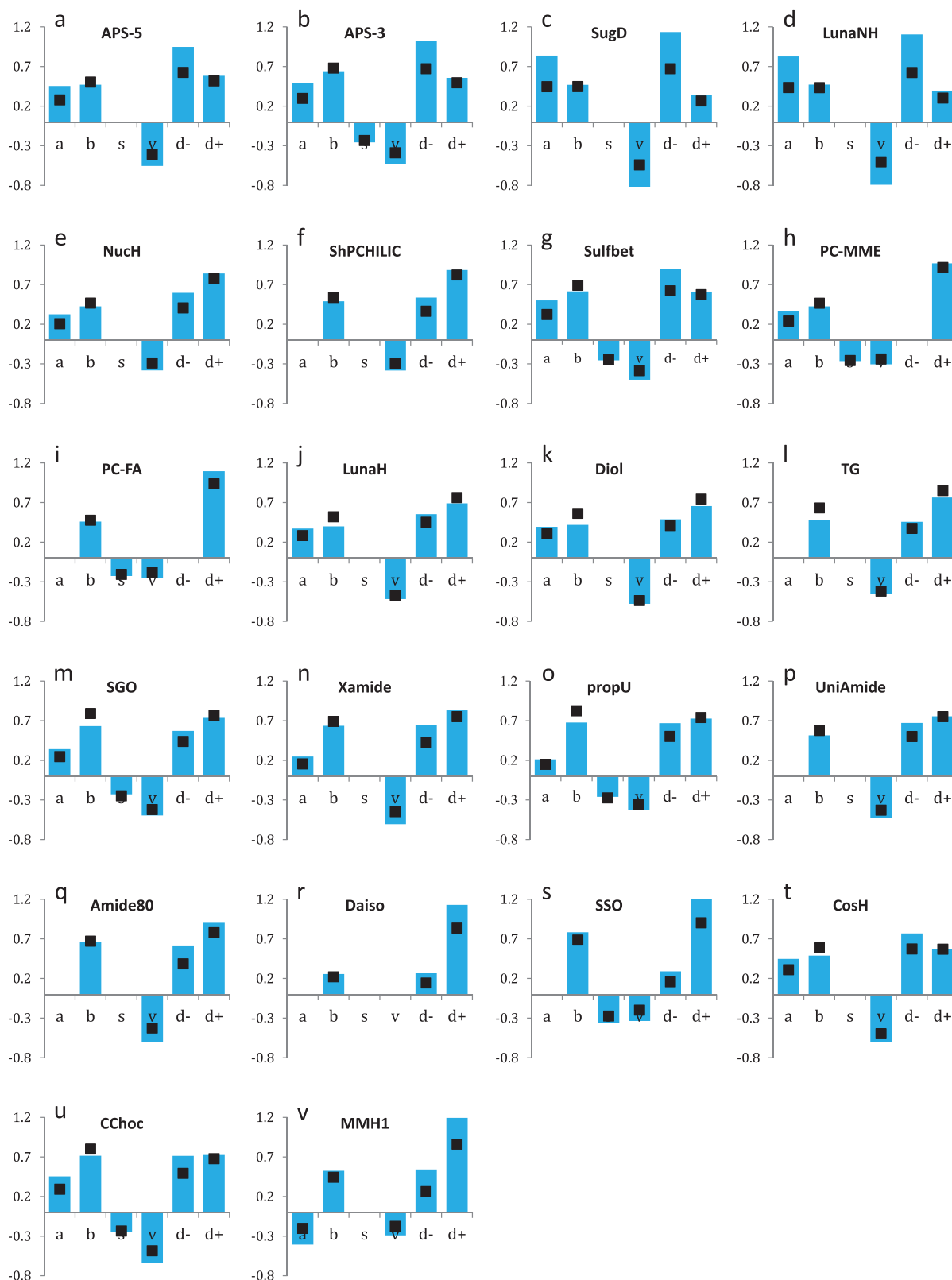


Fig. 4. Obtained system constants computed by the analysis of retention factors of test probes from Table 1. The bars represent the obtained regression coefficients for Eq. (3), while black squares display the corresponding standardized coefficients (\hat{b}_i) calculated according to Eq. (6).

4.2.4. Amide modified columns

A longer retention time was exhibited on amide type columns compared to diol modified ones. Higher b coefficients emphasize a higher polarity and thicker water layer on the packing surface.

The experimental versus calculated $\log k$ plots are similar to diol and zwitterionic modified columns with an equal distribution of the solute groups along the trendline and justify their neutral classification (Fig. S5). Basic compounds can be found again

on the upper right-hand side, which emphasizes the impact of the charge state on the retention mechanism. Within the amide columns, three different coefficient patterns were observed. Xamide (Fig. 4n) and propU (Fig. 4o) show hydrogen bond acceptor properties which are insignificant on UniAmide (Fig. 4p) and Amide80 (Fig. 4q). Amide80 is known to have a slightly acidic background as a result of the synthesis process [58,59], which endorses our previous observation that acidic modifications may reduce the impact of the a coefficient to the retention. Therefore, UniAmide may also have a slight acidic background or a low coverage which enables acidic silanol groups to contribute to the retention mechanism. Within the propU chromatographic system, the polarizability coefficient s contributes slightly to the partition towards the MP. It may be due to the urea group but could also result from our in-house synthesis protocol as almost all our columns have a significant s contribution. Additionally, ν is smaller compared to the other amide columns, while an affinity similar to UniAmide was found towards negatively charged molecules.

4.2.5. Acidic modified columns

In our predefined set of acidic columns we originally only expected bare silica (Daiso) and SSO. However, the Daiso column was found to be the least one to fit to the linear solvation equation. Only hydrogen bond donation and the analytes' charge state constituted a significant contribution to the retention mechanism (Fig. 4r). All effects that accounts for the partition into the MP are summed up by the constant c . Furthermore, the magnitude of b is very small compared to all other columns. Our results denote a predominately electrostatic interaction driven retention mechanism with a very limited impact of the hydrophilic partition, under the given conditions. In 2011 Wikberg et al. examined the state of water in neat silica compared to zwitterionic modified SPs [8]. They showed that considerable more "non-freezing-water" was found on grafted silica particles compared to bare particles. It might be an indication of a thicker water layer associated on modified columns. However, the LSER model may not truly display the interaction within the HILIC system in combination with the Daiso silica. The $\log k$ plot (Fig. S6a) is in accordance to PC-MME and PC-FA which were previously re-evaluated as acidic columns. A cluster is formed for neutral and acidic columns in the lower left region of the trendline. Basic and zwitterionic analytes are assembled at the upper right half. The same trend was found for SSO (Fig. S6b).

Like all acidic columns, SSO also shows no significant hydrogen bond acceptor probability which can be related to the negatively charged sulfonic acid group (Fig. 4s). Retention is mainly facilitated by hydrogen donor interactions and the charge state of the analyte. Acidic compounds are thereby repulsed from the SP and exhibit higher affinity towards the hydro-organic MP (reduced d^- value).

4.2.6. Mixed modified SP

The last columns to be discussed are CosH, CChoc and MMH1. It is not easy to heuristically classify these columns, as they show different ligand modifications compared to the previously mentioned ones. CosH is an imidazole modified packing material which can be classified as a basic to neutral modified SP under the given experimental conditions. The coefficient magnitude is comparable to APS-5. However, the standardized d^- and d^+ values show a more equal contribution of the charge state (Fig. 4t). This is also shown in the even distribution of basic compounds along the retention window (S7a). Acidic solutes can be found in the middle range of the retention width. CChoc (Fig. S7b and Fig. 4u) is a Maillard modified packing material. As emphasized in the previously published article [60], the high complexity and diversity of the Maillard reaction makes it difficult to propose an unequivocal structure for the immobilized ligand. Maillard resins on the CChoc may consist of aza-heterocycles, diol and amino groups resulting from the aminopropyl starting material. Again, s was found significant. Hydrogen-bond donor and acceptor properties are comparable to basic modified columns, but with a higher b coefficient. On the contrary, the standardized coefficients for d^+ and d^- indicate that no strong repulsive electrostatic interactions affect positively charged analytes and indicate the reduction of the basic character of the starting material. Overall CChoc is arranged between basic and neutral diol type columns in reference to the retention mechanism. However, analyte retention and selectivity are higher compared to neutral diol columns. At last, MMH1 (Fig. S7c and Fig. 4v) can be grouped with acidic modified columns. Yet this column deviates from the usual coefficient pattern as the a coefficient is negative. Whether this is due to the C12 modification or if the model is just not correctly describing the retention is difficult to validate. The ν constant's magnitude is small and displays the lipophilic character of the column. Unfortunately, the exact selector coverage is unknown, thus information about the residual silanol background acting as acidic groups cannot be given. Nevertheless, acidic compounds were either excluded with the void time or only weakly

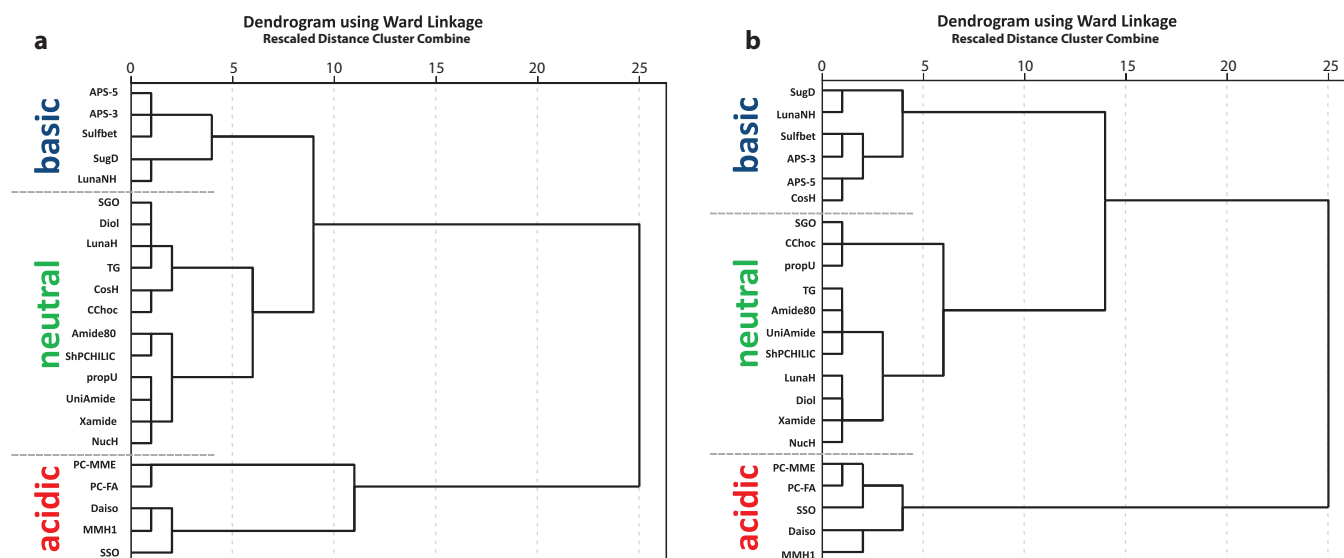


Fig. 5. Column classification by HCA. (a) Classification by means of normalized k values. (b) Classification according to the obtained normalized system constants.

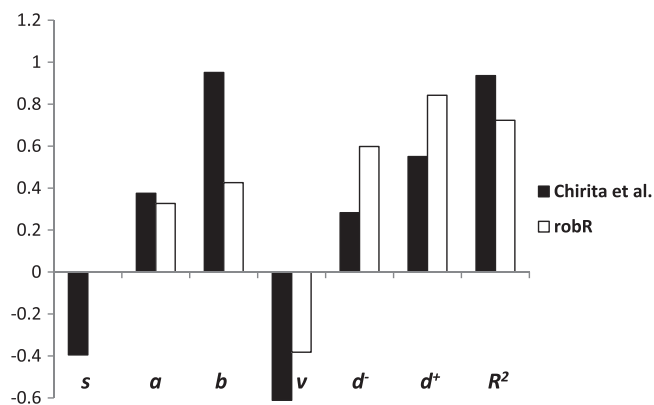


Fig. 6. Acquired LSER system constants for Nuch by robR compared to system constants found by Chirita et al. [42].

retained. Neutral compounds are arranged in the lower left part while basic and zwitterionic analytes are on the upper right region of the trendline as they are on Daiso, SSO, PC-MME and PC-FA.

4.3. Evaluation by hierarchical clustering

Finally, in order to compare all the columns according to their similarities, two HCAs were performed. At first, the phases were grouped using the normalized k values as input variables (Fig. 5a) followed by a second HCA according to the normalized obtained system constants (Fig. 5b).

In both ways, the columns are arranged into similar groups, although with a different order within the groups. The only deviation is the position of CosH. In Fig. 5a the column is positioned along the neutral systems next to CChoc, while it belongs to the basic group in Fig. 5b. This is in agreement with our observations discussed in Section 4.2.6. By applying the normalized k values we further see a clear separation of diol type and amide type/zwitterionic columns into distinct groups (Fig. 5a) while this information is lost to some extent when only the normalized system constants are used (Fig. 5b).

4.4. Summary

As one aim of this study was to evaluate the universality of Eq. (3) on HILIC systems, the result for Nuch is compared to the data published by Chirita et al. Fig. 6 shows the difference in the computed coefficients. Using a smaller amount of buffer salt in the MP promotes more sensitively and clearly electrostatic interactions to show up. This is in agreement with a higher magnitude for d^- and d^+ . Furthermore, a reduction of the water amount (20 → 10%) changes the phase ratio and the difference in s , a , b and v characteristics between the SP and MP should be reduced. Considering the retention interactions, the found results and the comparison are in agreement with the chemical nature of the systems. The biggest difference was observed in the quality of the LSER approach, with a lower R^2_{adj} of 0.723 compared to 0.936 [42]. Consequently it makes it impossible to use the regression equations to predict solute retention for the rather broad set of studied columns. If this outcome can be attributed again to the more strongly enabled electrostatic interactions is not fully clear, but it looks reasonable and may indicate the limitation of LSER models if not operated under a predominated HILIC partition mechanism.

5. Conclusion

As consequence of our experimental results and the comprehensive statistical treatment of the data we can only partially

confirm the suggested method to be a standardized protocol to characterize HILIC systems when operating conditions different to [42] are applied. Nevertheless, we confirm the significant contribution of the recently introduced D^- and D^+ parameter as valid representations of coulombic interactions as a part of the overall observed retention mechanisms. It emphasizes the preferred use of Eq. (3) over Eq. (1). Moreover, as for Sulfbet, CChoc, PC-MME and PC-FA, we demonstrated that the solvation parameter model can be used during column development to affirm or dismiss the preceding heuristic on how certain immobilized ligands will behave or which predominant mechanistic interactions will take place under HILIC conditions. However, LSER does not provide direct information of the different column performances in terms of selectivity, efficiency or stability. HCA, using either normalized k values or normalized system constants, was a convenient tool to arrange the SPs into three main groups with predominant interaction motifs. Acidic modified columns exhibit only weak hydrogen bond acceptor properties under the examined conditions, therefore, are less capable of achieving an even distribution of diverse analytes along the retention window. The exhibited repulsive effect on acids predominately reduces the area of operation to neutral and basic compounds. This effect may be reduced if a high hydrogen bond donor coefficient is present, which seems to compensate repulsive effects (e.g. SSO). Thus, this might indicate why basic and neutral columns are more frequently developed for HILIC applications than strong acidic HILIC columns [41]. In the group of “neutral” sorbents, amide-type and zwitterionic phases are preferably used to diol type materials as a wider retention window for almost all analytes was found, which is in accordance to Ref. [39]. This characteristic gives more freedom and possibilities for variations during method development.

To gain a wide selectivity and application range, we advise three HILIC column types (acidic, basic and neutral) as starting set. However, for the installation of a robust HILIC system, one might choose first a “neutral” modified column of the zwitterionic or amide type.

Acknowledgements

The authors thank Andrea Gargano for providing us with the PC-MME and PC-FA column.

Appendix A. Supplementary data

Supplementary data associated with this article can be found, in the online version, at <http://dx.doi.org/10.1016/j.chroma.2012.11.075>.

References

- [1] A.J. Alpert, J. Chromatogr. 499 (1990) 177.
- [2] F.M. Rabel, A.G. Caputo, E.T. Butts, J. Chromatogr. 126 (1976) 731.
- [3] P. Orth, H. Engelhardt, Chromatographia 15 (1982) 91.
- [4] P. Hemström, K. Irgum, J. Sep. Sci. 29 (2006) 1784.
- [5] D.V. McCalley, U.D. Neue, J. Chromatogr. A 1192 (2008) 225.
- [6] S.M. Melnikov, A. Holtzel, A. Seidel-Morgenstern, U. Tallarek, Anal. Chem. 83 (2011) 2569.
- [7] B.A. Olsen, J. Chromatogr. A 913 (2001) 113.
- [8] E. Wikberg, T. Sparrman, C. Viklund, T. Jonsson, K. Irgum, J. Chromatogr. A 1218 (2011) 6630.
- [9] A.J. Alpert, Anal. Chem. 80 (2008) 62.
- [10] A.E. Karatapanis, Y.C. Fiamegos, C.D. Stalikas, J. Chromatogr. A 1218 (2011) 2871.
- [11] W. Bicker, J.Y. Wu, H. Yeman, K. Albert, W. Lindner, J. Chromatogr. A 1218 (2011) 882.
- [12] D.V. McCalley, J. Chromatogr. A 1217 (2010) 3408.
- [13] M. Lämmerhofer, M. Richter, J. Wu, R. Nogueira, W. Bicker, W. Lindner, J. Sep. Sci. 31 (2008) 2572.
- [14] B. Chauve, D. Guillarme, P. Cléon, J.L. Veuthey, J. Sep. Sci. 33 (2010) 752.
- [15] C.T. Mant, R.S. Hodges, J. Sep. Sci. 31 (2008) 1573.
- [16] C.T. Mant, R.S. Hodges, J. Sep. Sci. 31 (2008) 2754.
- [17] G. Zauner, A.M. Deelder, M. Wührer, Electrophoresis 32 (2011) 3456.

- [18] J.M. Dreyfuss, C. Jacobs, Y. Gindin, G. Benson, G.O. Staples, J. Zaia, *Anal. Bioanal. Chem.* 399 (2011) 727.
- [19] O. Hernandez-Hernandez, R. Lebron-Aguilar, J.E. Quintanilla-Lopez, M.L. Sanz, F.J. Moreno, *Proteomics* 10 (2010) 3699.
- [20] M. Wuhler, A.R. de Boer, A.M. Deelder, *Mass Spectrom. Rev.* 28 (2009) 192.
- [21] X. Cai, J. Dong, L. Zou, X. Xue, X. Zhang, X. Liang, *Chromatographia* 74 (2011) 391.
- [22] Y.L. Loukas, Y. Dotsikas, *Chromatogr. Sci. Ser.* 103 (2011) 427.
- [23] B.A. Rappold, R.P. Grant, *J. Sep. Sci.* 34 (2011) 3527.
- [24] T. Zhang, D.J. Creek, M.P. Barrett, G. Blackburn, D.G. Watson, *Anal. Chem.* 84 (2012) 1994.
- [25] A. Mihailova, H. Maleroed, S.R. Wilson, B. Karaszewski, R. Hauser, E. Lundanes, T. Greibrokk, *J. Sep. Sci.* 31 (2008) 459.
- [26] P.S. Di, P.J. Boersema, A.J.R. Heck, S. Mohammed, *Anal. Chem.* 83 (2011) 3440.
- [27] M. Gilar, A. Jaworski, *J. Chromatogr. A* 1218 (2011) 8890.
- [28] D.S. Van, V. Vergote, A. Pezeshki, C. Burvenich, K. Peremans, S.B. De, *J. Sep. Sci.* 33 (2010) 728.
- [29] Y. Yang, R.I. Boysen, M.T.W. Hearn, *J. Chromatogr. A* 1216 (2009) 5518.
- [30] Y. Chen, W. Bicker, J. Wu, M. Xie, W. Lindner, *J. Agric. Food Chem.* 60 (2012) 4243.
- [31] R. Singh, P. Trivedi, D.U. Bawankule, A. Ahmad, K. Shanker, *J. Ethnopharmacol.* 141 (2012) 357.
- [32] H. Zhang, Z. Guo, W. Li, J. Feng, Y. Xiao, F. Zhang, X. Xue, X. Liang, *J. Sep. Sci.* 32 (2009) 526.
- [33] A.L.N. van Nuijs, I. Tarcomnicu, A. Covaci, *J. Chromatogr. A* 1218 (2011) 5964.
- [34] B. Buszewski, S. Noga, *Anal. Bioanal. Chem.* 402 (2012) 231.
- [35] Y. Guo, S. Gaiki, *J. Chromatogr. A* 1218 (2011) 5920.
- [36] T. Ikegami, H. Fujita, K. Horie, K. Hosoya, N. Tanaka, *Anal. Bioanal. Chem.* 386 (2006) 578.
- [37] P. Jandera, *J. Sep. Sci.* 31 (2008) 1421.
- [38] E. Lesellier, C. West, *J. Chromatogr. A* 1158 (2007) 329.
- [39] Y. Kawachi, T. Ikegami, H. Takubo, Y. Ikegami, M. Miyamoto, N. Tanaka, *J. Chromatogr. A* 1218 (2011) 5903.
- [40] N.P. Dinh, T. Jonsson, K. Irgum, *J. Chromatogr. A* 1218 (2011) 5880.
- [41] M.E.A. Ibrahim, Y. Liu, C.A. Lucy, *J. Chromatogr. A* 1260 (2012) 126.
- [42] R.I. Chirita, C. West, S. Zubrzycki, A.L. Finaru, C. Elfakir, *J. Chromatogr. A* 1218 (2011) 5939.
- [43] M. Vitha, P.W. Carr, *J. Chromatogr. A* 1126 (2006) 143.
- [44] C. West, E. Lesellier, *J. Chromatogr. A* 1110 (2006) 191.
- [45] C. West, E. Lesellier, *J. Chromatogr. A* 1191 (2008) 21.
- [46] U.D. Neue, B.A. Alden, P.C. Iraneta, M.R. Euerby, P. Petersson, C. Stella, J.-L. Veuthey, F. Steiner, L.R. Snyder, J.W. Dolan, U. Skogsberg, H. Händel, N. Welsch, K. Albert, *HPLC Made to Measure*, Wiley-VCH Verlag GmbH & Co. KGaA, Weinheim, Germany, 2008, p. 254.
- [47] B. Buszewski, S. Bocian, M. Matyska, J. Pesek, *J. Chromatogr. A* 1218 (2011) 441.
- [48] D.S. Van Meter, O.D. Stuart, A.B. Carle, A.M. Stalcup, *J. Chromatogr. A* 1191 (2008) 67.
- [49] C. West, S. Khater, E. Lesellier, *J. Chromatogr. A* 1250 (2012) 182.
- [50] P. Jandera, T. Hajek, V. Skerikova, J. Soukup, *J. Sep. Sci.* 33 (2010) 841.
- [51] M.H. Abraham, A. Ibrahim, A.M. Zissimos, *J. Chromatogr. A* 1037 (2004) 29.
- [52] P. Filzmoser, V. Todorov, *Anal. Chim. Acta* 705 (2011) 2.
- [53] P.J. Rousseeuw, A.M. Leroy, *Robust Regression and Outlier Detection*, John Wiley & Sons, Inc., Hoboken, New Jersey, 2005.
- [54] <https://ilab.acdlabs.com/ilab2/index.php>
- [55] <http://gruener.userpage.fu-berlin.de/spss-dialogs.htm>
- [56] E.E. Hills, M.H. Abraham, A. Hersey, C.D. Bevan, *Fluid Phase Equilib.* 303 (2011) 45.
- [57] J.Y. Wu, W. Bicker, W. Lindner, *J. Sep. Sci.* 31 (2008) 1492.
- [58] Y. Chen, W. Bicker, J. Wu, M.Y. Xie, W. Lindner, *J. Chromatogr. A* 1217 (2010) 1255.
- [59] Y. Guo, S. Srinivasan, S. Gaiki, *Chromatographia* 66 (2007) 223.
- [60] G. Schuster, W. Lindner, *Anal. Bioanal. Chem.* 400 (2011) 2539.

Supporting Information for Appendix II

Comparative characterization of hydrophilic interaction liquid chromatography columns by linear solvation energy relationships.

G. Schuster, W. Lindner.

Journal of Chromatography A 2012, 1273, 73-94

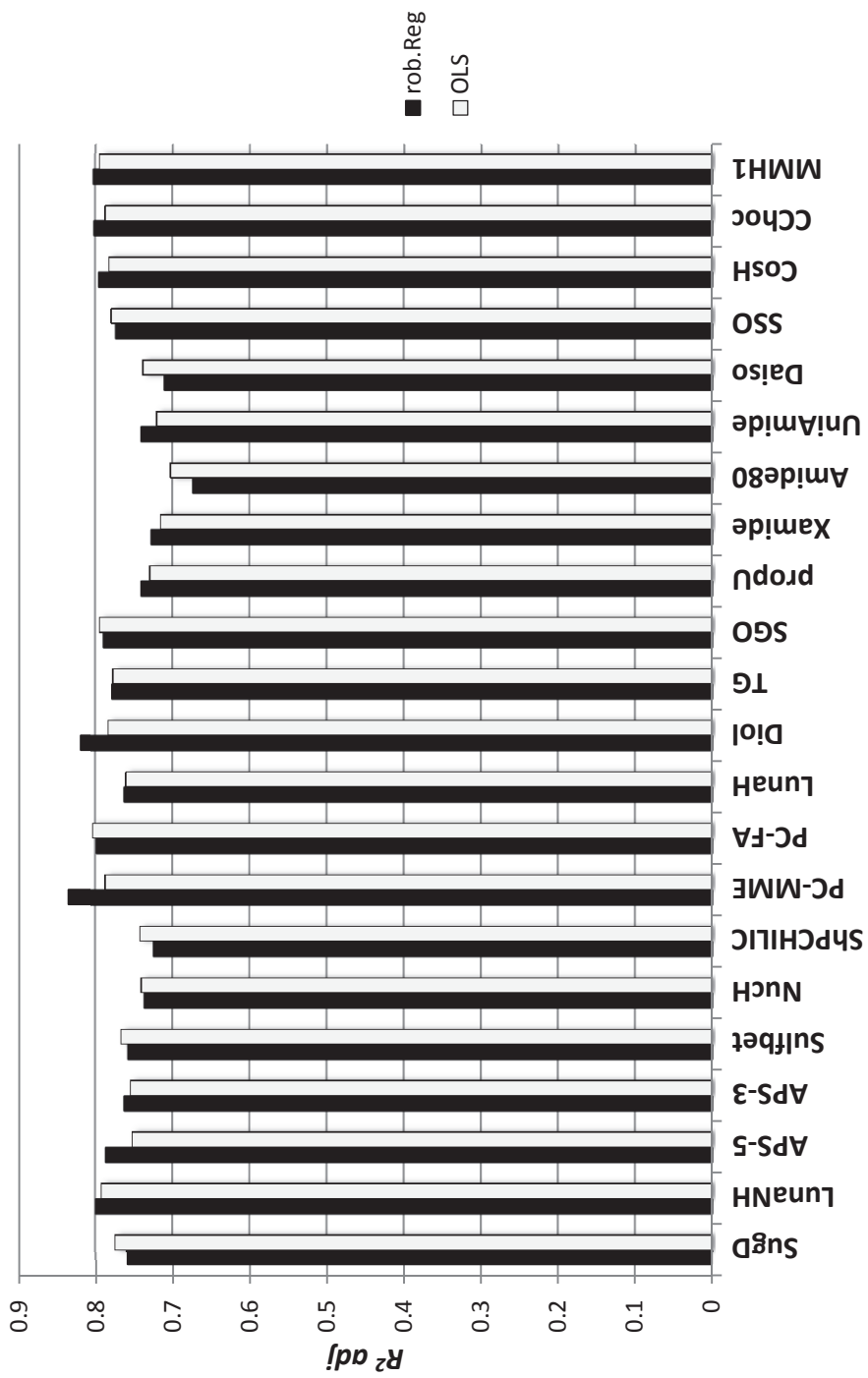


Fig. S1. Comparison of the achieved adjusted goodness of fit (R^2_{adj}) of the solvation model. Obtained either with robust regression (black) or ordinary least square regression (light grey)

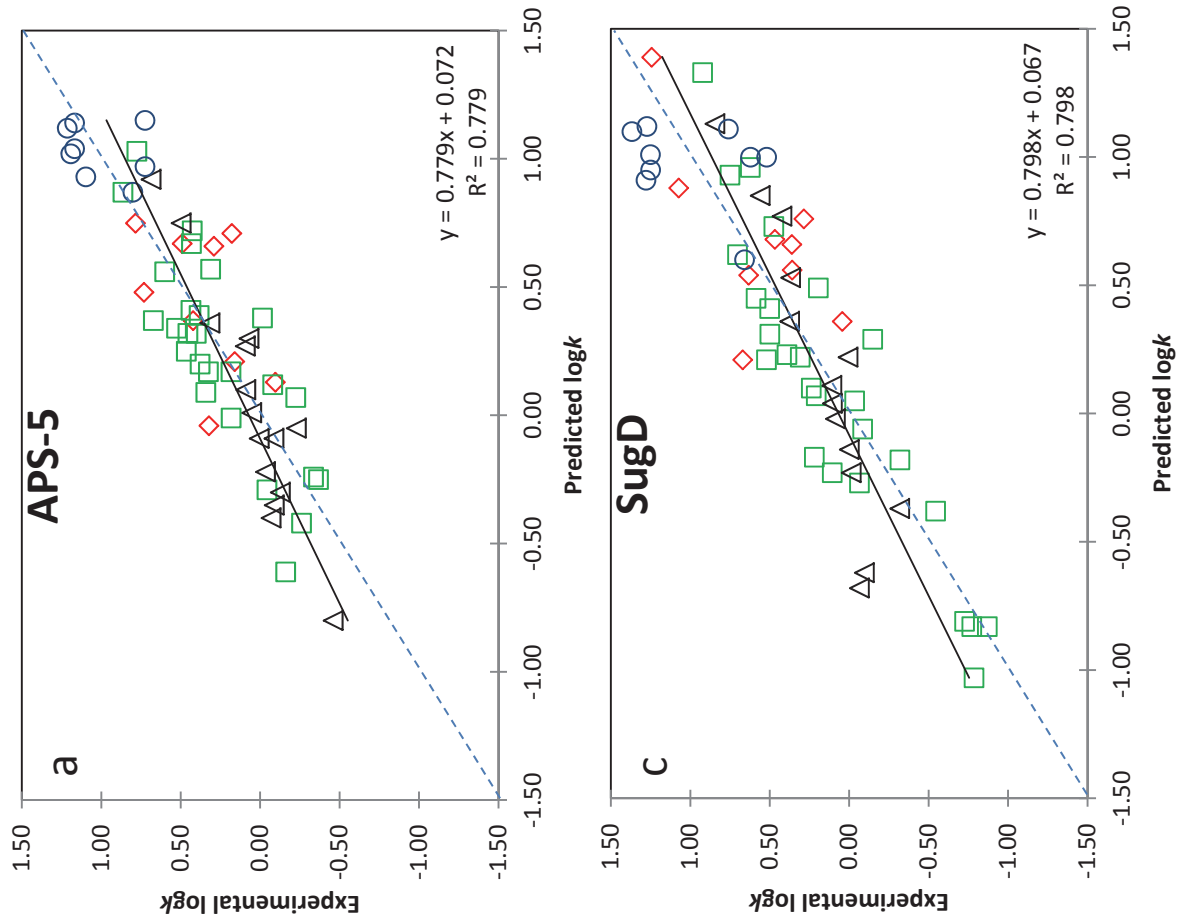
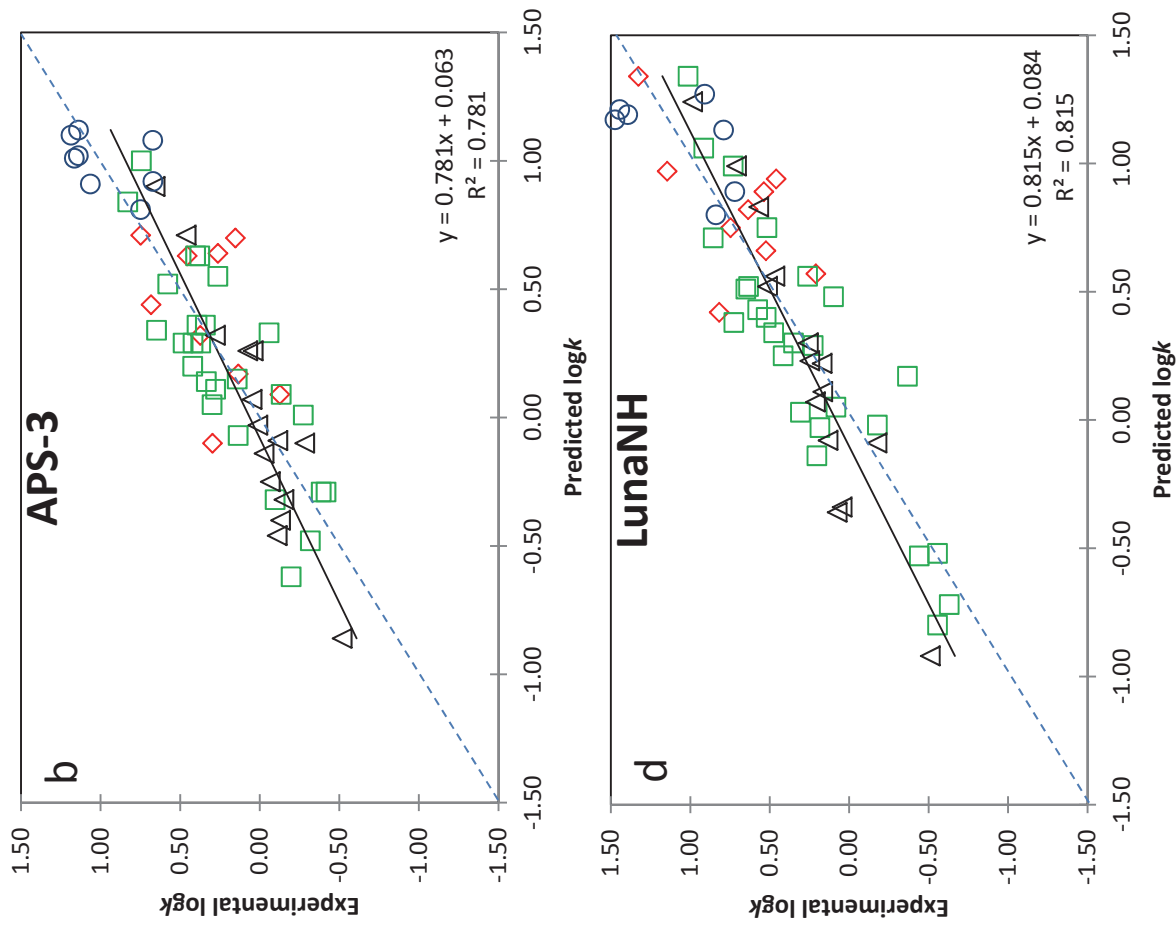


Fig. S2. Experimental logk versus predicted logk plots according to the model equations in Table 5.

Red diamonds \blacklozenge are acidic compounds, green squares \square are basic solutes, black triangles \blacktriangle are neutral species, blue circles \circ are zwitterionic species.



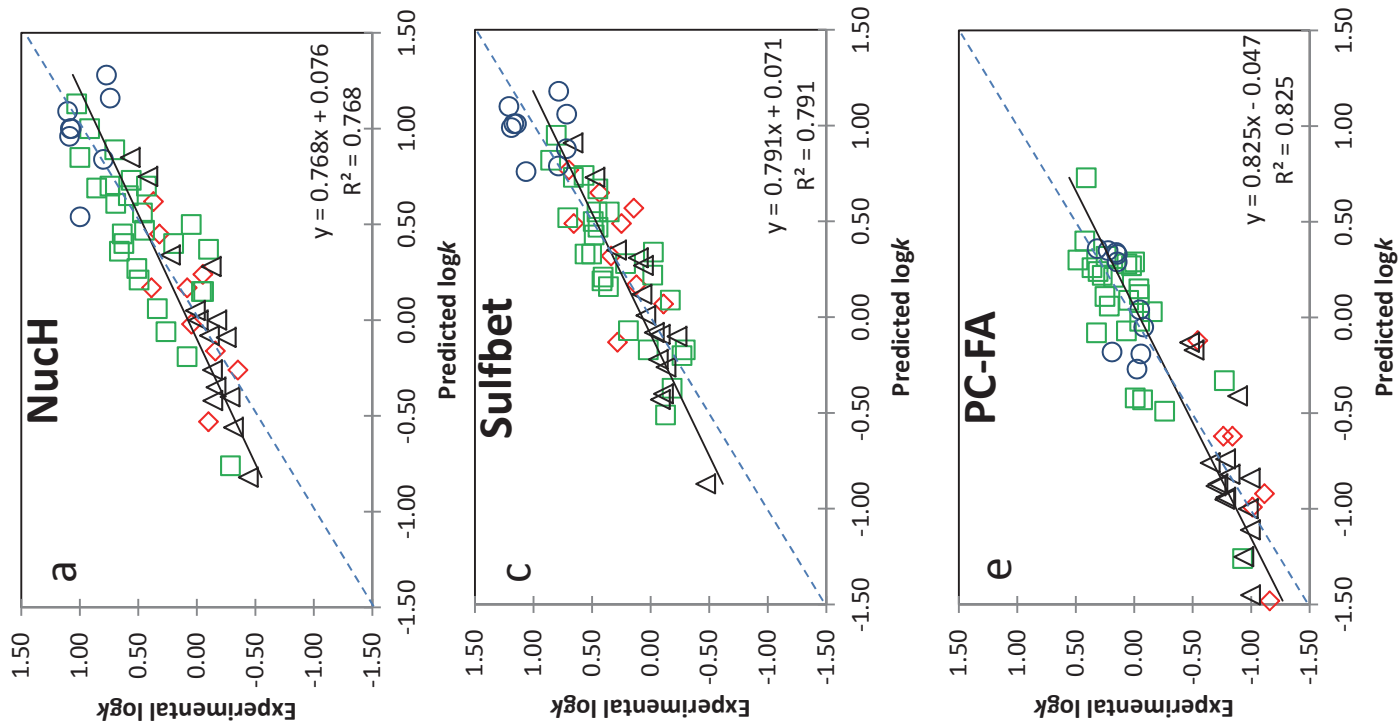


Fig. S3.

Experimental logk versus predicted logk plots according to the model equations in Table 5.

Red diamonds \diamond are acidic compounds, green squares \square are basic solutes, black triangles \triangle are neutral species, blue circles \circ are zwitterionic species.

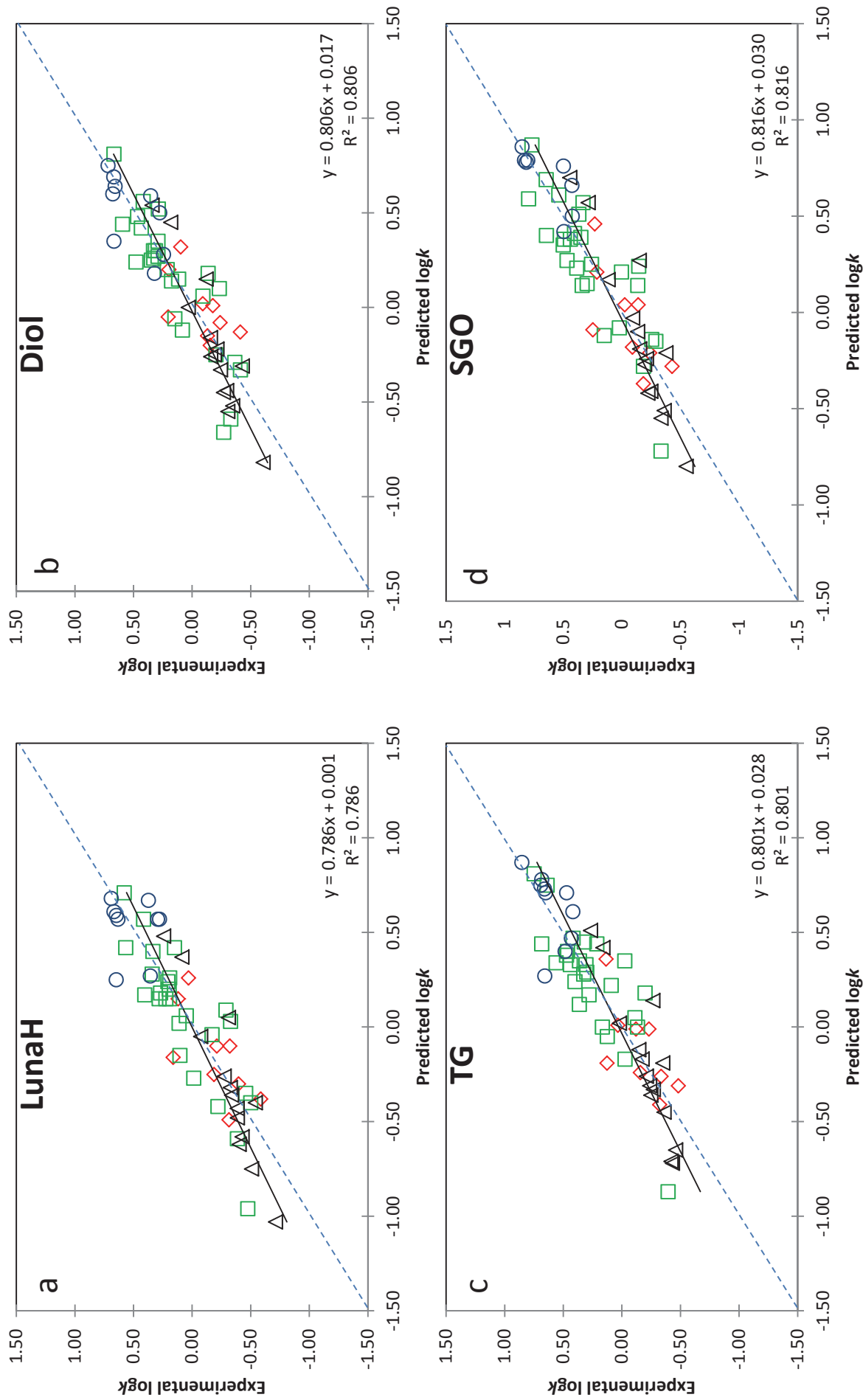


Fig. S4. Experimental logk versus predicted logk plots according to the model equations in Table 5.

Red diamonds \blacklozenge are acidic compounds, green squares \square are basic solutes, black triangles \blacktriangle are neutral species, blue circles \circ are zwitterionic species.

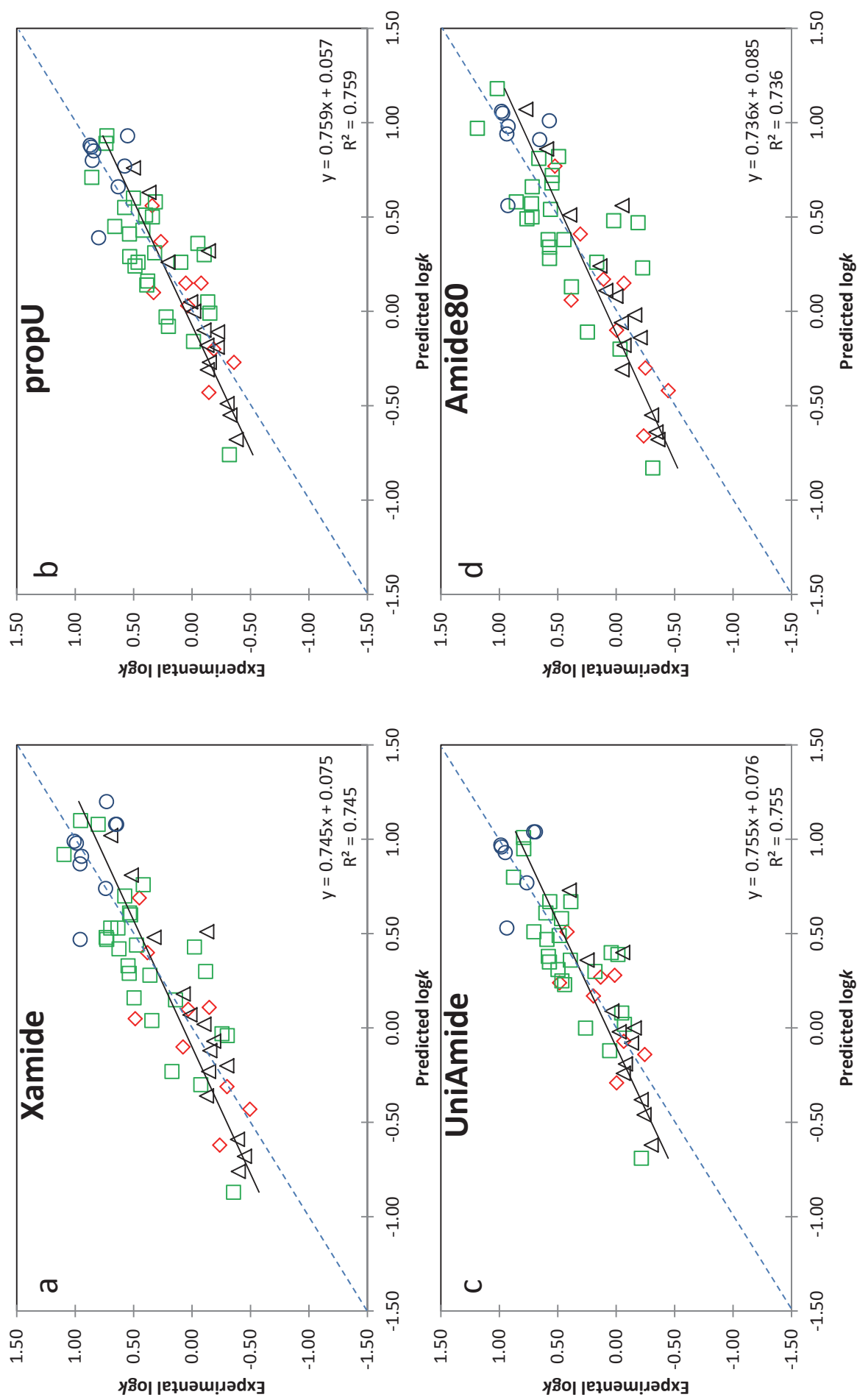


Fig. S5. Experimental $\log K$ versus predicted $\log K$ plots according to the model equations in Table 5. Red diamonds \blacklozenge are acidic compounds, green squares \square are basic solutes, black triangles \blacktriangle are neutral species, blue circles \circ are zwitterionic species.

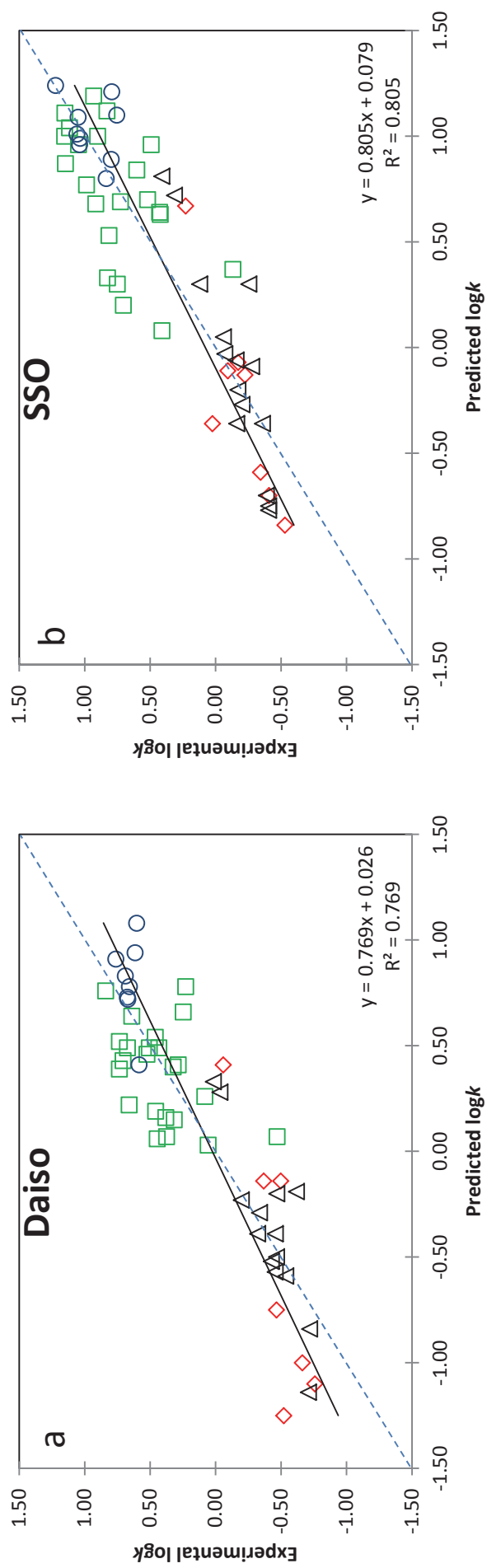


Fig. S6. Experimental logk versus predicted logk plots according to the model equations in Table 5. Red diamonds \blacklozenge are acidic compounds, green squares \square are basic solutes, black triangles \blacktriangle are neutral species, blue circles \circ are zwitterionic species.

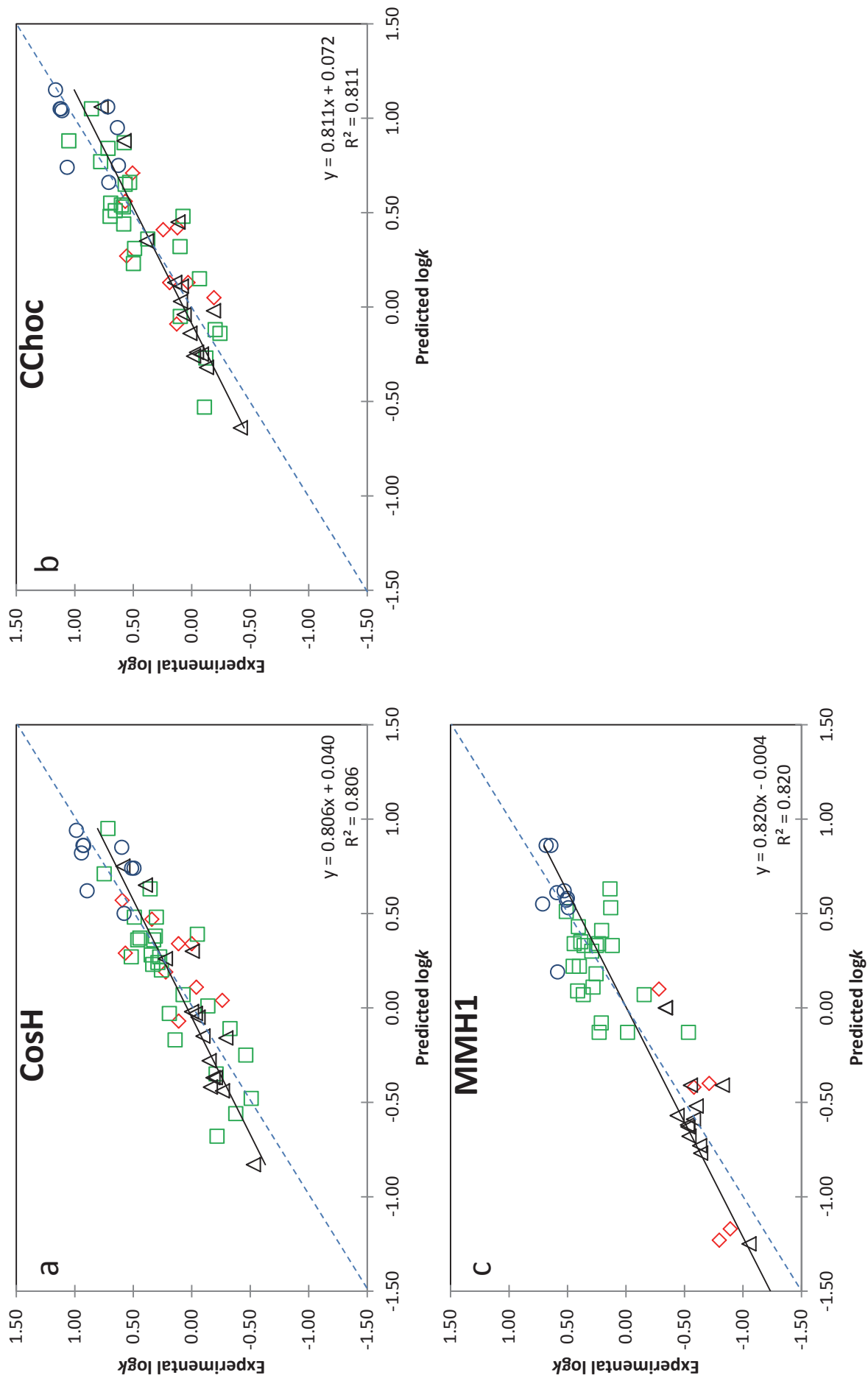


Fig. S7. Experimental logK versus predicted logK plots according to the model equations in Table 5. Red diamonds \blacklozenge are acidic compounds, green squares \square are basic solutes, black triangles \blacktriangle are neutral species, blue circles \circ are zwitterionic species.

APPENDIX III

Additional investigations into the retention mechanism of hydrophilic interaction liquid chromatography by linear solvation energy relationships.

G. Schuster, W. Lindner.

Submitted manuscript

1 **Additional investigations into the retention mechanism of Hydrophilic**
2 **Interaction Liquid Chromatography by Linear Solvation Energy**
3 **Relationships**

4
5
6
7
8 Georg Schuster, Wolfgang Lindner*

9
10
11
12 Department of Analytical Chemistry, University of Vienna, Waehringer Strasse 38,
13 A-1090 Vienna, Austria

14
15
16
17
18
19
20
21 *Corresponding author after publication:

22 Department of Analytical Chemistry, University of Vienna, Waehringer Strasse 38,

23 A-1090 Vienna, Austria

24 Tel.: +43-1-4277-52300, Fax: +43-1-4277-9523

25 E-mail address: wolfgang.lindner@univie.ac.at

26

27 **Abstract**

28 In analogy to our previous publication, the hydrophilic interaction liquid chromatography
29 (HILIC) mechanism were examined in terms of hydrogen bonding, coulombic interactions
30 and phase ratio using linear solvation energy relationships (LSER). At first, 23 commercially
31 available and in-house synthesized chromatographic supports are discussed in order to
32 obtained system constants at pH 5.0 with ammonium acetate as buffer salt. Subsequently we
33 compared these outcomes with our former results obtained at pH 3.0 with ammonium formate
34 as buffer additive. Goodness of fit in terms of the adjusted multiple correlation coefficient
35 (R^2_{adj}) was found to be reduced under the new conditions. No universal model which
36 simultaneously comprised acidic, basic and neutral analytes could be performed. A significant
37 enhancement of the HILIC systems hydrogen bond basicity was found when changing the pH
38 and buffer counter ions. Even though packing materials showed similar selectivity profiles
39 during the collection of the experimental retention data, different forces were found to
40 account for the overall retention (e.g. SHPCHILIC and Nuch). This indicates that HILIC type
41 selectivity is rather based on a sum of additive or multiplicative phenomena.

42

43 **Keywords**

44 HILIC, Hydrophilic Interaction Liquid Chromatography, LSER, Linear Solvation Energy
45 Relationship, Column Characterization

46

47 **1. Introduction**

48 Hydrophilic interaction liquid chromatography (HILIC) has become an important alternative
49 for analytical separation issues which cannot be adequately addressed by the still most
50 commonly used reversed phase (RP) chromatography, size exclusion chromatography or other
51 available chromatography modes. Its big advantage is due to the high retention of polar
52 solutes which are often rather poorly retained and separated on the former mentioned
53 methods, especially on RP. In HILIC, polar stationary phases are paired with hydro-organic
54 mobile phases (MP). Acetonitrile (ACN) was found to be the most favorable non-protic
55 organic solvent and is usually used with a low water content of 2-40%. However, some
56 publications proofed that other non-protic organic solvents may be used. Lindner and
57 coworkers exemplified the behavior of HILIC systems under non-aqueous conditions, in
58 which H₂O is exchanged with protic solvents (e.g. methanol (MeOH), ethanol, or 1,2-
59 ethandiol) [1]. Alpert et al, who introduced the name HILIC, originally suggested a partition
60 motivated mechanism [2]. Water molecules are driven towards the hydrophilic (polar) surface
61 of the stationary phase (SP) and form a stagnant water layer (SWL). Depending on the solutes
62 polarity, probes are then separated by their different partition coefficients between the SWL
63 and the bulk interface. Over the last 20 years, this rather simplified mechanism was emended
64 in terms of additional influences of adsorptive and electrostatic forces between the solutes and
65 the SPs. The large diversity of nowadays available HILIC SPs with their various
66 modifications like amino, urea, diol, betain on either silica or polymer support pose a
67 challenge for the estimation of combined mechanistic contributions towards the HILIC
68 retention mechanism. Approaches to depict the mechanistic forces of HILIC separations are
69 as widespread and diverse as the mechanism itself. Principal component analysis (PCA) and
70 hierarchical cluster analysis (HCA) as well as the analysis of test probes and evaluation of
71 subsequently calculated selectivity factors are powerful tools and the subject of several
72 interesting and enlightening publications [3-11]. Another proceeding which is quite common

73 for the characterization of RP columns is the use of linear solvation energy relationships
74 (LSER) [12-15]. However they are still rather scarcely found when it comes to mechanistic
75 studies in HILIC. Jandera et al. evaluated five SP in RP and HILIC mode using flavones and
76 phenolic acids [16], while Chirita et. al. investigated the behavior of zwitterionic stationary
77 phases based on 76 model compounds [17]. Recently, we published a study on the
78 characterization of 22 polar SPs under HILIC conditions [18]. We were able to show the
79 convenience of LSER models during column development and the ability of classifying them
80 according to the obtained system coefficients via HCA. Consequently, as sequel to our
81 previous work, the present study intends to expand the general view of the HILIC mechanism
82 in terms of the impact of MP changes on LSER models. Moreover, it shall encourage
83 researchers to make use of LSER models as complementary tools for the evaluation of
84 retention forces in the HILIC mechanism. In the following part, we will only shortly describe
85 the used LSER model and theory behind it. We request the reader to consolidate our former
86 publication for more information. By this means, both articles work as complementary parts
87 and thus sum up to a broader view on the investigated HILIC systems.

88
89 LSER models associate the retention of analytes in a certain chromatographic system to their
90 characteristics (physicochemical properties) described by solute descriptors. In this context,
91 Abraham solute parameters have been found adequate to explain chromatography systems. By
92 this means, equation 1 describes the initial solvation parameter model for neutral compounds
93 while equation 2 is modified for the charge state of ionizable compounds. D descriptors can
94 be obtained from equation 3 and 4, and were firstly introduced for HILIC applications by
95 Chirita et al. [17].

96

$$97 \log k = c + eE + sS + aA + bB + vV \quad (1)$$

98

99 $\log k = c + eE + sS + aA + bB + vV + d^-D^- + d^+D^+$ (2)

100

101 $D^- = \frac{10^{(pH-pK)}}{1+10^{(pH-pK)}}$ (4)

102

103 $D^+ = \frac{10^{(pK-pH)}}{1+10^{(pK-pH)}}$ (5)

104

105 In both equations, capital letters refer to the Abraham descriptors of the test compounds and
 106 therefore to interaction properties of the analytes. The complementary property of the SP or in
 107 this case HILIC system (SP and SWL) is represented by the italic lower case letters which are
 108 the computed regression constants. Phase ratio effects, unexplained retention effects and
 109 specific column parameters which are not provided by the chosen retention model are
 110 summarized in the system constant *c*. Interaction forces affiliated by the LSER model include
 111 the contribution from *n* and π electrons as displayed by *E* and *e* for the solute and the SP,
 112 respectively. *S* and *s* are an indication for dipolarity and polarizability. Hydrogen bond acidity
 113 (H-donor) characteristics are described by *A* and *b* while the hydrogen bond basicity (H-
 114 acceptor) is displayed by *B* and *a*. *V* is the McGowan characteristic volume in $\text{cm}^3\text{mol}^{-1}/100$
 115 and correlates with the ability of solute molecules to form cavities and disrupt solvent-solvent
 116 bonds. Additionally to these four original descriptors, which are by convention valid for
 117 neutral analytes, *D* descriptors were introduced to display the impact of coulombic
 118 interactions which arise from the positive or negative charge state of ionizable compounds.
 119
 120 Calculated system coefficients, the standardized coefficients as well as the experimental
 121 versus the predicted $\log k$ values have been consulted to observe the system changes. Thus,
 122 possible deviations associated to the forces which enable HILIC retention when changing the

123 buffer pH and buffer salts from $^w\text{pH}3$ and ammonium formate (NH_4FA) to $^w\text{pH}5$ and
124 ammonium acetate. (NH_4AcOH).

125
126 Apart from the construction of the LSER model to explain the mechanism within the system
127 and to predict retention values, the particular influence of the single descriptive forces
128 (individual variables) on the retention are more directly assessed from the obtained regression
129 coefficient. Consequently, standardized coefficients or beta values (\hat{b}_j) are formed according
130 to Eq. (6) in which the value of the regression coefficient j (b_j) is standardized by the ratio of
131 the standard deviation of the regression coefficient j (σ_{X_j}) and the standard deviation of the
132 dependent variable (σ_Y).

133

$$134 \quad \hat{b}_j = b_j \frac{\sigma_{X_j}}{\sigma_Y} \quad (6)$$

135

136 **2. Experimental**

137 **2.1. Materials**

138 ACN and acetone, both of HPLC gradient grade were purchased at VWR International
139 (Vienna, Austria). Analytical grade Acetic acid (AcOH) and NH_4AcOH were obtained from
140 Sigma–Aldrich (Vienna, Austria). Bi-distilled water was received in-house. All test
141 compounds were of analytical grade and commercially available by different manufacturers.
142 Table 1 shows the solutes with their corresponding molecular descriptors used for this
143 publication. For the analyte structures please refer to [18]. Examined SPs alongside their
144 dimensions, structures and manufacturers are listed in Table 2.

145

146 <Table 1>

147

148 <Table 2>

149

150 **2.1.1. Sample and Eluent Preparation**

151 Analytes were dissolved in concentrations of 0.02 - 1.0 mg mL⁻¹ in ACN/H₂O (v/v) ratios of
152 either 80:20 or 90:10 depending on their solubility. Buffer stock solutions were prepared by
153 dissolving 100 mM NH₄AcOH in bi-distilled water. The aqueous buffer was adjusted to ^wpH
154 5.0 with AcOH. The MP was obtained by mixing ACN and the buffer stock solution in ratios
155 of ACN/buffer (90:10; v/v) (10 mM NH₄AOH). The apparent ^spH, measured with a glass
156 electrode calibrated with aqueous calibration buffers, was ^wpH 7.6. According to IUPAC
157 standards, the aqueous pH and the apparent hydro-organic pH are annotated as ^wpH and
158 ^spH, respectively.

159

160 **2.1.2. Instrumentation**

161 Isocratic elution conditions with a linear flow velocity of 1.6 mm/s were used in combination
162 with a 1200 series HPLC system from Agilent (Waldbronn, Germany), equipped with a diode
163 array detector, to perform the chromatographic runs. The column compartment temperature
164 was set to 25°C. 15 - 20 column volumes of MP were allowed to pass the column prior to the
165 first analyte injection to guarantee stable equilibrium situations. Detection wavelengths were
166 set to 254 nm and 230 nm. Analytes were injected in volumes of 2 µL and acetone was used
167 as void time marker.

168

169 **2.2. Method and Data Analysis**

170 The methodology and data analysis for this study was carried out according to our previous
171 publication [18]. Abraham solute descriptors (A, B, S, E, V) were obtained by ACD/Labs
172 i.Lab [19]. D^+ and D^- descriptors at s_w pH 7.6 were calculated with Eq. (4) and Eq. (5). ACD
173 Labs 7.0 calculator was used to predict pK and logD at s_w pH 7.6. SPSS 20.0 (PAWS
174 Statistics) equipped with the R essential package and Robust Regression dialog box was used
175 to calculate the LSER models [20]. The logarithm of the retention factor ($\log k$) served as
176 dependent variable, while Abraham solute descriptors and charge descriptors were used as
177 independent variables. The solute set was slightly different in the total number of analytes
178 used. High leverage and influential data points were evaluated by plotting the deleted
179 studentized residuals against the leverage values and subsequently removed from the model.

180

181 **2.2.1. Choice of Solutes**

182 The solute set was similar to Ref [18] but revalidated as described in section 2.2. Some
183 zwitterionic compounds of the betain type were removed during the model prediction as they
184 were found to be too influential data points. We had to assume an ineligible error as a result
185 from the computational parameter estimation since equal descriptors were obtained even
186 though the solutes differed at least in one methyl group. Descriptive statistics and histograms
187 of the solute parameter are shown in Table 3, Table 4 and Fig. S1, respectively.

188

189 <Table 3>

190

191 <Table 4>

192

193 **3. Results and Discussion**

194 **3.1. Apparent hydro-organic pH versus aqueous pH**

195 As stated in our preceding publication [18], it is important to evaluate the use of the ^spH or
196 ^wpH value to calculate the D descriptors. Formerly, we came to the conclusion that, while
197 working under acidic conditions with a low amount of water and salt content (ACN/H₂O
198 (90/10 v/v) + 10 mM NH₄FA) to enable electrostatic interaction under HILIC conditions, the
199 use of ^wpH 3.0 is more appropriate to mimic the charge state of ionizable solutes than ^spH
200 5.4. However, during the evaluation under neutral/basic conditions we came to the opposite
201 that ^spH 7.6 reflects better the analytes charge state than ^wpH 5.0 to calculate the D
202 descriptors.

203

204 **3.2. Influence of MP composition on LSER Model**

205 The original idea behind this study was to examine the influence of pH on the forces which
206 enable retention, thus, also the influence on the LSER model for previously characterized
207 columns [18]. However, after the analysis of our solute set, the acquisition of the
208 corresponding $\log k$ values and the application thereof to the multiple linear regression (MLR),
209 we found a severe lack in correlation compared to the analysis at ^wpH 3 (e.g. APS-5: $R^2_{\text{adj}(\text{pH} 3)} = 0,763 \rightarrow R^2_{\text{adj}(\text{pH} 5)} = 0.540$; Xamide: $R^2_{\text{adj}(\text{pH} 3)} = 0,724 \rightarrow R^2_{\text{adj}(\text{pH} 5)} = 0.450$).

211 Thus, it seemed that changing the buffer composition from NH₄FA to NH₄AcOH not only
212 changed the analytes ionization state of acidic and basic compounds but also the retention
213 forces within the HILIC system. As a result, the combined incorporation of neutral-, acidic-
214 and basic analytes to the LSER equation did not result in suitable models, anymore. Again,
215 this study was conducted under enabled or increased additional electrostatic interactions due
216 to the rather low amount of buffer salt and H₂O content. Yet to overcome the lack of
217 correlation and to investigate the HILIC system more selectively we divided our solute set
218 into two subgroups containing neutrals + acids and neutrals + bases. For both sets, the neutral
219 analytes were kept constant and only the charged analytes were different in terms of their

220 ionic status. The arrangement of the analytes to the specific group is shown in Table 1.
221 Zwitterionic and amphoteric compounds were excluded from the model because a more
222 complicated and multidimensional retention mechanisms may be expected to take place.
223 Although the neutral analytes were in both subsets the same, we observed different a/b ratios
224 which account for the hydrogen bond basicity and acidity of the HILIC systems. Thus the
225 analyte type had a slight influence on the modeling of the LSER equations. While calculating
226 the LSER for acidic and neutral compounds an enhanced hydrogen acceptor characteristic of
227 the system was found while higher b coefficients were mostly the result for neutrals alongside
228 basic compounds. This is not a very unexpected result since acidic solutes with high A terms
229 or basic solutes with higher B terms interact stronger with basic (a) or acidic (b) hydrogen
230 bond moieties within the HILIC system. However, to somehow counterbalance this effect we
231 challenged this concept by combining the individually obtained LSER equations for
232 neutrals+acids and neutrals+bases and formed a “mean model equations”. Consequently, we
233 took the mean value of the obtained a , b , and v coefficients and the single determined d and
234 d^+ coefficients. Prediction of solutes was consulted to evaluate the validity of this equation
235 (Fig. S2 – Fig. S6). For the evaluation of the “mean linear solvation energy model”, we added
236 amino acids which were not present in the training set (see Table S1).

237
238 In the following section, the columns will be discussed according to their arrangement into
239 groups of similar retention forces. Although the overall selectivity pattern may be slightly
240 different within these new groups, the retention seems to be governed in similar manners. We
241 think that this is no contradictory methodology as LSER models try to compartmentalize the
242 HILIC system into single retention effects (hydrogen bonding, charge interactions, partition
243 ratio) which then may contribute in an additively or multiplicatively way to gain the overall
244 selectivity pattern of the single columns.

245

246 3.3.Evaluation of system coefficients

247

248 <Fig 1>

249

250 Some basic principles of this study need to be kept in mind while interpreting the results.

251 Most importantly, this study only examines the interactions between the HILIC systems and

252 small aromatic UV active compounds and different results may be observed if aliphatic

253 compounds are considered. Consequently, the LSER models were reduced to the solute

254 descriptors A, B, V, D⁺ and D⁻. This seems applicable as aromatic compounds show a high

255 correlation between the polarizability contributions from n and π electrons and the overall

256 hydrogen bond acceptor capability. Hence, the system constant e was mostly found to be

257 insignificant or if significant found to down regulate the effect of b . S was originally included

258 in the LSER calculations but found to be insignificant which was already the case in our

259 previous publication. Nevertheless, *dipole-dipole* interactions may possibly affect the

260 retention within the HILIC system but might not be assessed with the chosen solute sets. Dinh

261 et al showed that dipole-dipole interactions play a role but this effect was predominately

262 found for PolySulfA and ZIC [4]. Unfortunately, the number of solute retention data used for

263 the solvation parameter model varies within the column set as some analytes eluted with the

264 void time especially acids on acidic columns. As mentioned above, the discussion is based on

265 \hat{b}_j -values (Fig. 1, Table 5 – Table 7) and not on the obtained regression coefficients to display

266 the impact of the independent variables to the overall model.

267

268 The system constant c is negative for all columns and involves the phase ratio and column

269 specific phenomena which participate in the repartition of the analytes towards the mobile

270 phase and are not adequately described by the set LSER model. These effects may be the

271 impact of polarizability and dipolarity which was excluded from our model and found to

272 account rather for elution than retention [17]. Nevertheless, due to the complexity of the c
273 term a stringent interpretation should be avoided.

274

275 Coherent distributions between the forces which apply either towards the MP or SP were
276 found for the remaining coefficient. It is in agreement with our previous publication but also
277 with publications of former working groups who performed LSER on HILIC systems [16,17].
278 Indeed, hydrogen bonding in terms of H-bond acidity (b) and H-bond basicity (a) are positive
279 and contribute to the retention of solutes. Moreover, d^+ and d^- were found to be positive as
280 well. Thus, solute retention is governed by an elevated hydrophilicity due to the analytes
281 charge state and electrostatic solute-sorbent interactions. Furthermore, ion-pairing and salt
282 bridge phenomena may take place between the solute and the buffer ions within the SWL.
283 Contrarily, v is negative and quantifies the stronger distribution towards the MP. The ACN
284 molecules are less organized compared to the hydrogen bonded H₂O molecule network in the
285 water layer. Hence, a lower energy is needed to let the solute form a cavity and enter the
286 solvent. As a result, bigger (and more lipophilic) molecules will most likely prefer to stay in
287 the organic compartment of the MP if no other strong hydrophilic interactions assist to
288 penetrate into the water layer. All this findings are in agreement with hydrophilic/polar
289 interaction driven chromatography (HILIC/NP) and are orthogonal to LSER models for RP
290 systems (e.g. [13,15]).

291

292 **3.4.Retention of acidic and neutral analytes within HILIC systems**

293

294 <Table 5>

295

296 Table 5 displays the obtained model equations for neutral and acidic compounds with
297 corresponding beta values. The columns could be arranged into roughly four groups according

298 to the obtained coefficient patterns. The first group contains APS-5, APS-3, Sulfbet, CosH,
299 SugD and LunaNH. Within this group of mainly basic SPs the hydrogen bond donor and
300 acceptor characteristics of the HILIC system (a and b coefficient) and the analytes charge
301 state, hence the HILIC systems affinity towards anions, exhibit equal contribution to the
302 retention. It is to mention that SugD and LunaNH have a slightly higher contribution of the d'
303 coefficient. Thus, reflecting the dominating influence of electrostatic interactions compared to
304 hydrogen bonding. This can be explained by the higher basicity of the tert. and sec. amine
305 groups present on SugD and also presumably present on LunaNH. Although a different ligand
306 type is specified for LunaNH the same effect was already observed for the LSER study under
307 pH_w 3 and suggest the existents of not only primary amino modifications for this support.
308 APS-5 and APS-3 contain primary amino functionalities while CosH features a triazol ring.
309 Both ligand types seem to be partially protonated and partially dissociated, respectively under
310 the given conditions. Thus attractive forces with acids are reduced and may also be further
311 decreased due to the additional ionized residual silanol groups. Despite the basic character of
312 the Sulfbet based on the tert. amine modification the column interacts more in the range of
313 APS-5 and APS-3 than SugD or LunaNH. Hence, this leads to the conclusion that the added
314 sulfonic acid residue counterbalance the stronger attraction for acids but it is not sufficient
315 enough to repartition this column towards more “neutral” packings.
316
317 In the second group (LunaH, propU, Xamide, UniAmide, Amide80, ZIC and NuchH,
318 PolySulfA) partition of acidic compounds between the MP and the SP/SWL seem to be the
319 main retentive force as it is shown by the high contribution of the b and v coefficient with a
320 slightly lower effect of the hydrogen acceptor capability a (mean b/a ratio = 1.14). The charge
321 effect (d') plays a minor role. Only NuchH, LunaH and Amide80 show an equal magnitude for
322 a and b . One column that does not quite equally fit into this group is PolySulfA. It exhibits a
323 very low a coefficient but the highest contribution of the d' coefficient for all columns. This

324 might be due to the polymeric background of the column which seems to be able to swell.
325 Consequently, it may form a higher amount of adsorbed water resulting in a thicker SWL in
326 comparison to more brush type base columns. Recently, Noga et al. measured the excess
327 adsorption isotherms of water onto surfaces of chemically bonded stationary phases [21].
328 Their results support our finding as Polyhydroxyethyl A, which is closely related to the
329 PolySulfA, exhibited the largest excess adsorption of water for all columns tested. Yet again,
330 it confirms the impact of the diffuse or stagnant water layer onto the HILIC systems hydrogen
331 bond acidity (*b*).

332
333 On Diol, SGO, CChoc and ShPCHILIC, acids are stronger retained due to hydrogen bond
334 interactions. The low *d'* coefficient may result from repulsive forces which can derive either
335 from residual ionized silanol groups on Diol, SGO or CChoc and from the negatively charged
336 phosphocholin group of ShPCHILIC. However, the attractive forces or the partition within the
337 SWL are still strong enough to facilitate sufficient retention of acidic compounds.

338
339 On almost all acidic columns like Daiso, SSO, PC-MME and PC-FA (see Table 2) acidic
340 analytes are excluded while carrying a negative charge. Although TG is very similar to SGO
341 it shows a general lower retention for all compounds and residual ionized silanol groups have
342 a higher impact on the repulsion process compared to SGO. Even though both column
343 loadings are quite similar (see Table 2) the bulkiness of the sulfinylgroup compared to the
344 thioether group seems able to better shield the silanol groups and to inhibit repulsive effects
345 [22]. The slightly positive *d'* coefficient of PC-FA is only a result of the model uncertainty for
346 this coefficient which was also found to be insignificant. Thus, if an acid is retained it may
347 only happen via hydrogen bonding as the amido-amino function seems less effective to
348 neutralize the strong acid moiety. A high *b* coefficient is commonly associated to the H-bond
349 acidity of the SWL. However, only low *b* system parameters were obtained. Thus, it is

350 reasonable to assume that these columns only have a very limited adsorbed water layer and
351 are more likely to undergo adsorptive single point interactions rather than hydrophilic
352 multipoint interactions. The group of Knut Irgum found similar results for bare silica columns
353 via PCA and nuclear magnetic resonance studies [4,23]. Furthermore, Kumar et al. observed a
354 lower adsorption of water on bare silica and attributed this effect to the preferential
355 association of ACN molecules onto siloxane bridges [8]. Both, the obtained low b and ν value
356 assist these statements. Rather low k values were obtained for neutral analytes.

357

358 **3.5. Retention of basic and neutral analytes within HILIC systems**

359

360 <Table 6>

361

362 Table 6 displays the obtained model equations for neutral and basic compounds. Again, the
363 first group contains the basic columns APS-5, APS-3, Sulfbet, CosH, SugD and LunaNH (see
364 Table 2). While the hydrogen donor to acceptor ratio was mostly equal to 1.0 for acidic
365 compounds, a higher b coefficient was obtained for basic compounds, which would support a
366 partition enhanced mechanism. Additionally, the relatively high contribution of the charge
367 state (d^+) for APS-5, APS-3, Sulfbet and CosH shows the lower impact of electrostatic
368 repulsion and the lower basicity of these columns at s_w pH 7.6 compared to SugD and
369 LunaNH for which a d^+/d^- ratio can be calculated of 0.5 or 0.7, respectively. Consequently,
370 basic solutes seem to experience some repulsive forces. However, they are not as strongly
371 affected as acids on acidic columns as no bases were found to elute with t_0 on equally charged
372 SPs.

373

374 On the “neutral” diol modified columns TG, SGO and Diol, d^+ shows the highest contribution
375 towards the retention and emphasizes an electrostatically dominated mechanism overlaying

376 the partition between the MP and the SP. Residual negatively charged silanol groups are most
377 likely to account for this phenomenon. Apart from that, the hydrogen acceptor and donor
378 probability of these phases account to an equal amount towards the retention of analytes.
379 Similar to these columns are LunaH, CChoc, UniAmide, propU, Xamide, Amide80 and
380 PolySulfA. On all these columns the b coefficient is higher than the a coefficient.
381 Furthermore, UniAmide and propU exhibit higher d^+ coefficients than a and b which pin
382 point once more to residual negatively charged silanols. However, since the d^+ coefficient was
383 generally obtained with a high magnitude it may also simply indicates that the charge state
384 has an generally higher impact on the retention of bases than it has for acids, for which the
385 hydrogen acceptor and donor capability of the HILIC systems predominately determines the
386 extend of retention. Although a high d^+ was found for PolySulfA, the additional attractive
387 forces due to the sulfonic acid residues may not be too high since the retention span for bases
388 is similar to diol modified columns which are the lowest retentive ones in this column group.
389 Also some repulsive forces from background aminopropyl groups of the grafting process may
390 reduce the retention. And thus PolySulfA seems more partition dominated. Zwitterionic
391 modified columns can be separated into two groups. ZIC and NucH both are similar to the
392 previously described “neutral” columns with equal contributions of hydrogen donor/acceptor
393 as well as the charge state. Hereby, NucH offers higher electrostatic interactions compared to
394 ZIC. The more brush type modification of NucH and the possibility of residual silanols
395 compared to the polymeric modification of ZIC may be accountable for this effect.
396 Furthermore, the ligand coverage can contribute to these deviations. Consequently, although
397 the modification density is not specified the LSER model indicates a higher sulfobetain
398 loading of NucH compared to ZIC. In comparison, ShPCHILIC (phosphocholin modified)
399 facilitates retention due to high coulombic interactions with regard to the negatively charged
400 phosphoric acid group. Furthermore this HILIC system is generally a better hydrogen bond
401 acceptor than donor under the given test conditions which pinpoints a more dominant

402 adsorption driven mechanism with underlying partition effects. The result is very interesting
403 as ShPCHILIC showed similar selectivity profiles according to NucH even though these two
404 columns seem to have different interaction forces to generally retain solutes.
405 The acidic supports, SSO, PC-FA and PC-MME facilitate retention of basic compounds via
406 electrostatic interactions as shown by the high magnitude of the d^+ coefficient compared to
407 the minor contribution of a and b .

408

409 3.6.Column comparison according to “mean model equations” and pH

410

411 <Table 7>

412

413 Mean model coefficients are summarized in Table 7. Bar graphs of the standardized system
414 constants for ^wpH 5.0 and ^wpH 3.0 are shown in Fig. 1. If we examine the predictions made
415 by the “mean model equation” compared to the actual $\log k$ values (Fig. S2 – S6) we observe a
416 general overestimation of the actual retention values. Thus, not all forces are adequately
417 displayed or captured using this LSER model. Discussed dipole-dipole driven partition
418 towards the MP may be one of these forces. This is of course furthermore displayed in the
419 lower R^2_{adj} compared to studies in which predominately high buffer capacities in combination
420 with a higher H_2O amount was used [17]. However, this is, next to our previous publication
421 [18], one of the first studies to examine a various amount of columns under electrostatically
422 enhanced HILC conditions. Consequently, the rather complex mixed-modal character of the
423 retention mechanism adds a not negligible uncertainty to the whole outcome. Moreover,
424 dissociated acids should have a higher hydrogen acceptor capability which is not displayed by
425 the calculated Abraham descriptors. This effect most likely takes place on packings with
426 adsorptive interaction sites. A similar effect regarding the prolonged retention of acids was
427 found by Kumar et al. [8] and Guo et. al. [24]. The latter examined the influence of pH

428 change on the retention of salicylic acid and acetylsalicylic acid. No change in k was found
429 for salicylic acid opposed to a longer retention of acetylsalicylic acid at elevated pH.
430 Furthermore, our proposition on the importance of hydrogen bond for the retention of acidic
431 compounds is illustrated by comparing the changes in retention for 4-hydroxybenzoic acid
432 and salicylic acid. Both acids only differ in the position of the hydroxyl group. However, the
433 change of the retention factor for 4-hydroxybenzoic acid from $^w\text{pH}3$ to $^w\text{pH}5$ is around
434 14 times higher than for salicylic acid which did not change significantly. Due to the ortho
435 position of the OH group in salicylic acid, the carboxylate group can form an intramolecular
436 hydrogen bond with the hydroxyl group, which reduces or even inhibits the addressability of
437 both functional groups. On the contrary, 4-hydroxybenzoic acid is not able to undergo this
438 intramolecular hydrogen bonding and offers two interaction sites in favor to the HILIC
439 mechanism. As a result, the ionized ortho hydroxyl acid retains around 10 times longer than
440 the ionized para form. This strong effect of hydroxyl groups was primarily observed for acids
441 and only slightly for basic compounds. It becomes more and more obvious that it is important
442 to adapt the available or computable Abraham descriptors of neutral molecules to their
443 ionized forms in order to obtain high quality results if electrostatic and adsorptive interactions
444 shall be taken into account. Despite the relatively low R^2_{adj} retention predictions were still
445 possible to a certain extent, albeit it was not the focus of our study. To validate the “mean
446 model” we added amino acids which were not part of the training set. The equally good fit of
447 prediction for these compounds compared to the training set shows, that it is possible to use
448 this mean equations to get a “global view” on the retention phenomena. This was not possible
449 when acids, bases and neutrals were added combined to the MLR.

450

451 If we compare the results from the system in combination with NH_4FA $^w\text{pH} 3.0$ or
452 NH_4AcOH $^w\text{pH}5.0$ a longer retention was observed for almost all compounds which is

453 represented by a higher magnitude of the *b* coefficient. Only CChoc, ShPCHILIC, SSO, TG
454 and SGO exhibited lower hydrogen bond acidity. For all columns the hydrogen bond basicity
455 property got higher and in terms of acidic columns even turned significant. One reason that
456 accounts for this phenomenon may be the dissociation of acidic groups or residual silanol
457 groups which would serve as stronger hydrogen acceptors. Subsequently, a higher adsorption
458 of the strong hydrogen bond donor H₂O takes places which results in a higher solvation of the
459 chromatographic support.

460 Furthermore the change from formate to acetate may influence the thickness of the layer. The
461 higher molecular volume of acetate ions could lead to a swelling of the water layer compared
462 to the use of formate buffer. Apart from this the acetate or ammonia buffer ions may
463 contribute to the HILIC systems in terms of forming ion pairs or salt bridges. Elevated
464 retention is known to emerge when formate is exchanged to acetate [25]. Thus, we think that
465 the phase is not only more solvated but the higher retention and the clear rise of the hydrogen
466 basicity as shown by the LSER model is due to the change in the buffer salt in combination
467 with dissociated silanol functions on columns which are based on silica support materials.

468 Another peculiarity that we observed similar to Bicker et al. [25] was the loss in retention for
469 arylsulfonic acids (data not shown). Albeit the high negative logD values (~ -2 - -5) and the
470 permanent negative charge which would favor hydrophilic interactions they are found to elute
471 faster on all columns. A closer look at the descriptors of the acids (see Table 1) show higher B
472 and lower A values which is opposed to the parameters of carboxylic acids used during the
473 study. As mentioned above, thioether based columns (TG, SGO and SSO) lost some of their
474 H-bond acidic capacity during the pH change. We may be able to reciprocally transfer this
475 effect. Thus, the chosen conditions in combination with the changed buffer counter ions are
476 affecting the solvation of sulfur containing compounds and render their hydrogen bond
477 capacity. Furthermore, the referred rise of the H-bond basicity may lead to the observed loss

478 in retention which promotes the retention of carboxylic acids. However, these statements are
479 only preliminary observations and need further investigations.

480

481 Finally, in addition to the presented results, the complete set of experiments was also carried
482 out at ^wpH 8.0 or ^spH 7.8, respectively (data not shown). No significant changes on
483 selectivity differences or the obtained LSER models were observed which we attest to the
484 negligible change in ^spH from 7.6 to 7.8.

485

486 **4. Conclusion**

487 In accordance with the phrase “all roads lead to Rome” many different ways are nowadays
488 used to classify hydrophilic packing materials and to elucidate HILIC retention mechanisms
489 and interaction forces. Yet mainly PCA or selectivity plots are consulted to depict different
490 retention phenomena in the HILIC mode [3-11]. We showed that LSER methods can give
491 similar results in terms of SP/SWL-solute- interactions with additional predictive character.
492 The main drawbacks of linear solvation energy studies under enhanced electrostatic driven
493 HILIC interactions were found to be the unadjusted solute descriptors for anions and cations
494 which are generally computed for their neutral species. However, the hydrogen acidity and
495 basicity of the molecule is changing which plays an important role if adsorption is one of the
496 dominant retention facilitating forces. This statement is underlined by the reduction in R^2_{adj} at
497 ^wpH 5 compared to our previous study at ^wpH 3. Due to the elevated pH, more solutes are
498 ionized as acids become deprotonated while most basic compounds still stayed positively
499 charged. The problematic in generating one universal equation with the need of deriving
500 specific equations for solute families may be directly related to this phenomenon. Acids seem
501 to be more affected by the hydro-organic environment than basic compounds. Thus we

502 emphasize a focus on the correction of these descriptors for ionized species in upcoming
503 studies. Another approach would be the screening of HILIC chromatography materials at
504 higher water and buffer salt content which attenuates the mixed modal character of the phases,
505 which was shown by Chirita et. al. [17]. Apart from that, we showed that the change from
506 formate to acetate elevates the hydrogen bond basicity of the HILIC system. Furthermore,
507 intramolecular hydrogen bonding in acids reduces the number of interaction sites and lowers
508 their overall hydrophilicity. Thus, electrostatic attraction is somewhat inhibited. Finally, we
509 want to remind the reader that the HILIC mechanism is very divers although partition seem to
510 be dominant on many columns. Hence, the presented results may only be attributed to our
511 specific test setting and can vary under different elution conditions.

512

513 **Figure legends**

514

515 **Fig. 1** Obtained standardized system constants (calculated according to Eq. 6).derived from
516 the analysis of retention factors of test probes from Table 1. The white bar represents the
517 standardized regression coefficients for $^w\text{pH } 3$ [18] while the black, the blue diagonal striped
518 and the red horizontal striped bar display the standardized coefficients for the mean solvation
519 equation at $^w\text{pH } 5$, the neutral+basic analytes and the neutral+acidic analytes, respectively.

520

521

522 **References**

- 523 [1] W. Bicker, J. Wu, M. Lämmerhofer, W. Lindner, J. Sep. Sci. 31 (2008) 2971.
524 [2] A.J. Alpert, J. Chromatogr. 499 (1990) 177.
525 [3] R.-I. Chirita, C. West, A.-L. Finaru, C. Elfakir, J. Chromatogr. A 1217 (2010)
526 3091.
527 [4] N.P. Dinh, T. Jonsson, K. Irgum, J. Chromatogr. A 1218 (2011) 5880.
528 [5] Y. Guo, S. Gaiki, J. Chromatogr. A 1218 (2011) 5920.
529 [6] M.E.A. Ibrahim, Y. Liu, C.A. Lucy, J. Chromatogr. A 1260 (2012) 126.
530 [7] Y. Kawachi, T. Ikegami, H. Takubo, Y. Ikegami, M. Miyamoto, N. Tanaka, J.
531 Chromatogr. A 1218 (2011) 5903.
532 [8] A. Kumar, J.C. Heaton, D.V. McCalley, J. Chromatogr. A 1276 (2013) 33.
533 [9] M. Lämmerhofer, M. Richter, J. Wu, R. Nogueira, W. Bicker, W. Lindner, J.
534 Sep. Sci. 31 (2008) 2572.
535 [10] D.V. McCalley, J. Chromatogr. A 1217 (2010) 3408.
536 [11] A. Periat, B. Debrus, S. Rudaz, D. Guillarme, J. Chromatogr. A 1282 (2013)
537 72.
538 [12] J. Gotta, S. Keunchkarian, C. Castells, M. Reta, J. Sep. Sci. 35 (2012) 2699.
539 [13] L. He, M. Zhang, W. Zhao, J. Liu, X. Jiang, S. Zhang, L. Qu, Talanta 89 (2012)
540 433.
541 [14] S. Studzińska, B. Buszewski, Chromatographia 75 (2012) 1235.
542 [15] K. Vyňuchalová, P. Jandera, Anal. Lett. 44 (2011) 1640.
543 [16] P. Jandera, T. Hajek, V. Skerikova, J. Soukup, J. Sep. Sci. 33 (2010) 841.
544 [17] R.I. Chirita, C. West, S. Zubrzycki, A.L. Finaru, C. Elfakir, J. Chromatogr. A
545 1218 (2011) 5939.
546 [18] G. Schuster, W. Lindner, J. Chromatogr. A 1273 (2013) 73.
547 [19] <https://ilab.acdlabs.com/iLab2/index.php>.
548 [20] <http://gruener.userpage.fu-berlin.de/spss-dialogs.htm>.
549 [21] S. Noga, S. Bocian, B. Buszewski, J. Chromatogr. A 1278 (2013) 89.
550 [22] J.Y. Wu, W. Bicker, W. Lindner, J. Sep. Sci. 31 (2008) 1492.
551 [23] E. Wikberg, T. Sparrman, C. Viklund, T. Jonsson, K. Irgum, J. Chromatogr. A
552 1218 (2011) 6630.
553 [24] Y. Guo, S. Gaiki, J. Chromatogr. A 1074 (2005) 71.
554 [25] W. Bicker, J.Y. Wu, H. Yeman, K. Albert, W. Lindner, J. Chromatogr. A 1218
555 (2011) 882.
556
557
558

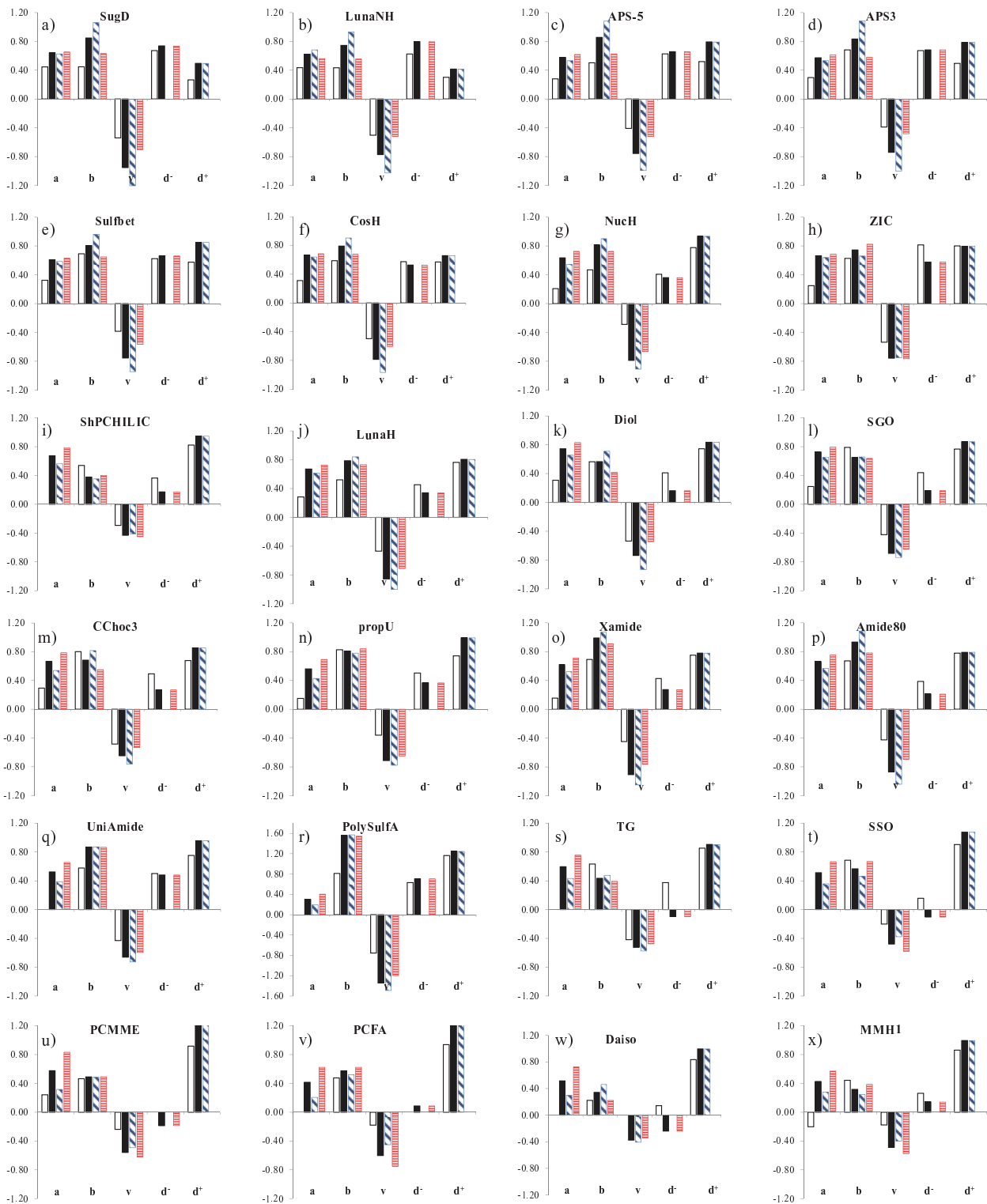





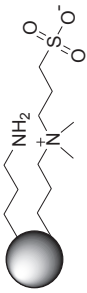
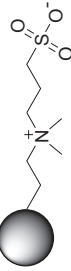
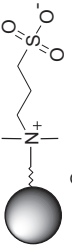

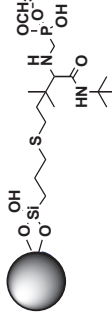
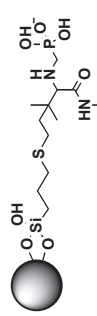
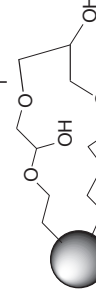
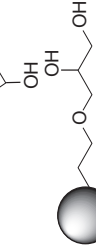
Table 1 LSER test compounds and their corresponding descriptors. Solute structures can be found in Table S1. The last column indicates the affiliation of this analyte to a certain test set. The red circle and blue square symbolizes the “neutral+acidic” and “neutral+basic” test set, while a green diamond represents the validation set.

Nr.	Analytes	A	B	S	E	V	D _{7.6}	D ⁺ _{7.6}	Log D _{o/w} (pH 7.6)	Acid pK	Basic pK	test set
1	Adenine	0.70	1.13	1.80	1.68	0.923	0.00	0.00	-0.03	9.85	4.20	● ■ ◆
2	Adenosine	0.97	2.22	2.64	2.69	1.754	0.02	0.00	-1.02	13.11, 9.23	3.40	● ■ ◆
3	Deoxyadenosine	0.72	1.94	2.38	2.49	1.695	0.00	0.00	-0.55	13.79	3.40	● ■ ◆
4	Uracil	0.44	1.00	1.00	0.81	0.752	0.02	0.00	-0.72	9.20		● ■ ◆
5	Uridine	0.90	2.29	2.35	1.88	1.582	0.17	0.00	-1.69	13.58, 8.28		● ■ ◆
6	Deoxyuridine	0.74	1.92	2.14	1.65	1.524	0.14	0.00	-1.77	13.37, 9.23	1.69	● ■ ◆
7	Thymine	0.44	1.03	1.00	0.80	0.893	0.02	0.00	-1.12	9.84		● ■ ◆
8	Thymidine	0.74	1.93	2.09	1.62	1.665	0.01	0.00	-0.12	14.04, 9.23		● ■ ◆
9	Cytosine	0.60	1.02	1.90	1.43	0.793	0.00	0.00	-1.71	12.20	4.18	● ■ ◆
10	Cytidine	0.87	2.62	2.21	2.09	1.623	0.00	0.00	-1.93	13.43	3.27	● ■ ◆
11	Guanine	0.97	1.20	1.60	1.80	0.982	0.01	0.00	-0.98	12.6, 9.63	3.15	● ■ ◆
12	Guanosine	1.34	2.86	2.82	2.56	1.812	0.02	0.00	-1.73	13.37, 9.28	1.69	● ■ ◆
13	Deoxyguanosine	1.09	2.58	2.56	2.36	1.754	0.02	0.00	-1.37	13.96, 9.31	1.90	● ■ ◆
14	Xanthine	0.97	1.07	1.60	1.50	0.941	0.50	0.00	-1.11	13.93, 7.60	1.00	● ◆
15	Hypoxanthine	0.60	1.18	1.82	1.38	0.882	0.05	0.00	-1.21	8.90	2.20	● ■ ◆
16	Caffeine	0.05	1.28	1.72	0.50	1.363	0.00	0.00	-0.13		0.73	● ■
17	Theophylline	0.54	1.34	1.60	1.50	1.222	0.09	0.00	-0.22	8.60	1.70	● ■
18	Theobromine	0.50	1.38	1.60	1.50	1.222	0.00	0.00	-0.72	9.90	0.59	● ■
19	Dyphylline	0.54	1.86	2.44	1.88	1.762	0.00	0.00	-1.10	15.05, 13.66	0.70	● ■
20	Nicotinic acid	0.57	0.73	1.21	0.79	0.891	1.00	0.00	-2.96	2.20	4.80	●
21	Nicotinamide	0.63	1.00	1.09	1.01	0.932	0.00	0.00	-0.11		3.54	● ■ ◆
22	Isoniazid	0.47	1.39	1.85	1.19	1.032	0.00	0.00	0.25	12.55	3.06	● ■ ◆
23	4-Hydroxybenzenesulfonic acid	0.81	1.15	2.02	1.10	1.115	1.08	0.00	-5.20	8.66, -0.23		● ◆

24	4-Methylbenzenesulfonic acid	0.31	0.88	1.72	0.89	1.197	1.00	0.00	-2.57	-0.43	2.45	◆
25	2-Aminobenzenesulfonic acid	0.54	1.19	2.17	1.15	1.156	1.00	0.00	-3.41	-1.41	2.45	◆
26	Salicylic acid	0.71	0.38	0.84	0.89	0.990	1.00	0.00	-1.07	3.01		●
27	5-Methylsalicylic acid	0.70	0.40	1.04	0.93	1.131	1.00	0.00	-0.60	13.99, 3.30		●
28	4-Hydroxybenzoic acid	0.81	0.56	0.90	0.93	0.990	1.02	0.00	-1.37	9.22, 4.57		◆
29	4-Aminobenzoic acid	0.94	0.60	1.65	1.08	1.032	1.00	0.00	-1.76	4.86	2.51	◆
30	4-Hydroxyphenylacetic acid	0.97	0.78	1.32	0.94	1.131	1.00	0.00	-2.24	10.19, 4.50		◆
31	3,4-Dihydroxyphenylacetic acid	1.35	0.86	1.47	1.12	1.190	1.01	0.00	-2.91	9.84, 4.42		◆
32	3-Phenoxyacetic acid	0.72	0.76	0.93	0.91	1.131	1.01	0.00	-2.95	9.59, 4.19		◆
33	Mandelic acid	0.74	0.89	1.05	0.9	1.131	1.00	0.00	-2.69	15.65, 3.41		◆
34	3,4-(Methylenedioxy) mandelic acid	0.74	1.28	1.33	1.22	1.281	1.00	0.00	-2.84	15.65, 3.39		◆
35	Propranolol	0.17	1.42	1.43	1.88	2.148	0.00	0.97	1.56	13.84	9.14	■
36	Atenolol	0.69	2.00	1.88	1.45	2.176	0.00	0.97	-1.46	13.88	9.16	◆
37	Salbutamol sulfate	1.19	1.82	1.26	1.43	1.978	0.00	0.98	-1.60	9.99	9.22	◆
38	Sotalol	0.74	1.75	1.86	1.52	2.101	0.01	0.97	-1.27	9.55	9.18	◆
39	Melamine	0.68	1.21	1.88	1.61	0.893	0.00	0.01	-1.37		5.66	◆
40	1-(4-nitrophenyl)ethanamine	0.21	0.79	1.51	1.06	1.272	0.00	0.92	0.08		8.65	◆
41	Benzyltrimethylammonium	0.00	0.15	0.56	0.36	1.401	0.00	1.00	-2.31			■
42	1-Ethylpyridin-1-ium bromide	0.00	0.11	0.58	0.39	0.979	0.00	1.00	-3.66			■
43	1-Butylpyridin-1-ium bromide	0.00	0.12	0.59	0.39	1.260	0.00	1.00	-3.30			■
44	Benzylamine	0.15	0.72	0.77	0.83	0.957	0.00	0.98	-0.7		9.22	◆
45	Dopamine	1.20	1.04	1.46	1.35	1.215	0.02	1.00	-1.83	12.68, 9.39	10.11	◆
46	Tyramine	0.71	0.94	1.17	1.01	1.157	0.01	1.00	-1.55	9.51	10.49	◆
47	2-Amino-1-phenylethanol	0.46	1.19	1.10	1.03	1.157	0.00	0.87	-0.43	12.04	8.43	◆
48	Phenylephrine	0.88	1.37	1.17	1.20	1.356	0.01	0.98	-1.65	9.76	9.22	◆
49	Phenylalanine	0.78	1.02	1.39	0.95	1.313	1.00	0.98	-1.65	2.21	9.20	◆
50	Tyrosine	1.28	1.29	1.60	1.18	1.372	1.00	0.98	-2.13	10.01, 2.25	9.35	◆
51	Tryptophan	1.09	1.23	1.80	1.62	1.543	1.00	0.99	-1.47	2.30	9.51	◆

52	α -Methyltryptophan	1.09	1.24	1.75	1.59	1.684	1.00	0.99	-1.12	2.34	9.51	◆
53	5-Methyltryptophan	1.09	1.23	1.74	1.64	1.684	1.00	0.99	-1.01	2.26	9.52	◆
54	Tryptophanamide	1.01	1.45	2.27	1.87	1.584	0.00	0.79	-0.57		8.18	◆
55	Deoxycytidine	0.71	2.25	2.00	1.86	1.565	1.00	0.00	-1.88	14.03, 3.59		◆

Table 2 Stationary phases used during the LSER study

Abbreviation	Stationary Phase	Manufacturer	Modification	ligand density	Dimensions	Particle Size	Pore Size	Surface
SugD	SugarD	Waters		n/a	150x4.6 mm	5.0 μm	120 Å	n/a
LunaNH	Luna NH2	Phenomenex	Amino, endcapped	n/a	150x3.0 mm	5.0 μm	100 Å	400 m ² g ⁻¹
APS-5	3-aminopropyl silica	in-house		3.4 μmol/m ²	150x4.0 mm	5.0 μm	100 Å	300 m ² g ⁻¹
APS-3	3-aminopropyl silica	in-house		2.4 μmol/m ²	150x4.0 mm	3.0 μm	100 Å	300 m ² g ⁻¹
Sulfbet	Sulfobetain	in-house		1.9 μmol N/m ² 1.7 μmol S/m ²	150x4.0 mm	5.0 μm	100 Å	300 m ² g ⁻¹
NucH	NucleodurHILIC	Macherey & Nagel		7 % C	150x4.6 mm	3.0 μm	110 Å	n/a
ZIC	ZIC HILIC	SeQuant		n/a	150x4.6 mm	3.5 μm	100 Å	n/a
ShPCHILIC	PC HILIC	Shiseido		n/a	150x4.6 mm	3.0 μm	100 Å	350 m ² g ⁻¹
PCMME	Amidoamino phosphonate (monomethylester)	in-house		0.8 μmol/m ²	150x4.0 mm	5.0 μm	100 Å	300 m ² g ⁻¹
PCFA	Amidoamino phosphonate (free acid)	in-house		0.4 μmol/m ²	150x4.0 mm	5.0 μm	100 Å	300 m ² g ⁻¹
LunaH	Luna HILIC	Phenomenex		5.7 % C	150x4.6 mm	5.0 μm	200 Å	200 m ² g ⁻¹
Diol	ProntosilDiol	Bischoff Chromatography		4 % C	150x4.0 mm	5.0 μm	100 Å	300 m ² g ⁻¹

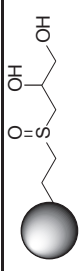
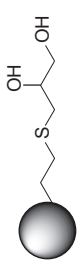
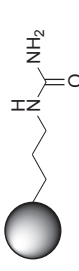
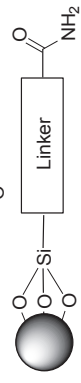

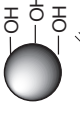
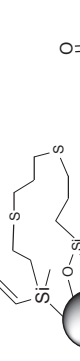
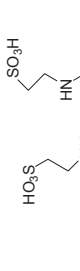
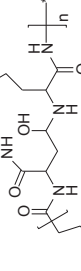
SGO	Sulfinylglycerol	in-house		2.3 $\mu\text{mol}/\text{m}^2$	150x4.0 mm	5.0 μm	100 Å	300 $\text{m}^2 \cdot \text{g}^{-1}$
TG	Thioglycerol	in-house		2,7 $\mu\text{mol}/\text{m}^2$	150x4.0 mm	5.0 μm	100 Å	300 $\text{m}^2 \cdot \text{g}^{-1}$
propU	nPropUrea	in-house		1.81 $\mu\text{mol}/\text{m}^2$	150x4.0 mm	5.0 μm	100 Å	300 $\text{m}^2 \cdot \text{g}^{-1}$
Xamide	XBridge Amide	Waters Corporation		7.5 $\mu\text{mol}/\text{m}^2$	150x3.0 mm	3.5 μm	135 Å	185 $\text{m}^2 \cdot \text{g}^{-1}$
Amide80	TSKGelAmid80	Tosoh		n/a	150 x 2.0 mm	3.0 μm	100 Å	450 $\text{m}^2 \cdot \text{g}^{-1}$
UniAmide	UnisolAmide(HILIC)	Agela Techn. Inc.	hydrophilic amide group	8 % C	150x4.6 mm	5.0 μm	100 Å	410 $\text{m}^2 \cdot \text{g}^{-1}$
Daiso	Daisogel (bare silica)	Daiso Chemical		-	150x4.0 mm	5.0 μm	100 Å	300 $\text{m}^2 \cdot \text{g}^{-1}$
SSO	Sulfosulfoxyde	in-house		0.85 $\mu\text{mol}/\text{m}^2$	150x4.0 mm	5.0 μm	100 Å	300 $\text{m}^2 \cdot \text{g}^{-1}$
PolySulfa	PolySULFOETHYL A	PolyLC Inc.		n/a	150x4.6 mm	5.0 μm	300 Å	n/a
CosH	CosmosilHILIC	Nacalai Tesque		n/a	150x4.6 mm	5.0 μm	120 Å	300 $\text{m}^2 \cdot \text{g}^{-1}$
CChoc	C-Choc HILIC	in-house	Maillard Modified	19.2 $\mu\text{mol C}/\text{m}^2$	150x4.0 mm	3.0 μm	100 Å	300 $\text{m}^2 \cdot \text{g}^{-1}$

Table 3 Descriptive Statistic for the solutes (see Table 1) considered during the multiple linear regression.

	E	S	A	B	V	D ⁻	D ⁺
Minimum	0.360	0.560	0.000	0.110	0.752	0.000	0.000
Maximum	2.690	2.820	1.350	2.860	2.176	1.080	1.000
Mean	1.306	1.564	0.663	1.236	1.282	0.297	0.264
Median	0.552	0.570	0.331	0.644	0.373	0.446	0.437
Standard deviation	1.195	1.600	0.705	1.165	1.174	0.015	0.000
Median absolute deviation	0.305	0.430	0.185	0.340	0.206	0.015	0.000

Table 4 Correlation matrix for the solute descriptors of the compounds considered during the multiple linear regression (see Table 1)

	A	B	S	E	V	D ⁻	D ⁺
A	1.000	0.477	0.443	0.553	0.183	0.223	-0.315
B		1.000	0.839	0.855	0.673	-0.398	-0.201
S			1.000	0.838	0.472	-0.199	-0.420
E				1.000	0.546	-0.331	-0.268
V					1.000	-0.308	0.316
D ⁻						1.000	-0.405
D ⁺							1.000

Table 5 System constants for 23 stationary phases computed according to Eq.3 for neutral and acidic compounds with the corresponding statistics. R^2_{adj} is the adjusted correlation coefficient, SE is the standard error of the fit, F the Fisher's statistics, n the number of solutes considered in the regression. Italic numbers represent the standardized coefficients \hat{b}_j .

	<i>c</i>	<i>a</i>	<i>b</i>	<i>v</i>	<i>d</i>	<i>n</i>	<i>R</i>	R^2_{adj}	<i>SE</i>	<i>F</i>
SugD	-0.224 ±0.23	1.706 ±0.24	0.613 ±0.22	-1.371 ±0.33	0.996 ±0.18	33	0.916	0.815	0.269	36
		<i>0.653</i>	<i>0.632</i>	<i>-0.702</i>	<i>0.737</i>					
LunaNH	-0.267 ±0.20	1.362 ±0.19	0.556 ±0.19	-1.040 ±0.28	1.058 ±0.15	35	0.933	0.854	0.242	51
		<i>0.562</i>	<i>0.556</i>	<i>-0.519</i>	<i>0.795</i>					
APS-5	-0.426 ±0.21	1.222 ±0.20	0.513 ±0.20	-0.854 ±0.30	0.717 ±0.16	35	0.884	0.751	0.257	27
		<i>0.619</i>	<i>0.627</i>	<i>-0.520</i>	<i>0.657</i>					
APS-3	-0.532 ±0.20	1.235 ±0.19	0.486 ±0.19	-0.812 ±0.29	0.769 ±0.16	35	0.899	0.782	0.246	32
		<i>0.612</i>	<i>0.580</i>	<i>-0.481</i>	<i>0.682</i>					
Sulfbet	-0.388 ±0.20	1.219 ±0.19	0.517 ±0.19	-0.903 ±0.28	0.701 ±0.15	35	0.892	0.769	0.244	30
		<i>0.630</i>	<i>0.649</i>	<i>-0.565</i>	<i>0.661</i>					
CosH	-0.353 ±0.18	1.112 ±0.17	0.455 ±0.17	-0.815 ±0.25	0.473 ±0.14	35	0.877	0.738	0.217	25
		<i>0.685</i>	<i>0.678</i>	<i>-0.605</i>	<i>0.527</i>					
NucH	-0.305 ±0.21	1.283 ±0.20	0.531 ±0.19	-0.976 ±0.30	0.352 ±0.16	35	0.860	0.704	0.252	21
		<i>0.725</i>	<i>0.726</i>	<i>-0.665</i>	<i>0.361</i>					
ZIC	-0.224 ±0.25	1.352 ±0.18	0.711 ±0.19	-1.271 ±0.28	0.656 ±0.14	34	0.914	0.813	0.225	37
		<i>0.685</i>	<i>0.826</i>	<i>-0.765</i>	<i>0.577</i>					

ShPCHILJC	-0.352 ±0.20	1.231 ±0.20	0.260 ±0.20	-0.547 ±0.29	0.148 ±0.15	33	0.841	0.666	0.221	17
		<i>0.784</i>	<i>0.403</i>	<i>-0.450</i>	<i>0.172</i>					
LunaH	-0.451 ±0.18	1.096 ±0.17	0.457 ±0.17	-0.886 ±0.25	0.285 ±0.14	35	0.858	0.701	0.215	21
		<i>0.728</i>	<i>0.732</i>	<i>-0.708</i>	<i>0.341</i>					
Diol	-0.384 ±0.15	1.108 ±0.15	0.233 ±0.15	-0.604 ±0.22	0.121 ±0.12	34	0.871	0.726	0.184	23
		<i>0.832</i>	<i>0.420</i>	<i>-0.543</i>	<i>0.162</i>					
TG	-0.452 ±0.17	1.046 ±0.18	0.203 ±0.16	-0.468 ±0.23	-0.063 ±0.13	32	0.805	0.596	0.194	12
		<i>0.757</i>	<i>0.392</i>	<i>-0.474</i>	<i>-0.097</i>					
SGO	-0.409 ±0.15	1.120 ±0.15	0.372 ±0.15	-0.733 ±0.22	0.148 ±0.12	35	0.880	0.744	0.186	26
		<i>0.795</i>	<i>0.639</i>	<i>-0.624</i>	<i>0.190</i>					
CChoc	-0.308 ±0.19	1.305 ±0.18	0.375 ±0.18	-0.732 ±0.27	0.250 ±0.14	33	0.881	0.743	0.222	24
		<i>0.786</i>	<i>0.551</i>	<i>-0.532</i>	<i>0.269</i>					
propU	-0.351 ±0.16	0.957 ±0.15	0.484 ±0.15	-0.755 ±0.23	0.284 ±0.12	35	0.865	0.714	0.193	22
		<i>0.691</i>	<i>0.838</i>	<i>-0.648</i>	<i>0.365</i>					
Xamide	-0.245 ±0.18	1.185 ±0.17	0.631 ±0.17	-1.059 ±0.26	0.253 ±0.14	35	0.882	0.748	0.218	26
		<i>0.712</i>	<i>0.910</i>	<i>-0.764</i>	<i>0.272</i>					
Amide80	-0.228 ±0.19	1.302 ±0.18	0.571 ±0.18	-1.008 ±0.27	0.204 ±0.15	35	0.880	0.745	0.228	26
		<i>0.752</i>	<i>0.781</i>	<i>-0.695</i>	<i>0.209</i>					
UniAmide	-0.394 ±0.20	1.010 ±0.17	0.549 ±0.17	-0.757 ±0.25	0.381 ±0.13	30	0.866	0.71	0.206	19
		<i>0.656</i>	<i>0.866</i>	<i>-0.594</i>	<i>0.481</i>					

PolySulfa	-0.311 ±0.27	0.822 ±0.28	1.381 ±0.30	-1.965 ±0.39	0.739 ±0.23	31	0.820	0.672	0.308	13
	<i>0.404</i>	<i>1.545</i>	<i>0.706</i>	<i>-1.197</i>	<i>0.706</i>					
SSO	-0.370 ±0.23	1.201 ±0.23	0.462 ±0.21	-0.805 ±0.31	-0.098 ±0.16	32	0.857	0.694	0.246	19
	<i>0.666</i>	<i>0.667</i>	<i>-0.579</i>	<i>-0.102</i>						
PC-MME	-0.474 ±0.17	1.086 ±0.19	0.276 ±0.19	-0.650 ±0.27	-0.149 ±0.16	31	0.834	0.649	0.204	15
	<i>0.834</i>	<i>0.493</i>	<i>-0.624</i>	<i>-0.186</i>						
PC-FA	-0.724 ±0.17	0.953 ±0.19	0.326 ±0.19	-0.731 ±0.26	0.066 ±0.16	30	0.831	0.64	0.198	14
	<i>0.624</i>	<i>0.624</i>	<i>-0.750</i>	<i>0.087</i>						
Daiso	-0.501 ±0.29	1.342 ±0.28	0.171 ±0.28	-0.527 ±0.41	-0.247 ±0.22	34	0.741	0.487	0.345	9
	<i>0.728</i>	<i>0.223</i>	<i>-0.346</i>	<i>-0.239</i>						

Table 6 System constants for 23 stationary phases computed according to Eq.3 for neutral and basic compounds with the corresponding statistics. R^2 is the adjusted correlation coefficient, SE is the standard error of the fit, F the Fisher's statistics, n the number of solutes considered in the regression. Italic numbers represent the standardized coefficients \hat{b}_j .

	c	a	b	v	d^+	n	R	$R^2_{adj.}$	SE	F
Sugd	-0.085 ± 0.18	1.044 ± 0.30 <i>0.627</i>	0.813 ± 0.26 <i>1.062</i>	-1.349 ± 0.31 <i>-1.204</i>	0.521 ± 0.19 <i>0.495</i>	29	0.844	0.665	0.270	15
LunaNH	-0.236 ± 0.14	1.119 ± 0.21 <i>0.683</i>	0.767 ± 0.21 <i>0.933</i>	-1.180 ± 0.24 <i>-1.026</i>	0.453 ± 0.15 <i>0.415</i>	29	0.912	0.804	0.210	30
APS-5	-0.287 ± 0.15	0.753 ± 0.22 <i>0.533</i>	0.762 ± 0.21 <i>1.082</i>	-1.016 ± 0.25 <i>-0.993</i>	0.758 ± 0.15 <i>0.792</i>	30	0.872	0.722	0.220	20
APS-3	-0.362 ± 0.15	0.748 ± 0.22 <i>0.533</i>	0.76 ± 0.21 <i>1.086</i>	-1.017 ± 0.25 <i>-0.998</i>	0.748 ± 0.15 <i>0.786</i>	30	0.871	0.721	0.219	20
Sulfbet	-0.297 ± 0.14	0.848 ± 0.22 <i>0.586</i>	0.695 ± 0.21 <i>0.963</i>	-0.990 ± 0.24 <i>-0.944</i>	0.834 ± 0.15 <i>0.85</i>	29	0.885	0.748	0.215	23
CosH	-0.238 ± 0.14	0.833 ± 0.22 <i>0.641</i>	0.585 ± 0.21 <i>0.905</i>	-0.908 ± 0.25 <i>-0.966</i>	0.582 ± 0.15 <i>0.658</i>	30	0.851	0.68	0.220	16
NucH	-0.219 ± 0.16	0.841 ± 0.24 <i>0.545</i>	0.691 ± 0.23 <i>0.902</i>	-1.009 ± 0.26 <i>-0.909</i>	0.973 ± 0.16 <i>0.935</i>	30	0.876	0.731	0.235	21
ZIC	-0.171 ± 0.19	1.039 ± 0.28 <i>0.641</i>	0.537 ± 0.26 <i>0.662</i>	-0.906 ± 0.29 <i>-0.751</i>	0.884 ± 0.19 <i>0.796</i>	31	0.842	0.664	0.275	16
ShPCHLIC	-0.092 ± 0.18	0.749 ± 0.27	0.232 ± 0.23	-0.449 ± 0.26	0.906 ± 0.18	32	0.818	0.619	0.270	14

		0.198	1.572	-1.49	1.246				
SSO	-0.122 ± 0.18	0.530 ± 0.23	0.353 ± 0.21	-0.504 ± 0.25	1.180 ± 0.18	31	0.886	0.752	0.260
		0.359	0.466	-0.376	1.075				24
PC-MME	-0.343 ± 0.14	0.543 ± 0.21	0.422 ± 0.20	-0.653 ± 0.22	1.487 ± 0.15	32	0.933	0.852	0.218
		0.318	0.488	-0.492	1.224				46
PC-FA	-0.624 ± 0.13	0.343 ± 0.18	0.449 ± 0.17	-0.640 ± 0.20	1.499 ± 0.14	34	0.939	0.866	0.212
		0.207	0.523	-0.451	1.231				55
Daiso	-0.273 ± 0.18	0.428 ± 0.23	0.350 ± 0.24	-0.446 ± 0.28	0.993 ± 0.19	32	0.832	0.646	0.272
		0.302	0.462	-0.406	0.997				15

Table 7 Calculated mean LSER model and beta values for 23 stationary phases for neutral and basic compounds with the corresponding statistics. R^2 is the fit of experimental to calculated logk values. *Italic numbers* represent the mean standardized coefficients \hat{b}_j . The stated RSD is the deviation between the single LSER models from Table 4 and Table 5

Column	c	a	b	v	d⁻	d⁺	R²
SugD	-0.155 ± 0.10	1.375 ± 0.47	0.713 ± 0.14	-1.360 ± 0.02	0.996	0.521	0.787
		<i>0.640 ± 0.02</i>	<i>0.847 ± 0.30</i>	<i>-0.953 ± 0.35</i>	<i>0.737</i>	<i>0.495</i>	
LunaNH	-0.252 ± 0.02	1.241 ± 0.17	0.662 ± 0.15	-1.110 ± 0.10	1.058	0.453	0.815
		<i>0.623 ± 0.09</i>	<i>0.745 ± 0.27</i>	<i>-0.773 ± 0.36</i>	<i>0.795</i>	<i>0.415</i>	
APS-5	-0.357 ± 0.10	0.988 ± 0.33	0.638 ± 0.18	-0.935 ± 0.11	0.717	0.758	0.755
		<i>0.576 ± 0.06</i>	<i>0.855 ± 0.32</i>	<i>-0.757 ± 0.33</i>	<i>0.657</i>	<i>0.792</i>	
APS-3	-0.447 ± 0.12	0.992 ± 0.34	0.623 ± 0.19	-0.915 ± 0.15	0.769	0.748	0.759
		<i>0.573 ± 0.06</i>	<i>0.833 ± 0.36</i>	<i>-0.740 ± 0.36</i>	<i>0.682</i>	<i>0.786</i>	
Sulfbet	-0.343 ± 0.06	1.034 ± 0.26	0.606 ± 0.13	-0.947 ± 0.06	0.701	0.834	0.752
		<i>0.608 ± 0.03</i>	<i>0.806 ± 0.22</i>	<i>-0.755 ± 0.27</i>	<i>0.661</i>	<i>0.85</i>	
CosH	-0.296 ± 0.08	0.973 ± 0.20	0.520 ± 0.09	-0.862 ± 0.07	0.473	0.582	0.783
		<i>0.663 ± 0.03</i>	<i>0.792 ± 0.16</i>	<i>-0.786 ± 0.25</i>	<i>0.527</i>	<i>0.658</i>	
NucH	-0.262 ± 0.06	1.062 ± 0.31	0.611 ± 0.11	-0.993 ± 0.02	0.352	0.973	0.769
		<i>0.635 ± 0.13</i>	<i>0.814 ± 0.12</i>	<i>-0.787 ± 0.17</i>	<i>0.361</i>	<i>0.935</i>	
ZIC	-0.198 ± 0.04	1.196 ± 0.22	0.624 ± 0.12	-1.089 ± 0.26	0.656	0.884	0.754
		<i>0.663 ± 0.03</i>	<i>0.744 ± 0.12</i>	<i>-0.758 ± 0.01</i>	<i>0.577</i>	<i>0.796</i>	
ShPCHILIC	-0.222 ± 0.18	0.990 ± 0.34	0.246 ± 0.02	-0.498 ± 0.07	0.148	0.906	0.749
		<i>0.675 ± 0.15</i>	<i>0.379 ± 0.03</i>	<i>-0.430 ± 0.03</i>	<i>0.172</i>	<i>0.947</i>	
LunaH	-0.385 ± 0.09	0.954 ± 0.20	0.504 ± 0.07	-0.919 ± 0.05	0.285	0.722	0.771
		<i>0.672 ± 0.08</i>	<i>0.787 ± 0.08</i>	<i>-0.854 ± 0.21</i>	<i>0.341</i>	<i>0.806</i>	
Diol	-0.288 ± 0.14	0.943 ± 0.23	0.325 ± 0.13	-0.706 ± 0.14	0.121	0.677	0.725
		<i>0.745 ± 0.12</i>	<i>0.566 ± 0.21</i>	<i>-0.737 ± 0.27</i>	<i>0.162</i>	<i>0.835</i>	
TG	-0.302 ± 0.21	0.754 ± 0.41	0.233 ± 0.04	-0.473 ± 0.01	-0.063	0.644	0.709
		<i>0.596 ± 0.23</i>	<i>0.435 ± 0.06</i>	<i>-0.524 ± 0.07</i>	<i>-0.097</i>	<i>0.905</i>	
SGO	-0.326 ± 0.12	0.937 ± 0.26	0.373 ± 0.00	-0.700 ± 0.05	0.148	0.707	0.786
		<i>0.725 ± 0.10</i>	<i>0.649 ± 0.01</i>	<i>-0.681 ± 0.08</i>	<i>0.19</i>	<i>0.87</i>	
CChoc	-0.183 ± 0.18	0.982 ± 0.46	0.449 ± 0.10	-0.747 ± 0.02	0.250	0.768	0.766
		<i>0.663 ± 0.17</i>	<i>0.684 ± 0.19</i>	<i>-0.648 ± 0.16</i>	<i>0.269</i>	<i>0.854</i>	
propU	-0.218 ± 0.19	0.729 ± 0.32	0.473 ± 0.02	-0.719 ± 0.05	0.284	0.815	0.728

		0.559 ± 0.19	0.808 ± 0.04	-0.713 ± 0.09	0.365	0.991	
Xamide	-0.203 ± 0.06	0.960 ± 0.32 0.618 ± 0.13	0.685 ± 0.08 0.990 ± 0.11	-1.041 ± 0.03 -0.908 ± 0.21	0.253 0.272	0.739 0.779	0.788
Amide80	-0.204 ± 0.03	1.075 ± 0.32 0.660 ± 0.13	0.693 ± 0.18 0.932 ± 0.21	-1.061 ± 0.08 -0.868 ± 0.24	0.204 0.209	0.796 0.789	0.782
UniAmide	-0.289 ± 0.15	0.735 ± 0.39 0.523 ± 0.19	0.552 ± 0.00 0.870 ± 0.00	-0.697 ± 0.09 -0.660 ± 0.09	0.381 0.481	0.743 0.957	0.771
PolySulfa	-0.414 ± 0.15	0.589 ± 0.33 0.301 ± 0.15	1.467 ± 0.12 1.559 ± 0.02	-1.874 ± 0.13 -1.344 ± 0.21	0.739 0.706	1.345 1.246	0.700
SSO	-0.246 ± 0.18	0.866 ± 0.47 0.513 ± 0.22	0.408 ± 0.08 0.567 ± 0.14	-0.655 ± 0.21 -0.478 ± 0.14	-0.098 -0.102	1.180 1.075	0.829
PC-MME	-0.409 ± 0.09	0.815 ± 0.38 0.576 ± 0.36	0.349 ± 0.10 0.491 ± 0.00	-0.652 ± 0.00 -0.558 ± 0.09	-0.149 -0.186	1.487 1.224	0.844
PC-FA	-0.674 ± 0.07	0.648 ± 0.43 0.416 ± 0.29	0.388 ± 0.09 0.574 ± 0.07	-0.686 ± 0.06 -0.601 ± 0.21	0.066 0.087	1.499 1.231	0.832
Daiso	-0.387 ± 0.16	0.885 ± 0.65 0.515 ± 0.30	0.261 ± 0.13 0.343 ± 0.17	-0.487 ± 0.06 -0.376 ± 0.04	-0.247 -0.239	0.993 0.997	0.691

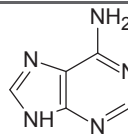
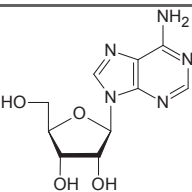
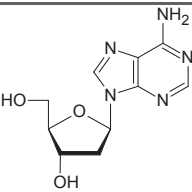
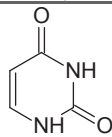
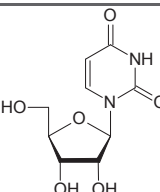
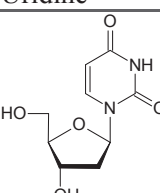
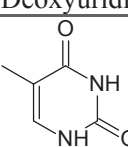
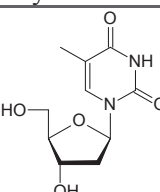
Supporting Information for Appendix III

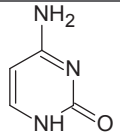
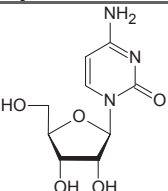
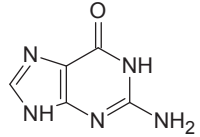
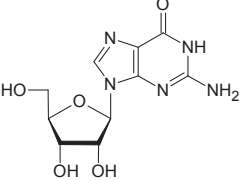
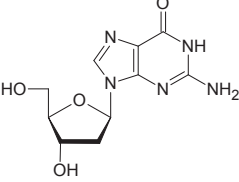
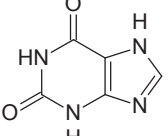
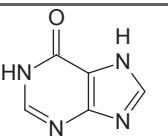
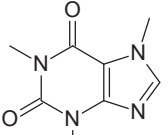
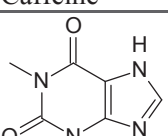
Additional investigations into the retention mechanism of hydrophilic interaction liquid chromatography by linear solvation energy relationships.

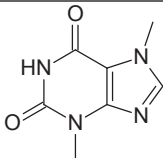
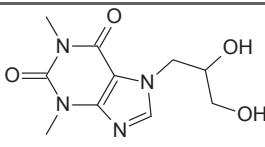
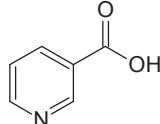
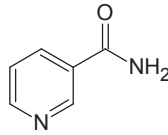
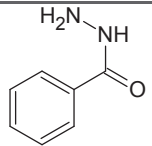
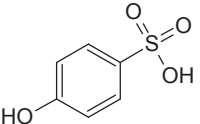
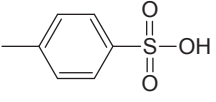
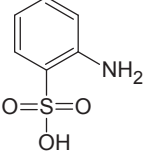
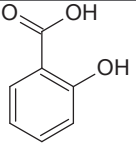
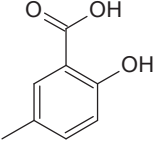
G. Schuster, W. Lindner.

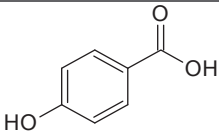
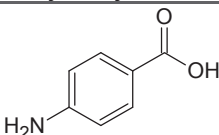
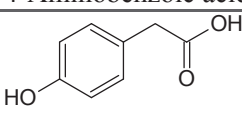
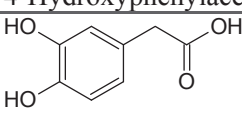
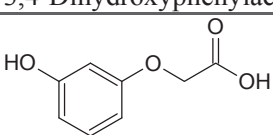
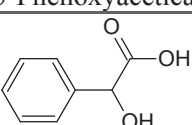
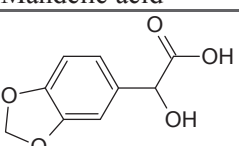
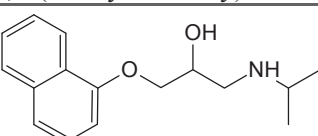
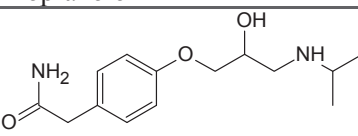
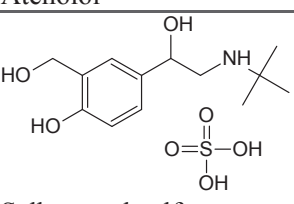
Submitted manuscript

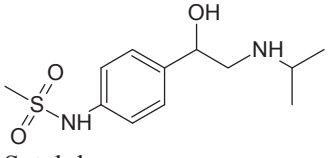
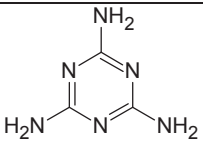
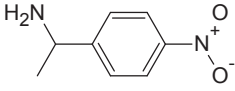
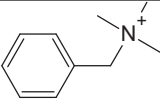
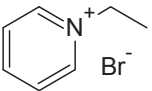
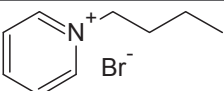
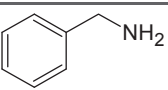
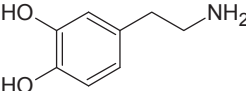
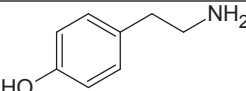
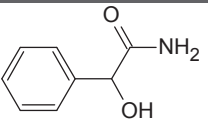
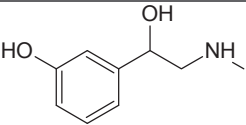
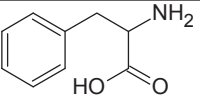
Table S1 Chemical structures for the test analytes considered during the multiple linear regression.

Nr.	Analytes	prediction set: neutral + acidic solutes	prediction set: neutral + basic solutes	validation set: “mean model equation”
1	 Adenine	X	X	X
2	 Adenosine	X	X	X
3	 Deoxyadenosine	X	X	X
4	 Uracil	X	X	X
5	 Uridine	X	X	X
6	 Deoxyuridine	X	X	X
7	 Thymine	X	X	X
8	 Thymidine	X	X	X

9		X	X	X
	Cytosine			
10		X	X	X
	Cytidine			
11		X	X	X
	Guanine			
12		X	X	X
	Guanosine			
13		X	X	X
	Deoxyguanosine			
14		X		X
	Xanthine			
15		X	X	X
	Hypoxanthine			
16		X	X	
	Caffeine			
17		X	X	
	Theophylline			

18		X	X	
	Theobromine			
19		X	X	
	Dyphylline			
20		X		
	Nicotinic acid			
21		X	X	X
	Nicotinamide			
22		X	X	X
	Isoniazid			
23		X	X	X
	4-Hydroxybenzenesulfonic acid			
24		X		X
	4-Methylbenzenesulfonic acid			
25		X		X
	2-Aminobenzenesulfonic acid			
26		X		
	Salicylic acid			
27		X		
	5-Methylsalicylic acid			

28		X		X
	4-Hydroxybenzoic acid			
29		X		X
	4-Aminobenzoic acid			
30		X		X
	4-Hydroxyphenylacetic acid			
31		X		X
	3,4-Dihydroxyphenylacetic acid			
32		X		X
	3-Phenoxyacetic acid			
33		X		X
	Mandelic acid			
34		X		X
	3,4-(Methylenedioxy) mandelic acid			
35			X	
	Propranolol			
36		X	X	X
	Atenolol			
37			X	X
	Salbutamol sulfate			

38			X	X
	Sotalol			
39		X	X	X
	Melamine			
40			X	X
	1-(4-nitrophenyl)ethanamine			
41			X	
	Benzyltrimethylammonium			
42			X	
	1-Ethylpyridin-1-ium bromide			
43			X	
	1-Butylpyridin-1-ium bromide			
44			X	X
	Benzylamine			
45			X	X
	Dopamine			
46			X	X
	Tyramine			
47			X	X
	2-Amino-1-phenylethanol			
48			X	X
	Phenylephrine			
49				X
	Phenylalanine			

50	<p>Tyrosine</p>	X
51	<p>Tryptophan</p>	X
52	<p>α-Methyltryptophan</p>	X
53	<p>5-Methyltryptophan</p>	X
54	<p>Tryptophanamide</p>	X
55	<p>Deoxycytidine</p>	X

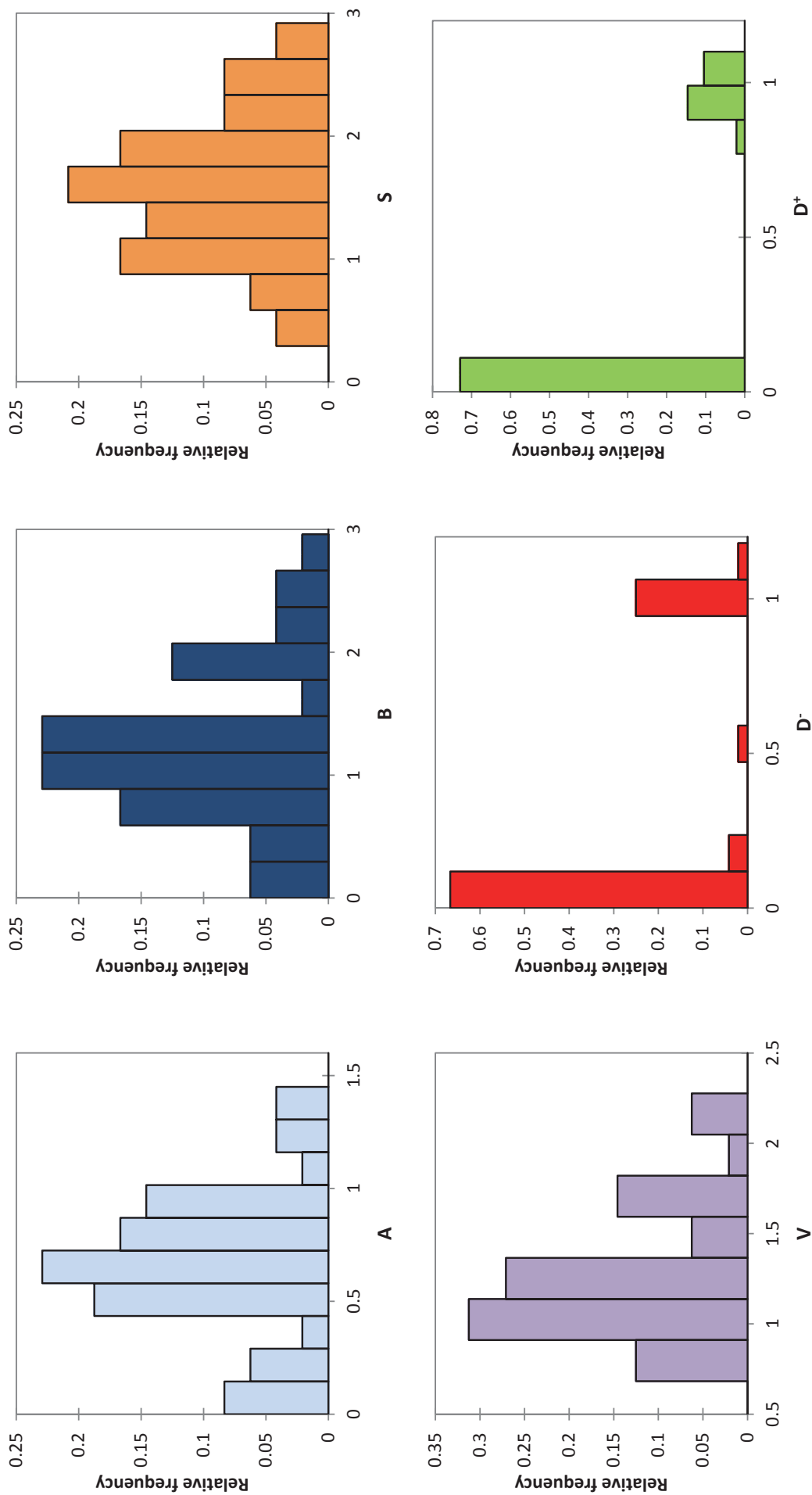
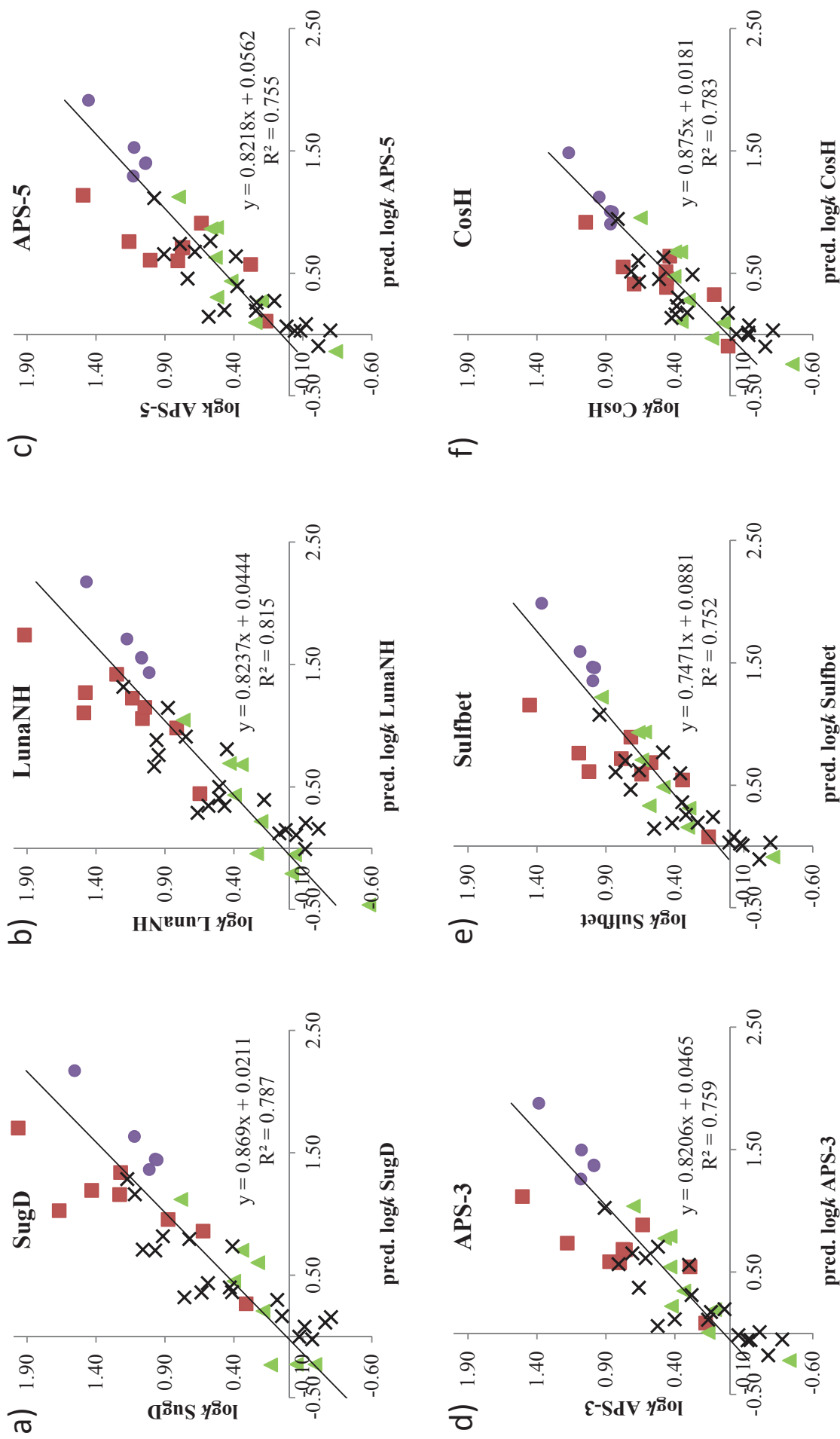


Fig. S1. Frequency plots of the Abraham and *D* descriptors of the test compounds from Table 1

**Fig. S2.**

Experimental logk versus predicted logk plots according to the mean model equations in Table 6. Red squares ■ are basic solutes, purple circles ● are neutral species, green triangles ▲ are acidic compounds, black crosses X are amino acids.

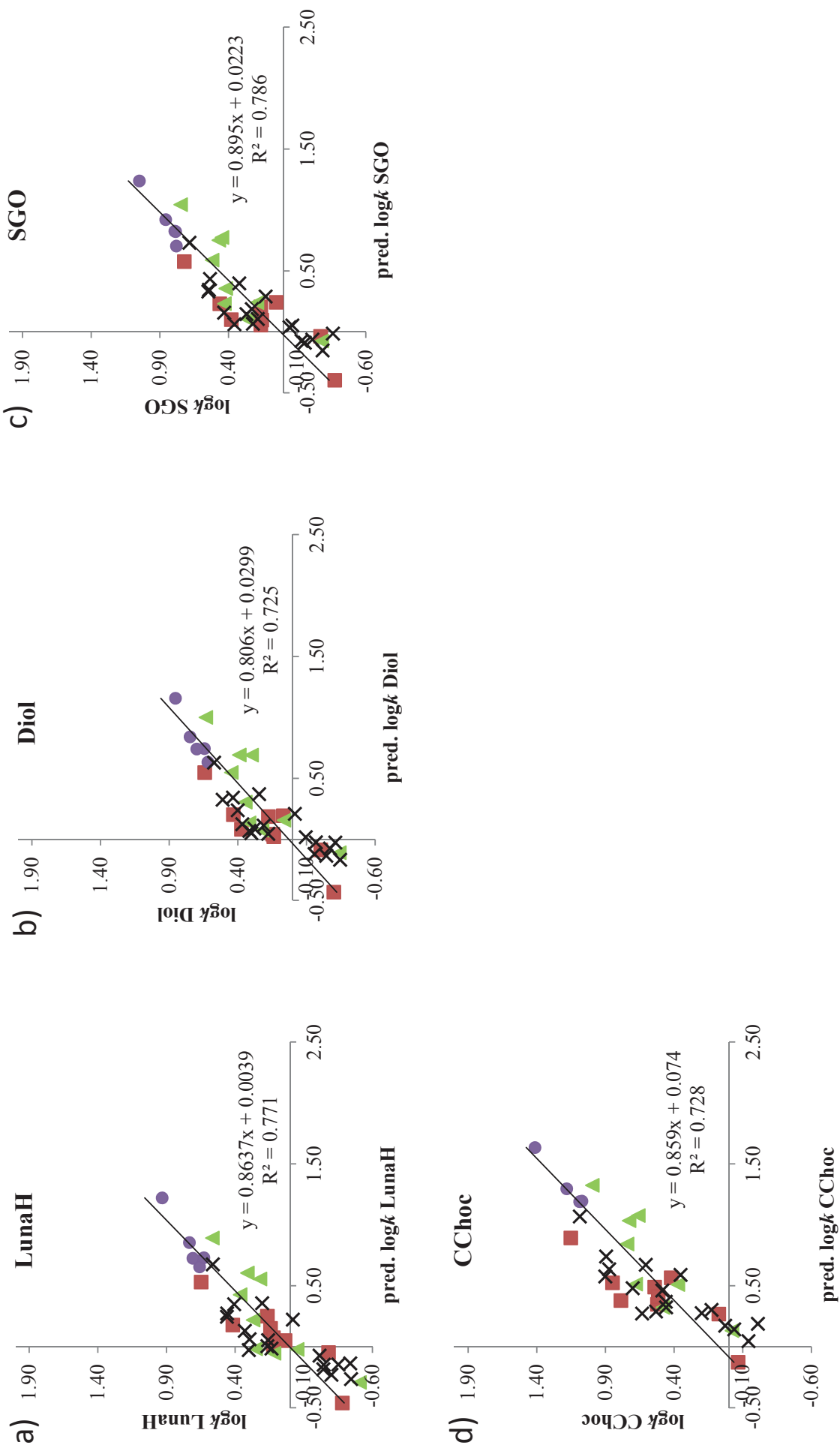
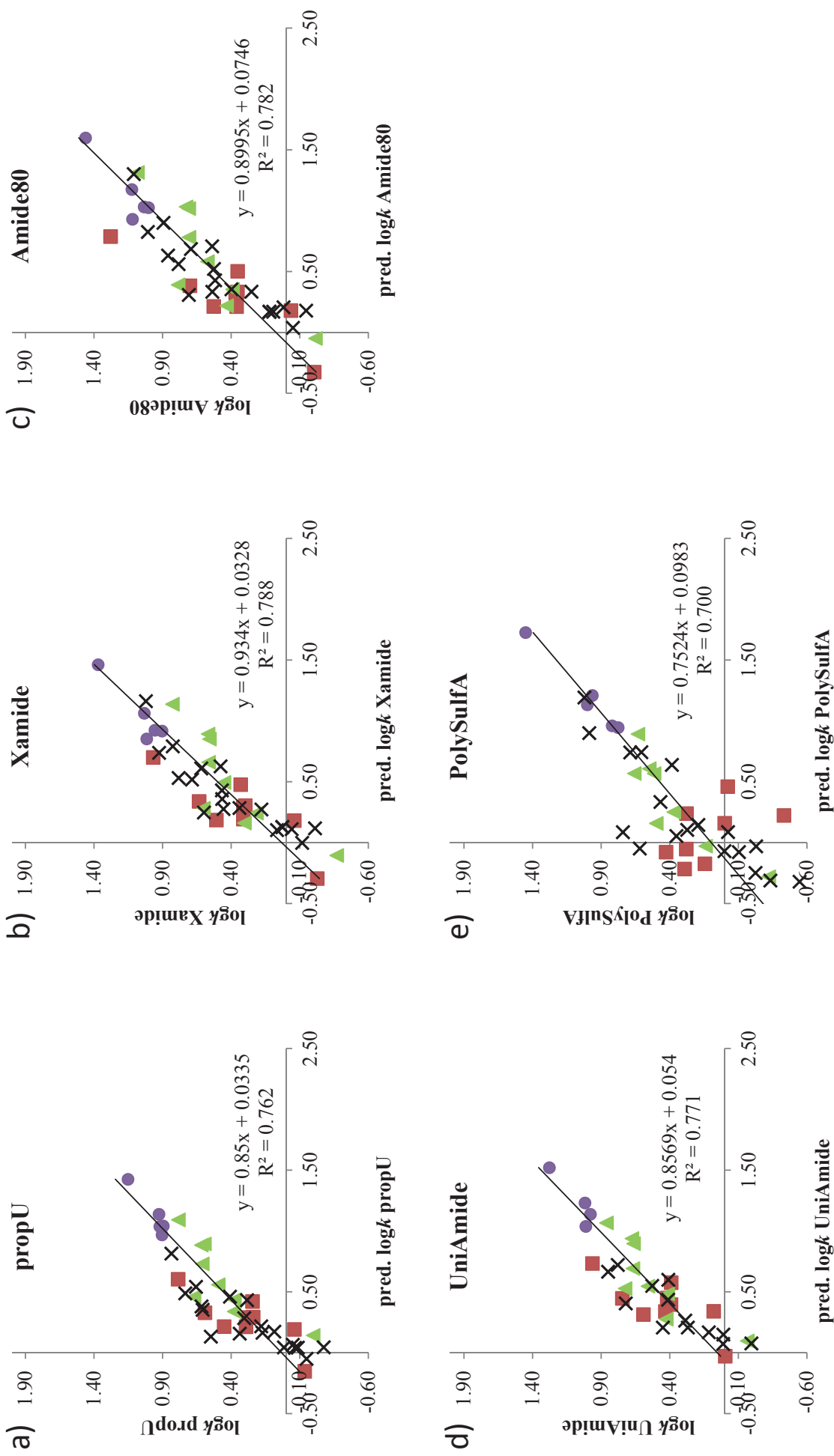


Fig. S3.

Experimental logk versus predicted logk plots according to the mean model equations in Table 6. Red squares ■ are basic solutes, black crosses X are neutral species, green triangles ▲ are acidic compounds, purple circles ● are amino acids.

**Fig. S4.**

Experimental $\log k$ versus predicted $\log k$ plots according to the mean model equations in Table 6. Red squares ■ are basic solutes, purple circles ● are neutral species, green triangles ▲ are acidic compounds, black crosses X are amino acids.

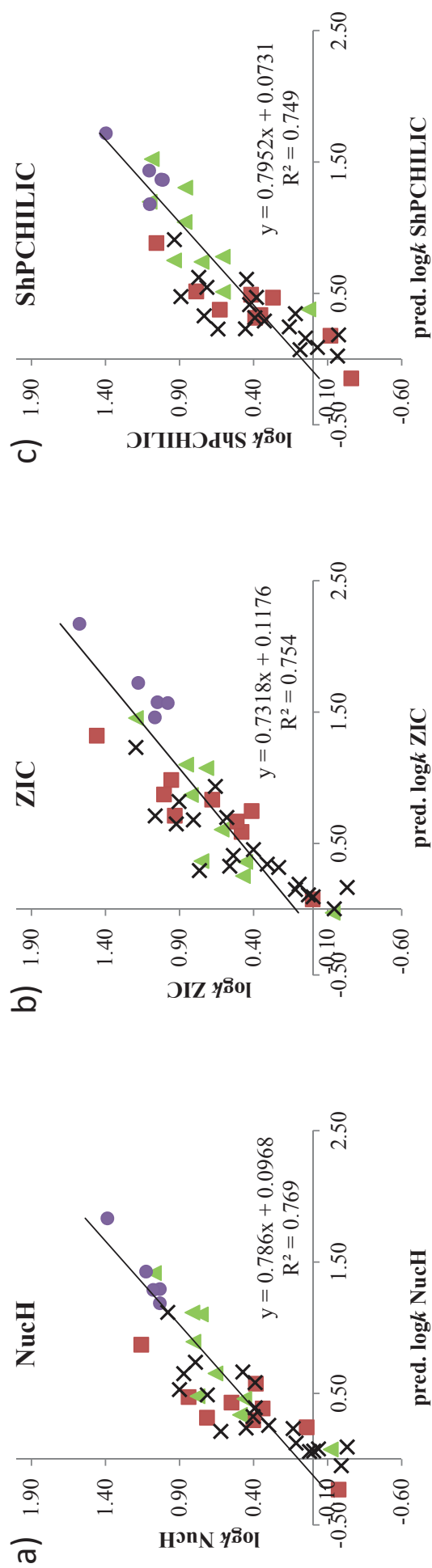


Fig. S5.

Experimental $\log k$ versus predicted $\log k$ plots according to the mean model equations in Table 6. Red squares ■ are acidic compounds, green triangles ▲ are basic solutes, black crosses X are neutral species, purple circles ● are amino acids.

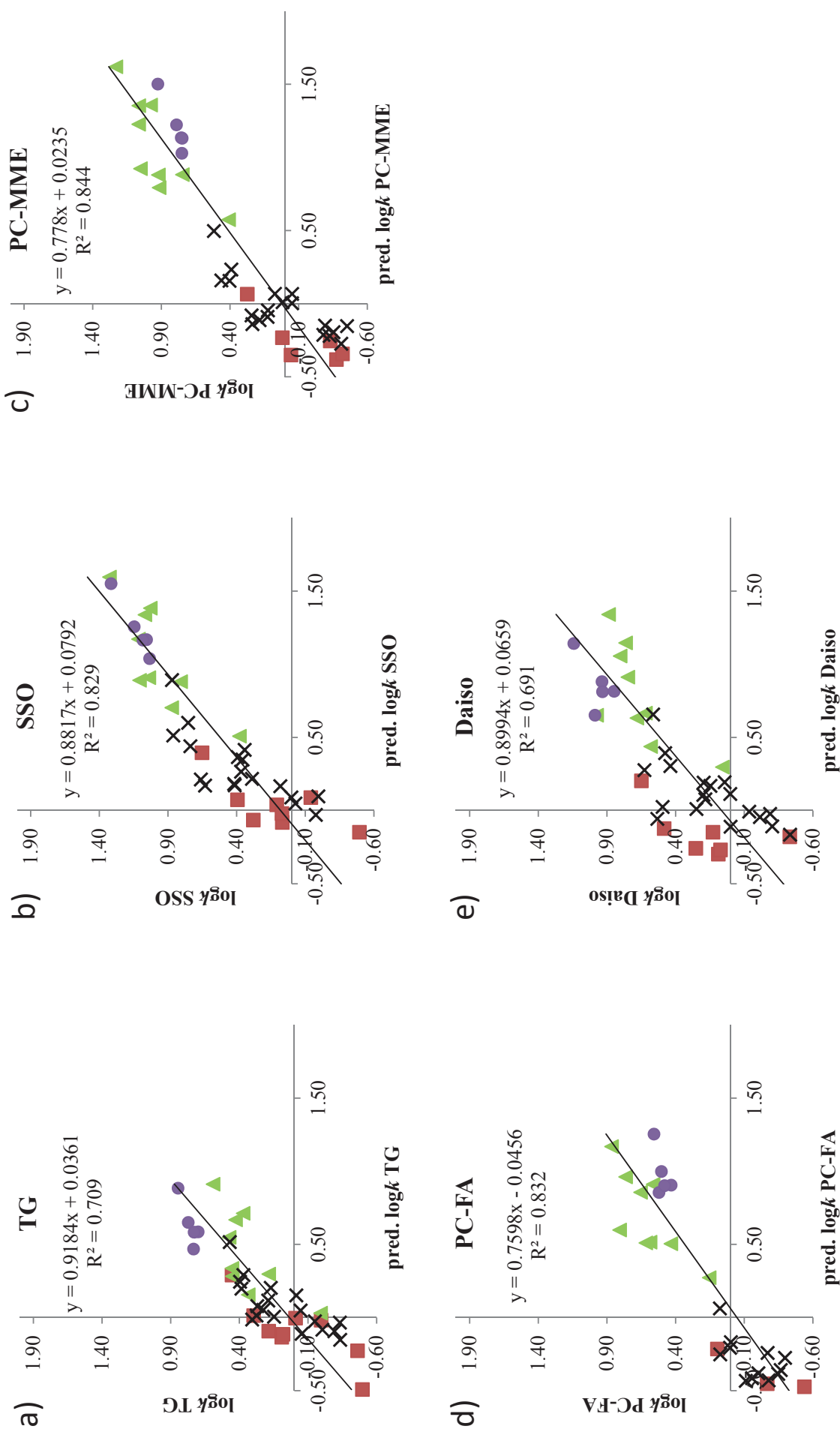


Fig. S6. Experimental $\log k$ versus predicted $\log k$ plots according to the mean model equations in Table 6. Red squares ■ are basic solutes, black crosses X are neutral species, green triangles ▲ are acidic compounds, purple circles ● are amino acids.

APPENDIX IV

Enantioseparation of chiral sulfonates by liquid chromatography and subcritical fluid chromatography.

R.Pell, G. Schuster, M. Lämmerhofer, W. Lindner.

Journal of Separation Science 2012, 35, 2521-2528

Reinhard Pell
Georg Schuster
Michael Lämmerhofer*
Wolfgang Lindner

Department of Analytical
Chemistry, University of Vienna,
Vienna, Austria

Received May 4, 2012
Revised May 25, 2012
Accepted May 25, 2012

Research Article

Enantioseparation of chiral sulfonates by liquid chromatography and subcritical fluid chromatography

Tert-butylcarbamoyl-quinine and -quinidine weak anion-exchange chiral stationary phases (Chiralpak® QN-AX and QD-AX) have been applied for the separation of sodium β -ketosulfonates, such as sodium chalconesulfonates and derivatives thereof. The influence of type and amount of co- and counterions on retention and enantioresolution was investigated using polar organic mobile phases. Both columns exhibited remarkable enantiodiscrimination properties for the investigated test solutes, in which the quinidine-based column showed better enantioselectivity and slightly stronger retention for all analytes compared to the quinine-derived chiral stationary phase. With an optimized mobile phase (MeOH, 50 mM HOAc, 25 mM NH₃), 12 of 13 chiral sulfonates could be baseline separated within 8 min using the quinidine-derivatized column. Furthermore, subcritical fluid chromatography (SubFC) mode with a CO₂-based mobile phase using a buffered methanolic modifier was compared to HPLC. Generally, SubFC exhibited slightly inferior enantioselectivities and lower elution power but also provided unique baseline resolution for one compound.

Keywords: Chiral separation / Chiral sulfonates / Cinchona alkaloid / Liquid chromatography / Subcritical fluid chromatography
DOI 10.1002/jssc.201200448

1 Introduction

Liquid chromatography using chiral stationary phases (CSPs) is nowadays routinely used for direct separation of enantiomers in both analytical and preparative scale [1]. Among the vast number of commercially available CSPs, *tert*-butylcarbamoyl-quinine- and -quinidine (Fig. 1) exhibit remarkable enantiodiscrimination properties toward chiral acids, such as *N*-protected amino acids, aryl carboxylic acids, *N*-protected aminophosphonic, and phosphinic acids [2–5]. The CSPs are preferentially operated with slightly acidic polar organic or hydro organic mobile phases, which protonates the quinuclidine tertiary amine of the chiral selector (SO) and deprotonates the acidic selectand (SA) thus enabling a weak anion-exchange retention mechanism. Additional interactions between the SO and SA, such as hydrogen bonding, π – π stacking, van der Waals, or steric interactions working in

concert with each other, may support the ion pairing process and thus facilitate enantiodiscrimination [6, 7].

Chiral sulfonic acids (or their sulfonate salts, respectively) gained distinct importance as resolving agents. For instance, camphor sulfonic acid, 3-bromocamphorsulfonic acid, and 1-phenylethanesulfonic acid were successfully employed for resolving racemic amines and amino acids via diastereomeric salt formation [8]. Chalconesulfonic acid and derivatives thereof were used in the “Dutch Resolution” process, a smooth variation of the classical Pasteur resolution, where mixtures of resolving agents are used instead of one single resolving agent [9]. Since sulfonic acids are isosteric to carboxylates, they show potential for pharmaceutical applications. For example, 6-gingesulfonic acid, a 1,3-ketosulfonic acid derivative found in ginger (*zingiberis rhizoma*), shows antiulcer activity [10, 11]. (*R*)-Saclofen, the sulfonic acid analogue of baclofen, is a potent GABA_A receptor antagonist [12].

Acquiring enantiomerically pure sulfonic acids was either achieved by asymmetric synthesis or synthesis of the racemate following a resolution via diastereomeric salt formation. For example, the preparation of enantiopure chalconesulfonic acid was accomplished via homogenous catalysis using a quinine- or quinidine-modified catalyst [13] or via Dutch Resolution with (*R*)-4-methylphenylglycinol [14]. However, enantioresolution of a broad set of free (unprotected) sulfonic acids via chromatography has not been reported so far.

Correspondence: Prof. Dr. Wolfgang Lindner, Department of Analytical Chemistry, University of Vienna, Währinger Strasse 38, 1090 Vienna, Austria
E-mail: wolfgang.lindner@univie.ac.at
Fax: +43-1-42779523

Abbreviations: CitOH, citric acid; CSP, chiral stationary phase; DEA, diethylamine; FA, formic acid; HOAc, acetic acid; MalOH, malonic acid; MeOH, methanol; QD-AX, *tert*-butylcarbamoyl-quinidine anion exchanger; QN-AX, *tert*-butylcarbamoyl-quinine anion exchanger; SA, selectand; SO, chiral selector; SucOH, succinic acid; TEA, triethylamine

*Current address: Michael Lämmerhofer, Institute of Pharmaceutical Sciences, Eberhard Karls University Tübingen, Tübingen, Germany.

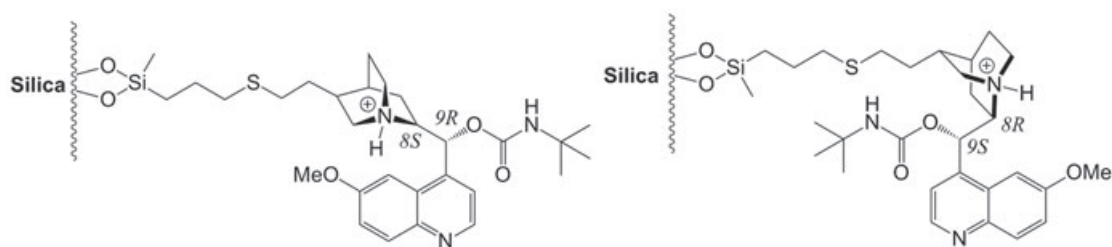


Figure 1. Structures of weak anion exchangers QN-AX (left) and QD-AX (right).

Only camphorsulfonic acid, three N-protected aminosulfonic acids and alpha-perfluoromethyl branched perfluorooctane sulfonate (1*m*-PFOS) were separated in their enantiomers on a quinine carbamate type weak anion-exchange CSP [2, 3, 15]. Furthermore, camphorsulfonic acid was resolved by indirect enantioseparation using an achiral diol stationary phase with quinine as chiral mobile phase additive [16].

Hence, we herein report the application of *tert*-butylcarbamoyl-quinine and -quinidine CSPs (Fig. 2) for enantioseparation of β -ketosulfonic acids (applied as their sodium salts) by HPLC and subcritical fluid chromatography (SubFC). Employing a polar organic mobile phase, the influence of type, and amounts of acidic and basic additives was investigated. Additionally, the separation performance of SubFC for the same analyte set was also examined.

2 Experimental

2.1 Materials

Compounds 1–4 were kind gifts of Syncom (Groningen, the Netherlands). 2,4-Dichlorobenzaldehyde, acetophenone, benzaldehyde, 2',4'-dichloroacetophenone, 2,4-dimethoxybenzaldehyde, 2',4'-dimethoxyacetophenone, 2-methoxybenzaldehyde, 2'-methoxyacetophenone, coumarin, phenalen-1-one, NaHSO₃, and NaOH were purchased from Sigma-Aldrich (Vienna, Austria) in reagent grade or higher quality. Ethanol (96%), CH₂Cl₂, and methanol (MeOH) were purchased from VWR (Vienna, Austria) and water was bidistilled in house. Mobile phases for HPLC (or modifiers for SubFC, respectively) were prepared with HPLC grade solvents and analytical grade reagents and were degassed in the ultrasonication bath prior to use. Mobile phases containing HOAc/NH₃ (where HOAc is defined as acetic acid) buffers were prepared by combining ammonium acetate with HOAc.

2.2 Synthesis of sodium β -ketosulfonate test compounds

The synthesis of chalconesulfonate derivatives 6–12 was accomplished by 1,4-addition (Thia-Michael addition) of sodium bisulfite to the corresponding chalcone derivatives, which were synthesized via aldol condensation. The synthetic protocol followed the published procedure by Kel-

logg et al. [14]. Accordingly, sodium β -ketosulfonates 5 and 13 were also prepared via 1,4-addition of NaHSO₃ to the α,β -unsaturated carbonyl compound starting materials: 20.0 mmol of coumarin (2.93 g, for synthesis of 5) or phenalen-1-one (3.61 g, for synthesis of 13) were suspended in 20 mL 96% ethanol. A total of 2.08 g (20.0 mmol, 1 eq.) NaHSO₃ were dissolved in 10 mL water and added to the ethanolic solution. The mixture was heated and refluxed overnight. After cooling to r.t. and evaporation of solvent crude 5 or 13 were obtained, which were then purified by flash chromatography (CH₂Cl₂/MeOH 10:1, then 1:1; v/v).

Compound 5, yield 45%, white powder; ¹H-NMR [CD₃OD]: δ = 3.22 (m, 2H), 4.34 (dd, 1H), 6.87 (m, 2H), 7.17 (m, 2H). ¹³C-NMR [CD₃OD]: δ = 31.2 (CH₂), 56.3 (CH), 116.6 (C_{ar}H), 121.0 (C_{ar}H), 122.7 (C_{ar}), 125.4 (C_{ar}H), 130.7 (C_{ar}H), 154.8 (C_{ar}), 170.5 (C = O). MS (ESI, negative): 227.1 [M-Na]⁻

Compound 6, yield 33%, white crystals; ¹H-NMR [D₂O]: δ = 3.72 (dd, 1H), 3.82 (dd, 1H), 5.14 (dd, 1H), 7.05 (dd, 1H), 7.26 (t, 2H), 7.32 (t, 2H), 7.41 (t, 1H), 7.66 (d, 2H). ¹³C-NMR [D₂O]: δ = 40.7 (CH₂), 57.0 (CH), 127.7 (C_{ar}H), 128.5 (C_{ar}H), 129.2 (C_{ar}H), 129.6 (C_{ar}H), 129.9 (C_{ar}H), 132.5 (C_{ar}), 134.2 (C_{ar}), 134.6 (C_{ar}H), 135.9 (C_{ar}), 136.2 (C_{ar}), 200.3 (C = O). MS (ESI, negative): 357.0 [M-Na]⁻

Compound 7, yield 34%, white powder; ¹H-NMR [D₂O]: δ = 3.68 (dd, 1H), 3.81 (dd, 1H), 4.48 (dd, 1H), 7.11 (dd, 1H), 7.17–7.31 (m, 7H). ¹³C-NMR [D₂O]: δ = 44.2 (CH₂), 62.2 (CH), 127.8 (C_{ar}H), 128.8 (C_{ar}H), 129.0 (C_{ar}H), 129.6 (C_{ar}H), 130.7 (C_{ar}H), 130.9 (C_{ar}H), 132.0 (C_{ar}), 135.2 (C_{ar}), 135.8 (C_{ar}), 138.0 (C_{ar}), 201.8 (C = O). MS (ESI, negative): 357.0 [M-Na]⁻

Compound 8, yield 50%, white powder; ¹H-NMR [D₂O]: δ = 3.60 (s, 6H), 3.63–3.78 (m, 2H), 5.02 (dd, 1H), 6.37 (d, 2H), 7.21 (d, 1H), 7.29 (t, 2H), 7.45 (t, 1H), 7.67 (d, 2H). ¹³C-NMR [D₂O]: δ = 40.7 (CH₂), 53.9 (CH), 55.7 (OCH₃), 56.4 (OCH₃), 99.2 (C_{ar}H), 105.9 (C_{ar}H), 116.8 (C_{ar}H), 128.5 (C_{ar}H), 129.2 (C_{ar}H), 129.4 (C_{ar}H), 134.4 (C_{ar}H), 136.3 (C_{ar}), 159.0 (C_{ar}), 160.3 (C_{ar}), 201.7 (C = O). MS (ESI, negative): 349.1 [M-Na]⁻

Compound 9, yield 66%, white powder; ¹H-NMR [D₂O]: δ = 3.68 (d, 6H), 3.72 (d, 2H), 4.45 (dd, 1H), 6.31 (m, 2H), 7.26 (m, 6H). ¹³C-NMR [D₂O]: δ = 44.5 (CH₂), 55.9 (OCH₃), 56.0 (OCH₃), 62.8 (CH), 98.7 (C_{ar}H), 106.4 (C_{ar}H), 119.7 (C_{ar}), 128.6 (C_{ar}H), 128.9 (C_{ar}H), 129.5 (C_{ar}H), 132.9 (C_{ar}H), 135.7 (C_{ar}), 161.4 (C_{ar}), 165.2 (C_{ar}), 200.7 (C = O). MS (ESI, negative): 349.1 [M-Na]⁻

Compound 10, yield 97%, yellowish powder; ¹H-NMR [D₂O]: δ = 3.66 (s, 3H), 3.69–3.85 (m, 2H), 5.14 (dd, 1H), 6.87

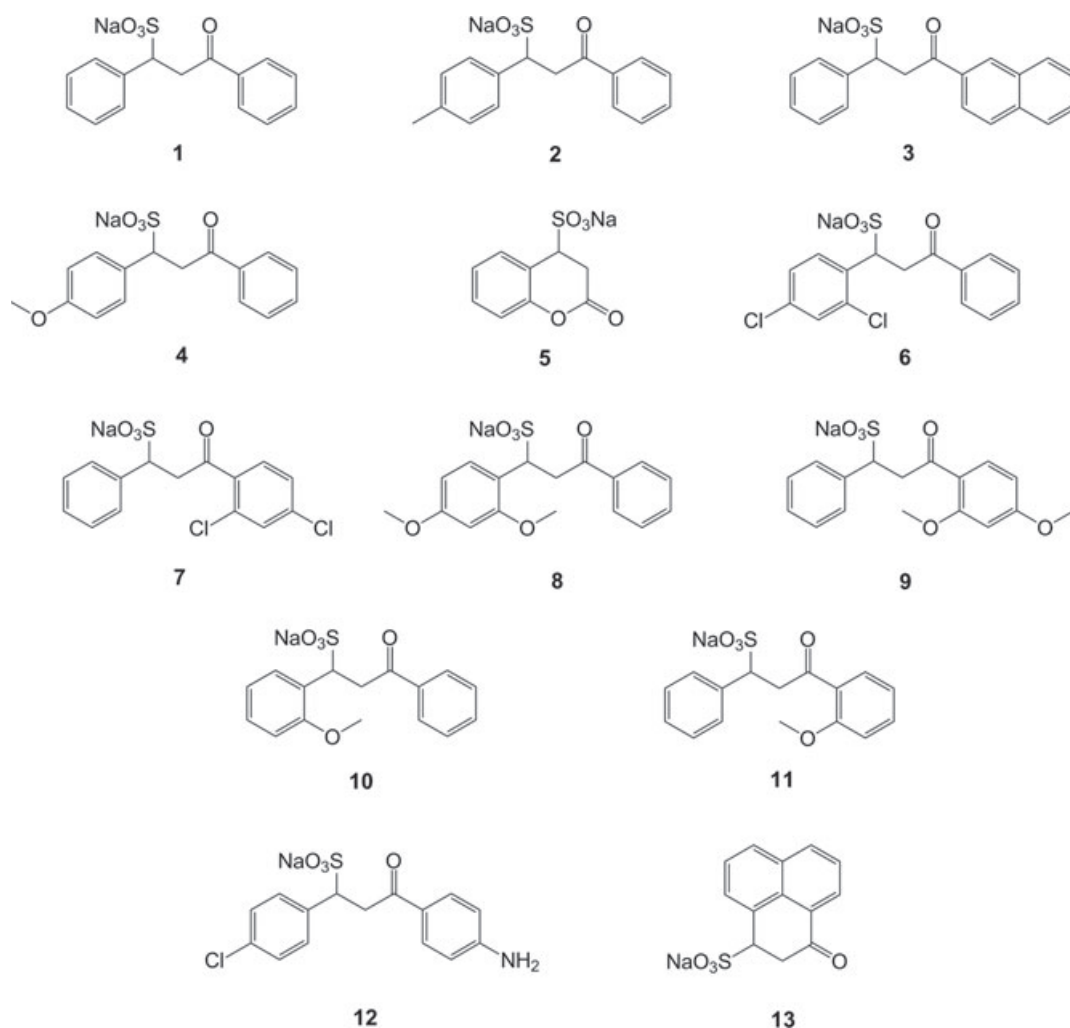


Figure 2. Structural formulas of the investigated analytes.

(dd, 2H), 7.20 (t, 1H), 7.36 (t, 3H), 7.51 (t, 1H), 7.73 (d, 2H). $^{13}\text{C-NMR}$ [D_2O]: $\delta = 40.7$ (CH_2), 54.2 (CH), 56.5 (OCH_3), 112.4 ($\text{C}_{\text{ar}}\text{H}$), 121.3 ($\text{C}_{\text{ar}}\text{H}$), 124.1 ($\text{C}_{\text{ar}}\text{H}$), 128.5 ($\text{C}_{\text{ar}}\text{H}$), 128.6 ($\text{C}_{\text{ar}}\text{H}$), 129.2 ($\text{C}_{\text{ar}}\text{H}$), 129.9 ($\text{C}_{\text{ar}}\text{H}$), 134.5 ($\text{C}_{\text{ar}}\text{H}$), 136.3 (C_{ar}), 157.9 (C_{ar}), 201.8 ($\text{C}=\text{O}$). MS (ESI, negative): 319.0 [M-Na] $^-$

Compound 11, yield 74%, white powder; $^1\text{H-NMR}$ [D_2O]: $\delta = 3.72$ (s, 3H), 3.73–3.85 (m, 2H), 4.45 (dd, 1H), 6.84 (t, 1H), 6.96 (d, 1H), 7.24 (m, 6H), 7.41 (t, 1H). $^{13}\text{C-NMR}$ [D_2O]: $\delta = 44.8$ (CH_2), 56.0 (CH), 62.7 (OCH_3), 112.9 ($\text{C}_{\text{ar}}\text{H}$), 121.1 ($\text{C}_{\text{ar}}\text{H}$), 127.0 (C_{ar}), 128.7 ($\text{C}_{\text{ar}}\text{H}$), 128.9 ($\text{C}_{\text{ar}}\text{H}$), 129.6 ($\text{C}_{\text{ar}}\text{H}$), 130.2 ($\text{C}_{\text{ar}}\text{H}$), 135.2 ($\text{C}_{\text{ar}}\text{H}$), 135.5 (C_{ar}), 158.6 (C_{ar}), 203.7 ($\text{C}=\text{O}$). MS (ESI, negative): 319.1 [M-Na] $^-$

Compound 12, yield 60%, yellowish powder; $^1\text{H-NMR}$ [D_2O]: $\delta = 3.64$ (dd, 2H), 4.50 (dd, 1H), 6.58 (d, 2H), 7.17 (d, 2H), 7.25 (d, 2H), 7.57 (d, 2H). $^{13}\text{C-NMR}$ [D_2O]: $\delta = 39.8$ (CH_2), 61.2 (CH), 115.7 ($\text{C}_{\text{ar}}\text{H}$), 126.1 ($\text{C}_{\text{ar}}\text{H}$), 126.8 ($\text{C}_{\text{ar}}\text{H}$), 126.9 (C_{ar}), 128.4 (C_{ar}), 128.9 ($\text{C}_{\text{ar}}\text{H}$), 130.6 ($\text{C}_{\text{ar}}\text{H}$), 131.0 (C_{ar}), 133.4 (C_{ar}), 135.7 ($\text{C}_{\text{ar}}\text{H}$), 200.2 ($\text{C}=\text{O}$). MS (ESI, negative): 338.1 [M-Na] $^-$

Compound 13, yield 65%, yellow powder; $^1\text{H-NMR}$ [D_2O]: $\delta = 3.04$ (dd, 1H), 3.27 (dd, 1H), 4.63 (m, 1H), 7.47 (m, 2H),

7.57 (d, 1H), 7.82 (d, 1H), 7.92 (d, 1H), 8.01 (d, 1H). $^{13}\text{C-NMR}$ [D_2O]: $\delta = 39.2$ (CH_2), 62.2 (CH), 114.9 ($\text{C}_{\text{ar}}\text{H}$), 126.3 (C_{ar}), 128.9 ($\text{C}_{\text{ar}}\text{H}$), 130.9 ($\text{C}_{\text{ar}}\text{H}$), 131.5 ($\text{C}_{\text{ar}}\text{H}$), 133.8 (C_{ar}), 134.4 (C_{ar}), 153.6 (C_{ar}), 198.8 ($\text{C}=\text{O}$). MS (ESI, negative): 261.1 [M-Na] $^-$

2.3 Instrumentation and chromatography

All HPLC experiments were conducted on a 1200 series HPLC systems from Agilent Technologies (Waldbronn, Germany) consisting of a solvent degasser, a quaternary pump, an autosampler, a column thermostat, and a diode array detector. Chemstation software version Rev. B.01.03 was used for data acquisition and analysis. The mobile phase flow rate was 1.0 mL/min using a 5 μm particle size, 150 \times 4 mm i.d. column. The test compounds were dissolved in MeOH in a concentration of 1.0–2.0 mg/mL. The injection volume varied between 5 and 10 μL and column temperature was 25°C. The void volume was determined by injecting a solution of acetone in MeOH. Before switching from stronger to

weaker acid as mobile phase counterion, the CSP was washed with MeOH containing 1% (v/v) triethylamine (TEA) with a flow of 2 mL/min for about 10 min followed by plain MeOH with 2 mL/min for 10 min, in order to remove the high-affinity counterion and achieve reproducible retention times with subsequent additive.

SubFC experiments were carried out on a Thar Discovery system from Thar Technologies Inc., equipped with a combined CO₂ and modifier pump, a combined column oven and column selector valve for six columns, an automated back pressure regulator, a water bath, and a Gilson UV variable wavelength detector. Instrument control and data acquisition were carried out with Thar SuperChrome software and Thar ChromScope software, respectively. The runs were performed in isocratic mode with 25% modifier content at a flow rate of 4.0 mL/min, 40°C, and 150 bar backpressure. The analytes were dissolved in MeOH in a concentration of 3–5 mg/mL and the void time was determined by injecting a methanolic solution of acetone.

3 Results and discussion

3.1 General remarks

First, the sulfonic acid test compounds were applied as their sodium salts. However, no differences in chromatographic separation properties are observed between sulfonic acid and sodium sulfonate analytes, as sulfonic acids are strong acids and thus fully dissociated under the applied mobile phase conditions. Second, polar organic mode with MeOH as bulk solvent was chosen for the HPLC studies. The sulfonate analytes 1–13 show high solubility in MeOH that is advantageous for potential preparative separations. Taking analyte solubility into account, also reversed phase mode could have been chosen. However, operation of QN-AX or QD-AX (where QN-AX and QD-AX are defined as *tert*-butylcarbamoyl-quinine anion exchanger and *tert*-butylcarbamoyl-quinidine anion exchanger) CSPs with hydro organic mobile phases cause prolonged retention and eventually decreased enantioselectivity due to the activation of nonspecific hydrophobic interactions [2]. Moreover, regarding preparative separations, one tries to avoid water in the mobile phase due to higher energy costs in the evaporation process.

3.2 Influence of counterion type and strength

The interaction, and thus retention and separation, between the quinine carbamate type SOs and the SAs is dominated by long range electrostatic forces [6, 7]. Hence, under slightly acidic mobile phase conditions, the protonated tertiary amine in the quinuclidine moiety (see Fig. 1) undergoes an ionic interaction with the corresponding deprotonated (ionized) acidic analyte. The anion-exchange retention mechanism following a stoichiometric displacement model is strongly de-

pendent on the type and amount of counterions in the mobile phase.

The counterion effect was systematically studied by Gyimesi-Forrás et al. [17] for carboxylic acid analytes. Sulfonic acids have not yet been explored in this regard. We therefore investigated five different mono-, bi-, and trivalent acids as acidic additives (counterions) using MeOH as bulk solvent (the apparent pH was adjusted to 6.1 with TEA). An increase of competitor acid (counterion) concentration in the mobile phase led to a decrease of retention times for all sulfonate test compounds 1–13. Plots of the logarithm of the retention factor ($\log k_1$) versus the logarithm of the counterion concentration ($\log [C]$) gave a linear relationship that clearly indicates an anion-exchange mechanism following the stoichiometric displacement model (Eq. (1)) [2, 18].

$$\log k = \log K_z - Z \cdot \log [C] \quad (1)$$

where in k is the retention factor, $[C]$ the molar concentration of the counterion in the eluent, Z is the slope of the linear regression line, and $\log K_z$ the intercept with the system-specific constant K_z being defined by Eq. (2).

$$K_z = \frac{K \cdot S \cdot (q_x)^Z}{V_0} \quad (2)$$

wherein K is the ion-exchange equilibrium constant, S the surface area, q_x the charge density on the surface, i.e. the number of ion-exchange sites available for adsorption and V_0 the mobile phase volume. Hence, the intercept $\log K_z$ can be regarded as measure for the affinity of the solute toward the ion exchanger under given conditions and represents the $\log k$ value at 1 M concentration of counterion. The slope Z in Eq. (1) is indicative for the charges involved in the ion-exchange process and is directly proportionally depending on the ratio of the effective charge numbers of solute ($z_{\text{eff,S}}$) and counterion ($z_{\text{eff,C}}$) [19, 20].

Thus, both intercept and slope are characteristic for the given ion-exchange process and can be used for retention prediction. Table 1 depicts the values of slopes and intercepts of the linear relationship for compounds 9 and 11. They can also be used to illustrate the elution strength of different counterions.

As can be seen from Table 1, the strongest acids within this study, citric acid (CitOH) and malonic acid (MalOH), exhibited the lowest values for the intercept (−1.19 and −1.92, respectively). On the contrary, for HOAc as the weakest acid investigated, the value was 0.55. Hence, the more competitive the counterion (the stronger and polyprotic the acid) the lesser amount is needed to achieve isoelutotropic conditions. This findings corroborate earlier investigations made for carboxylic acid analytes [17], but the effect is more pronounced for the sulfonate compounds. For instance, to adjust k_1 to 4.5 for compound 9, only 2 mM of CitOH are needed compared to 214 mM of HOAc (Table 1). However, employing such low concentrations of counterions may be detrimental for the peak shapes or for the reproducibility of retention times (especially in preparative chromatography under high sample loads). Thus, CitOH or MalOH may be avoided as

Table 1. Influence of counterion concentration on retention of first eluted enantiomers of **9** and **11** on CSP **2^a** according to Eq. (1)

Acid (counter-ion)	Compound 9				Compound 11			
	<i>c</i> (mM) ^b	Slope	Intercept	<i>c</i> _{iso} (M) ^c	<i>c</i> (mM)	Slope	Intercept	<i>c</i> _{iso} (M) ^c
HOAc	25–100	−0.33	0.43	0.214	25–100	−0.33	0.39	0.166
FA	25–100	−0.70	−0.23	0.055	25–100	−0.71	−0.28	0.048
CitOH	2–10	−0.70	−1.19	0.002	2–10	−0.76	−1.36	0.002
SucOH	25–100	−0.64	−0.16	0.053	25–100	−0.64	−0.20	0.048
MalOH	2–10	−1.22	−1.92	0.008	2–10	−1.28	−2.01	0.008

a) pH_a of methanolic mobile phase was adjusted with TEA to 6.1.

b) Employed concentration range of acid in MP.

c) Calculated concentrations for isoelutotropic conditions ($k_1 = 4.5$).

counterions, unless analytes are extremely strongly retained such as polyprotic acids.

In sharp contrast, a variation of the counterion concentration showed insignificant effects on enantioselectivity. Moreover, the type of counterion (acidic additive) exhibited also only a minor influence on α (note: the pH_a was always adjusted to 6.1 with TEA). For instance, the α -value for **9** varied from 1.31 to 1.36 using different types of acidic additives (data not shown).

To summarize, separation of sodium β -ketosulfonates on quinine- and quinidine-derived CSPs follows an ion-exchange mechanism as it was observed for other acidic (anionic) analytes such as carboxylic, phosphonic, and phosphinic acids. This means in practical terms that retention can easily be adjusted by the amount or type of acidic additive without significantly changing enantioselectivity.

3.3 Influence of the co-ion

Basic additives act as co-ions in the anion-exchange dominated retention process and can also be influential for separation of chiral acids on cinchona alkaloid derived CSPs. Primarily, they are utilized to adjust the pH of the eluent. Since cinchona carbamate type SOs are weak anion exchangers and are operated with weak acids as mobile phase additives, the apparent pH (and thus the ionization state of SOs and SAs) plays a decisive role for retention and enantioselectivity [21]. Typically, small amounts of organic amines are only needed to establish weakly acidic conditions, which also favors repeatability, shortens retention times, and improves peak shape (compared to the sole addition of acidic additives) [22]. Under the given slightly acidic mobile phase conditions, the decreased retention can be explained by the competition between the protonated quinuclidinium moiety of the SO and the protonated amine additive to form ion pairs with the deprotonated acidic analyte. It seems that the competitive effect is necessary to balance the electrostatic interaction between the SO and SA.

In this study, three amines with differing alkyl substitution degree, namely NH_3 , DEA (diethylamine), and TEA,

were chosen as basic additives. In previous studies for carboxylic acid solutes, they showed increasing elution strength on QN-AX or QD-AX CSPs in the following order: $NH_3 < DEA < TEA$ [22]. First, the mobile phase acid to base ratio (i.e. the pH_a of the mobile phase being responsible for the protonation state of the SO and dissociation state of the SA) was optimized in matters of short retention times with adequate resolution of the chiral compounds (data not shown). Hence, an acid to base ratio of 2:1 was chosen with HOAc as acidic additive. Figure 3 depicts the influence of the various amine additives on chromatographic parameters (retention k_1 , enantioselectivity α , plate number N_1 , and resolution R_s). Unlike for the acidic counterions, the type of the basic co-ions showed negligible influence on separation performance (note that the pH_a for all three additive combinations was almost constant, namely 6.8 for HOAc/ NH_3 , 6.9 for HOAc/DEA, and 6.9 for HOAc/TEA, each 50 mM acid and 25 mM base).

On the contrary, employing a different combination of acidic and basic additives, such as formic acid (FA) and DEA, yielded strongly differing results (see right bars in Fig. 3). Compared to HOAc/DEA, the use of FA/DEA led to a sixfold increased retention, but also to a better separation performance. The higher retention times may be related to the lower pH_a of FA/DEA ($pH_a = 5.6$ for 50 mM FA and 25 mM DEA in MeOH) and may be a combined effect of altered ionization states, in particular reduced counterion dissociation. Therefore, the observed overall ionic interaction of the analytes with the SOs is strengthened because of less counterion competition.

3.4 Separation performance of QN-AX and QD-AX CSP

A set of 13 sodium β -ketosulfonates was chosen to investigate the separation performance of QN-AX and QD-AX CSP toward chiral sulfonate compounds. Analytes **2–4** and **6–12** are derivatives of chalconesulfonate **1**. They comprise either electron donating or electron withdrawing groups on their phenyl rings turning them π -basic or π -acidic. Besides,

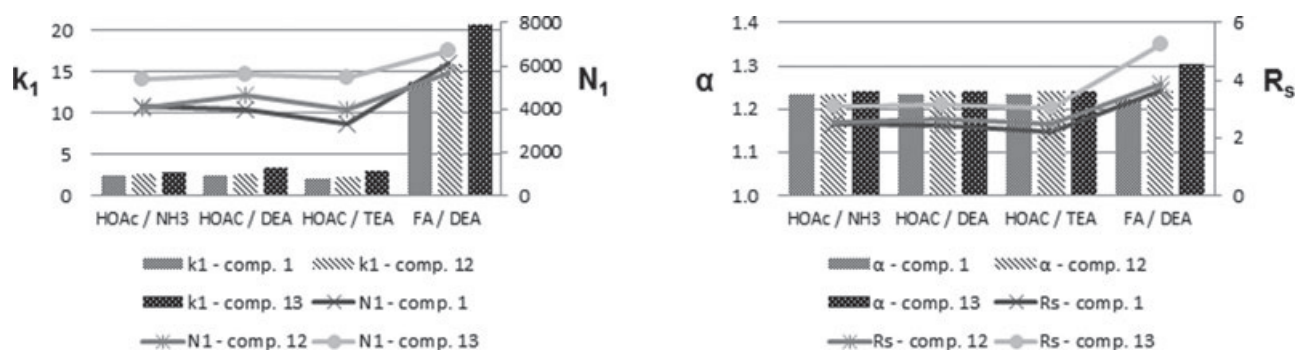


Figure 3. Effect of acidic and basic additives on chromatographic behavior of compounds **1**, **12**, and **13** on QD-AX CSP. Left diagram: retention factors and plate numbers of the first eluted peak. Right diagram: enantioselectivity and resolution. Mobile phases: MeOH, 50 mM acid and 25 mM base.

Table 2. Enantiomer separation of compounds **1–13** on QN-AX and QD-AX CSP in HPLC mode^{a)}

Analyte	QN-AX CSP				QD-AX CSP			
	k_1	α	R_s	$N_1(m^{-1})$	k_1	α	R_s	$N_1(m^{-1})$
1	1.75	1.21	2.5	47 700	2.14	1.23	2.8	47 800
2	1.86	1.21	2.3	38 000	2.27	1.24	2.9	46 300
3	2.86	1.16	2.0	38 400	3.74	1.17	2.4	45 200
4	1.94	1.22	2.4	40 200	2.63	1.27	3.2	42 100
5	1.88	1.10	1.2	12 900	2.12	1.24	3.0	45 200
6	1.90	1.00	0.0	18 000	2.33	1.05	0.7	36 200
7	2.09	1.14	1.8	43 200	2.64	1.15	2.0	44 900
8	1.92	1.07	0.8	21 600	2.39	1.24	2.8	39 800
9	1.88	1.29	3.2	44 200	2.37	1.32	3.6	42 900
10	1.90	1.00	0.0	20 800	2.16	1.19	2.4	45 300
11	1.77	1.23	2.6	40 800	2.21	1.26	3.0	44 400
12	1.88	1.19	2.0	35 700	2.33	1.26	2.9	38 500
13	2.96	1.05	0.6	35 500	3.26	1.28	3.5	44 000

a) Conditions: mobile phase: MeOH, 50 mM HOAc, 25 mM NH₃; 1.0 mL/min, 25°C, detection 254 and 230 nm; $t_0 = 1.51$ min.

compounds **5** and **13** possess a more rigid molecular structure compared to the conformationally more flexible chalconesulfonates (and derivatives thereof).

MeOH with 50 mM HOAc and 25 mM NH₃ was employed as mobile phase that was a good compromise between fast analyte elution, good separation performance, and high buffer volatility for a potential LC-MS hyphenation. As summarized in Table 2, QD-AX CSP outperformed the QN-AX column in terms of enantioselectivity and resolution values, and yielded baseline resolution for 12 of the 13 test compounds. Nevertheless, also the quinine-based column achieved at least partial separation of 11 sodium β -ketosulfonates with eight of them being baseline resolved with the given conditions.

Regarding the structure-enantioselectivity relationship, some trends became evident: disubstituted chalconesulfonates derivatives with their substituents at the phenyl ring next to the carbonyl group were better resolved on both columns than their constitutional isomers having the

phenyl-substitution in vicinity of the sulfonate group (for instance, **7** and **9** showed higher α -values than **6** and **8**). *Ortho*-substitution at the sulfonate group containing aromatic ring seems to be detrimental for the enantiodiscrimination properties, as α -values for **10** are lower than for its *para*-substituted isomer **4** (Fig. 4).

Furthermore, pronounced retention characteristics were not observed. Both electron donating and electron withdrawing substituents caused slightly increased retention for the chalconesulfonate derivatives compared to the unsubstituted chalconesulfonate. Furthermore, naphthyl group containing compounds **3** and **13** were retained strongest.

3.5 SubFC enantioseparation of sodium β -ketosulfonates

Recently, we reported on separation of chiral carboxylic acids on QN-AX and QD-AX CSPs by SubFC [23]. By applying supercritical (sc) CO₂ and a methanolic modifier (containing buffer salts), we achieved separation performance similar to HPLC experiments using polar organic mobile phases. Although SubFC does not appear to be the first choice technique for separation of such polar compounds such as sulfonic acids (sulfonates), it was examined herein for SubFC enantioseparation of the sulfonate analytes on QN-AX and QD-AX CSP, respectively (Fig. 5).

Table 3 summarizes the data obtained for both columns in SubFC mode using sc CO₂ with 25% modifier content (MeOH, 200 mM HOAc, 100 mM NH₃). Generally, enantioselectivity and plate numbers are slightly lower than in HPLC mode using MeOH, 50 mM HOAc, 25 mM NH₃ as mobile phase (compare Tables 2 and 3). However, compound **6** could only be baseline separated when applying QD-AX CSP in SubFC mode. Moreover, the “separation profile” for all analytes on both CSPs is similar for SubFC and HPLC, which implies the same chiral recognition mechanism in both modes.

Elution strength is lower in SubFC due to a lower dielectric constant of the eluent that renders electrostatic

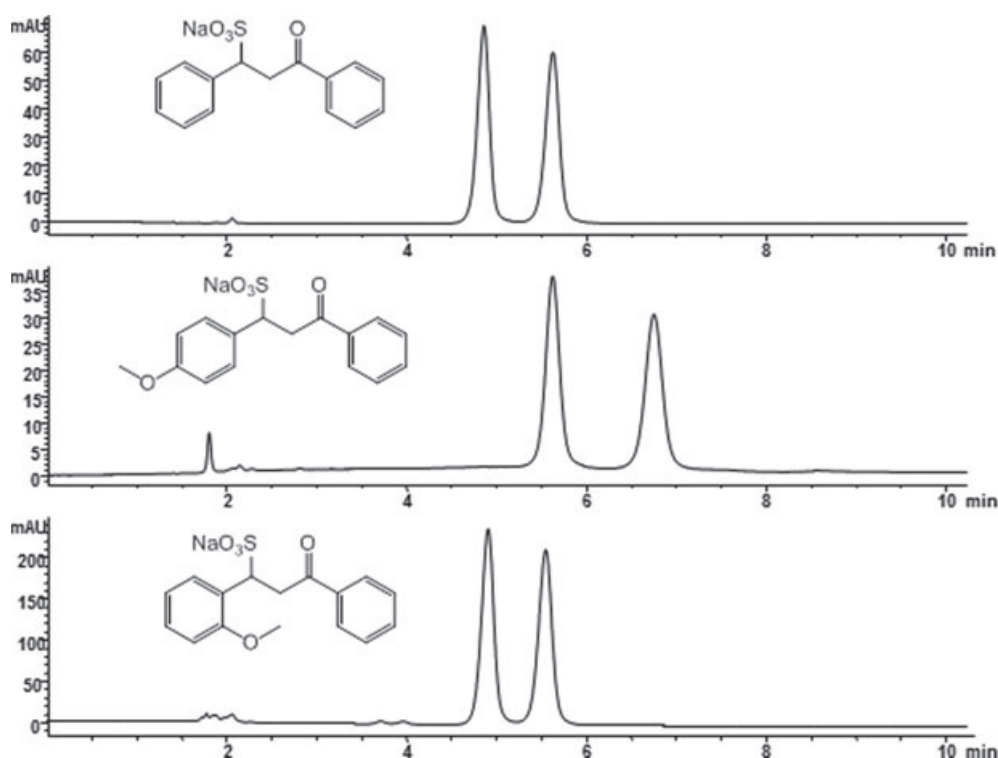


Figure 4. HPLC enantioseparations of **1** (top), **4** (middle), and **10** (bottom) on QD-AX CSP. Mobile phase: MeOH, 50 mM HOAc, 25 mM NH₃; 1.0 mL/min, 25°C UV detection at 280 nm.

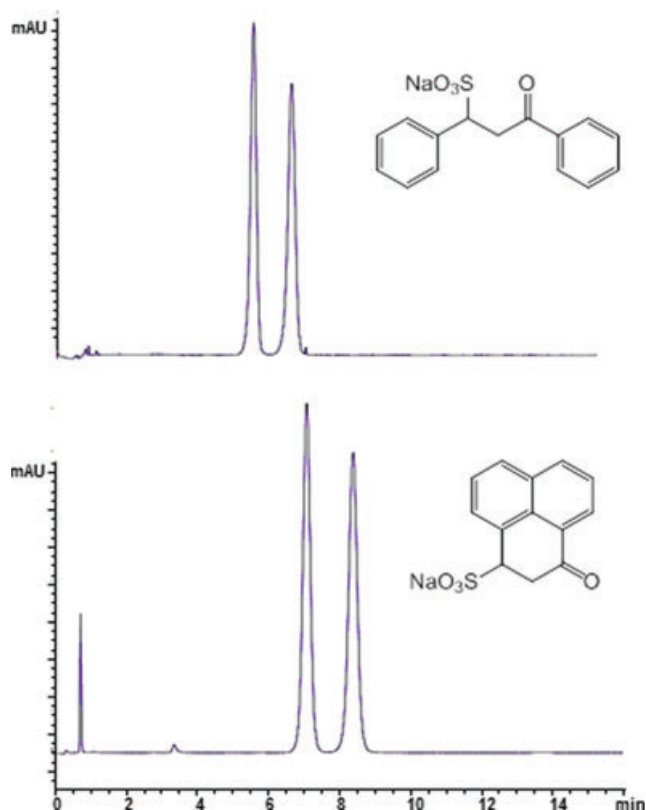


Figure 5. SubFC enantioseparations of **1** (top) and **13** (bottom) on QD-AX CSP. Conditions: 25% modifier (MeOH, 200 mM HOAc, 100 mM NH₃); 4.0 mL/min, 40°C, 150 bar; UV detection at 254 nm.

Table 3. Enantioseparation of analytes **1–13** on QN-AX and QD-AX CSP in SubFC mode^{a)}

Analyte	QN-AX CSP				QD-AX CSP			
	k_1	α	R_s	N_1 (m ⁻¹)	k_1	α	R_s	N_1 (m ⁻¹)
1	10.35	1.16	2.2	31 100	10.27	1.25	3.3	36 800
2	9.37	1.08	1.2	34 400	9.61	1.21	2.9	35 900
3	21.29	1.10	1.5	33 700	21.98	1.15	2.3	36 500
4	10.31	1.18	2.5	30 900	11.04	1.24	3.2	38 200
5	10.59	1.12	1.7	35 400	9.98	1.18	2.8	42 600
6	14.37	1.05	0.7	23 300	13.82	1.09	1.5	41 400
7	12.02	1.11	1.7	34 700	12.16	1.15	2.2	38 400
8	8.96	1.05	0.7	20 200	9.12	1.16	2.3	36 300
9	10.73	1.26	3.1	36 300	11.22	1.29	3.6	39 400
10	9.76	1.00	0.0	27 900	9.22	1.15	2.3	37 100
11	10.49	1.21	2.7	29 300	10.90	1.23	3.1	37 400
12	38.22	1.13	1.7	26 600	35.08	1.20	3.3	35 900
13	14.69	1.00	0.0	25 700	13.71	1.19	2.9	40 900

a) Conditions: 25% modifier (MeOH, 200 mM HOAc, 100 mM NH₃); 4.0 mL/min, 40°C, 150 bar backpressure; detection 254 and 230 nm; $t_0 = 0.49$ min.

interactions stronger and is reflected in roughly fivefold higher k_1 values. However, due to the low viscosity of the sc CO₂-methanolic mobile phase, this disadvantage can almost be compensated by application of a fourfold higher mobile phase flow rate. Additionally, the higher temperature for SubFC measurements (40°C compared to 25°C in HPLC) caused slightly decreased selectivity according to the

enthalpically controlled chiral recognition mechanism observed on cinchona carbamate type CSPs [23, 24].

4 Concluding remarks

Chiral sodium β -ketosulfonates, such as chalconesulfonates and derivatives thereof, were successfully separated on cinchona alkaloid derivatized CSPs using HPLC and SubFC. It was demonstrated that also for sulfonic acid compounds anion exchange is the dominating retention mechanism. Hence, retention can be adjusted by using different counterion concentrations without affecting enantioselectivity. However, acid–base equilibria are superimposed to the ion-exchange process, as the protonation state of both weak anion-exchange type SO and weak competitor acid is dependent on the apparent pH. From a practical point of view, this means that the ratio or type of the acidic and basic additives, respectively, cause pronounced influence not only on retention but also on enantioselectivity and peak shape.

HPLC turned out to be superior to SubFC in terms of faster solute elution but employing the same co- and counterion strength in the mobile phase. However, for some analytes, SubFC afforded the highest magnitude of resolution values. Moreover, SubFC could be considered a valuable alternative for preparative applications due to ease of solvent evaporation.

The authors thank Dario Bianchi for synthesizing test compounds 12 and 13 and Peter Frühauf for packing the columns.

The authors have declared no conflicts of interest.

5 References

- [1] Francotte, E., Lindner, W., *Chirality in Drug Research*, Wiley-VCH, Weinheim 2006.
- [2] Lämmerhofer, M., Lindner, W., in: Grinberg, N., Grushka, E. (Eds.), *Advances in Chromatography*, CRC Press, Boca Raton, FL 2008, pp. 1–107.
- [3] Lämmerhofer, M., Lindner, W., *J. Chromatogr. A* 1996, 741, 33–48.
- [4] Zarbl, E., Lämmerhofer, M., Hammerschmidt, F., Wuggenig, F., Hanbauer, M., Maier, N. M., Sajovic, L., Lindner, W., *Anal. Chim. Acta* 2000, 404, 169–177.
- [5] Lämmerhofer, M., Hebenstreit, D., Gavioli, E., Lindner, W., Mucha, A., Kafarski, P., Wiczorek, P., *Tetrahedron: Asymmetry* 2003, 14, 2557–2565.
- [6] Mandl, A., Nicoletti, L., Lämmerhofer, M., Lindner, W., *J. Chromatogr. A* 1999, 858, 1–11.
- [7] Maier, N. M., Schefzick, S., Lombardo, G. M., Feliz, M., Rissanen, K., Lindner, W., Lipkowitz, K. B., *J. Am. Chem. Soc.* 2002, 124, 8611–8629.
- [8] Newman, P., *Optical Resolution Procedures for Chemical Compounds: Amines and Related Compounds*, Optical Resolution Information Center, Riverdale, NY 1978.
- [9] Sluis, S. v. d., Hulshof, L., Kooistra, J., Vries, T., Wynberg, H., Echten, E. v., Koek, J., Hoeve, W. T., Kellogg, R. M., Broxterman, Q. B., Minnaard, A., Kaptein, B., *Angew. Chem. Int. Ed.* 1998, 37, 2349–2354.
- [10] Macchiarulo, A., Pellicciari, R., *J. Mol. Graphics Modell.* 2007, 26, 728–739.
- [11] Yoshikawa, M., Yamaguchi, S., Kunimi, K., Matsuda, H., Okuno, Y., Yamahara, J., Murakami, N., *Chem. Pharm. Bull.* 1994, 42, 1226–1230.
- [12] Kerr, D. I. B., Ong, J., Vaccher, C., Berthelot, P., Flouquet, N., Vaccher, M.-P., Debaert, M., *Eur. J. Pharmacol.* 1996, 308, R1–R2–R1–R2.
- [13] Moccia, M., Fini, F., Scagnetti, M., Adamo, M. F. A., *Angew. Chem. Int. Ed.* 2011, 50, 6893–6895.
- [14] Kellogg, R. M., Nieuwenhuijzen, J. W., Pouwer, K., Vries, T. R., Broxterman, Q. B., Grimbergen, R. F. P., Kaptein, B., Crois, R. M., de Wever, E., Zwaagstra, K., van der Laan, A. C., *Synthesis* 2003, 1626–1638.
- [15] Wang, Y., Beesoon, S., Benskin, J. P., De Silva, A. O., Genuis, S. J., Martin, J. W., *Environ. Sci. Technol.* 2011, 45, 8907–8914.
- [16] Pettersson, C., No, K., *J. Chromatogr. A* 1983, 282, 671–684.
- [17] Gyimesi-Forrás, K., Akasaka, K., Lämmerhofer, M., Maier, N. M., Fujita, T., Watanabe, M., Harada, N., Lindner, W., *Chirality* 2005, 17, S134–S142.
- [18] Ståhlberg, J., *J. Chromatogr. A* 1999, 855, 3–55.
- [19] Hinterwirth, H., Lämmerhofer, M., Preinerstorfer, B., Gargano, A., Reischl, R., Bicker, W., Trapp, O., Brecker, L., Lindner, W., *J. Sep. Sci.* 2010, 33, 3273–3282.
- [20] Millot, M. C., Debranche, T., Pantazaki, A., Gherghi, I., Sébille, B., Vidal-Madjar, C., *Chromatographia* 2003, 58, 365–373.
- [21] Lämmerhofer, M., Maier, N. M., Lindner, W., *Am. Lab.* 1998, 30, 71–78.
- [22] Xiong, X., Baeyens, W. R. G., Aboul-Enein, H. Y., De-langhe, J. R., Tu, T., Ouyang, J., *Talanta* 2007, 71, 573–581.
- [23] Pell, R., Lindner, W., *J. Chromatogr. A* 2012, 1245, 175–182.
- [24] Oberleitner, W. R., Maier, N. M., Lindner, W., *J. Chromatogr. A* 2002, 960, 97–108.

Curriculum vitae

Dipl.-Ing. (FH) Georg Schuster

Year and Place of Birth: 1984 in Bad Tölz, Germany

Citizenship: German

Contact: georg.schuster@univie.ac.at

Education

10/2009 – 04/2013

University of Vienna

Vienna, Austria

PhD in Analytical Chemistry

Thesis Title: „Development of polar chromatography sorbents and attempts to describe retention mechanisms of hydrophilic interaction chromatography systems“

Supervisor: Professor W. Lindner

Department of Analytical Chemistry

09/2007 – 03/2008

LMU Munich

Munich, Germany

Diploma Student

Thesis Title: *Implementation of Beckman Coulter Capillary Electrophoresis P/ACE™ System MDQ for Protein Characterization*

Supervisor: Professor W. Frieß

Department of Pharmaceutical Technology and Biopharmacy

09/2004 – 03/2008

NTA Isny

Isny, Germany

Diploma Studies in Pharmaceutical Chemistry

Naturwissenschaftlich Technische Akademie Isny

State approved university of applied sciences

Graduation as Diplom Ingenieur (FH) Pharmazeutische Chemie

2000-2002

Fachoberschule

Bad Tölz, Germany

Specialized secondary school

Main focus: Economy

Teaching Experience and Work Experience

2008 – 2012 <i>University of Vienna</i> Vienna, Austria	Mentoring of diploma students Teaching Assistant Laboratory courses in analytical chemistry for undergraduate students of chemistry and biology
07/2012 – 10/2011 <i>Novartis Pharma AG</i> Basel, Switzerland	Research on the behaviour of polar stationary phases in Supercritical Fluid Chromatography
06/2008 – 08/2008 <i>Coriolis Pharma Service GmbH</i> Munich, Germany	Development and analysis of biopharmaceutical drug formulations

Training and Qualifications

Languages	German (native speaker) English (fluent) French (basic knowledge)
Computer skills	MS Office IBM SPSS Statistics, XLStat, R CS ChemOffice Agilent ChemStation LC Applied Biosystems/MDS Sciex Analyst®
Other	Quality Assurance in the Chemical Laboratory (University Course, Montanuniversität Leoben, 2012-2013)

Scientific Contributions

Oral Presentations

HILIC: A systematic column characterization

29th international Symposium on Chromatography, September 2012, Toruń, Poland

HILIC: A systematic column characterization (*Awarded best scientific talk*)

Junganalytiker Forum, June 2012, Universität Salzburg, Austria,

Articles in Peer-Reviewed Journals

Comparative characterization of hydrophilic interaction liquid chromatography columns by linear solvation energy relationships,

Authors: G. Schuster, W. Lindner

Journal of chromatography A., 2013, 1273, 73-94

Enantioseparation of Chiral Sulfonates by Liquid Chromatography and Subcritical Fluid Chromatography,

Authors: R. Pell, G. Schuster, M. Lämmerhofer, W. Lindner

Journal of Separation Science, 2012, 35, 2521-2528

Chocolate HILIC phases: development and characterization of novel saccharide-based stationary phases by applying non-enzymatic browning (Maillard reaction) on amino-modified silica surfaces,

Authors: G. Schuster, W. Lindner

Journal of Analytical and Bioanalytical Chemistry, 2011, 400, 2539-2554

Special issue *Analytical Sciences in Austria*

Poster Presentations

How many HILIC columns do we need? A systematic column characterization study,

Authors: G. Schuster, W. Lindner

HPLC 2012 (June 19 - 23, Budapest, Hungary)

Characterization of a Novel Sugar-based Polar Stationary Phase and Its Aminopropyl Modified Starting Material,

Author: G. Schuster, W. Lindner

ANAKON 2011 (March 22 - 25, 2011, Zurich, Switzerland)

Hydrophilic Interaction Liquid Chromatography: Retention Studies on Sugar-based Polar Stationary Phases,

Authors: G. Schuster, T. Hüser, W. Lindner

28th International Symposium on Chromatography September 12 - 16, 2010, Valencia, Spain